

EXPLORING THE REGULATORY MECHANISMS OF IRE1 SIGNALING IN  
BIOTIC AND ABIOTIC STRESS RESPONSES IN *ARABIDOPSIS*

By

TAIABA AFRIN

KAROLINA MUKHTAR, COMMITTEE CHAIR  
ZSUZSANNA BEBOK  
MELISSA L. HARRIS  
SHAHID M. MUKHTAR  
JEANMARIE VERCHOT

A DISSERTATION

Submitted to the graduate faculty of The University of Alabama at Birmingham,  
in partial fulfillment of the requirements for the degree of  
Doctor of Philosophy

BIRMINGHAM, ALABAMA

2023

Copyright by  
Taiaba Afrin  
2023

# EXPLORING THE REGULATORY MECHANISMS OF IREA SIGNALING IN BIOTIC AND ABIOTIC STRESS RESPONSES IN ARABIDOPSIS

TAIABA AFRIN

BIOLOGY

## ABSTRACT

Given their stationary existence, plants have evolved various defensive strategies for their survival. Among many survival mechanisms, one crucial characteristic of plants is their ability to recognize stressors and respond appropriately. When faced with various environmental and intracellular signals, plant cells respond by undergoing significant changes in the transcription and translation of stress response regulators. Many of these changes depend on the processing within the endoplasmic reticulum (ER). This surge in protein synthesis might surpass the capacity for precise protein quality control, resulting in a buildup of unfolded and/or incorrectly folded proteins. This situation sets off a mechanism known as the unfolded protein response (UPR). UPR is a complex, multilayered regulatory network consisting of three primary branches in eukaryotic systems.

Among the three branches of UPR signaling, the IRE1-mediated pathway is the most conserved. In Arabidopsis, IRE1 splices bZIP60 mRNA and produces a functional transcription factor which then induces cytoprotective genes in the nucleus to maintain cellular homeostasis. One of my project's findings indicated that different Arabidopsis accessions have single nucleotide polymorphisms (SNPs) in the promoter regions of IRE1. These SNPs affect how IRE1 and its regulatory network react under different stresses. The various natural accessions demonstrated varying levels of promoter activity for both IRE1a and IRE1b, as well as distinct expression patterns for IRE1a and IRE1b

and differential downstream cascade when subjected to heat stress, tunicamycin, and salicylic acid treatment.

One of IRE1's primary roles is to activate the pro-survival pathway by splicing the bZIP60 mRNA. When plants are subjected to acute ER stress, the pro-survival pathway switches to the pro-death pathway. However, the critical regulator which acts as the molecular switch has not been discovered yet. In my final chapter, I propose a novel microRNA, miR5658, which acts as the molecular switch and activates the pro-death pathway. Furthermore, long non-coding RNAs (lncRNAs) play critical roles in maintaining ER homeostasis, which must be studied more deeply.

In summary, my thesis dissected the crucial roles of the IRE1a/bZIP60 pathway in managing the ER stress response. Additionally, it highlighted the vital functions of the novel miR5658 in determining cell fate by regulating the IRE1a/bZIP60 pathway during acute ER stress. Understanding the role of miR5658 on bZIP60 mRNA target is very critical to agricultural industries as it will be able to create novel options for biotechnologists to alleviate the ER stress for quality crop production.

Keywords: ER stress, IRE1, bZIP60, lncRNA, miRNA, Cell death

## **ACKNOWLEDGMENTS**

My deepest gratitude goes to my mentor, Dr. Karolina Mukhtar, for her unwavering support and inspiration throughout my graduate study at UAB. Her profound expertise as a scientist, coupled with her exceptional mentoring abilities, have been invaluable. Dr. Mukhtar enlightened me on dissecting and addressing scientific inquiries while providing boundless guidance in my research endeavors. I am immensely thankful for her dedicated efforts in refining my skills in both oral presentations and written communication. Her mentorship has been instrumental in shaping me into a self-confident and independent researcher.

I would also like to thank all my committee members, Drs. Zsuzsanna Bebok, Melissa Harris, Shahid Mukhtar, and Jeanmarie Verchot. The critical input I've received has been a significant catalyst propelling my research endeavors. I owe particular gratitude to Dr. Shahid Mukhtar, whose constructive insights during our joint lab meetings have been invaluable. I extend my heartfelt thanks to all past and present members of both Dr. Karolina Mukhtar's and Dr. Shahid Mukhtar's labs, who have embodied the spirit of teamwork over the past six years. I wish to acknowledge Dr. Xiaoyu Liu especially, for her technical guidance, engaging dialogues, and unwavering support at all times. I am deeply grateful to my lab mates, Danish Diwan and Regina Bedgood, who have provided consistent support during the varying tides of academic and

personal life over the last few years. I'm thankful to all the dedicated undergraduates I've enjoyed working with throughout my PhD journey.

My profound gratitude is extended to my cherished parents and brothers for their infinite love, unwavering support, countless sacrifices, and constant encouragement that have steered my life. Thank you for believing in me and encouraging me to pursue my dreams.

In conclusion, but of no less importance, I wish to express my heartfelt appreciation to my husband, Raiful Hasan. His unwavering support and understanding have been of immeasurable value. He has been there for me, encouraging me to remain optimistic even in the face of adversity. His immense contribution and sacrifice have made my PhD journey much more fulfilling and enjoyable than I could have ever envisaged. Treading this path of pursuing PhDs together was a journey filled with a mix of challenges and pleasures, but together we embraced and savored every moment.

## TABLE OF CONTENTS

ABSTRACT.....	ii
ACKNOWLEDGEMENTS.....	iv
LIST OF TABLES.....	vii
LIST OF FIGURES.....	viii
LIST OF ABBREVIATIONS.....	x
INTRODUCTION.....	1
Plant Pathogen Interactions.....	1
The Master Regulator of Plant Immune Signaling.....	7
Endoplasmic Reticulum Stress Signaling in Plant Immunity.....	9
The Regulatory Roles of Small RNA in Plant Stress Response.....	15
CHAPTER 1 MULTILEVEL REGULATION OF ENDOPLASMIC RETICULUM STRESS RESPONSES IN PLANTS: WHERE OLD ROADS AND NEW PATHS MEET.....	20
CHAPTER 2 ARABIDOPSIS GCN2 KINASE CONTRIBUTES TO ABA HOMEOSTASIS AND STOMATAL IMMUNITY .....	53
CHAPTER 3 THE INTERPLAY OF GTP-BINDING PROTEIN AGB1 WITH ER STRESS SENSORS IRE1A AND IRE1B MODULATES ARABIDOPSIS UNFOLDED PROTEIN RESPONSE AND BACTERIAL IMMUNITY .....	95
CHAPTER 4 PROBING NATURAL VARIATION OF IRE1 EXPRESSION AND ENDOPLASMIC RETICULUM STRESS RESPONSES IN ARABIDOPSIS ACCESSIONS.....	125
CHAPTER 5 ELUCIDATING THE ROLE OF NATURAL ANTISENSE RNA LOCI AS PRO-SURVIVAL TO PRO-DEATH MOLECULAR SWITCH IN THE IRE1A SIGNALING PATHWAY IN ARABIDOPSIS THALIANA.....	172
DISCUSSIONS AND FUTURE DIRECTIONS.....	227
REFERRENCE.....	238
APPENDIX A SUPPLEMENTAL FIGURES.....	254
APPENDIX B SUPPLEMENTAL TABLES.....	274

## LIST OF TABLES

### CHAPTER 1 MULTILEVEL REGULATION OF ENDOPLASMIC RETICULUM STRESS RESPONSES IN PLANTS: WHERE OLD ROADS AND NEW PATHS MEET

Box 1. Key developments in understanding the function of ER stress signaling in plant development and stress responses.....	35
---	----

### CHAPTER 3 THE INTERPLAY OF GTP-BINDING PROTEIN AGB1 WITH ER STRESS SENSORS IRE1A AND IRE1B MODULATES ARABIDOPSIS UNFOLDED PROTEIN RESPONSE AND BACTERIAL IMMUNITY

Table 1. P-values from independent sample (two-tailed) t-test for fresh weight data resulting from the Tm treatment experiments.....	104
Table 2. P-values from independent sample (two-tailed) t-test for fresh weight data resulting from the DTT treatment experiments.....	106
Table 3. P-values from independent sample (two-tailed) t-test for root length data resulting from the DTT treatment experiments.....	107

### CHAPTER 4 PROBING NATURAL VARIATION OF IRE1 EXPRESSION AND ENDOPLASMIC RETICULUM STRESS RESPONSES IN ARABIDOPSIS ACCESSIONS

Table 1: Selected accessions for IRE1a and IRE1b genes, characterized in this study...	132
Table 2: SNPs found in IRE1a promoter regions across different Arabidopsis accessions.....	137

### CHAPTER 5 ELUCIDATING THE ROLE OF NATURAL ANTISENSE RNA LOCI AS PRO-SURVIVAL TO PRO-DEATH MOLECULAR SWITCH IN THE IRE1A SIGNALING PATHWAY IN ARABIDOPSIS THALIANA

Table 1: Predicted miRNAs that can target both spliced and unspliced bZIP60 transcript.....	182
---	-----

## LIST OF FIGURES

### CHAPTER 1 MULTILEVEL REGULATION OF ENDOPLASMIC RETICULUM STRESS RESPONSES IN PLANTS: WHERE OLD ROADS AND NEW PATHS MEET

Figure 1: Three arms of ER stress response in plants.....	25
Figure 2. Conserved domain architecture of IRE1 proteins in Arabidopsis.....	30
Figure 3. Stress-mediated activation of UPR.....	33

### CHAPTER 2 ARABIDOPSIS GCN2 KINASE CONTRIBUTES TO ABA HOMEOSTASIS AND STOMATAL IMMUNITY

Figure 1. AtGCN2 is required for <i>P. syringae</i> -triggered eIF2 $\alpha$ phosphorylation and TBF1 translational derepression.....	58
Figure 2. AtGCN2-TBF1 cascades transcriptionally manipulate ABA signaling components during preinvasive stage.....	63
Figure 3. AtGCN2 contributes to stomatal immunity and affects disease susceptibility at the preinvasive stage of the infection event.....	67
Figure 4. AtGCN2 affects disease susceptibility by promoting ABA accumulation and negatively affecting ABA signaling components accumulation.....	71
Figure 5. A model representing the key targets of AtGCN2 in immune responses during preinvasive and postinvasive stages of bacterial pathogen infection.....	79

### CHAPTER 3 THE INTERPLAY OF GTP-BINDING PROTEIN AGB1 WITH ER STRESS SENSORS IRE1A AND IRE1B MODULATES ARABIDOPSIS UNFOLDED PROTEIN RESPONSE AND BACTERIAL IMMUNITY

Figure 1. Representative phenotypes of Arabidopsis plants used in the study .....	101
Figure 2. Analysis of chemical ER stress sensitivity to 0.3 $\mu$ g/ml tunicamycin (Tm) on fresh weight of indicated genotypes .....	105
Figure 3. Analysis of chemical ER stress sensitivity to 0.75 mM DTT on fresh weight of indicated genotypes .....	106
Figure 4. Analysis of root length in response to a chemical ER stress triggered by exposure to 0.75 mM DTT of indicated genotypes.....	108
Figure 5. Bacterial infection with <i>Pseudomonas syringae</i> pv. tomato DC3000.....	110

CHAPTER 4 PROBING NATURAL VARIATION OF IRE1 EXPRESSION AND  
ENDOPLASMIC RETICULUM STRESS RESPONSES IN ARABIDOPSIS  
ACCESSIONS

Figure 1: Geographical distribution and representative phenotypes of selected Arabidopsis natural accessions used in this study.....	133
Figure 2: Analysis of relative IRE1a and IRE1b expression levels in selected accessions before and after heat stress .....	134
Figure 3: Transient MUG assay to determine basal and heat-induced activities of IRE1a and IRE1b promoters from selected ecotypes.....	139
Figure 4: Analysis of ER stress sensitivity and relative heat-induced mRNA expression levels of spliced bZIP60 in selected accessions.....	142
Figure 5. Quantification of relative mRNA levels of IRE1a and IRE1b following Salicylic Acid treatment.....	148
Figure 6. Quantification of bZIP60 splicing efficacy and relative mRNA levels of ER stress markers BiP3 and ERDJ3B.....	151
Figure 7. Natural variation of resistance to <i>Pseudomonas syringae</i> pv. tomato DC3000 among selected Arabidopsis accessions.....	155
Figure 8: Heat map comparisons of differential gene expression, whole-plant ER stress sensitivity, and pathology phenotypes of selected Arabidopsis accessions.....	157

CHAPTER 5 ELUCIDATING THE ROLE OF NATURAL ANTISENSE RNA LOCI AS  
PRO-SURVIVAL TO PRO-DEATH MOLECULAR SWITCH IN THE IRE1A  
SIGNALING PATHWAY IN ARABIDOPSIS THALIANA

Figure 1: The analysis of relative miRNA expression level .....	184
Figure 2: Characterization of <i>NAT<sub>SRCl</sub></i> and <i>srcl</i> mutants.....	188
Figure 3: Transient activity of mutated bZIP60 and pathogenic resistance.....	191
Figure 4: Cell Death Analysis of control and mutant lines.....	194
Figure 5: Upstream and downstream signaling markers quantification.....	198
Figure 6: The proposed model for miR5658 expression and activity.....	206

## LIST OF ABBREVIATIONS

ABA	abscisic acid
AGB1	Arabidopsis GTP-binding protein b1
AGI	Arabidopsis Genome Initiative
ATF4	activating transcription factor 4
ATF6	activating transcription factor 6
BABA	$\beta$ -aminobutyric acid
BiP	binding immunoglobulin protein
BR	brassinosteroids
bZIP60	basic leucine zipper 60
circRNA	circular ncRNA
COR	Coronatine
DTT	Dithiothreitol
EF-Tu	elongation factor Tu
EFR	EF-Tu receptor
eIF2 $\alpha$	eukaryotic translation initiation factor 2 $\alpha$
ER	Endoplasmic Reticulum
ERAD	ER-associated degradation
ERQC	ER quality control

ET	ethylene
ETI	effector-triggered immunity
ETS	effector-triggered susceptibility
FLC	Flowering locus C
FLS2	FLAGELLIN SENSING 2
G proteins	Guanine nucleotide-binding proteins
GA	gibberellic acid
GarVX	Garlic virus X
GCN2	General Control Non-repressible 2
GFP	green fluorescent protein
HR	hypersensitive response
IRE1	inositol-requiring enzyme 1
JA	jasmonic acid
lincRNA	long intronic/intergenic RNA
lncNAT	long non-coding natural antisense transcript
lncRNA	long non-coding RNA
LRR	leucine-rich repeat
MAMPs	microbe-associated molecular patterns
MAPK	mitogen-activated protein kinase
miRNA	microRNA
mRNAs	messenger RNAs
MTI	microbe-associated molecular patterns
NATs	natural antisense transcript

NBS	nucleotide-binding site
ncRNAs	non-coding RNAs
NPR1	NONEPRESSOR OF PR GENES1
PAMPs	pathogen associated molecular patterns
PCD	programmed cell death
PERK	protein kinase RNA-like ER kinase
PIAMV	<i>Plantago asiatica mosaic virus</i>
piRNA	Piwi-associated RNA
PR	pathogenesis-related
<i>Pst</i>	<i>Pseudomonas syringae</i>
PTI	PAMP triggered immunity
R genes	resistance genes
RBSDV	<i>Rice black streak dwarf virus</i>
RIDD	regulated IRE1-dependent decay
RIDS	regulated IRE1-dependent splicing
RIN4	RPM1- interacting protein
RNS	reactive nitrogen species
ROS	reactive oxygen species
RPM1	Resistance to <i>Pseudomonas syringae</i> pv. <i>maculicola</i> -1
rRNA	ribosomal RNA
S1P	site-1 protease
S2P	site-2 protease
SA	Salicylic acid

SAR	systemic acquired resistance
siRNA	small interfering RNA
snoRNA	small nucleolar RNA
SNP	single nucleotide
snRNA	small nuclear RNA
TF	transcription factor
TM	Tunicamycin
tRNA	transfer RNA
TTSS	type-III secretion system
TuMV	Turnip mosaic virus
uORFs	upstream open reading frames
UPR	unfolded protein response

## **GENERAL INTRODUCTION**

Throughout the evolutionary history of photosynthetic eukaryotes, spanning over a billion years, numerous algae have successfully adapted to terrestrial environments. It is believed that plants originated from a type of aquatic green algae. Over time, they developed significant adaptations for terrestrial life, such as vascular tissues, seeds, and flowers. These key evolutionary advancements enhanced the plant's ability to thrive in dryland environments. Given that plants are immobile, they are constantly subjected to a multitude of stressors from various biotic organisms, in addition to the abiotic factors in their environment. All these stressors have influenced the evolution of plants over time.

In this dissertation, I will delve into plant immunity: the processes by which plants identify stressors, initiate stress response mechanisms and acquire immunity. I will discuss three different pathways activated in response to the unfolded protein response (UPR) that play a role in maintaining endoplasmic reticulum (ER) homeostasis.

Additionally, I will briefly discuss the emerging significance of lncRNA/lncNAT in regulating plant ER homeostasis.

## **Plant-Pathogen Interactions**

In their natural habitats, plants regularly face multiple stressors either concurrently or in succession, particularly in the context of a fluctuating environment and global warming. This is especially true in environments where pathogens and herbivores

are prevalent. Due to their autotrophic nature, plants serve as an attractive food source for many exploitative species, including microbes, insects, and higher animals. (W. Zhang et al., 2017). The survival and well-being of plants depend on their capacity to recognize and deploy effective defensive strategies against these exploitative species. Therefore, plants have developed complex, multilayered defense systems to flourish in natural environments. Unlike animals, plants possess a unique, innate immune system, where each cell expresses innate immune receptors to detect signs of invasion (Jones & Dangl, 2006). A transcriptome response study involving various stress combinations in the model plant *Arabidopsis thaliana* (hereafter: Arabidopsis) has demonstrated that plants have evolved to manage multiple stressors simultaneously (Rasmussen et al., 2013). When a pathogen encounters a plant, it deploys a set of effectors to target areas within the host cell; these effectors substantially play a significant role in determining the pathogen's virulence. Pathogen effectors are dispatched to various compartments within the host cell, where they likely interact with one or more targets to suppress, postpone, and obstruct host defense responses. Conversely, a plant's innate immunity serves as the initial line of defense for its survival. Surface pattern recognition receptors (PRRs) function as early detection systems that identify pathogen/microbe-associated molecular patterns (PAMPs)/(MAMPs). As an example, FLS2 (FLAGELLIN SENSING 2) is responsible for detecting flagellin, a component of bacterial flagella, while EFR (EF-Tu receptor) recognizes bacterial elongation factor Tu (EF-Tu) (Gómez-Gómez & Boller, 2000; Zipfel et al., 2006). When PAMPs are detected, PRRs trigger a fundamental resistance response known as PAMP/MAMP-triggered immunity (PTI/MTI) (Jones & Dangl, 2006; Zipfel, 2014). PTI typically inhibits non-adapted microbes from causing

infection, thus serving as a crucial first-layer barrier against disease. The MTI safeguards plants by initiating various defense responses. These include the generation of reactive oxygen species (ROS) and reactive nitrogen species (RNS), the influx of calcium and hydrogen ions, deposition of callose, activation of the mitogen-activated protein kinase (MAPK) cascade, transcriptional activation of defense-related genes, and secretion of pathogenesis-related (PR) proteins (Ausubel, 2005; Cook et al., 2015). Certain pathogens have evolved to produce effector molecules that function as virulence factors, designed to delay, obstruct, or suppress MTI and suppress basic defense mechanisms, leading to a condition known as effector-triggered susceptibility (ETS) (Dangl et al., 2013). The effectors AvrPto and AvrPtoB derived from *Pseudomonas syringae* have been extensively studied and are known to inhibit PAMP-triggered signaling by targeting the complexes formed by PAMP receptors (Göhre et al., 2008; Xiang et al., 2008). In addition, other effectors such as HopAI1 and HopF2 can target and inhibit the MAPK cascades, thereby blocking PAMP-induced signaling (Wang et al., 2010; Zhang et al., 2007). plants have also evolved host resistance genes (*R* genes) whose products are capable of recognizing effector proteins produced by pathogens. Most disease resistance genes in plants are variants of nucleotide-binding site leucine-rich repeat (NBS-LRR) proteins. These proteins are characterized by the presence of nucleotide-binding site (NBS) and leucine-rich repeat (LRR) domains, along with variable amino- and carboxy-terminal domains (McHale et al., 2006). When an NB-LRR protein identifies just a single effector from the multitude a pathogen delivers into its host, the host reacts swiftly and robustly. This reaction stunts the pathogen's growth and sets off a heightened, quicker defense reaction, leading to what is known as effector-triggered immunity (ETI)

(Chisholm et al., 2006; Dangl & Jones, 2001; Jones & Dangl, 2006). The R protein RRS1-R in Arabidopsis exhibits a direct interaction with the effector protein Pop2 from *Ralstonia solanacearum* (*R. solanacearum*), resulting in the induction of effector-triggered immunity (ETI) response (Deslandes et al., 2003). In the guard model, certain plant R proteins are involved in monitoring the modification of host proteins mediated by effectors. Upon detecting such modifications, these R proteins initiate an effector-triggered immunity (ETI) response (Dangl & Jones, 2001). Host protein RIN4 (RPM1 [Resistance to *Pseudomonas syringae* pv. *maculicola*-1]-interacting protein) can undergo modification by the effectors AvrRpm1, AvrB, and AvrRpt2 derived from *Pseudomonas syringae* (Axtell & Staskawicz, 2003; Kim et al., 2005; Mackey et al., 2003). Recognition of the modified RIN4 by the host R proteins RPM1 and RPS2 triggers and establishes ETI responses (Chung et al., 2011; Mackey et al., 2002). Effector-triggered immunity (ETI) restores and enhances the basic transcriptional programs and antimicrobial defenses of pattern-triggered immunity (PTI). It is often linked with localized plant cell death, known as the hypersensitive response (HR) (Dangl & Jones, 2001; Jones & Dangl, 2006).

The recognition of pathogen effectors triggers HR in most cases through programmed cell death (PCD), production of reactive oxygen species (ROS), and antimicrobial compound synthesis in the infected tissue (Dangl & Jones, 2001; Lam, 2004; Nimchuk et al., 2003). HR is a characteristic plant defense mechanism that involves rapid and localized cell death at infected locations in host tissues. Leaves that have not been exposed to pathogens before, gain systemic resistance/immunity after a plant has undergone a resistance response involving the HR on one or more leaves. In many instances, there is no distinct difference in between PTI and ETI (Thomma et al.,

2011), and ETI is referred to as amplified PTI (Jones & Dangl, 2006). Hence, plant immune systems are considered unique surveillance systems that detect intrusions and employ defense responses (Gust et al., 2017). Usually, PTI mediated PCD appears after several days of infection, while ETI-triggered HR PCD happens within hours of infection (Lam, 2004). These local resistance reactions stimulate a more enduring systemic immunity, termed systemic acquired resistance (SAR), which prepares uninfected tissues for potential future pathogen attacks (Fu & Dong, 2013). SAR results in enhanced resistance across the entire plant, effectively protecting against secondary infections for extended periods ranging from weeks to months (Fu & Dong, 2013).

One of the ancient families of enzymes, proteases, cleaves protein substrates to contribute to cellular signaling and play critical roles in regulated cell death signaling (Salvesen et al., 2016). Caspases are intracellular proteases that initiate a series of signaling cascades during programmed cell death, cell proliferation, and inflammation. Caspases can be categorized as apoptotic and pro-inflammatory, while apoptotic can further be grouped into initiator (caspase-8, -9, and -10) and effector (caspase-3, -6, and -7) caspases (Salvesen et al., 2016). Apoptosis is the best-described form of PCD in animals, whereas the crucial apoptotic regulators' Caspases and B cell lymphoma 2 (Bcl-2) family proteins are absent in plants (Bozhkov & Lam, 2011). The disparities between plant and animal cellular structures are accountable for the divergence during the process of cell death. The rigid cell walls of plant cells hinder the formation of apoptotic bodies. Even though the plant genome sequencing data failed to establish the presence of caspases (Uren et al., 2000), caspase-like proteolytic activity has been observed during HR and disease-related plant cell death (Bonneau et al., 2008; Sueldo & van der Hoorn,

2017; Vercammen et al., 2007). Hence the caspase-like proteases are the leading executioner of HR-mediated cell death. The whole genome sequencing results of the *Arabidopsis* revealed that its genome lacks any true caspase-encoding genes, and that PCD is instead dependent on other proteases with caspase-like function. Metacaspases are closest plant structural homologs of caspases (Minina et al., 2017; Tsatsiani et al., 2011). However, both the specificity for substrates and the regulation of metacaspases diverge from those of caspases (Minina et al., 2020). Even so, metacaspases have been functionally linked to cell death triggered by both development and stress, whether biotic or abiotic. In animals, autophagy represents another type of nonapoptotic programmed cell death (PCD) (Edinger & Thompson, 2004). Autophagy can function additively with metacaspases during cell death (Coll et al., 2014). Interestingly, there are studies to claim that autophagy (a pro-survival mechanism) negatively regulates HR PCD and functions with other prodeath pathways parallelly in plants' innate immune system (Hofius et al., 2009; Liu et al., 2005; Patel & Dinesh-Kumar, 2008). *Arabidopsis* encodes a total of nine metacaspases, falling into two categories: type I, represented by AtMC1-3, and type II, encompassing AtMC4-9 (Uren et al., 2000). The involvement of reactive oxygen species (ROS) in activating PCD in animals, plants, and yeast is well established (Lam et al., 2001). Several studies reported the production of an "oxidative burst" during the early and late phases of plant-pathogen interaction, as well as the role of ROS in cell death response and signaling (Lam, 2004). Multiple studies have suggested that proteins related to membrane channels play an integral role in hypersensitive response (HR)-mediated cell death. Furthermore, alterations in cytosolic ionic homeostasis emerge as a pivotal

event during the course of HR-mediated cell death (Clarke et al., 2000; Clough et al., 2000; Devoto et al., 1999; Mittler et al., 1995).

### **The Master Regulator of Plant Immune Signaling**

The relationship between plant hormone signaling and plant-pathogen interactions is intricate and interconnected. Numerous pathways are involved in the synthesis, perception, and effects of plant hormones, contributing to the complexity of their interaction. These hormones, at first, were primarily known for their complex impacts on plant growth and development. However, it's now clear that plant hormone signaling notably affects the results of interactions between plants and pathogens (Grant & Jones, 2009). Salicylic acid (SA) and jasmonic acid (JA) serve as the primary defense hormones responsible for safeguarding plants against biotrophic and necrotrophic pathogens, respectively (Glazebrook, 2005). Upon recognizing pathogen-associated molecular patterns (PAMPs) during PTI/MTI and ETI, SA, a phenolic compound, is synthesized from a primary metabolite chorismate (Mishina & Zeier, 2007). Salicylic acid (SA) is a well-described regulator of SAR. It has been identified as one of the phytohormones that modulate hypersensitive response (HR) cell death in various environmental conditions (Alvarez, 2000). At the site of pathogen infection, higher concentrations of synthesized SA work in conjunction with other signals to induce cell death in infected cells. On the other hand, a reduced concentration of SA, produced at the site of infection, is transported to adjacent uninfected cells, serving as a survival signal for these cells (Alvarez, 2000). But pre-existing SAR downregulates the HR mediated cell death upon avirulent pathogen infection (Devadas & Raina, 2002). The regulatory protein

NONEXPRESSOR OF PR GENES1 (NPR1) is the master regulator of defense gene expressions as well as plant immunity and is highly conserved in plant species (Chern et al., 2001; Mou et al., 2003).

NPR1 plays a significant role in controlling signaling pathways downstream of SA. Upon activation by SA, NPR1 acts as a transcriptional coactivator, regulating a wide array of defense-related genes (Dong, 2004; Moore et al., 2011). The NPR1 protein facilitates SA signaling by activating downstream PR genes, thereby enhancing SAR (Pajerowska-Mukhtar et al., 2013). Moreover, when salicylic acid (SA) is present, NPR1 has the ability to enhance its own expression (Chen et al., 2019). As a result, NPR1 is subjected to a dual level of regulation, both at the transcriptional co-regulation stage and the post-transcriptional phase (Ding & Ding, 2020). The movement of NPR1 into the nucleus plays a crucial role in salicylic acid (SA) signaling. In a plant cell's quiescent state, NPR1 primarily resides in the cytoplasm, forming an oligomer bonded together by intermolecular disulfide linkages. Yet, when Systemic Acquired Resistance (SAR) is triggered, accompanied by a rise in salicylic acid (SA), the plant cells transition to a more reduced state. This change transforms the oligomeric NPR1 into its monomeric form. The monomeric NPR1 then moves into the nucleus, where it regulates the expression of genes related to SAR (Kinkema et al., 2000; Mou et al., 2003). The NPR1 monomers that consistently move into the nucleus, undergo ubiquitination and are directed toward the proteasome; this process prevents the untimely activation of genes targeted by NPR1 (Spoel et al., 2009). NPR1 proteins can govern immunity by interacting with other hormone regulatory pathways and by restructuring extensive gene expression networks (van Butselaar & Van den Ackerveken, 2020). NPR1 interacts with members of the basic

leucine zipper (bZIP) transcription factor family to trigger defense responses after entering the nucleus (Fan & Dong, 2002). These bZIP transcription factors are known to induce the expression of PR genes by binding to specific promoter regions (Fan & Dong, 2002). This interaction is crucial in promoting both local and systemic resistance mechanisms.

### **Endoplasmic Reticulum Stress Signaling in Plant Immunity**

The endoplasmic reticulum (ER) serves as a vital hub within the cell's secretory pathway, handling key operations such as protein synthesis and folding. It operates as a pivotal processing center for these critical cellular functions (Stefano et al., 2015; Vitale & Denecke, 1999). Within the ER, newly synthesized proteins undergo folding and modifications with the help of various proteins, such as BiP, calnexin, and protein disulfide isomerase (PDI) (Mori, 2000). These proteins play essential roles in facilitating proper protein folding and ensuring the integrity of the protein structure within the ER environment. The ER relies on its intrinsic quality control machinery to provide a favorable cellular environment, including ER retention and retrieval pathways. These mechanisms actively monitor and regulate protein synthesis and assembly within the ER lumen (Ellgaard & Helenius, 2003; Sitia & Braakman, 2003). Plant cells, similar to yeast and mammalian cells, possess their own ER quality control (ERQC) system (Liu & Li, 2014). This implies that plants can effectively manage increased levels of unfolded or misfolded proteins by utilizing their ERQC system. Nevertheless, under certain circumstances, such as when plants encounter unexpected stresses, the capacity of the ERQC machinery may not be sufficient to cope with the demands placed upon it.

Consequently, a substantial accumulation of misfolded proteins within the ER can occur, resulting in a condition known as ER stress and that can have potentially lethal consequences (Kaufman et al., 2002). A significant amount of research has been carried out to explore the processes behind endoplasmic reticulum (ER) stress signaling in yeast (Wu et al., 2014), mammals (Latham, 2015; Wu et al., 2014), and plants (Afrin, Diwan, et al., 2020; Iwata et al., 2008; Korner et al., 2015). In plants, ER stress can be triggered in multiple means, including the application of specific treatments such as chemicals (e.g., tunicamycin (TM) (Afrin et al., 2022; Afrin, Seok, et al., 2020; Koizumi et al., 2001; Moreno et al., 2012); dithiothreitol (DTT) (Iwata et al., 2008; Martinez & Chrispeels, 2003); salicylic acid (SA) (Afrin, Seok, et al., 2020; S. J. Lu et al., 2012; Moreno et al., 2012); L-azetidine-2-carboxylic acid (Irsigler et al., 2007); cyclopiazonic acid (CPA) (Zuppini et al., 2004)), as well as exposure to viral and bacterial pathogens (Moreno et al., 2012; Verchot & Pajerowska-Mukhtar, 2021; Vitale & Ceriotti, 2004; Ye et al., 2011), heat stress (Deng et al., 2011; S. J. Lu et al., 2012; S. S. Zhang et al., 2017), salt stress (Lee et al., 2006), and even during normal growth and developmental processes (Y. Deng et al., 2013; Iwata et al., 2008; Vitale & Ceriotti, 2004). The chemical ER stressor TM disrupts the N-linked glycosylation process of secreted glycoproteins, hindering their normal folding process (Iwata & Koizumi, 2005). On the other hand, as a reducing agent, DTT interferes with the proper formation of disulfide bonds by disturbing the oxidizing environment required for their correct folding (Braakman et al., 1992). To restore protein synthesis homeostasis, plant cells under stress employ various strategies, including: (i) upregulating the expression of genes encoding ER chaperones and foldases, which accelerate protein folding processes (Helenius & Aebi, 2004; Kamauchi et al.,

2005; Martinez & Chrispeels, 2003); (ii) enhancing the expression of components involved in ER-associated degradation (ERAD), which facilitates the efficient removal of misfolded proteins (Doblas et al., 2013; Pollier et al., 2013); and (iii) decreasing the synthesis of secretory proteins, reducing the burden of misfolded protein accumulation (Chen & Brandizzi, 2013; Mishiba et al., 2013; Moreno et al., 2012). When adequately handled, brief episodes of ER stress can be mitigated and resolved, thus reinstating a beneficial cellular environment. If ER stress persists, it can have severe consequences such as triggering autophagy, resulting in the breakdown and recycling of cellular components, or even leading to cell death. In more extreme cases, prolonged and unmitigated ER stress can ultimately lead to the death of the entire plant (Cai et al., 2014; Williams et al., 2014).

In order to combat ER stress, cells activate a series of protective signaling mechanisms known as the "unfolded protein response" (UPR) (Walter & Ron, 2011). The UPR operates at both the transcriptional and translational levels, aiming to bolster the ER's capacity for protein folding and eliminate unfolded or misfolded proteins. Specific regulatory mechanisms are activated under mild, temporary stress at the transcriptional level. These mechanisms increase the expression of genes that encode for ER-resident chaperones and foldases, as well as components of the ERAD system. These pathways primarily focus on the unfolded proteins present within the ER. They either repair faulty proteins, end unsuccessful folding attempts, or remove proteins that have been misfolded or damaged (Howell, 2013; Schröder & Kaufman, 2005; Walter & Ron, 2011). In contrast, long-term or chronic stress typically triggers regulatory changes in protein synthesis, which prevent the translation of additional messenger RNAs (mRNAs)

(Maurel et al., 2014; Schröder & Kaufman, 2005; Walter & Ron, 2011). In extreme conditions, when neither form of UPR regulation can restore protein homeostasis, processes such as autophagy or even PCD may be triggered. These processes remove the damaged organelles or in some cases, the entire cell (Hetz, 2012; Xu et al., 2005). In multicellular organisms, several UPR signaling pathways have been divided into three main types. These either involve an activating transcription factor 6 (ATF6) associated with the ER membrane, an inositol-requiring enzyme 1 (IRE1), or a protein kinase RNA-like ER kinase (PERK) (Schröder & Kaufman, 2005).

Plant cells have signaling pathways that correspond functionally to the three branches of the mammalian UPR (Afrin, Diwan, et al., 2020; Bao & Howell, 2017; Korner et al., 2015). The most conserved branch of these pathways is the IRE1-mediated pathway. This pathway includes a sensor domain in the N-terminal ER lumen and a kinase/endonuclease domain in the C-terminal. The genomes of several plants - including *Arabidopsis*, rice, soybean, maize, and *Nicotiana attenuata* - contain two homologs, *IRE1a* and *IRE1b* (Afrin, Seok, et al., 2020; Li et al., 2012; Silva et al., 2015; Wakasa et al., 2012; Xu et al., 2019). These homologs are highly similar in sequence and have conserved domain architecture. Recently, another homolog of *IRE1*, known as *IRE1c*, was discovered in *Arabidopsis* (Mishiba et al., 2019). Upon encountering stress within the ER, IRE1 responds by dimerization and trans-autophosphorylation, resulting in an atypical mRNA splicing event involving the bZIP60 transcription factor (TF). This process is referred to as regulated IRE1-dependent splicing (RIDS) (Deng et al., 2011; Moreno et al., 2012). In *Arabidopsis*, the spliced variant of AtbZIP60 acts as an active transcription factor, moving into the nucleus to trigger the expression of genes responsive

to ER stress. Recent findings have shown that the bZIP60 in Arabidopsis can also migrate from localized tissues to systemic tissues, thereby disseminating the UPR signal to remote parts of the plant (Lai et al., 2018).

The second branch involves the membrane-associated transcription factors AtbZIP17 and AtbZIP28. This pathway is similar to the mammalian ATF6 pathway, which also includes a bZIP domain and is activated by ER stress through its separation from the membrane (Yan Deng et al., 2013; Howell, 2013). Under stress-free conditions, the plant protein BiP attaches itself to the ATF6-like bZIP17/bZIP28 in Arabidopsis, which remains embedded in the endoplasmic reticulum (ER) membrane (Kim et al., 2018; Srivastava et al., 2013). When the ER undergoes stress, BiP detaches from bZIP17/bZIP28 and the detached bZIP28 re-routes to the Golgi apparatus where it undergoes proteolytic processing by S1P/S2P and gets released from the membrane (Kim et al., 2018; Srivastava et al., 2014). Following its release, the bZIP domain of the trans-acting factor is transported to the nucleus. Once there, it works in harmony with the heterotrimeric NF-Y complex to trigger the activation of UPR genes (Liu & Howell, 2010). In addition to ER stress, bZIP17 can also be activated in response to salt stress. Under this specific stress condition, bZIP17 undergoes regulated translocation to the Golgi apparatus and is subjected to cleavage facilitated by the enzymes S1P and S2P. This process enables the liberation of its N-terminal transcription factor (TF) domain, which is then transported to the nucleus. Once in the nucleus, it collaborates with bZIP60 to stimulate salt stress-responsive promoters and a subset of ER stress-induced promoters (Henriquez-Valencia et al., 2015; Liu et al., 2007).

Recent studies have highlighted the phosphorylation of eIF2 $\alpha$  as a third arm of UPR mechanisms in plants, which underlines the similarities between the mechanisms of UPR signaling in both animal and plant domains (Liu et al., 2019). The plant genomes of *Arabidopsis thaliana* and *Nicotiana benthamiana*, contain a single instance of a GCN2 kinase. This kinase is activated by a range of ER-related stressors, both of abiotic and biotic nature. Examples of such stressors include amino acid deprivation, exposure to the herbicide glyphosate (Faus et al., 2015), ultraviolet and cold stress, physical damage, and exposure to salicylic acid (SA) (Lageix et al., 2008). The GCN2 kinase also responds to infections caused by pathogens (Li et al., 2018; Liu et al., 2015; Monaghan & Li, 2010). Recent findings have shown that AtGCN2 is crucial for managing levels of abscisic acid (ABA), a plant hormone, and for controlling the immunity of stomata, small openings on plant leaf surfaces. Additionally, AtGCN2 has been observed to control the translation of a TF, TBF1, by reinitiating translation at upstream open reading frames (uORFs), a mechanism that is quite similar to the action of mammalian ATF4 and yeast GCN4 proteins (Liu et al., 2019; Pajerowska-Mukhtar et al., 2012). Even though plants lack a direct equivalent of the primary mammalian ER stress sensor, PERK, and the activation mechanism of plant GCN2 is still unclear, the link between AtGCN2 signaling and ER stress responses is reinforced through its downstream target, AtTBF1. AtTBF1 is the central regulator of genes associated with the secretory pathway during a pathogen infection (Pajerowska-Mukhtar et al., 2012). It binds to their promoters via the *TLI cis*-regulatory motif, a type of DNA sequence that controls the transcription of nearby genes (Wang et al., 2005).

## **The Regulatory Roles of Small RNA in Plant Stress Responses**

Plants have developed sophisticated molecular mechanisms to cope with extreme biotic and abiotic stress throughout the course of evolution. These intricate mechanisms play a vital role in the survival and sustainability of plants in challenging environmental conditions. Interestingly, non-protein-coding DNA plays an equally significant role as protein-coding DNA in contributing to this complex adaptation process. Usually, protein-coding loci are transcribed at higher levels, whereas the most of non-protein-coding loci transcribe at lower levels in a controlled manner and regulate complex developmental processes (Mattick & Makunin, 2006). Contrary to its previous label as "junk" DNA, non-protein-coding DNA has emerged as a valuable component that transcribes a significant portion of the transcriptional unit called non-coding RNAs (ncRNAs). These ncRNAs play essential roles in diverse regulatory processes (Urquiaga et al., 2020). In eukaryotes, only about 2% of RNA out of 90% encodes protein (Rai et al., 2019). ncRNAs can be categorized into two broad categories: housekeeping and regulatory ncRNA. They can further be categorized depending on different aspects. Generally based on their structure and function, transfer RNA (tRNA), ribosomal RNA (rRNA), small nuclear RNA (snRNA), and small nucleolar RNA (snoRNA) are expressed constitutively and known as housekeeping ncRNA, while microRNA (miRNA), small interfering RNA (siRNA), Piwi-associated RNA (piRNA) and long non-coding RNA (lncRNA, >200 nucleotides) are known as regulatory ncRNAs (Ponting et al., 2009). lncRNAs can further be categorized into: i) sense (the lncRNA overlap with one or more exons of a

different transcript on the same strand), ii) long non-coding natural antisense transcript (lncNAT, the lncRNA overlap with one or more exons of a different transcript on the opposite strand), iii) bidirectional (when the location of the transcription start site of lncRNA and the opposite strand are in close proximity), iv) long intronic (lincRNA, the lncRNA derived from intronic region), v) long intergenic (lincRNA, the lncRNA originate from the interval region of two genes) and vi) circular ncRNA (circRNA, lncRNA transcribe from back spliced exons) (Kung et al., 2013; Mattick & Rinn, 2015; Ponting et al., 2009).

Earlier lncRNAs were considered as “transcriptional noise” and speculated that they play a crucial role during transcriptional and post-transcriptional gene expression regulation. In the last several years, several studies in plant model system unveiled the vital regulatory roles of lncRNA during the developmental process, and biotic and abiotic stress responses (Fan et al., 2016; X. Sun et al., 2020; Y. Wang et al., 2014; Zhang et al., 2016). Deviant from protein-coding genes, ncRNA genes are poorly conserved and do not have large homologous families, but sequence conservation was observed among subsets of lncRNA across species (Necsulea et al., 2014; Zhao et al., 2021). The genomic location of lncRNA plays a critical role in their regulatory potential, and they can bind to DNA/RNA through cis-acting or trans-acting sequences and regulate the functions. Particularly in plants, most of the reported lncRNA is involved with stress responses (Shafiq et al., 2016). For instance, lncRNA ELENA1 (bacterial speck disease), TAR-66, TAR67, TAR-191, TAR-197, TAR-224 (wilt disease) in *Arabidopsis*; ALEX1 (bacterial leaf blight) in *Oryza*; TalnRNA5, TalnRNA9, TapmlnRNA2, TapmlnRNA7, TapmlnRNA19 (powdery mildew), TalncRNA18, TalncRNA73, TalncRNA106,

TalncRNA108 (stripe rust disease) in *Triticum*, Slylnc0195, Slylnc1077 (TYLCV infection) in *Solanum* (Seo et al., 2017; Wang et al., 2015; Wang et al., 2017; Xin et al., 2011; Yu et al., 2020; Zhang et al., 2013; Zhu et al., 2014). The mode of action of lncRNAs exhibits significant variation as they engage in diverse interactions. They can interact with other genes, hormones, proteins, and ncRNAs. Additionally, lncRNAs can serve as precursors for miRNAs and siRNAs or act as target mimics for other miRNAs. Furthermore, lncRNAs can be co-induced with neighboring defensive genes, enhancing their regulatory functions in response to different stimuli (Seo et al., 2017; Y. Sun et al., 2020; Wang et al., 2015; Xin et al., 2011; Yu et al., 2020; Zhu et al., 2014). However, their role and mechanism in plants' defense response are not fully deciphered yet. Recent studies have been shedding light on the notable significance of a specific lncRNA, known as lncNAT, in the defense response mechanisms of plants. These findings underscore the crucial role played by lncNAT in modulating plant defense and highlight its potential as a critical regulatory molecule in plant immune responses (Kumar & Chakraborty, 2021; Wang et al., 2015).

NATs are a class of lncRNAs that play critical roles in regulating gene expression. They have been identified to be involved in various abiotic and biotic stress response mechanisms across multiple species, including *Homo sapiens*, *Mus musculus*, *Saccharomyces cerevisiae*, *Plasmodium falciparum*, *Oryza*, *Zea mays*, *Triticum*, *Brassica rapa*, and *Arabidopsis* (Borsani et al., 2005; He et al., 2008; Katayama et al., 2005; Liu et al., 2012; T. Lu et al., 2012; Oono et al., 2017; Siegel et al., 2014; H. Wang et al., 2014; Xu et al., 2017; Yassour et al., 2010; Yu et al., 2013). These diverse organisms highlight the widespread importance of NATs in mediating adaptive responses to environmental

challenges. lncNATs can regulate the expression levels of sense transcripts (Marquardt et al., 2014; Sun et al., 2013). NATs can be categorized into two groups based on their effect on sense transcripts: concordant and discordant. Concordant NATs are characterized by coordinated expression patterns between the NAT and sense transcripts, while discordant NATs exhibit opposite expression patterns between the NAT and sense transcript (Jabnoune et al., 2013; Swiezewski et al., 2009; H. Wang et al., 2014). In the case of Arabidopsis, the COOLAIR lncRNA represses the expression of the Flowering locus C (FLC) sense transcript by inducing changes in histone marks (Swiezewski et al., 2009). Additionally, in Rice, a cis-NAT enhances the translation of its corresponding sense mRNA to maintain phosphate homeostasis and promote overall plant fitness (Jabnoune et al., 2013). These examples highlight how NATs can exert diverse regulatory effects on sense transcripts in different species. The specific biological functions and regulatory mechanisms employed by NATs still need to be discovered due to their wide-ranging nature. However, researchers have demonstrated that NATs utilize a variety of mechanisms to regulate the transcriptional or post-transcriptional expression of sense transcripts. These mechanisms include modulation of translation initiation (Wilusz et al., 2009), regulation of mRNA stability (Faghihi et al., 2008), involvement in transcription termination (Georg et al., 2009), impact on DNA methylation (Lewis et al., 2004), influence on histone methylation (Zhao et al., 2018), facilitation of translational enhancement (Deforges et al., 2019; Jabnoune et al., 2013), engagement in RNA interference (Prescott & Proudfoot, 2002), participation in gene silencing (Katiyar-Agarwal et al., 2006), induction of alternative splicing through RNA masking (Hastings

et al., 1997), and contribution to RNA editing (Peters et al., 2003). These discoveries underscore the wide range of mechanisms NATs utilize to modulate gene expression.

Many NATs have been identified in plants, with approximately 7-9% of all transcripts overlapping as cis-NATs (T. Lu et al., 2012). In Arabidopsis, it has been observed that approximately 88% of cis-NAT pairs involve protein-coding genes and non-protein coding transcripts (Okamoto et al., 2010). These cis-NATs have the potential to form a complex regulatory network; however, their precise roles and functions still need to be better understood. Several studies conducted in Arabidopsis have revealed the crucial involvement of NATs in various developmental processes. For example, they play roles during germination (Fedak et al., 2016), flowering (Csorba et al., 2014), and gametophyte development (Wunderlich et al., 2014). Moreover, NATs have been associated with stress response mechanisms in different plant species. In Arabidopsis, they are involved in salt tolerance (Borsani et al., 2005; Yu et al., 2013) and cold acclimation (Kindgren et al., 2018). In rice, NATs are implicated in phosphate starvation (Jabnoune et al., 2013) and leaf blade flattening (Liu et al., 2018), while in tomato, they are linked to oomycete resistance (Cui et al., 2017). Additionally, NATs can serve as precursors for siRNAs (Yu et al., 2013) and miRNA (Lu et al., 2008), adding to their functional diversity and regulatory potential. Chapter 5 of this Dissertation provides valuable insights into the molecular mechanisms of novel miR5658 in regulating the functions of the AtIRE1/bZIP60 mediated pathway in determining the cell fate during biotic stress.

## **CHAPTER 1**

### **MULTILEVEL REGULATION OF ENDOPLASMIC RETICULUM STRESS RESPONSES IN PLANTS: WHERE OLD ROADS AND NEW PATHS MEET**

by

TAIABA AFRIN<sup>1</sup>, DANISH DIWAN<sup>1</sup>, KATRINA SAHAWNEH<sup>1</sup>, AND KAROLINA PAJEROWSKA-MUKHTAR<sup>1</sup>

<sup>1</sup> Department of Biology, University of Alabama at Birmingham, 1300 University Blvd.,  
Birmingham, AL 35294, USA

Published, Journal of Experimental Botany, Vol. 71, No. 5 pp. 1659–1667, 2020,  
doi:10.1093/jxb/erz487

Copyright ©2019, Oxford University Press  
by  
Taiaba Afrin  
Used by permission  
Format adapted for dissertation

## **Abstract**

The sessile lifestyle of plants requires them to cope with a multitude of stresses in situ. In response to diverse environmental and intracellular cues, plant cells respond by massive reprogramming of transcription and translation of stress response regulators, many of which rely on endoplasmic reticulum (ER) processing. This increased protein synthesis could exceed the capacity of precise protein quality control, leading to the accumulation of unfolded and/or misfolded proteins that triggers the unfolded protein response (UPR). Such cellular stress responses are multilayered and executed in different cellular compartments. Here, we will discuss the three main branches of UPR signaling in diverse eukaryotic systems and describe various levels of ER stress response regulation that encompass transcriptional gene regulation by master transcription factors, post-transcriptional activities including cytoplasmic splicing, translational control, and multiple post-translational events such as peptide modifications and cleavage. In addition, we will discuss the roles of plant ER stress sensors in abiotic and biotic stress responses and speculate on the future prospects of engineering these signaling events for heightened stress tolerance.

**Keywords:** bZIP17, bZIP28, bZIP60, endoplasmic reticulum, GCN2, IRE1, UPR.

## **Integrated stress response in the endoplasmic reticulum**

The endoplasmic reticulum (ER) is the largest cellular organelle that controls the fundamental part of the protein homeostasis network by folding nascent peptides, packaging them, and sending them to their target locations (Chevet et al., 2001; Sunkar et al., 2006; Ron and Walter, 2007). The demand on the protein folding machinery can be increased by environmental conditions and endogenous factors, such as nutrient deficiency, oxidative stress, heat, or pathogen infection. When the folding demand is higher than the ER capacity, ER homeostasis becomes disrupted (Ron and Walter, 2007) while unfolded proteins begin to accumulate and aggregate, which collectively is referred to as ER stress (Walter and Ron, 2011). The cell has evolved effective mechanisms to adapt to this challenge, termed the unfolded protein response (UPR) (Kozutsumi et al., 1988). The UPR aims to resolve the ER stress by attenuating protein translation, reducing the amount of misfolded proteins, and inducing the expression of protein chaperones (Hetz et al., 2015). If the UPR cannot alleviate the ER stress, the cell switches its signaling into pro-death mode and activates apoptotic programs (Chen and Brandizzi, 2013).

The mammalian UPR is a three-prong signaling network. One branch includes a group of four kinases that mediate phosphorylation of eukaryotic translation initiation factor 2 $\alpha$  (eIF2 $\alpha$ ), including GCN2 (General Control Non-repressible 2) and PERK (RNA dependent Protein Kinase like ER kinase) (Wek et al., 2006). The phosphorylated eIF2 $\alpha$  allows for translational de-repression of mRNAs containing upstream ORFs (uORFs), such as activating transcription factor 4 (ATF4) (Rutkowski and Kaufman, 2003) that regulates survival under stress, autophagy (Luhr et al., 2019), apoptosis (Rozpedek et al.,

2016), tumor growth (Wortel et al., 2017), and polysomal decrease (Hofmann et al., 2012).

The other two branches of the mammalian UPR are mediated by transmembrane sensors spanning the ER lumen and cytosol: activating transcription factor 6 (ATF6) and inositol requiring enzyme 1 (IRE1,  $\alpha$  and  $\beta$  isoform) (Walter and Ron, 2011). Their activation is accomplished in response to accumulation of misfolded peptides in the ER lumen, leading to BiP (binding immunoglobulin protein) dissociation from these sensors and their activation by oligomerization or export (Maurel and Chevet, 2013). In animal systems, IRE1 can be activated by direct binding to unfolded proteins in the ER lumen or by changes in membrane lipid composition (Gardner and Walter, 2011; Promlek et al., 2011; Volmer et al., 2013). All three animal ER stress signaling branches participate in cellular responses to various external stimuli, including the regulation of metabolism (Oyadomari et al., 2008; Baird and Wek, 2012), immunity (Munn et al., 2005; Bunpo et al., 2010; Xia et al., 2018), tumorigenesis (Dey et al., 2015), and memory (Costa-Mattioli et al., 2005; Sidrauski et al., 2013).

### **UPR in plants: the next frontier for plant stress signaling**

While UPR has been a topic of active investigation in mammals and yeast for over three decades (Kozutsumi et al., 1988), it only recently has come to light as a complex stress response mechanism in plants (Koizumi et al., 2001; Liu et al., 2007b; Iwata et al., 2008; Lageix et al., 2008). Plant cells contain signaling pathways functionally corresponding to the three arms of the mammalian UPR (Korner et al., 2015; Bao and Howell, 2017; Park and Park, 2019) (Fig. 1). The most conserved arm is IRE1, equipped with

an N-terminal ER lumen sensor domain and a C-terminal kinase/endonuclease domain. The genomes of Arabidopsis, rice, soybean, maize, and *Nicotiana attenuata* contain two homologs, IRE1a and IRE1b that share high sequence similarity and conserved domain architecture (Li et al., 2012; Wakasa et al., 2012; Silva et al., 2015; Xu et al., 2019). Recently, it was reported that a third IRE1-like gene, designated IRE1c, exists in Arabidopsis (Mishiba et al., 2019, Preprint). Upon ER stress, IRE1 dimerizes, trans-autophosphorylates, and unconventionally splices mRNA for the bZIP60 transcription factor (TF) in a process termed regulated IRE1-dependent splicing (RIDS; see below). In Arabidopsis, the spliced form of AtbZIP60 is an active TF that translocates into the nucleus to drive the expression of ER stress responsive genes (Deng et al., 2011; Moreno et al., 2012). The IRE1 substrates from yeast and mammals, HAC1 and XBP1, also belong to the bZIP family and, akin to bZIP60, display conserved double stem-loop structures with specific nucleotide signatures required for mRNA processing (Back et al., 2005). Recently, Arabidopsis bZIP60 was also demonstrated to move from local to systemic tissues to propagate the UPR signal in distal parts of the plant (Lai et al., 2018b).

The second arm involves the membrane-associated TFs AtbZIP17 and AtbZIP28 (Srivastava et al., 2014; Kim et al., 2018). Their precursor forms are C-terminally anchored at the ER membrane, and upon ER stress translocate to the Golgi apparatus where they undergo sequential proteolytic cleavage by site-specific proteases S1P and S2P. Resulting N-termini, containing the bZIP and transcriptional activation domains, are transported to the nucleus, where they function as active TFs and up-regulate expression of stress response genes (Liu et al., 2007a, b; Che et al., 2010; Howell, 2013; Kim et al., 2018) (Fig. 1). Similar to the IRE1 branch, there is a considerable degree of conservation

between plant AtbZIP17/28 and mammalian ATF6 that also contains a bZIP domain and is activated by ER stress by cleavage from the membrane (Hillary and FitzGerald, 2018).

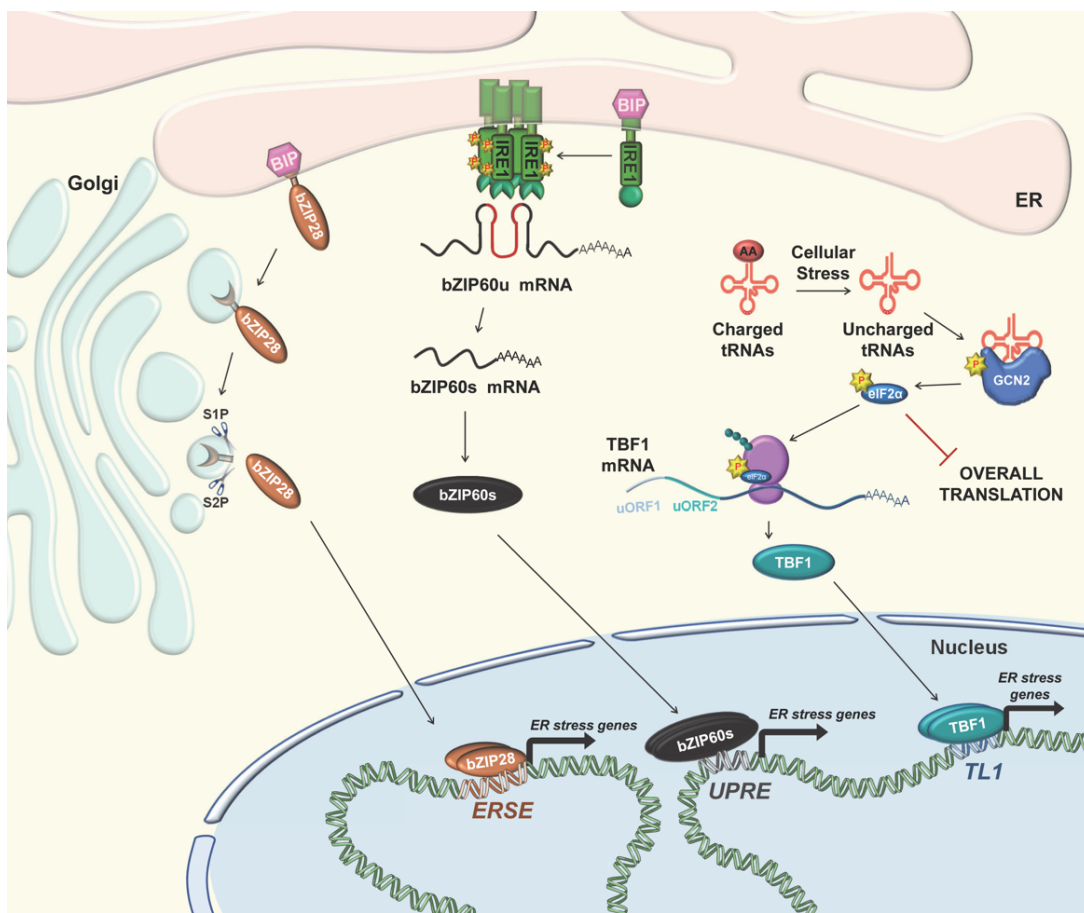


**Figure 1: Three arms of ER stress response in plants.** Accumulation of misfolded proteins leads BiP to dissociate from bZIP28, leading to its translocation to the Golgi where it is proteolytically cleaved by Site1 and Site 2 Proteases. The freed cytoplasmic domain enters the nucleus as a fully functional transcription factor and activates several ER stress genes through binding to their *ERSE* *cis*-regulatory motifs. Following ER stress, BiP also dissociates from IRE1, which enables it to oligomerize and trans-auto-phosphorylate. Thus activated, IRE1 cleaves cytoplasmic mRNA bZIP60u, which when spliced (bZIP60s) and translated enters the nucleus and activates several ER stress genes through binding to their *UPRE* *cis*-regulatory motifs. Cellular stress also causes a build-up of uncharged tRNAs, which are sensed and bound by GCN2, leading to its autophosphorylation. Thus activated, GCN2 phosphorylates eIF2 $\alpha$  to inhibit overall translation specifically de-repress translation of target mRNA TBF1 to form a transcription factor that enters the nucleus and activates several ER stress genes through binding to their *TL-1* *cis*-regulatory motifs.

Along with the well-established AtIRE1/AtbZIP60- and AtbZIP17/28-driven ER stress-mediating pathways, recently the eIF2 $\alpha$  phosphorylation was shown to be another cornerstone of cellular stress activation in plants, further emphasizing the resemblance between the mechanisms of the UPR signaling in the animal and plant kingdoms (Korner et al., 2015; Liu et al., 2019). Plant genomes (*Arabidopsis thaliana* and *Nicotiana benthamiana*) encode a single copy of a GCN2 kinase that responds to a variety of ER stress-related abiotic and biotic stimuli such as amino acid starvation, the herbicide glyphosate (Faus et al., 2015), UV and cold stress, wounding, and salicylic acid (SA) (Lageix et al., 2008), as well as pathogen infection (Monaghan and Li, 2010; Liu et al., 2015a; Li et al., 2018). Recently, AtGCN2 was shown to control abscisic acid (ABA) homeostasis and stomatal immunity, and regulate translation of a TF, TBF1, through uORF reinitiation, akin to mammalian ATF4 and yeast GCN4 (Pajerowska-Mukhtar et al., 2012; Liu et al., 2019). While plants do not possess a bona fide homolog of the main mammalian ER stress sensor PERK, and the plant GCN2 activation mechanism remains unknown, the connection of AtGCN2 signaling to the ER stress responses is strengthened by its downstream target AtTBF1, which is the master regulator of secretory pathway-related genes during pathogen infection (Pajerowska-Mukhtar et al., 2012) and binds to their promoters through the TL1 cis-regulatory motif (Wang et al., 2005).

### **Regulated IRE1-dependent splicing (RIDS)**

In plants, IRE1 splices two known mRNA orthologs: AtbZIP60 in *Arabidopsis* and OsbZIP50 in rice (Korner et al., 2015). AtbZIP60 was once thought to have been cleaved by proteolytic processing (Iwata et al., 2008); however, it does not have the

canonical S1P cleavage site and its activation does not require S1P or S2P. Consequently, it was demonstrated that it is subject to processing by IRE1 (Deng et al., 2011; Nagashima et al., 2011; Moreno et al., 2012). Splicing of AtbZIP60us mRNA (unspliced form) removes a 23 nt long intron, and tRNA ligase RLG1 catalyzes ligation of the resulting fragments (Nagashima et al., 2016), forming the bZIP60s (spliced) form. The reading frame of AtbZIP60s shifts, which eliminates a putative transmembrane domain normally present in AtbZIP60us (Deng et al., 2011) and instead encodes a nuclear localization signal (Parra-Rojas et al., 2015). AtbZIP60us and AtbZIP60s are not detectable under basal conditions when tagged with green fluorescent protein (GFP), even though the AtbZIP60us transcript was shown to be present (Parra-Rojas et al., 2015). The AtbZIP60s protein became detectable following ER stress or treatment with a proteasome inhibitor, suggesting rapid degradation of AtbZIP60us protein under basal conditions (Parra-Rojas et al., 2015), both of which are reminiscent of the regulation of XBP1 (Yoshida et al., 2001).

AtAGB1, the only G-protein β-subunit encoded by the Arabidopsis genome, was also demonstrated to act in concert with AtIRE1a and AtIRE1b to control two independent UPR pathways (Chen and Brandizzi, 2012). While *atagb1* mutants have shown a distinct sensitivity to tunicamycin, a potent inhibitor of N-linked glycosylation, this phenotype was further enhanced in *ire1a ire1b agb1* triple mutants. So far, AGB1 has only been implicated in the plant UPR, although the large numbers of often redundant G-protein complex members may hinder investigation of their involvement in the mammalian UPR (Chen and Brandizzi, 2013).

## **Regulated IRE1-dependent decay (RIDD)**

IRE1 is also known to engage in cleavage and bulk degradation of certain mRNAs in a process called regulated IRE1-dependent decay (RIDD) (Hollien and Weissman, 2006; Coelho and Domingos, 2014). In mammals, RIDD cleaves mRNAs at an XBP1-like consensus site but with an activity divergent from XBP1 mRNA splicing (Maurel et al., 2014). The exact function and nature of the degraded mRNAs is not completely understood, though it is known that RIDD is integral in the switch between pro-survival and pro-death IRE1 functions (Abdullah and Ravanan, 2018). While IRE1 splicing activity fully promotes pro-survival through activation of genes that help alleviate ER stress (Chen and Brandizzi, 2013), RIDD can tip the scales of cell fate depending on which specific mRNAs are degraded. While the cell is still in the pro-survival state, IRE1 degrades mRNAs encoding ER-resident proteins, decreasing the protein folding load in the ER. Recently, a study in Arabidopsis showed that many mRNAs encoding secretory pathway proteins that are known to be degraded upon treatment with tunicamycin are not degraded in *ire1a ire1b* double mutants. However, these targets are degraded in *bzip60* plants, indicating that this process is independent of RIDS (Mishiba et al., 2013). Defects in AtIRE1 lead to enhanced cell death as measured by ion leakage assays and inhibition of germination by tunicamycin. However, mammalian IRE1 $\alpha$  can also contribute to pro-death signaling through degradation of mRNAs of ER chaperones such as BiP, which decreases the protein folding capacity (Han et al., 2009). AtIRE1b RNase activity is also required for ER stress-induced autophagy in Arabidopsis through RIDD-mediated degradation of mRNAs that interfere with its induction (Bao et al., 2018).

## **Post-translational modifications of ER stress signaling components**

Early experimental work in mammals showed that mutation of catalytic residues in the IRE1 kinase domain disrupts RNase function, and inhibition of kinase activity leads to a loss of splicing in vivo (Shamu and Walter, 1996; Tirasophon et al., 1998). Mechanistic understanding of how phosphorylation affects the RNase activity of IRE1 in plants is of crucial importance for future agricultural interventions as it would allow tailoring IRE1 variants with altered ability to splice AtbZIP60, offering a strategy to fine-tune UPR during drought and pathogen infection. A site-specific mutation N820A in At-IRE1b leads to the abolishment of RNase activity (Deng et al., 2013), and three mutations within the kinase domain (D608N, K610N, and D628A) blocked autophosphorylation and AtbZIP60 splicing (Fig. 2A). Complementation analyses revealed that both kinase and RNase domains were required for normal vegetative growth, while a functional RNase domain was required for root elongation and shoot growth under stress conditions. Similarly, mutation K442A in AtIRE1a.1 (the only splice variant of AtIRE1a described to date) was reported to reduce its autophosphorylation activity (Noh et al., 2002). Intriguingly, in the subsequent iterations of the *Arabidopsis* genome annotation effort, it transpired that AtIRE1b occurs in three splicing variants, AtIRE1b.1, AtIRE1b.2, and AtIRE1b.3, that differ at their N-termini but are identical in their cytosol interfaces. Luminal domains of mammalian IRE1 are known to interact with numerous ER chaperones and co-chaperones, such as DNA-J and heat shock proteins, to form diverse complexes that can signal specific types and/or intensities of ER stress (Amin-Wetzel et al., 2017). Previous studies indicate that AtBiP1 and AtBiP2 may be primarily involved in biotic stress signaling, while AtBiP3 is implicated in heat stress (Wang et al., 2005; Zhang et

al., 2017). It would be intriguing to address whether sequence variation within plant IRE1 luminal domains can cause preferential interactions with specific chaperones, providing a stress-specific response, and whether it could be exploited to manipulate ER stress perception and sensitivity of crop plants. All AtIRE1 variants appear to contain the conserved residues involved in the activity of kinase and RNase domains (Fig. 2A, B),

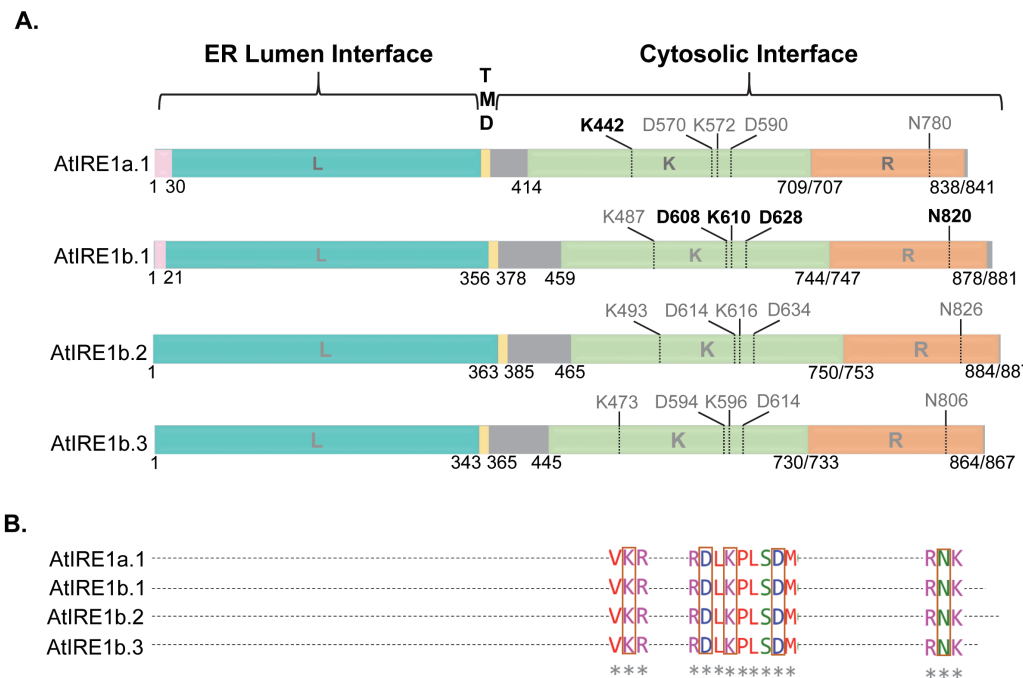


**Figure 2. Conserved domain architecture of IRE1 proteins in Arabidopsis.** (A) Amino acid sites K442 for AtIRE1a.1, and D680, K610, D628 and N820 for IRE1b.1, experimentally determined to be critical for function, are shown in black. Predicted conserved sites on other IRE1 proteins are labeled in gray. Signal peptides are marked in pink; no signal peptides were predicted in IRE1b.2 and IRE1b.3. Luminal domains (L) are shown in teal, transmembrane domains (TMD) in yellow, kinase domains (K) in green, and RNase domains (R) in orange. Gray shading corresponds to protein regions of unclassified domain nature. Numbers indicate predicted start and stop sites of individual domains as predicted by SMART database (<http://smart.embl-heidelberg.de/>), InterPro (<https://www.ebi.ac.uk/interpro/>) and SignalP-5.0 (<http://www.cbs.dtu.dk/services/SignalP/>). (B) A partial multiple sequence alignment showing a prediction of critical IRE1 amino acids (boxed and highlighted in color).

although their functionality remains to be tested. Further experimentation on these conserved residues could open up promising directions for tailoring the levels of ER signaling in crops, such as avoiding developmentally costly, spurious UPR activation.

Similar to IRE1, the GCN2 kinase is another ER stress sensor that is primarily controlled via phosphoregulation. GCN2 encodes a protein kinase with a conserved N-terminal kinase domain and a C-terminal region homologous to histidyl tRNA synthetase (HisRS) (Zhang et al., 2003). The GCN2 HisRS domain senses cellular stress by binding to uncharged tRNAs (Dong et al., 2000; Hao et al., 2005), which in turn stimulates its kinase activity, leading to di- or tetramerization, autophosphorylation on two threonine residues, and downstream phosphorylation of eIF2 $\alpha$  (Hinnebusch, 2005; Wek et al., 2006). Yeast GCN2 is thought to be kept inactive via phosphorylation at Ser577, which depends on TORC1 activity (Castilho et al., 2014). The mechanisms of GCN2 autophosphorylation or the presence of additional GCN2 kinases/ phosphatases have not yet been elucidated in plants, although it has been suggested that the TOR pathway is not involved in crosstalk with AtGCN2 (Lageix et al., 2008).

Another arm of the UPR that is activated through posttranslational regulation is ATF6 in animals and its two plant equivalents bZIP17 and bZIP28. Under unstressed conditions, ATF6 and its functional homologs reside in the ER membrane, where BiP is bound to their luminal domains. Dissociation of BiP from ATF6 unmasks Golgi localization signals, initiating the Golgi translocation (Shen et al., 2002; Srivastava et al., 2013). It is unknown whether bZIP28 translocates through this or another mechanism, since the Golgi localization signals are not found in bZIP28 (Srivastava et al., 2014) and, instead,

BiP binds to intrinsically disordered regions on bZIP28's luminal domain (Srivastava et al., 2013).

Once at the Golgi, ATF6 is cleaved first by site-1 protease (S1P), which reduces the size of the luminal domain and enables more efficient sequential cleavage at the trans-membrane domain by site-2 protease (S2P) (Shen and Prywes, 2004; Sun et al., 2015). It was assumed that the process was very similar to bZIP28, and Sun et al. even demonstrated that the S1P RRIL573 cleavage site is necessary for full activation of bZIP28 (Sun et al., 2015). However, Iwata et al. showed through genetic knockouts that S2P proteases, but not S1P proteases, were necessary for the activation of bZIP28 and claimed that the results of Sun et al. could have stemmed from a change in secondary structure or protein interactions affecting the ability of bZIP28 to sense ER stress or to translocate to the Golgi, but not necessarily because bZIP28 was cleaved at the RRIL573 site (Iwata et al., 2017). Regardless of the exact method of proteolytic cleavage, the liberated cytosolic domains of bZIP28 and ATF6 are able to translocate to the nucleus and bind to ER stress element (ERSE) cis-regulatory motifs to regulate ER stress genes (Yamamoto et al., 2004; Liu and Howell, 2010).

### **Roles of ER stress signaling in plant development and stress**

The vast majority of work dedicated to plant stress responses has focused on understanding the response mechanisms of plants against individual types of stresses. However, in their natural environment, plants are simultaneously exposed to multiple types of stress, including both abiotic and biotic factors. The ER deciphers and processes diverse inputs from inside and outside the cell, ensuring an optimal, integrated output response.

Among the abiotic stress factors, high temperature is one of the leading causes of ER stress and the UPR (Fig. 3). Several studies reported heat-induced bZIP60 splicing by IRE1 in Arabidopsis (Deng et al., 2011, 2016), maize (Li et al., 2012), and rice

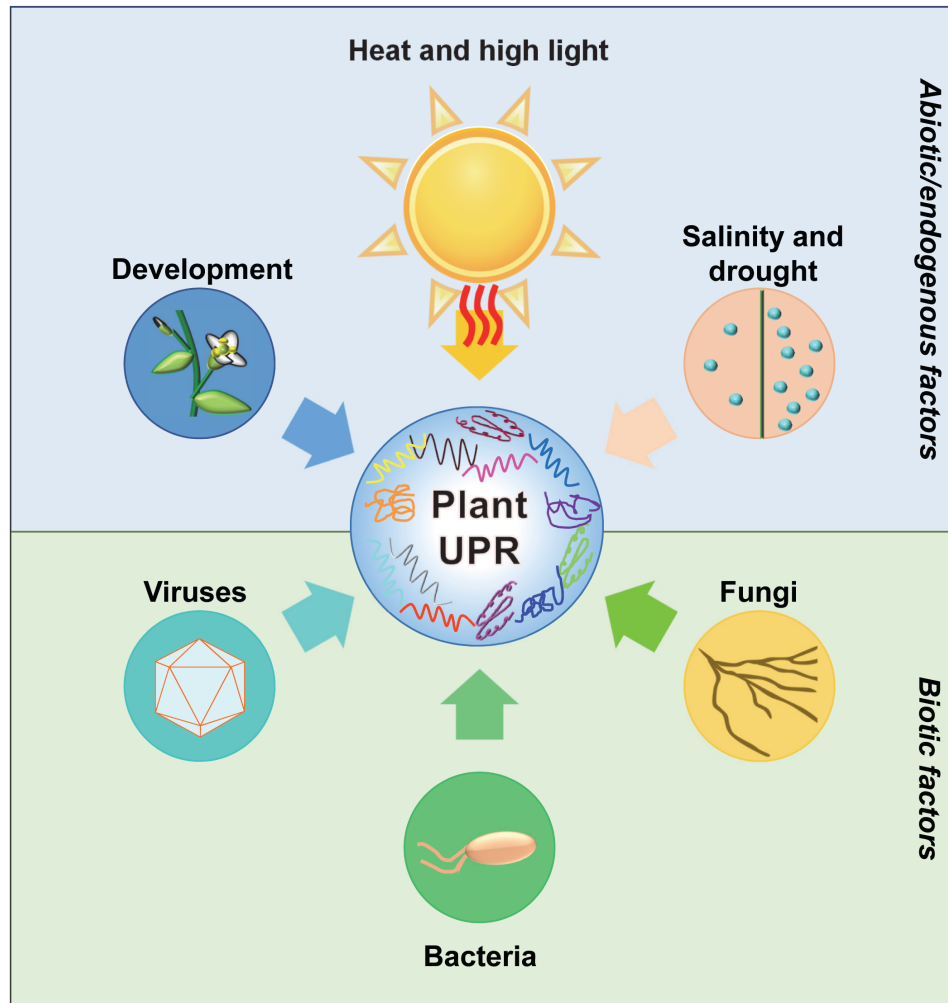


**Figure 3. Stress-mediated activation of UPR.** Abiotic and biotic stresses as well as developmental processes trigger the unfolded protein response (UPR) in *Arabidopsis*. Abiotic stresses, such as heat, high light intensity, salinity and drought, and biotic (infection with bacterial, fungal or viral phytopathogens), as well as normal developmental processes can lead to excessive accumulation of unfolded proteins in the ER or cause imbalances in amino acid supply, collectively leading to the activation of one or more arms of the UPR.

(OsbZIP50). Overexpression of BhbZIP60, an AtbZIP60 homolog from a resurrection plant *Boea hygrometrica*, resulted in heightened tolerance to drought and mannitol

stresses (Wang et al., 2017). Overexpression of bZIP60 yielded increased salt tolerance in Arabidopsis (Fujita et al., 2007). In the laboratory, bZIP60 splicing can be induced chemically by DTT or tunicamycin (Nagashima et al., 2011; Li et al., 2012; Moreno et al., 2012).

The AtIRE1/AtbZIP60 pathway was also reported to influence plant responses to pathogen infection (Fig. 3). *atire1a atire1b* and *atbzip60* loss-of-function plants are more susceptible to *Pseudomonas syringae* pv. *maculicola* strain ES4326 (Moreno et al., 2012). Several studies demonstrated that the AtIRE1/AtbZIP60 pathway is involved in anti-viral defenses, such as against *Turnip mosaic virus* (TuMV) in Arabidopsis (Zhang et al., 2015), *Rice black streak dwarf virus* (RBSDV) and *Garlic virus X* (GarVX) in *N. benthamiana* (Sun et al., 2013; Lu et al., 2016), as well as potexvirus, potyvirus, TuMV, and *Plantago asiatica mosaic virus* (PIAMV) in Arabidopsis, *N. benthamiana*, and potato (Gaguancela et al., 2016). Very recently, the IRE1/bZIP60 pathway was also shown to be required for *N. attenuata* resistance to a fungal pathogen *Alternaria alternata* (Xu et al., 2019). AtIRE1 and AtbZIP60 also play important roles in vegetative and reproductive developmental processes, notably root growth and pollen development (Chen and Brandizzi, 2012; Deng et al., 2013, 2016).

The AtGCN2 pathway is stimulated by a variety of ER stress-related stimuli such as amino acid starvation, the herbicide glyphosate, UV and cold stress, wounding, and SA (Lageix et al., 2008), infection with pathogens *Bemisia tabaci* (Li et al., 2018), *Hyaloperonospora arabidopsis*, *Golovinomyces cichoracearum*, *Pectobacterium carotovorum* subsp. *carotovorum* (Liu et al., 2015a), and various strains of *Pseudomonas*

*syringae* (Monaghan and Li, 2010; Liu et al., 2019), as well as developmental processes such as seed germination (Liu et al., 2015b) (Fig. 3).

**Box 1. Key developments in understanding the function of ER stress signaling in plant development and stress responses**

- In a recent study Liu *et al.* (2019) showed that bacterial infection activates *Arabidopsis General Control Non-derepressible 2* (GCN2) kinase pathway, leading to AtGCN2-mediated phosphorylation of eIF2 $\alpha$  and uORF-mediated translational de-repression of the transcription factor TBF1, which regulates ER stress responses and immunity (Liu et al., 2019). This study provides the first line of evidence that plants contain the eIF2 $\alpha$ -mediated signaling arm of UPR. AtGCN2 also plays a role in abscisic acid homeostasis and stomatal immunity by regulating stomatal closure and reopening in response to pathogenic bacteria or their toxin coronatine, respectively.
- Bao *et al.* recently (2019) showed that UPR is required for normal growth and development of plants. In their study, triple mutant *ire1a ire1b bzip17* showed impaired growth under normal growth condition, and also was defective in stress signaling pathways. They found that mobilization of bZIP17 into nucleus is required for normal growth and development (Bao et al., 2019).
- Lai *et al.* (2018) showed that NPR1 (Non-Expressor of PR1 genes 1; a master transcriptional immune co-regulator and one of salicylic acid receptors) negatively regulates the transcriptional regulation of bZIP60 and bZIP28. They also demonstrated that NPR1 can translocate to the nucleus and

physically interact with bZIP60 and bZIP28, helping alleviate ER stress (Lai, Renna, et al., 2018).

- Through micro-grafting experiments, Lai *et al.* (2018) demonstrated that Arabidopsis UPR signaling has both local (cell-autonomous) and systemic (non-cell-autonomous) components. Spliced bZIP60 can translocate from roots into shoots and participate in systemic propagation of UPR signaling (Lai, Stefano, et al., 2018).
- Bao *et al.* (2018) established that the functional endonuclease domain of IRE1b and RNase activity, but not its kinase domain and bZIP60 splicing, are required for activation of autophagy. They also showed that, upon ER stress, the RNase activity directs a promiscuous splicing and degradation of mRNAs encoding secreted proteins in a process termed RIDD (regulated IRE1-dependent decay). They identified and tested 12 gene targets of RIDD and concluded that three of them (BGLU21, ML and PR-14) are involved in downregulating autophagy by overexpression (Bao et al., 2018).
- Kim *et al.* (2018) studied the roles of bZIP17 in Arabidopsis development using genetic and genomic approaches. Unlike bZIP28 and bZIP60, bZIP17 is not a major UPR activator, but it functions in concert with bZIP28 to control genes required for development, especially root elongation, and stress maintenance (Kim et al., 2018).

Unlike the other two branches of the UPR, which in general have been associated with a variety of biotic and abiotic stresses (Qiang et al., 2012; Verchot, 2016; Fan et al.,

2018), the AtbZIP17/AtbZIP28 pathway has mainly been implicated in heat stress. Heat induces an increase in AtbZIP28 transcripts as well as stimulating its proteolytic cleavage and nuclear translocation (Gao et al., 2008). In addition, the *atbzip28* mutant displays a marked sensitivity to heat stress (Gao et al., 2008). AtbZIP17 was reported to be activated in response to salt and osmotic stress (Liu et al., 2007b) (Fig. 3).

While not directly implicated in any specific biotic stress, AtbZIP28 has been shown to be linked to PAMP (pathogen associated molecular pattern)-triggered immunity. Bacterial elicitor flg22 induces an accumulation of ER chaperone transcripts by down-regulating WRKY7, WRKY11, and WRKY17 TFs that repress the expression of AtbZIP28, which then up-regulates those ER chaperone genes (Arrano-Salinas et al., 2018).

### Concluding remarks

The field of plant UPR has enjoyed a rapid expansion during the past decade. Multiple signaling aspects have been elucidated, novel players have been discovered, and additional plant species have joined *Arabidopsis* as models to study ER stress, as highlighted in Box 1. These findings highlight the need to further explore the multifaceted interactions of ER signaling. The next challenge will be to identify connections and cross-talk between the pathways to understand how the plant cells integrate the abundance of qualitative and quantitative, biotic and abiotic stimuli to respond with an appropriate pro-survival or pro-death program. The ultimate goal is to extrapolate this knowledge for translational studies to develop and deploy crops with superb ER stress tolerance and yield performance in the field.

### **References:**

- Abdullah A, Ravanah P.** 2018. The unknown face of IRE1alpha - Beyond ER stress. *Eur J Cell Biol* **97**, 359-368.
- Amin-Wetzel N, Saunders RA, Kamphuis MJ, Rato C, Preissler S, Harding HP, Ron D.** 2017. A J-Protein Co-chaperone Recruits BiP to Monomerize IRE1 and Repress the Unfolded Protein Response. *Cell* **171**, 1625-1637 e1613.
- Arrano-Salinas P, Dominguez-Figueroa J, Herrera-Vasquez A, Zavala D, Medina J, Vicente-Carbajosa J, Meneses C, Canessa P, Moreno AA, Blanco-Herrera F.** 2018. WRKY7, -11 and -17 transcription factors are modulators of the bZIP28 branch of the unfolded protein response during PAMP-triggered immunity in *Arabidopsis thaliana*. *Plant Sci* **277**, 242-250.
- Back SH, Schroder M, Lee K, Zhang K, Kaufman RJ.** 2005. ER stress signaling by regulated splicing: IRE1/HAC1/XBP1. *Methods* **35**, 395-416.
- Baird TD, Wek RC.** 2012. Eukaryotic initiation factor 2 phosphorylation and translational control in metabolism. *Adv Nutr* **3**, 307-321.
- Bao Y, Bassham DC, Howell SH.** 2019. A Functional Unfolded Protein Response Is Required for Normal Vegetative Development. *Plant Physiol* **179**, 1834-1843.
- Bao Y, Howell SH.** 2017. The Unfolded Protein Response Supports Plant Development and Defense as well as Responses to Abiotic Stress. *Front Plant Sci* **8**, 344.
- Bao Y, Pu Y, Yu X, Gregory BD, Srivastava R, Howell SH, Bassham DC.** 2018. IRE1B degrades RNAs encoding proteins that interfere with the induction of autophagy by ER stress in *Arabidopsis thaliana*. *Autophagy* **14**, 1562-1573.

- Bartoszewski R, Brewer JW, Rab A, Crossman DK, Bartoszewska S, Kapoor N, Fuller C, Collawn JF, Bebok Z.** 2011. The unfolded protein response (UPR)-activated transcription factor X-box-binding protein 1 (XBP1) induces microRNA-346 expression that targets the human antigen peptide transporter 1 (TAP1) mRNA and governs immune regulatory genes. *J Biol Chem* **286**, 41862-41870.
- Behrman S, Acosta-Alvear D, Walter P.** 2011. A CHOP-regulated microRNA controls rhodopsin expression. *J Cell Biol* **192**, 919-927.
- Bunpo P, Cundiff JK, Reinert RB, Wek RC, Aldrich CJ, Anthony TG.** 2010. The eIF2 kinase GCN2 is essential for the murine immune system to adapt to amino acid deprivation by asparaginase. *J Nutr* **140**, 2020-2027.
- Byrd AE, Aragon IV, Brewer JW.** 2012. MicroRNA-30c-2\* limits expression of proadaptive factor XBP1 in the unfolded protein response. *J Cell Biol* **196**, 689-698.
- Castilho BA, Shanmugam R, Silva RC, Ramesh R, Himme BM, Sattlegger E.** 2014. Keeping the eIF2 alpha kinase Gcn2 in check. *Biochim Biophys Acta* **1843**, 1948-1968.
- Che P, Bussell JD, Zhou W, Estavillo GM, Pogson BJ, Smith SM.** 2010. Signaling from the endoplasmic reticulum activates brassinosteroid signaling and promotes acclimation to stress in *Arabidopsis*. *Sci Signal* **3**, ra69.
- Chen Y, Brandizzi F.** 2012. AtIRE1A/AtIRE1B and AGB1 independently control two essential unfolded protein response pathways in *Arabidopsis*. *Plant J* **69**, 266-277.
- Chen Y, Brandizzi F.** 2013. IRE1: ER stress sensor and cell fate executor. *Trends Cell Biol* **23**, 547-555.

**Chevret E, Cameron PH, Pelletier MF, Thomas DY, Bergeron JJ.** 2001. The endoplasmic reticulum: integration of protein folding, quality control, signaling and degradation. *Curr Opin Struct Biol* **11**, 120-124.

**Chitnis NS, Pytel D, Bobrovnikova-Marjon E, Pant D, Zheng H, Maas NL, Frederick B, Kushner JA, Chodosh LA, Koumenis C, Fuchs SY, Diehl JA.** 2012. miR-211 is a prosurvival microRNA that regulates chop expression in a PERK-dependent manner. *Mol Cell* **48**, 353-364.

**Coelho DS, Domingos PM.** 2014. Physiological roles of regulated Ire1 dependent decay. *Front Genet* **5**, 76.

**Costa-Mattioli M, Gobert D, Harding H, Herdy B, Azzi M, Bruno M, Bidinosti M, Ben Mamou C, Marcinkiewicz E, Yoshida M, Imataka H, Cuello AC, Seidah N, Sosin W, Lacaille JC, Ron D, Nader K, Sonenberg N.** 2005. Translational control of hippocampal synaptic plasticity and memory by the eIF2alpha kinase GCN2. *Nature* **436**, 1166-1173.

**Deng Y, Humbert S, Liu JX, Srivastava R, Rothstein SJ, Howell SH.** 2011. Heat induces the splicing by IRE1 of a mRNA encoding a transcription factor involved in the unfolded protein response in Arabidopsis. *Proc Natl Acad Sci U S A* **108**, 7247-7252.

**Deng Y, Srivastava R, Howell SH.** 2013. Protein kinase and ribonuclease domains of IRE1 confer stress tolerance, vegetative growth, and reproductive development in Arabidopsis. *Proc Natl Acad Sci U S A* **110**, 19633-19638.

**Deng Y, Srivastava R, Quilichini TD, Dong H, Bao Y, Horner HT, Howell SH.** 2016. IRE1, a component of the unfolded protein response signaling pathway, protects pollen development in Arabidopsis from heat stress. *Plant J* **88**, 193-204.

**Dey S, Sayers CM, Verginadis, II, Lehman SL, Cheng Y, Cerniglia GJ, Tuttle SW, Feldman MD, Zhang PJ, Fuchs SY, Diehl JA, Koumenis C.** 2015. ATF4-dependent induction of heme oxygenase 1 prevents anoikis and promotes metastasis. *J Clin Invest* **125**, 2592-2608.

**Dong J, Qiu H, Garcia-Barrio M, Anderson J, Hinnebusch AG.** 2000. Uncharged tRNA activates GCN2 by displacing the protein kinase moiety from a bipartite tRNA-binding domain. *Molecular cell* **6**, 269-279.

**Fan G, Yang Y, Li T, Lu W, Du Y, Qiang X, Wen Q, Shan W.** 2018. A Phytophthora capsici RXLR Effector Targets and Inhibits a Plant PPIase to Suppress Endoplasmic Reticulum-Mediated Immunity. *Mol Plant* **11**, 1067-1083.

**Faus I, Zabalza A, Santiago J, Nebauer SG, Royuela M, Serrano R, Gadea J.** 2015. Protein kinase GCN2 mediates responses to glyphosate in *Arabidopsis*. *BMC Plant Biol* **15**, 14.

**Fujita M, Mizukado S, Fujita Y, Ichikawa T, Nakazawa M, Seki M, Matsui M, Yamaguchi-Shinozaki K, Shinozaki K.** 2007. Identification of stress-tolerance-related transcription-factor genes via mini-scale Full-length cDNA Over-eXpressor (FOX) gene hunting system. *Biochem Biophys Res Commun* **364**, 250-257.

**Gaguancela OA, Zuniga LP, Arias AV, Halterman D, Flores FJ, Johansen IE, Wang A, Yamaji Y, Verchot J.** 2016. The IRE1/bZIP60 Pathway and Bax Inhibitor 1 Suppress Systemic Accumulation of Potyviruses and Potexviruses in *Arabidopsis* and *Nicotiana benthamiana* Plants. *Mol Plant Microbe Interact* **29**, 750-766.

- Gao H, Brandizzi F, Benning C, Larkin RM.** 2008. A membrane-tethered transcription factor defines a branch of the heat stress response in *Arabidopsis thaliana*. *Proc Natl Acad Sci U S A* **105**, 16398-16403.
- Gardner BM, Walter P.** 2011. Unfolded proteins are Ire1-activating ligands that directly induce the unfolded protein response. *Science* **333**, 1891-1894.
- Gupta S, Read DE, Deepti A, Cawley K, Gupta A, Oommen D, Verfaillie T, Matus S, Smith MA, Mott JL, Agostinis P, Hetz C, Samali A.** 2012. Perk-dependent repression of miR-106b-25 cluster is required for ER stress-induced apoptosis. *Cell Death Dis* **3**, e333.
- Han D, Lerner AG, Vande Walle L, Upton JP, Xu W, Hagen A, Backes BJ, Oakes SA, Papa FR.** 2009. IRE1alpha kinase activation modes control alternate endoribonuclease outputs to determine divergent cell fates. *Cell* **138**, 562-575.
- Hao S, Sharp JW, Ross-Inta CM, McDaniel BJ, Anthony TG, Wek RC, Cavener DR, McGrath BC, Rudell JB, Koehnle TJ.** 2005. Uncharged tRNA and sensing of amino acid deficiency in mammalian piriform cortex. *Science* **307**, 1776-1778.
- Hetz C, Chevet E, Oakes SA.** 2015. Proteostasis control by the unfolded protein response. *Nat Cell Biol* **17**, 829-838.
- Hillary RF, FitzGerald U.** 2018. A lifetime of stress: ATF6 in development and homeostasis. *J Biomed Sci* **25**, 48.
- Hinnebusch AG.** 2005. Translational regulation of GCN4 and the general amino acid control of yeast. *Annu Rev Microbiol* **59**, 407-450.

- Hofmann S, Cherkasova V, Bankhead P, Bukau B, Stoecklin G.** 2012. Translation suppression promotes stress granule formation and cell survival in response to cold shock. *Mol Biol Cell* **23**, 3786-3800.
- Hollien J, Weissman JS.** 2006. Decay of endoplasmic reticulum-localized mRNAs during the unfolded protein response. *Science* **313**, 104-107.
- Hong M, Luo S, Baumeister P, Huang JM, Gogia RK, Li M, Lee AS.** 2004. Under-glycosylation of ATF6 as a novel sensing mechanism for activation of the unfolded protein response. *J Biol Chem* **279**, 11354-11363.
- Howell SH.** 2013. Endoplasmic reticulum stress responses in plants. *Annu Rev Plant Biol* **64**, 477-499.
- Iwata Y, Ashida M, Hasegawa C, Tabara K, Mishiba KI, Koizumi N.** 2017. Activation of the Arabidopsis membrane-bound transcription factor bZIP28 is mediated by site-2 protease, but not site-1 protease. *Plant J* **91**, 408-415.
- Iwata Y, Fedoroff NV, Koizumi N.** 2008. Arabidopsis bZIP60 Is a Proteolysis-Activated Transcription Factor Involved in the Endoplasmic Reticulum Stress Response. *The Plant Cell* **20**, 3107-3121.
- Kim JS, Yamaguchi-Shinozaki K, Shinozaki K.** 2018. ER-Anchored Transcription Factors bZIP17 and bZIP28 Regulate Root Elongation. *Plant Physiol* **176**, 2221-2230.
- Koerner CJ, Du X, Vollmer ME, Pajerowska-Mukhtar KM.** 2015. Endoplasmic Reticulum Stress Signaling in Plant Immunity--At the Crossroad of Life and Death. *Int J Mol Sci* **16**, 26582-26598.

- Koizumi N, Martinez IM, Kimata Y, Kohno K, Sano H, Chrispeels MJ.** 2001. Molecular characterization of two *Arabidopsis* Ire1 homologs, endoplasmic reticulum-located transmembrane protein kinases. *Plant Physiol* **127**, 949-962.
- Kozutsumi Y, Segal M, Normington K, Gething MJ, Sambrook J.** 1988. The presence of malfolded proteins in the endoplasmic reticulum signals the induction of glucose-regulated proteins. *Nature* **332**, 462-464.
- Lageix S, Lanet E, Pouch-Pelissier MN, Espagnol MC, Robaglia C, Deragon JM, Pelissier T.** 2008. *Arabidopsis* eIF2alpha kinase GCN2 is essential for growth in stress conditions and is activated by wounding. *BMC Plant Biol* **8**, 134.
- Lai YS, Renna L, Yarema J, Ruberti C, He SY, Brandizzi F.** 2018a. Salicylic acid-independent role of NPR1 is required for protection from proteotoxic stress in the plant endoplasmic reticulum. *Proc Natl Acad Sci U S A* **115**, E5203-E5212.
- Lai YS, Stefano G, Zemelis-Durfee S, Ruberti C, Gibbons L, Brandizzi F.** 2018b. Systemic signaling contributes to the unfolded protein response of the plant endoplasmic reticulum. *Nat Commun* **9**, 3918.
- Lee RC, Feinbaum RL, Ambros V.** 1993. The *C. elegans* heterochronic gene lin-4 encodes small RNAs with antisense complementarity to lin-14. *Cell* **75**, 843-854.
- Lerner AG, Upton JP, Praveen PV, Ghosh R, Nakagawa Y, Igbaria A, Shen S, Nguyen V, Backes BJ, Heiman M, Heintz N, Greengard P, Hui S, Tang Q, Trusina A, Oakes SA, Papa FR.** 2012. IRE1alpha induces thioredoxin-interacting protein to activate the NLRP3 inflammasome and promote programmed cell death under irremediable ER stress. *Cell Metab* **16**, 250-264.

- Li N, Zhang SJ, Zhao Q, Long Y, Guo H, Jia HF, Yang YX, Zhang HY, Ye XF, Zhang ST.** 2018. Overexpression of Tobacco GCN2 Stimulates Multiple Physiological Changes Associated With Stress Tolerance. *Front Plant Sci* **9**, 725.
- Li Y, Humbert S, Howell SH.** 2012. ZmbZIP60 mRNA is spliced in maize in response to ER stress. *BMC Res Notes* **5**, 144.
- Liu C, Cheng H, Shi S, Cui X, Yang J, Chen L, Cen P, Cai X, Lu Y, Wu C, Yao W, Qin Y, Liu L, Long J, Xu J, Li M, Yu X.** 2013. MicroRNA-34b inhibits pancreatic cancer metastasis through repressing Smad3. *Curr Mol Med* **13**, 467-478.
- Liu JX, Howell SH.** 2010. bZIP28 and NF-Y transcription factors are activated by ER stress and assemble into a transcriptional complex to regulate stress response genes in Arabidopsis. *Plant Cell* **22**, 782-796.
- Liu JX, Srivastava R, Che P, Howell SH.** 2007a. An endoplasmic reticulum stress response in Arabidopsis is mediated by proteolytic processing and nuclear relocation of a membrane-associated transcription factor, bZIP28. *Plant Cell* **19**, 4111-4119.
- Liu JX, Srivastava R, Che P, Howell SH.** 2007b. Salt stress responses in Arabidopsis utilize a signal transduction pathway related to endoplasmic reticulum stress signaling. *Plant J* **51**, 897-909.
- Liu X, Afrin T, Pajerowska-Mukhtar KM.** 2019. Arabidopsis GCN2 kinase contributes to ABA homeostasis and stomatal immunity. *Commun Biol* **2**, 302.
- Liu X, Körner CJ, Hajdu D, Guo T, Ramonell KM, Argueso CT, Pajerowska-Mukhtar KM.** 2015a. Arabidopsis thaliana atGCN2 kinase is involved in disease resistance against pathogens with diverse life styles. *International Journal of Phytopathology* **4**, 93-104.

**Liu X, Merchant A, Rockett KS, McCormack M, Pajerowska-Mukhtar KM.** 2015b.

Characterization of *Arabidopsis thaliana* GCN2 kinase roles in seed germination and plant development. *Plant Signal Behav* **10**, e992264.

**Lu Y, Yin M, Wang X, Chen B, Yang X, Peng J, Zheng H, Zhao J, Lin L, Yu C, MacFarlane S, He J, Liu Y, Chen J, Dai L, Yan F.** 2016. The unfolded protein response and programmed cell death are induced by expression of Garlic virus X p11 in *Nicotiana benthamiana*. *J Gen Virol* **97**, 1462-1468.

**Luhr M, Torgersen ML, Szalai P, Hashim A, Brech A, Staerk J, Engedal N.** 2019. The kinase PERK and the transcription factor ATF4 play distinct and essential roles in autophagy resulting from tunicamycin-induced ER stress. *J Biol Chem* **294**, 8197-8217.

**Maurel M, Chevet E.** 2013. Endoplasmic reticulum stress signaling: the microRNA connection. *Am J Physiol Cell Physiol* **304**, C1117-1126.

**Maurel M, Chevet E, Tavernier J, Gerlo S.** 2014. Getting RIDD of RNA: IRE1 in cell fate regulation. *Trends Biochem Sci* **39**, 245-254.

**McMahon M, Samali A, Chevet E.** 2017. Regulation of the unfolded protein response by noncoding RNA. *Am J Physiol Cell Physiol* **313**, C243-C254.

**Mishiba K, Iwata Y, Mochizuki T, Matsumura A, Nishioka N, Hirata R, Koizumi N.** 2019. Unfolded protein-independent IRE1 activation contributes to multifaceted developmental processes in *Arabidopsis*. *bioRxiv*.

**Mishiba K, Nagashima Y, Suzuki E, Hayashi N, Ogata Y, Shimada Y, Koizumi N.** 2013. Defects in IRE1 enhance cell death and fail to degrade mRNAs encoding secretory pathway proteins in the *Arabidopsis* unfolded protein response. *Proc Natl Acad Sci U S A* **110**, 5713-5718.

- Misson J, Raghothama KG, Jain A, Jouhet J, Block MA, Bligny R, Ortet P, Creff A, Somerville S, Rolland N, Doumas P, Nacry P, Herrera-Estrella L, Nussaume L, Thibaudeau MC.** 2005. A genome-wide transcriptional analysis using *Arabidopsis thaliana* Affymetrix gene chips determined plant responses to phosphate deprivation. *Proc Natl Acad Sci U S A* **102**, 11934-11939.
- Monaghan J, Li X.** 2010. The HEAT repeat protein ILITYHIA is required for plant immunity. *Plant Cell Physiol* **51**, 742-753.
- Moreno AA, Mukhtar MS, Blanco F, Boatwright JL, Moreno I, Jordan MR, Chen Y, Brandizzi F, Dong X, Orellana A, Pajerowska-Mukhtar KM.** 2012. IRE1/bZIP60-mediated unfolded protein response plays distinct roles in plant immunity and abiotic stress responses. *PLoS One* **7**, e31944.
- Munn DH, Sharma MD, Baban B, Harding HP, Zhang Y, Ron D, Mellor AL.** 2005. GCN2 kinase in T cells mediates proliferative arrest and anergy induction in response to indoleamine 2,3-dioxygenase. *Immunity* **22**, 633-642.
- Nadanaka S, Okada T, Yoshida H, Mori K.** 2007. Role of disulfide bridges formed in the luminal domain of ATF6 in sensing endoplasmic reticulum stress. *Mol Cell Biol* **27**, 1027-1043.
- Nagashima Y, Iwata Y, Mishiba K, Koizumi N.** 2016. Arabidopsis tRNA ligase completes the cytoplasmic splicing of bZIP60 mRNA in the unfolded protein response. *Biochem Biophys Res Commun* **470**, 941-946.
- Nagashima Y, Mishiba K, Suzuki E, Shimada Y, Iwata Y, Koizumi N.** 2011. Arabidopsis IRE1 catalyses unconventional splicing of bZIP60 mRNA to produce the active transcription factor. *Sci Rep* **1**, 29.

- Nelson DE, Repetti PP, Adams TR, Creelman RA, Wu J, Warner DC, Anstrom DC, Bensen RJ, Castiglioni PP, Donnarummo MG, Hinche BS, Kumimoto RW, Maszle DR, Canales RD, Krolkowski KA, Dotson SB, Gutterson N, Ratcliffe OJ, Heard JE.** 2007. Plant nuclear factor Y (NF-Y) B subunits confer drought tolerance and lead to improved corn yields on water-limited acres. *Proc Natl Acad Sci U S A* **104**, 16450-16455.
- Noh SJ, Kwon CS, Chung WI.** 2002. Characterization of two homologs of Ire1p, a kinase/endoribonuclease in yeast, in *Arabidopsis thaliana*. *Biochim Biophys Acta* **1575**, 130-134.
- Oikawa D, Tokuda M, Hosoda A, Iwawaki T.** 2010. Identification of a consensus element recognized and cleaved by IRE1 alpha. *Nucleic Acids Res* **38**, 6265-6273.
- Oyadomari S, Harding HP, Zhang Y, Oyadomari M, Ron D.** 2008. Dephosphorylation of translation initiation factor 2alpha enhances glucose tolerance and attenuates hepatosteatosis in mice. *Cell Metab* **7**, 520-532.
- Pajerowska-Mukhtar KM, Wang W, Tada Y, Oka N, Tucker CL, Fonseca JP, Dong X.** 2012. The HSF-like transcription factor TBF1 is a major molecular switch for plant growth-to-defense transition. *Curr Biol* **22**, 103-112.
- Park CJ, Park JM.** 2019. Endoplasmic Reticulum Plays a Critical Role in Integrating Signals Generated by Both Biotic and Abiotic Stress in Plants. *Front Plant Sci* **10**, 399.
- Parra-Rojas J, Moreno AA, Mitina I, Orellana A.** 2015. The dynamic of the splicing of bZIP60 and the proteins encoded by the spliced and unspliced mRNAs reveals some unique features during the activation of UPR in *Arabidopsis thaliana*. *PLoS One* **10**, e0122936.

**Promlek T, Ishiwata-Kimata Y, Shido M, Sakuramoto M, Kohno K, Kimata Y.**

2011. Membrane aberrancy and unfolded proteins activate the endoplasmic reticulum stress sensor Ire1 in different ways. *Mol Biol Cell* **22**, 3520-3532.

**Qiang X, Zechmann B, Reitz MU, Kogel KH, Schafer P.** 2012. The mutualistic fungus Piriformospora indica colonizes Arabidopsis roots by inducing an endoplasmic reticulum stress-triggered caspase-dependent cell death. *Plant Cell* **24**, 794-809.

**Ron D, Walter P.** 2007. Signal integration in the endoplasmic reticulum unfolded protein response. *Nat Rev Mol Cell Biol* **8**, 519-529.

**Rozpedek W, Pytel D, Mucha B, Leszczynska H, Diehl JA, Majsterek I.** 2016. The Role of the PERK/eIF2alpha/ATF4/CHOP Signaling Pathway in Tumor Progression During Endoplasmic Reticulum Stress. *Curr Mol Med* **16**, 533-544.

**Rutkowski DT, Kaufman RJ.** 2003. All roads lead to ATF4. *Dev Cell* **4**, 442-444.

**Shamu CE, Walter P.** 1996. Oligomerization and phosphorylation of the Ire1p kinase during intracellular signaling from the endoplasmic reticulum to the nucleus. *EMBO J* **15**, 3028-3039.

**Shen J, Chen X, Hendershot L, Prywes R.** 2002. ER stress regulation of ATF6 localization by dissociation of BiP/GRP78 binding and unmasking of Golgi localization signals. *Dev Cell* **3**, 99-111.

**Shen J, Prywes R.** 2004. Dependence of site-2 protease cleavage of ATF6 on prior site-1 protease digestion is determined by the size of the luminal domain of ATF6. *J Biol Chem* **279**, 43046-43051.

**Sidrauski C, Acosta-Alvear D, Khoutorsky A, Vedantham P, Hearn BR, Li H, Gamache K, Gallagher CM, Ang KK, Wilson C, Okreglak V, Ashkenazi A, Hann B,**

- Nader K, Arkin MR, Renslo AR, Sonnenberg N, Walter P.** 2013. Pharmacological brake-release of mRNA translation enhances cognitive memory. *Elife* **2**, e00498.
- Silva PA, Silva JC, Caetano HD, Machado JP, Mendes GC, Reis PA, Brustolini OJ, Dal-Bianco M, Fontes EP.** 2015. Comprehensive analysis of the endoplasmic reticulum stress response in the soybean genome: conserved and plant-specific features. *BMC Genomics* **16**, 783.
- Srivastava R, Deng Y, Howell SH.** 2014. Stress sensing in plants by an ER stress sensor/transducer, bZIP28. *Front Plant Sci* **5**, 59.
- Srivastava R, Deng Y, Shah S, Rao AG, Howell SH.** 2013. BINDING PROTEIN is a master regulator of the endoplasmic reticulum stress sensor/transducer bZIP28 in Arabidopsis. *Plant Cell* **25**, 1416-1429.
- Sun L, Zhang SS, Lu SJ, Liu JX.** 2015. Site-1 protease cleavage site is important for the ER stress-induced activation of membrane-associated transcription factor bZIP28 in Arabidopsis. *Sci China Life Sci* **58**, 270-275.
- Sun Z, Yang D, Xie L, Sun L, Zhang S, Zhu Q, Li J, Wang X, Chen J.** 2013. Rice black-streaked dwarf virus P10 induces membranous structures at the ER and elicits the unfolded protein response in Nicotiana benthamiana. *Virology* **447**, 131-139.
- Sunkar R, Kapoor A, Zhu JK.** 2006. Posttranscriptional induction of two Cu/Zn superoxide dismutase genes in Arabidopsis is mediated by downregulation of miR398 and important for oxidative stress tolerance. *Plant Cell* **18**, 2051-2065.
- Tirasophon W, Welihinda AA, Kaufman RJ.** 1998. A stress response pathway from the endoplasmic reticulum to the nucleus requires a novel bifunctional protein kinase/endoribonuclease (Ire1p) in mammalian cells. *Genes Dev* **12**, 1812-1824.

**Verchot J.** 2016. How does the stressed out ER find relief during virus infection? *Curr Opin Virol* **17**, 74-79.

**Volmer R, van der Ploeg K, Ron D.** 2013. Membrane lipid saturation activates endoplasmic reticulum unfolded protein response transducers through their transmembrane domains. *Proc Natl Acad Sci U S A* **110**, 4628-4633.

**Wakasa Y, Hayashi S, Ozawa K, Takaiwa F.** 2012. Multiple roles of the ER stress sensor IRE1 demonstrated by gene targeting in rice. *Sci Rep* **2**, 944.

**Walley J, Xiao Y, Wang JZ, Baidoo EE, Keasling JD, Shen Z, Briggs SP, Dehesh K.** 2015. Plastid-produced interorgannellar stress signal MEcPP potentiates induction of the unfolded protein response in endoplasmic reticulum. *Proc Natl Acad Sci U S A* **112**, 6212-6217.

**Walter P, Ron D.** 2011. The unfolded protein response: from stress pathway to homeostatic regulation. *Science* **334**, 1081-1086.

**Wang B, Du H, Zhang Z, Xu W, Deng X.** 2017. BhbZIP60 from Resurrection Plant *Boea hygrometrica* Is an mRNA Splicing-Activated Endoplasmic Reticulum Stress Regulator Involved in Drought Tolerance. *Front Plant Sci* **8**, 245.

**Wang D, Weaver ND, Kesarwani M, Dong X.** 2005. Induction of protein secretory pathway is required for systemic acquired resistance. *Science* **308**, 1036-1040.

**Wek RC, Jiang HY, Anthony TG.** 2006. Coping with stress: eIF2 kinases and translational control. *Biochem Soc Trans* **34**, 7-11.

**Wightman B, Ha I, Ruvkun G.** 1993. Posttranscriptional regulation of the heterochronic gene lin-14 by lin-4 mediates temporal pattern formation in *C. elegans*. *Cell* **75**, 855-862.

- Wortel IMN, van der Meer LT, Kilberg MS, van Leeuwen FN.** 2017. Surviving Stress: Modulation of ATF4-Mediated Stress Responses in Normal and Malignant Cells. *Trends Endocrinol Metab* **28**, 794-806.
- Xia X, Lei L, Qin W, Wang L, Zhang G, Hu J.** 2018. GCN2 controls the cellular checkpoint: potential target for regulating inflammation. *Cell Death Discov* **4**, 20.
- Xu Z, Song N, Ma L, Wu J.** 2019. IRE1-bZIP60 Pathway Is Required for Nicotiana attenuata Resistance to Fungal Pathogen *Alternaria alternata*. *Front Plant Sci* **10**, 263.
- Yoshida H, Matsui T, Yamamoto A, Okada T, Mori K.** 2001. XBP1 mRNA is induced by ATF6 and spliced by IRE1 in response to ER stress to produce a highly active transcription factor. *Cell* **107**, 881-891.
- Zhang L, Chen H, Brandizzi F, Verchot J, Wang A.** 2015. The UPR branch IRE1-bZIP60 in plants plays an essential role in viral infection and is complementary to the only UPR pathway in yeast. *PLoS Genet* **11**, e1005164.
- Zhang Y, Dickinson JR, Paul MJ, Halford NG.** 2003. Molecular cloning of an *Arabidopsis* homologue of GCN2, a protein kinase involved in co-ordinated response to amino acid starvation. *Planta* **217**, 668-675.

## **CHAPTER 2**

### **ARABIDOPSIS GCN2 KINASE CONTRIBUTES TO ABA HOMEOSTASIS AND STOMATAL IMMUNITY**

by

Xiaoyu Liu<sup>1,2</sup>, Taiaba Afrin<sup>1</sup> & Karolina M. Pajerowska-Mukhtar<sup>1</sup>

<sup>1</sup> Department of Biology, University of Alabama at Birmingham, 1300 University Blvd.,  
Birmingham, AL 35294, USA

Published, COMMUNICATIONS BIOLOGY, (2019) 2:302,  
<https://doi.org/10.1038/s42003-019-0544-x>

Copyright ©2019, Springer Nature  
by  
Taiaba Afrin  
Used by permission  
Format adapted for dissertation

## Abstract

General Control Non-derepressible 2 (GCN2) is an evolutionarily conserved serine/threonine kinase that modulates amino acid homeostasis in response to nutrient deprivation in yeast, human and other eukaryotes. However, the GCN2 signaling pathway in plants remains largely unknown. Here, we demonstrate that in Arabidopsis, bacterial infection activates AtGCN2-mediated phosphorylation of eIF2 $\alpha$  and promotes TBF1 translational derepression. Consequently, TBF1 regulates a subset of abscisic acid signaling components to modulate pre-invasive immunity. We show that GCN2 fine-tunes abscisic acid accumulation and signaling during both pre-invasive and post-invasive stages of an infection event. Finally, we also demonstrate that AtGCN2 participates in signaling triggered by phytotoxin coronatine secreted by *P. syringae*. During the preinvasive phase, AtGCN2 regulates stomatal immunity by affecting pathogen-triggered stomatal closure and coronatine-mediated stomatal reopening. Our conclusions support a conserved role of GCN2 in various forms of immune responses across kingdoms, highlighting GCN2's importance in studies on both plant and mammalian immunology.

## Introduction

Cellular robustness and resilience, universal features of all biological systems, allow organisms to withstand internal and environmental perturbations<sup>1,2</sup>. Cells respond to these changes by trading off growth-related processes with stress-associated signaling cascades that are manifested by distinctive regulatory programs<sup>3,4</sup>. These responses require the activation of specific master regulator(s) to maintain cellular homeostasis<sup>5</sup>. General Control Non-derepressible 2 (GCN2), a universal regulator, is an evolutionarily conserved sensor involved in perception of nutrient starvation, stress signal transduction cascades and diverse immune responses<sup>5,6</sup>. *GCN2* encodes a protein kinase with a conserved N-terminal kinase domain and a C-terminal region homologous to histidyl-tRNA synthetase (HisRS)<sup>7</sup>. In yeast and mammals, GCN2 senses amino acid starvation by binding with the uncharged tRNAs *via* its HisRS domain<sup>8,9</sup>. This in turn stimulates the kinase activity of GCN2 and initiates a downstream signaling cascade<sup>10,11</sup>. In particular, GCN2 phosphorylates eukaryotic initiation factor alpha (eIF2 $\alpha$ ), causing its reduced mRNA scanning capacity, which leads to an arrest of general translation but initiates translation of the main GCN4 ORF (mORF)<sup>11,12</sup>. The GCN2/eIF2 $\alpha$ -mediated translation switch of GCN4 activates downstream target genes and alleviates the starvation stress in yeast. Likewise, mammals also possess a functional eIF2 $\alpha$  phosphorylation switch that can be activated by four diverse kinases including GCN2<sup>13</sup>. Upon the perception of stress caused by essential amino acid starvation, eIF2 $\alpha$  phosphorylation allows for uORF-mediated translation of ATF4 TF. *Arabidopsis* contains a single copy of GCN2 (General Control Non-derepressible 2, At3g59410) that was shown to functionally complement  $\Delta gcn2$  yeast mutant strain<sup>7</sup>. Similar to the mammalian and yeast systems, AtGCN2 was

demonstrated to bind with tRNA molecules and phosphorylate Arabidopsis eIF2 $\alpha$  under branched amino acid deprivation and diverse abiotic stress conditions, including treatments with herbicides, phytohormones, as well as wounding<sup>14-18</sup>, suggesting the functional conservation of these molecules across kingdoms. AtGCN2 stress signaling was also demonstrated to be inducible by BABA ( $\beta$ -aminobutyric acid)<sup>19,20</sup>. BABA-induced priming is associated with eIF2 $\alpha$  phosphorylation, which was absent in the *atgcn2* mutant plants<sup>19</sup>. The *atgcn2* mutants are more tolerant to BABA-induced growth repression, but display normal BABA-induced resistance against *H. arabidopsidis* isolate Cala2, which is virulent on the *Ler* accession<sup>19</sup>.

Previously, we showed the roles of AtGCN2 in gibberellic acid (GA)-mediated plant and seed development<sup>21</sup>. Moreover, we identified a heat-shock factor-like protein, TBF1 (HSF4/HsfB1) that contains uORFs in its 5' UTR, reminiscent of the mammalian ATF4 and yeast GCN4<sup>3,22,23</sup>. We also demonstrated that TBF1 is translationally regulated through uORF-mediated translation de-repression upon pathogen infection<sup>3</sup>. This body of evidence collectively suggests possible existence of a GCN2-mediated signaling cascade in Arabidopsis that could play important roles in plant growth and development as well as immune responses<sup>21,24</sup>.

The plant immune system utilizes an array of phytohormones to coordinate the defense response. The fine-tuned signaling interplay among salicylic acid (SA), jasmonic acid (JA), ethylene (ET), abscisic acid (ABA), GA and brassinosteroids<sup>4,25,26</sup> facilitates an integrated defense response<sup>4,27</sup> that often relies on antagonistic hormone action<sup>28</sup>. For instance, over-accumulation of SA inversely affects JA levels and these events positively contribute to the establishment of immunity against bacterium *Pseudomonas syringae* pv.

*tomato* DC3000 (*Pst* DC3000)<sup>29,30</sup>. Virulent pathogens manipulate this hormonal cross-talk to diminish immune responses and thus drive the cell towards susceptibility. For example, *Pst* DC3000 delivers virulence factors (hereafter effectors) through type-III secretion system (TTSS) into the host cell<sup>31,32</sup>. *Pst* DC3000 *hrcC* strain, a mutant defective in TTSS, is almost nonpathogenic<sup>33</sup>. In addition to the effectors, *Pst* DC3000 also delivers toxin coronatine (COR), a structural mimic of JA-isoleucine (an active form of JA) to antagonize SA-mediated defenses and cause plant disease<sup>34-36</sup>.

Emerging roles of ABA during different phases of bacterial infection have also been described<sup>34,37</sup>. A positive role for ABA in defense during early (pre-invasive) stages of bacterial infection is supported by its well-known function in the regulation of ion channels flux, facilitating the closure of stomata. On the contrary, ABA can suppress defense responses through its antagonistic interaction with SA and possibly other hormones, in the later (post-invasive) phase of infection<sup>37</sup>.

We previously reported that AtGCN2 negatively regulates defense responses against phytopathogens with diverse lifestyles<sup>24</sup>. Here, we set out to study pathogen infection-triggered AtGCN2-mediated signaling. We demonstrated that bacterial infection initiates AtGCN2-dependent eIF2α phosphorylation. Moreover, our genetic data indicate that AtGCN2 participates in uORF-mediated translational derepression of TBF1 and executes dual roles in stomatal immunity by contributing to pathogen-triggered ABA-dependent stomatal closure and to COR-mediated stomatal reopening. Conversely, however, AtGCN2 acts as a negative regulator of plant immunity during the post-invasive stage of infection, mainly by regulating ABA accumulation and TBF1-dependent

transcription of ABA signaling components. In summary, we uncovered opposing roles of AtGCN2 in regulating different layers of plant immunity.

## Results

### *Pathogen triggers AtGCN2-dependent eIF2 $\alpha$ phosphorylation.*

Activation of the GCN2/eIF2 $\alpha$  signaling and uORF-mediated translational de-repression of a master TF(s) has been described in mammals and yeast<sup>10,11</sup>. To determine the existence of such a pathway in Arabidopsis in response to a bacterial infection, we first analyzed the eIF2 $\alpha$  phosphorylation status in the wild-type *Ler* and *atgcn2* loss-of-function mutant that is completely deficient in AtGCN2 transcription (Supplementary Fig. 1a). We used a phosphorylation state-specific anti-human eIF2 $\alpha$  antibody, which can specifically recognize phosphorylated eIF2 $\alpha$  in Arabidopsis in response to various

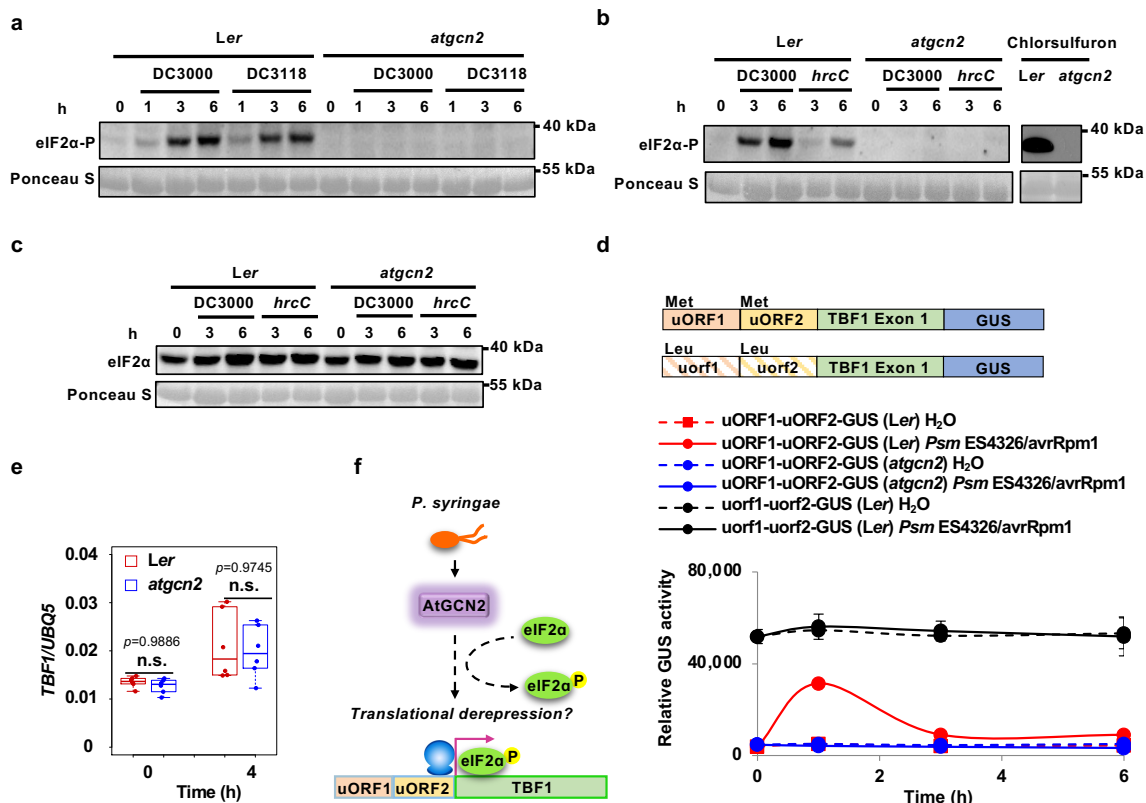


**Figure 1.** AtGCN2 is required for *P. syringae*-triggered eIF2 $\alpha$  phosphorylation and TBF1 translational derepression. a Detection of phosphorylated form of eIF2 $\alpha$  in the samples prepared from 2-week-old plants treated with *Pst* DC3000 or *Pst* DC3118 (OD600 nm = 0.02). Phosphorylation state-specific (S51) antihuman eIF2 $\alpha$  antibody was used. Ponceau S staining shows loading amounts. Full blots are shown in Supplementary Fig. 1b. b Detection of phosphorylated form of eIF2 $\alpha$  in the samples prepared from 2-week-old plants treated with *Pst* DC3000 or *Pst* hrcC (OD600 nm = 0.02). Phosphorylation state-specific (S51) antihuman eIF2 $\alpha$  antibody was used. Ponceau S staining shows loading amounts. Full blots are shown in Supplementary Fig. 1d. c Time course total eIF2 $\alpha$  protein accumulation in 2-week-old plants upon *Pst* DC3000 or *Pst* hrcC (OD600 nm = 0.02) challenge. Ponceau S staining shows loading amounts. Full blots are shown in Supplementary Fig. 1h. d Schematic diagram of constructs used for quantification of GUS activity. Start codon and mutated start codon are labeled as Met and Leu, respectively. GUS activity is shown in T3 plants uORF1-uORF2-GUS (Ler), uorf1-uorf2-GUS (Ler), and uORF1-uORF2-GUS (atgcn2) at designated time points after inoculation with *Psm* ES4326/avrRpm1 or control. Error bars represent standard deviation of three technical replicates. Experiments were conducted in three independent biological replications with similar results. e Transcript accumulation of TBF1 was measured in 4-week-old Ler and atgcn2 plants that were sprayed with salicylic acid (SA; 0.5 mM) using real-time RT-PCR. The boxes plots extend from the 25th to 75<sup>th</sup> percentiles and the whiskers extend from the minimum to the maximum level. Median values are plotted in the boxes with data generated from three independent biological replicates. Statistical analysis was performed with two-way ANOVA with Tukey's test (significance set at P ≤ 0.05) and n.s. denotes not significant. f Schematic representation of AtGCN2- and TBF1-mediated signaling events following *P. syringae* infection. AtGCN2 phosphorylates eIF2 $\alpha$  following *P. syringae* infection and might be directly or indirectly involved in translational regulation of TBF1.

abiotic stressors, including starvation, UV irradiation, wounding, cold temperature, NaCl and H<sub>2</sub>O<sub>2</sub><sup>3,15,18</sup>. We detected eIF2 $\alpha$  phosphorylation in the wild-type plants as early as 1 hour post inoculation (hpi) with the virulent bacterium *Pst* DC3000 and mutant COR-deficient strain *Pst* DC3118<sup>38</sup> (Fig. 1a, Supplementary Fig. 1b). As expected, the control treatment did not induce eIF2 $\alpha$  phosphorylation, confirming its specificity to pathogen challenge (Supplementary Fig. 1c, d). This phosphorylated form of eIF2 $\alpha$  continued to

accumulate at 3 hpi and 6 hpi but was absent in the *atgcn2* mutant plants at all the tested time points, suggesting the requirement of AtGCN2 in eIF2 $\alpha$  phosphorylation during plant infection (Fig. 1a and Supplementary Fig. 1c, d). Subsequently, we tested if virulent effectors contribute to eIF2 $\alpha$  phosphorylation by comparing Pst DC3000 and Pst DC3000 hrcC strain that is defective in TTSS-mediated effector delivery. Pst hrcC induced a much weaker eIF2 $\alpha$  phosphorylation than DC3000, indicating that the effector proteins or type-III pilus itself are required for the full extent of eIF2 $\alpha$  phosphorylation (Fig. 1b and Supplementary Fig. 1e). Chlorsulfuron-treated plants were used as a positive control as this herbicide was previously shown to act as a powerful trigger of eIF2 $\alpha$  phosphorylation<sup>15</sup>. Moreover, AtGCN2-dependent eIF2 $\alpha$  phosphorylation can also be induced by *P. syringae* pv. *maculicola* ES4326 (Psm ES4326) expressing avrRpm1, confirming that AtGCN2 universally responds to stress caused by *P. syringae* infection irrespective of the strain (Supplementary Fig. 1f, g). The levels of transcript and total eIF2 $\alpha$  protein in wild-type and *atgcn2* plants were comparable (Fig. 1c and Supplementary Fig. 1h–k), further confirming that the observed response is dynamic, and phosphorylation mediated. Overall, these data suggest that AtGCN2 is required for the eIF2 $\alpha$  phosphorylation following microbial infection.

### ***TBF1 translational de-repression is AtGCN2-dependent.***

The high degree of structural and functional conservation of GCN2/ eIF2 $\alpha$  in Arabidopsis, yeast and human prompted us to investigate their downstream uORF-mediated targets<sup>10,11,39–41</sup>. Among others, the Arabidopsis TF TBF1 was proposed to be a possible target given that its mRNA contains two uORFs upstream of the main ORF (mORF)

(Fig. 1d) and was shown to be translationally regulated<sup>3</sup>. To test the requirement of AtGCN2 in TBF1 translational derepression, we employed reporter constructs by fusing in-frame either wild-type uORFs or uorf (mutated form of uORF harboring a mutation in the initiator codon, i.e., ATG to CTG) and the first exon of mORF TBF1 to GUS reporter coding sequences as previously described<sup>3</sup>. The resulting constructs were transformed into *Ler* and *atgcn2* plants to generate stable transgenic lines. We challenged *Ler* plants expressing uORF1-uORF2-GUS or uorf1- uorf2-GUS as well as *atgcn2* expressing uORF1-uORF2-GUS with an avirulent bacterial pathogen and quantified GUS activity. As shown in Fig. 1d, we detected an eightfold increase in the GUS activity in the uORF1-uORF2-GUS (in *Ler* background) plants, while this induction was completely abolished in the uorf1-uorf2- GUS (in *Ler* background) and uORF1-uORF2-GUS (in *atgcn2* background) plants. The uorf1-uorf2-GUS (in *Ler* background) plants lost their translational-level inhibition and displayed a high output of basal level translation, which is not further inducible, since the uORF cassette is mutated and not reactive to stimulation (Fig. 1d). Given that the *atgcn2* mutant displays no defects in accumulating TBF1 transcript (Fig. 1e), and comparable levels of *uidA-TBF1* chimeric transcript expression were detected in the three transgenic reporter lines following pathogen challenge (Supplementary Fig. 1i, j), the measured GUS activity represents the rate of translation reinitiation at the TBF1 mORF. Taken together, our data indicate that *Arabidopsis* GCN2 is implicated in translational regulation of TBF1 in plant immune signaling (Fig. 1f).

### ***AtGCN2 and TBF1 regulate pre-invasive stage ABA signaling.***

To elucidate candidate cellular processes downstream of AtGCN2-dependent eIF2 $\alpha$  phosphorylation, we conducted bioinformatics analyses of the TBF1-dependent immune transcriptome<sup>3</sup>. We discovered an enrichment of differentially expressed genes encoding ABA receptors, ABA biosynthetic enzymes and ABA-related transcriptional regulators (Fig. 2a, b and detailed information in Supplementary Table 1). We classified these genes into two categories, TBF1-induced and TBF1-repressed. Given that ABA was postulated to play dual roles during different stages of plant infection<sup>37</sup>, we proposed that the AtGCN2/eIF2 $\alpha$ -mediated and TBF1-dependent signaling may differentially contribute to preinvasion- and postinvasion- associated defenses (Fig. 2c). Among the ABA-related TBF1-repressed genes, we selected two canonical negative ABA response regulators, *PP2CA* (*Protein Phosphatase type 2C*) and *ABI2* (*Abscisic Acid Insensitive 2* that also encodes a PP2C) for expression profiling analyses. Promoter sequence analyses of *PP2CA* and *ABI2* confirmed the presence of conserved *TL1* elements (*GAA-GAAGAA*, the binding site for TBF1), in their upstream regulatory regions<sup>3</sup> (Supplementary Table 1). This indicates that *ABI2* and *PP2CA* may be transcriptionally regulated by TBF1. To experimentally support this observation, we carried out a real-time qPCR and analyzed expression profiles of these two genes in response to microbial challenge using the previously published loss-of-function *tbfl* mutant (Col-0 background)<sup>3</sup>. We observed transcriptional repression of *PP2CA* and *ABI2* in the Col-0 plants during the preinvasive stage of *Pst hrcC* infection; this suppression, however, was not detected in the *tbfl* mutant (Fig. 2d, f). Thus, this repression likely constitutes a general, and not effector-specific, regulatory effect of TBF1 on the ABA pathway in response to bacterial infection.

To examine the roles of AtGCN2 in the preinvasive phase of plant immunity, we monitored the temporal expression patterns of these ABA-responsive genes in the *atgcn2* plants in response to *Pst hrcC*. We observed a repression of *PP2CA* and *ABI2* mRNA levels in the wild-type infected with *Pst hrcC*, while the transcripts of these two ABA-related

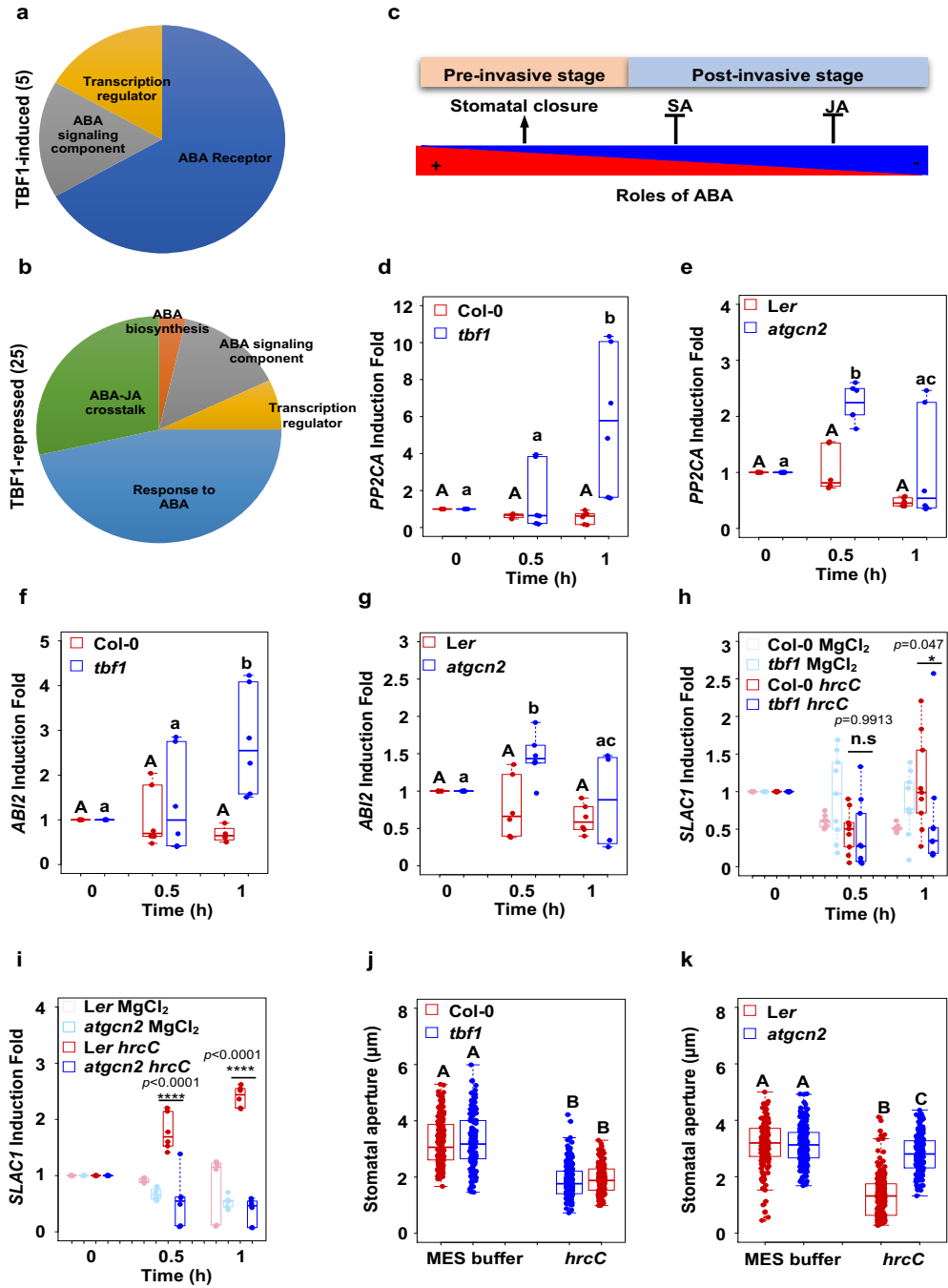


**Figure 2.** AtGCN2-TBF1 cascades transcriptionally manipulate ABA signaling components during preinvasive stage. Pie charts of GO terms of genes that are transcriptionally induced (a) and repressed (b) by TBF1 upon *elf18* treatment. Details are listed in Supplementary Table 1. c Diagrammatic representation of a model illustrating the opposing roles of ABA in preinvasive and postinvasive phases of pathogen infection. Positive and negative contributions of ABA in plant defense are depicted in blue and red colors, respectively. Salicylic acid (SA) and jasmonic acid (JA) are shown [adopted from Ton et al.<sup>37</sup>]. Real-time RT-PCR analyses were performed on leaf samples of plants spray inoculated with Pst hrcC ( $OD_{600nm} = 0.2$ ) and transcript levels of PP2CA (d, e), ABI2 (f, g), and SLAC1 (h, i), respectively, were quantified. The box plots are prepared as described above. Median values are plotted in the boxes with data generated from three independent biological replicates. For d–g, two-way ANOVA with Tukey's test (significance set at  $p \leq 0.05$ ) was performed; capital letters denote difference in wild-type plants (Ler or Col-0), and lower-case letters denote difference in mutant plants (*tbfl* or *atgcn2*). For h, i, two-way ANOVA with Tukey's test was performed and asterisks above the bars signify statistically significant differences between Pst hrcC challenged Col-0 and *tbfl* or Ler and *atgcn2* plants (\*\* $p \leq 0.01$ , \*\*\* $p \leq 0.001$ , n.s.—not significant). j, k Stomatal aperture width was measured in epidermal peels of 4-week-old *tbfl* mutants (in Col-0 background; j) and *atgcn2* mutants (in Ler background; k) that were treated with Pst hrcC ( $OD_{600nm} = 0.2$ ) for 1 h. The box plots are prepared as described above. Median values are plotted in the boxes with data generated from stomata derived from three independent biological replicates. One-way ANOVA with Tukey's test (significance set at  $p \leq 0.05$ ) was performed and letters above the bars signify statistically significant differences among groups.

genes were elevated in the *atgcn2* mutant (Fig. 2e, g). The resemblance of *PP2CA* and *ABI2* transcriptional trends in *tbfl* and *atgcn2* plants indicates that TBF1 might function as one of the AtGCN2 targets to regulate the ABA response during the preinvasive stage of pathogen challenge.

Besides regulating TBF1 translational derepression, AtGCN2-mediated eIF2α phosphorylation leads to general attenuation of protein synthesis<sup>15</sup>. In yeast, GCN2 activation requires functional interactors Gcn1 and Gcn20<sup>42–44</sup>. Recently, *Arabidopsis* GCN1 and GCN20 were reported to share sequence similarity with yeast Gcn1 and Gcn20 and shown to play an important role in regulating stomatal immunity<sup>45–47</sup>.

Moreover, another recent report illuminated the function of Arabidopsis GCN4, an AAA<sup>+</sup>-ATPase family protein, as a key regulator of stomatal aperture during stress<sup>48</sup>. Stomata, which serve as gateways for gas exchange, respond to environmental cues by changes in osmotic pressure within guard cells, allowing fine-tune regulation of the stomatal aperture<sup>49</sup>. It has been shown that treatments with immune stimuli result in a rapid stomata closure to restrict pathogen entrance<sup>50</sup>. In general, stomatal closure is executed through an efflux of ions through ion channels. Among them, an S-type anion channel SLAC1 (SLOW ANION CHANNEL- ASSOCIATED 1) plays a critical role in the pathogen-induced stomatal closure<sup>50</sup>. Quantification of *SLAC1* transcripts upon *Pst hrcC* challenge revealed that both the *tbf1* and *atgcn2* mutants are impaired in this response compared with their respective wild types (Fig. 2h, i), further implying a possible regulatory relationship between these two factors. Finally, we tested the *atgcn2* and *tbf1* mutants for their ability to execute stomatal closure in response to *Pst hrcC*. Our results demonstrated that the *atgcn2* mutant is less effective in closing the stomata following *Pst hrcC* infection (Fig. 2k), while *tbf1* plants show near wild-type levels of stomatal closure (Fig. 2j). This less severe stomatal phenotype of *tbf1* plants is consistent with the fact that TBF1 constitutes only one of many potential downstream targets of AtGCN2 and suggests that other factors might be able to compensate this response in the *tbf1* plants. Overall, our results demonstrate that AtGCN2 contributes to the regulation of ABA signaling and stomatal immunity during the preinvasive stage of bacterial infection. Moreover, AtGCN2 might have a regulatory relationship with the key immune TF TBF1 during the preinvasive infection stage.

***AtGCN2 is required for coronatine-mediated stomatal reopening.***

As a deliberate countermeasure against the host stomatal closure, selected phytopathogenic bacteria, and most prominently a number of *P. syringae* strains are able to secret COR to reopen the stomata<sup>35,51</sup>. To examine if AtGCN2 is involved in COR- mediated stomatal reopening, we investigated stomatal immunity using two different types of pathogen infection assays, i.e., syringe pressure infiltration and spray inoculation, and employed *Pst* DC3000 and the COR-deficient mutant strain *Pst* DC3118. In the syringe pressure infiltration assay, bacteria were forcefully delivered at the abaxial side of a leaf through the stomata into intercellular spaces, whereas the bacterial entry through the stomata in the spray inoculation assay was controlled by the natural stomatal immunity<sup>52</sup>. This pair-wise comparison of immune responses allowed us to probe the role of AtGCN2 in COR- dependent stomatal reopening. In the syringe infiltration assay, we detected enhanced disease resistance against *Pst* DC3000 and *Pst* DC3118 in the *atgcn2* mutant (Fig. 3a and Supplementary Fig. 2a, c). In spray inoculation, however, we observed a differential strain-specific response. While the *atgcn2* mutant displayed enhanced resistance against spray inoculation with *Pst* DC3000, this phenotype was lost when *Pst* DC3118 was used (Fig. 3b). To further quantify the responses of *atgcn2* to *P. syringae* infection, we conducted a comprehensive analysis of pathogen biomass accumulation in *Ler* and *atgcn2* plants following infection with *Pst* DC3000, *Pst* DC3118, and *Pst* *hrcC* delivered by pressure infiltration or spray on a time course of 4, 12, 24, 36, 48, 60, and 72 hpi (Supplementary Fig. 2). This fine-resolution dataset recapitulated our earlier observations done with traditional colony counts at 72 hpi (Fig. 3a, b), and allowed us to glean additional insights into the dynamics of

infection as a function of *P. syringae* strain and the delivery method. In the pressure-infiltrated plants, we observed differential accumulation of *P. syringae* bacteria throughout the course of infection, resulting in markedly lower bacterial loads in the

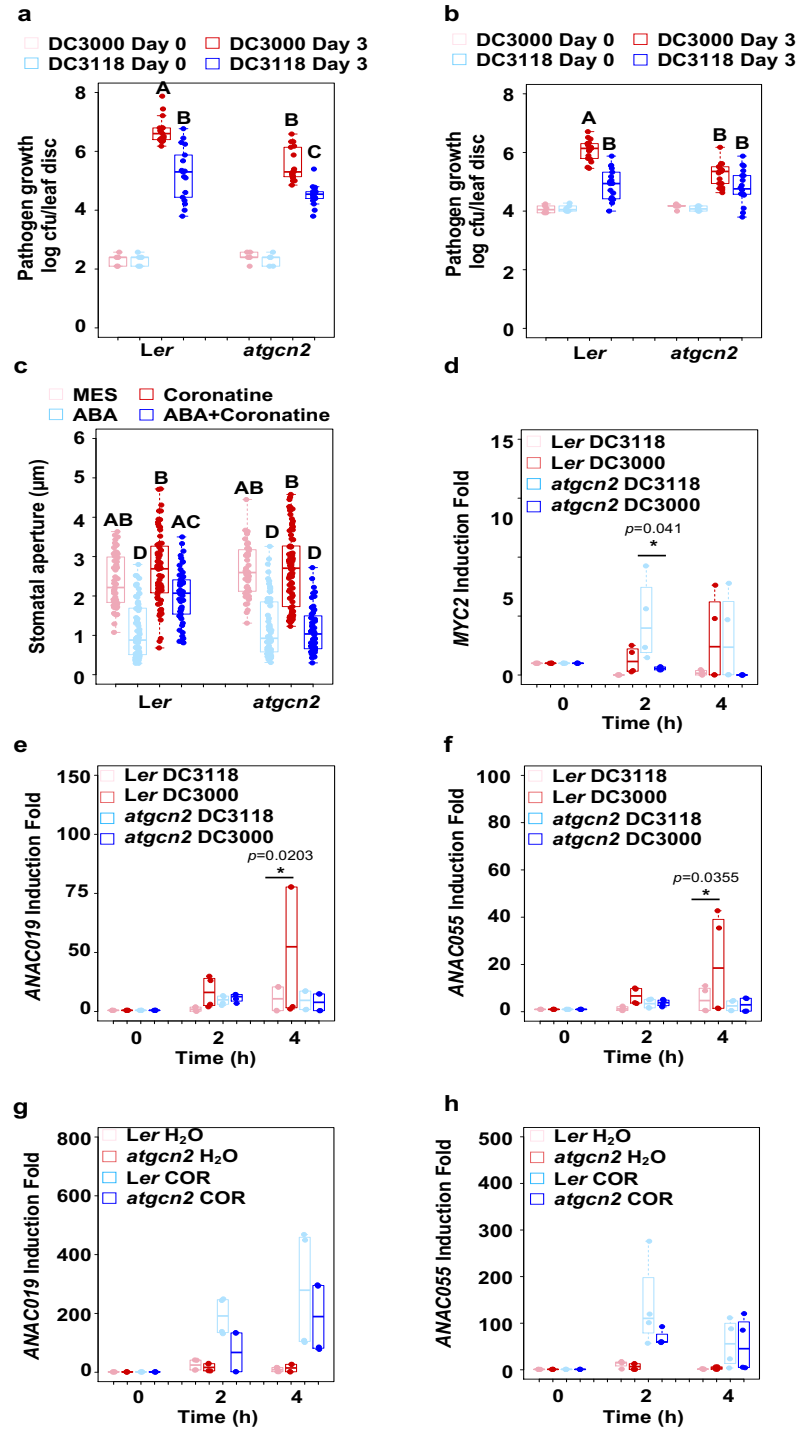


**Figure 3.** AtGCN2 contributes to stomatal immunity and affects disease susceptibility at the preinvasive stage of the infection event. Pathogen growth was quantified in 4-week-old plants infected with *Pst* DC3000 or *Pst* DC3118 at 3 days using syringe inoculation ( $OD_{600\text{ nm}} = 0.0002$ ) (a) and spray inoculation ( $OD_{600\text{ nm}} = 0.2$ ) (b). The box plots are prepared as described above. Median values are plotted in the boxes with data generated from three independent biological replicates with two different technical replicates of each biological replicate (day 0) or three independent biological replicates with six technical replicates of each biological replicate (day 3). Statistical analysis was performed by two-way ANOVA with Tukey's test, letters above the bars signify statistically significant differences among groups ( $p \leq 0.05$ ). (c) Stomatal aperture width was measured in epidermal peels of 4-week-old plants that were treated with MES buffer (control), ABA (10  $\mu\text{M}$ ), coronatine (0.5 ng/ $\mu\text{l}$ ), or ABA (10  $\mu\text{M}$ ) and coronatine (0.5 ng/ $\mu\text{l}$ ) combination for 3 h. The box plots are prepared as described above. Median values are plotted in the boxes with data generated from stomata derived from three independent biological replicates. Statistical analysis was performed by two-way ANOVA followed by Tukey's test; letters above the bars signify statistically significant differences among groups ( $p \leq 0.05$ ). Real-time RT-PCR analyses were performed on leaf samples that were dip inoculated with *Pst* DC3000 or *Pst* DC3118 ( $OD_{600\text{ nm}} = 0.2$ ) to determine transcript induction of MYC2 (d), ANAC019 (e), and ANAC055 (f), respectively. Time in hours (h) is indicated. The box plots are prepared as described above. Median values are plotted in the boxes with data generated from three independent biological replicates. Two-way ANOVA with Tukey's test was performed and asterisks above the bars signify statistically significant differences between *Pst* DC3118 and *Pst* DC3000 treatments ( $p \leq 0.05$ ). Transcript induction of ANAC019 (g) and ANAC055 (h) was determined in 2-week-old plants upon treatments with coronatine (0.5 ng/ $\mu\text{l}$ ) or control using real-time RT-PCR. The box plots are prepared as described above. Median values are plotted in the boxes with data generated from three independent biological replicates. Two-way ANOVA with Bonferroni's test was performed and asterisks above the bars signify statistically significant differences between *Ler* and *atgcn2* upon COR treatments (\* $p \leq 0.05$ )

*atgcn2* mutants at 72 hpi (Supplementary Fig. 2a, c, e). In spray-inoculated *atgcn2*, we confirmed the trend of enhanced resistance to *Pst* DC3000 (Fig. 3b and Supplementary Fig. 2b), while the bacterial biomass was not consistently different between *Ler* and *atgcn2* sprayed with *Pst* DC3118 (Supplementary Fig. 2d), in concordance with the colony count data (Fig. 3b).

To further solidify our findings, we next tested vacuum infiltration inoculation (equivalent to syringe infiltration, Supplementary Fig. 3a) and dip inoculation (equivalent to spray inoculation, Supplementary Fig. 3b), and we observed consistent

trends of bacterial growth in the *atgcn2* mutant. Akin to our *Pst hrcC* results, we detected deficiency of the *atgcn2* mutant in *Pst* DC3118-mediated stomatal closure and *SLAC1* transcript accumulation (Supplementary Fig. 3c, d). Therefore, a direct comparison of stomatal aperture upon *Pst* DC3000 or *Pst* DC3118 challenge was not optimal. Since the initial wave of ABA-induced stomatal closure is intact in the *atgcn2* plants, we decided to adopt an alternate approach, and chose to directly observe the effect of pure COR as well as a combination of ABA and COR on the induction of stomatal reopening. While the control ABA pretreatment effectively closed the stomata in both *Ler* and *atgcn2*, the opposite was the case for COR. Unlike in *Ler*, the stomata remained closed in the *atgcn2* mutant even in the presence of COR (Fig. 3c) indicating that AtGCN2 is involved in COR-mediated stomatal reopening and consequently the entry of bacteria into the leaf.

Previously, COR was shown to induce the MYC2 TF that in turn upregulates several NAC TFs to confer virulence<sup>51</sup>. To gain additional insights into the mechanism of COR insensitivity in the *atgcn2* mutant, we quantified the *MYC2* transcript after infection with *Pst* DC3000 or *Pst* DC3118. Although not statistically significant, *MYC2* was induced in *Ler* plants when challenged with *Pst* DC3000 as compared with *Pst* DC3118, confirming that COR recognition promotes *MYC2* transcription in wild-type plants<sup>48</sup>. However, no induction of *MYC2* was detected in the *atgcn2* mutant when challenged with *Pst* DC3000 (Fig. 3d). Consistent with the previous findings that COR induces NAC TFs through MYC2, we detected a stronger induction of *ANAC019* and *ANAC055* transcripts in the *Ler* plants when challenged with *Pst* DC3000 compared with *Pst* DC3118. Akin to *MYC2*, no such effect was observed

in the *atgcn2* mutant (Fig. 3e, f). We also analyzed the transcript accumulation of *ANAC019* and *ANAC055* after COR infiltration and found that the *atgcn2* mutant displays a less pronounced transcriptional induction of *ANAC019* and *ANAC055* upon COR treatment compared with the wild-type plants (Fig. 3g, h). Overall, those results collectively demonstrate that AtGCN2 is implicated in COR recognition through the proper regulation of MYC2 and NAC TFs (also see Supplementary Discussion).

#### ***AtGCN2 regulates ABA accumulation and ABA signaling.***

To investigate additional roles of AtGCN2 in ABA signaling, we first measured changes in the accumulation of total ABA in response to *Pst* DC3000 and *Pst* DC3118. It is known that COR-mediated stomatal re-opening begins at 3 hpi with *Pst* DC3000<sup>50</sup>; thus, we elected to consider the initial 4 h as the preinvasive stage of plant immunity. We did not observe a significant difference in the ABA concentration in wild-type and *atgcn2* in the early phase of pathogen infection with either *Pst* DC3000 and *Pst* DC3118 (Supplementary Fig. 4a, b). However, elevated ABA levels were detected at multiple time points between 10 and 16 h after *Pst* DC3000 challenge in Ler plants (Fig. 4a), consistent with the upregulation of ABA biosynthesis genes NCED5 and ABA3 (Fig. 4b, c). This *Pst* DC3000-induced ABA accumulation was less pronounced in the *atgcn2* plants. Moreover, we also revealed that over-accumulation of ABA between 10 h and 16 h is diminished in the wild-type plants infected with *Pst* DC3118 (Fig. 4d), which correlates with the expression levels of NCED5 and ABA3 (Fig. 4e, f). Collectively, these data indicate that COR contributes to over-production of ABA during the late phase of infection

with virulent bacterial strains, and AtGCN2 is involved in the regulation of this process.

Next, we measured the transcript accumulation of PP2CA and ABI2 in Ler and atgcn2

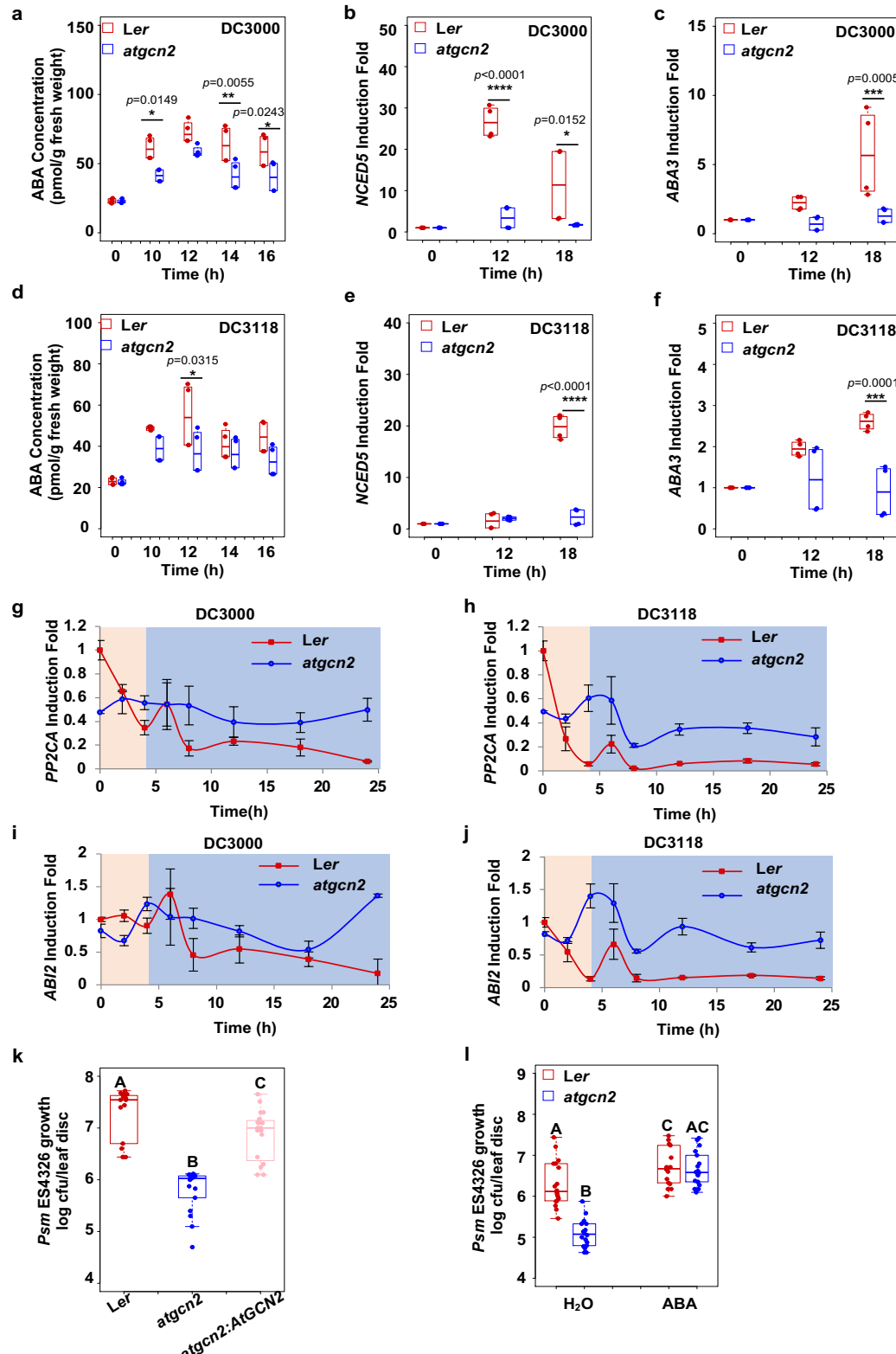


**Figure 4.** AtGCN2 affects disease susceptibility by promoting ABA accumulation and negatively affecting ABA signaling components accumulation. (a) ABA concentration was determined in 4-week-old plants after *Pst* DC3000 (OD<sub>600nm</sub>=0.2) spray inoculation. Median values represent three biological replicates. Two-way ANOVA with Bonferroni's test was performed; asterisks indicate significant differences compared with wild type (\* $p \leq 0.05$  and \*\* $p \leq 0.01$ ). qRT-PCR was performed on 2-week-old plants spray inoculated with *Pst* DC3000 (OD<sub>600nm</sub>=0.2) and transcript levels of NCED5 (b) and ABA3 (c) were quantified. Median values represent three biological replicates. Two-way ANOVA with Bonferroni's test was performed; asterisks indicate significant differences compared with wild type (\*\*\*\* $p \leq 0.0001$  and \*\*\* $p \leq 0.001$ ). d ABA concentration was determined in 4-week-old Ler and atgcn2 plants after *Pst* DC3118 (OD<sub>600nm</sub>=0.2) spray inoculation. Median values represent three biological replicates. Two-way ANOVA with Bonferroni's test was performed; asterisks indicate significant differences compared with wild type Ler (\* $p \leq 0.05$ ). Real-time RT-PCR analyses were performed on 4-week-old Ler and atgcn2 plants spray inoculated with *Pst* DC3118 (OD<sub>600nm</sub>=0.2) and transcript levels of NCED5 (e) and ABA3 (f) were quantified. Median values represent three biological replicates. Two-way ANOVA with Bonferroni's test was performed; asterisks indicate significant differences compared with wildtype (\*\*\*\* $p \leq 0.0001$  and \*\*\* $p \leq 0.001$ ). Real-time RT-PCR analyses were performed on leaf samples spray inoculated with *Pst* DC3000 (OD<sub>600nm</sub> =0.2) (g, i) or *Pst* DC3118 (OD<sub>600nm</sub>=0.2) (h, j) and transcript levels of PP2CA (g, h), and ABI2 (i, j) were quantified. Ler and atgcn2 mutants are shown in red and blue lines, respectively. Pink background represents the preinvasive stage while light blue background corresponds to the postinvasive stage. Data represent the mean and SE of three independent biological replicates. k Bacterial growth was quantified in 4-week-old *Psm* ES4326 syringe inoculated plants at 3dpi (OD<sub>600nm</sub>=0.0001). l Bacterial growth was quantified in 4-week-old mock- or 10mM ABA-treated Ler and atgcn2 two days post syringe inoculation (OD<sub>600nm</sub>=0.001). Median values represent three biological replicates. Statistical analysis was performed by one-way ANOVA (k, l) followed by Tukey's test; letters above the bars signify statistically significant differences among groups ( $p \leq 0.05$ ).

plants upon *Pst* DC3000 and *Pst* DC3118 challenge over the course of 24 hpi and observed that pathogen-triggered transcriptional repression of PP2CA and ABI2 was absent in atgcn2 (Fig. 4g–j), suggesting that AtGCN2 might indirectly impair the transcription of ABA negative regulators to benefit pathogen virulence. To test the possible contribution of AtGCN2 to basal disease resistance, we infected wild-type Ler, *atgcn2*, and a

transgenic complementation line expressing functional AtGCN2 under its native promoter (*atgcn2*: AtGCN2) with Psm ES4326. We revealed that *atgcn2* displayed enhanced basal disease resistance and exhibited ten times less pathogen growth than Ler, while the bacterial load in the *atgcn2*: AtGCN2 complementation line showed elevated pathogen growth compared with the *atgcn2* mutant (Fig. 4k). On contrary, exogenous application of ABA suppressed the enhanced resistance phenotypes the *atgcn2* mutant, which resulted in the establishment of disease susceptibility levels equal to those of wild-type plants (Fig. 4l). In summary, these data indicate that the virulent bacterial pathogen utilizes AtGCN2 to promote ABA over-accumulation and transcriptional repression of ABA negative regulators, resulting in heightened virulence at the post-invasive stage of infection.

## Discussion

In the present study, we found that bacterial pathogens induce the phosphorylation of eIF2 $\alpha$  and this process is dependent on the functional AtGCN2 (Fig. 1a, b and Supplementary Fig. 1c–e). Our previous work identified TBF1, a master immune TF that undergoes a translational derepression following biotic stress. We also previously demonstrated that pathogen infection leads to increased accumulation of both uncharged and charged tRNA<sup>Phe</sup>, as well as induced eIF2 $\alpha$  phosphorylation<sup>3</sup>. Given that activation of yeast and mammalian GCN2 is known to result in translational derepression of a key TF<sup>8,9</sup>, and in light of the genetic data presented in this study that provided preliminary insights into a regulatory relationship of AtGCN2 on TBF1 translational derepression (Fig. 1d), it is therefore likely that a similar activation mechanism exists

in Arabidopsis. Hence, our study points to a possibility that plants might possess a translational derepression pathway involving AtGCN2, eIF2 $\alpha$ , and TBF1 that is triggered during pathogen infection and reminiscent of the yeast GCN2- eIF2 $\alpha$ -GCN4 and mammalian GCN2/PERK-eIF2 $\alpha$ -ATF4 pathways.

In a recent study, Xu et al. found that AtGCN2-mediated eIF2 $\alpha$  phosphorylation is not required for elf18-induced TBF1 translation or disease resistance<sup>53</sup>. GCN2 has the ability to sense and respond to the external amino acid homeostasis, and it is plausible that degradation products of flg22 and elf18, often delivered in excessive concentrations during treatments, could cause amino acid imbalance, indirectly leading to AtGCN2 activation. Thus, we deemed treatments with in vitro synthesized MAMPs inadequate and inconclusive for our experiments.

Moreover, the *atgcn2* mutant allele used in the Xu et al. study is different from the one described in our study. Xu et al. used an allele GABI\_862B02 with the T-DNA insertion positioned near the 3' end of the gene (exon 27). We opted to use a different allele that has the insertion in the gene's first intron (also described by Lageix et al.<sup>15</sup>).

In another recent study, Izquierdo et al. described roles of Arabidopsis GCN1, GCN2, and GCN20 in various stress responses<sup>45</sup>. However, they failed to detect *P. syringae* and SA- induced eIF2 $\alpha$  phosphorylation, while we demonstrate that pathogen-mediated eIF2 $\alpha$  phosphorylation is dependent upon AtGCN2. Our results are in agreement with a previous report<sup>15</sup>, which showed eIF2 $\alpha$  phosphorylation by a wide range of biotic and abiotic treatments including SA. Moreover, they also did not observe any immune phenotypes of *atgcn2* mutant plants, which is contrary to enhanced disease resistance phenotypes to both bacterial (this study) and biotrophic

fungal pathogens<sup>24</sup>. We hypothesize that the inability of Izquierdo et al.<sup>45</sup> to detect eIF2α phosphorylation and immune-related phenotypes of *atgcn2* is possibly due to different immuno-detection methods, type and developmental stage of plant tissues used, and differences between bacterial strains and application methods.

Our results support a function for AtGCN2 in the plant immune system. Recently, it was also shown that global translational reprogramming is a fundamental layer of immune regulation in *Arabidopsis*<sup>53</sup> and that the uORFs within the TBF1 mRNA can function autonomously in translational regulation when transformed into rice<sup>54</sup>. What's more, the GCN2 kinase also contributes to mammalian innate immune responses upon pathogen attack<sup>13,55–57</sup>. The functions of animal GCN2 also span additional aspects of cellular activities, such as regulating inflammation, establishing adaptive immunity and manipulating disease progression. In addition, the nutrient sensing mechanism of the mammalian GCN2 is also linked with mammalian target of rapamycin (mTOR1), which is a central research focus in immunology and biology of aging<sup>58,59</sup>. Moreover, the down-stream ATF4 TF in human is directly recruited by TLR4 receptor and required for the inflammatory cytokine production<sup>60</sup>, akin to the plant TBF1 that is a key factor in growth-to-defense transition<sup>3</sup>. This highlights the crucial roles of the GCN2-mediated activation of various defenses and lends additional support in the overall functional conservation of GCN2-controlled immune processes in mammals and plants.

Phytohormones perform essential roles in every aspect of plant life<sup>61</sup> and engage in a multitude of synergistic and antagonistic interactions at various regulatory levels to maintain cellular homeostasis. Our bioinformatics analysis identified a set of TBF1-

dependent differentially expressed genes that are implicated in ABA biosynthesis and signaling. Additional experiments confirmed that two very well defined negative regulators of ABA signaling, PP2CA and ABI2<sup>62</sup>, are misregulated in both *atgcn2* and *tbfl* mutants in response to virulent bacterial pathogens. Likewise, genetic analyses of positive and negative regulators of ABA in conjunction with different methods of pathogen delivery, showed that ABA signaling interacts antagonistically or synergistically with SA or JA to contribute to the plant immune system throughout different infection phases<sup>63</sup>. These previously proposed, opposing functions of ABA are in concordance with our genetic and pathology data. During the late phase of infection with *Pst* DC3000, low accumulation of ABA in *atgcn2* is correlated with a decrease in transcript accumulation of ABA biosynthetic genes *NCED5* and *ABA3* (Fig. 4b, c) and increased *PP2CA* and *ABI2* gene expression (Fig. 4g, i). This suggests that virulent bacterial pathogens might utilize AtGCN2 to potentiate disease susceptibility. It was recently reported that members of the AvrE effector family from *Pst* DC3000 target PP2A complexes in susceptible hosts via direct interaction/association with specific B' regulatory subunits<sup>64</sup>. Interestingly, Ton et al. previously hypothesized that ABA plays opposing roles in pre and postinvasive phases of pathogen infection<sup>37</sup>. While ABA positively contributes to stomatal immunity (detailed below), virulent pathogens hijack ABA biosynthesis and signaling that in turn suppresses SA-mediated defenses at the later infection stage. It is plausible, therefore, that the lower levels of ABA in the *atgcn2* mutant allow for higher SA accumulation. Consistent with these data, we previously observed a marked increase in the SA bio-synthetic gene *SID2* levels in the *atgcn2* plants at 12 and 24 h after SA spray as well as increased levels of resistance to

biotrophic powdery mildew fungus *Golovinomyces cichoracearum*<sup>24</sup>. Taken together, we propose that AtGCN2 is a positive regulator of ABA biosynthesis and signaling, and virulent pathogens potentially target AtGCN2 to establish disease susceptibility. Consistent with the previous reports, our data confirm the opposing functions of ABA in different phases of pathogen infection.

In addition to the roles of ABA in postinvasive immunity, a plethora of genetic, biochemical and infection studies in the last decade has demonstrated that the core components of ABA pathway including RCAR, SLAC1, and PP2CA play positive roles in preinvasive immunity<sup>62,65–68</sup>. We provided evidence that AtGCN2 positively contributes to immunity through the ABA signaling, in particular the activities of ion channels in the guard cells (Fig. 2h, i). Stomata, which serve as the gas exchange pores, can alter their aperture in response to environmental cues or pathogen attack<sup>50,69,70</sup>. Recently, SCORD5 (susceptible to coronatine-deficient *Pst* DC3000), which encodes an ATP-binding cassette protein AtGCN20/AtABCF3, was shown to be involved in regulating stomatal aperture<sup>47</sup>. Intriguingly, the GCN1-GCN20 complex interacts with GCN2 and contributes to activation of downstream translational reinitiation in yeast<sup>42–44</sup>. It remains to be tested whether AtGCN2 and AtGCN20 form a functional complex; however, it was shown that C-terminal region of AtGCN1 (ILITYHIA) interacts with AtGCN2 and contributes to AtGCN2-dependent eIF2α phosphorylation<sup>71</sup>. AtGCN1 and AtGCN4 are also implicated in the regulation of stomatal aperture upon pathogen attack<sup>46–48</sup>. Additional players, such as yeast Yih1 protein and its mammalian ortholog IMPACT, compete with GCN2 for GCN1 binding and inhibit eIF2α phosphorylation in yeast and mammals, respectively<sup>72,73</sup>. However, no such orthologs

have been isolated in Arabidopsis. Future genetic and biochemical experiments could identify such novel regulators of AtGCN2 activation and stomatal immunity.

It is also remarkable that *atgcn2*, despite being affected in ABA signaling during both early and late stages of infection (Fig. 5a, b), can perceive the initial ABA signal and respond correctly with the stomatal closure. Although the ABA receptor-related transcripts are misregulated in the *tbf1* mutant following immune stress (Fig. 2), their basal levels are normal when comparing *tbf1* to Col-0<sup>3</sup> and we hypothesize that resulting translation of ABA perception and signaling components is sufficient for a successful initial trigger. While a number of ABA signaling genes are mis-regulated in the *atgcn2* plants, their expression is not completely absent, and early ABA accumulation is unchanged (Supplementary Fig. 4), thus it is likely that un-challenged *atgcn2* plants possess the necessary elements of the ABA perception and signaling machinery. External application of ABA at a concentration much higher than the physiologically active levels may be over-saturating the ABA receptor and signaling pathway to permit successful perception and transduction of the ABA signal and uninterrupted initial wave of ABA-induced stomatal closure (Fig. 3c).

We also demonstrated that AtGCN2 is involved in COR-mediated stomatal reopening, a hallmark of virulent bacterial infection. Upon delivery, COR, a structural mimic of the active form of JA, directly binds to the JA receptor and consequently leads to the derepression of MYC2, a central transcriptional regulator of JA signaling. Among the direct downstream MYC2 targets, a set of NAC TFs was shown to exert inhibitory effects on SA biosynthesis and metabolism<sup>51</sup>. It was recently suggested that MYC2 might be under translational control during seed germination<sup>74</sup>. We

demonstrated that AtGCN2 is required for COR recognition through proper regulation of MYC2 and NAC TFs. While COR suppresses the SA-mediated immunity to reopen the stomata, the complete mechanism governing this phenomenon is still lacking. We propose that AtGCN2 is an upstream regulator of this process that may serve as an additional player in hormonal interplay during preinvasive immunity (Fig. 5a, Supplementary Discussion). Collectively, this body of evidence highlights the expanding repertoire of AtGCN2-associated regulators and further supports the recently emerging concept of translational regulation in stomatal immunity.

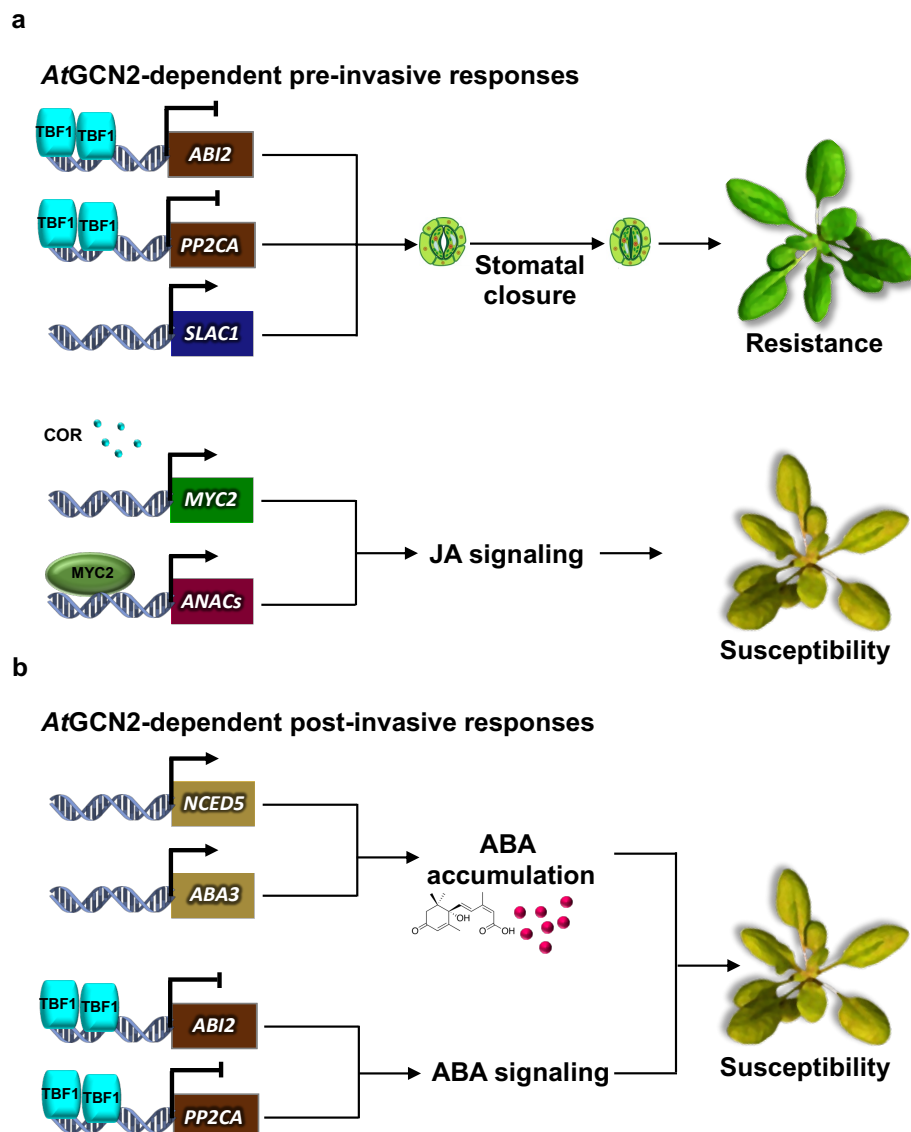


**Figure 5.** A model representing the key targets of AtGCN2 in immune responses during preinvasive and postinvasive stages of bacterial pathogen infection. (a) AtGCN2 exhibits dual roles in the plant immunity during the preinvasive stage of an infection event. AtGCN2 contributes to plant immunity by enhancing pathogen-triggered stomatal closure through TBF1-mediated repression of negative regulators of ABA signaling, ABI2 and PP2CA, as well as via upregulation of ion transporter SLAC1. Moreover, AtGCN2 is also required for coronatine-mediated virulence by enhancing the expression of the key JA signaling modulator, MYC2, and consequently its transcriptional targets ANAC019 and ANAC055. b During the postinvasive stage of bacterial infection, AtGCN2 promotes ABA accumulation through indirect positive regulation of ABA biosynthetic genes NCED5 and ABA3, as well as through TBF1-mediated repression of negative regulators of ABA signaling, ABI2 and PP2CA

In conclusion, we discovered AtGCN2 as an immune regulator that triggers eIF2 $\alpha$ -mediated downstream signaling events. We gathered evidence indicating a possibility of AtGCN2 being directly or indirectly implicated in translational control of TBF1, which leads to the repression of ABA signaling components upon pathogen infection. We demonstrated the opposing roles of AtGCN2 in regulating ABA accumulation and signaling that contribute to pre and postinvasive plant immunity. Finally, our conclusions suggest a conserved role of GCN2 in various forms of immune responses across kingdoms, highlighting AtGCN2 as a molecule of interest for plant and mammalian immunology.

## Methods

### ***Plant materials and growth conditions.***

Wild-type *Arabidopsis thaliana* (L.) Heynh. accessions Columbia-0 and Landsberg *erecta* (*Ler*) were used in this study. The *atgcn2* Genetrap insertion line GT8359 (*Ler* background) was obtained from Cold Spring Harbor Laboratory, New York. The *tbf1* T-DNA insertion line SALK\_104713 was obtained from ABRC. *Agrobacterium*

*tumefaciens* carrying *uORF1-uORF2-GUS* or *uorf1-uorf2-GUS* were used to transform *Ler* and the *atcgn2* plants to generate stable Arabidopsis transgenic lines as described previously<sup>3</sup>. Plants were grown on Super Fine Germination Mix soil (Sun Gro Horticulture) under a 12h light/12h dark photoperiod (21°C, 100 µmol/m<sup>2</sup>/s light intensity and 40% relative humidity).

### ***Pathogen strains***

*Pseudomonas syringae* pv. *maculicola* ES4326 (*Psm* ES4326), *Psm* ES4326 carrying avirulent effector *avrRpm1*, *Pseudomonas syringae* pv. *tomato* DC3000 (*Pst* DC3000) and *Pst* DC3118 defective in coronatine production and *Pst* DC3000 *hrcC* defective in TTSS-mediated effectors delivery were used in this study.

### ***Pathogen infection and quantification assays***

For quantifying disease resistance during post-invasive stage, four-week-old plants were syringe infiltrated with *Pst* DC3000 (OD<sub>600nm</sub> = 0.0002) or *Pst* DC3118 (OD<sub>600nm</sub> = 0.0002) and bacterial growth was quantified three days post inoculation as described previously<sup>39</sup>. For characterizing the defense response during the post-invasive stage in early developmental stage, two-week-old plants were vacuum inoculated with *Pst* DC3000 (OD<sub>600nm</sub> = 0.002) or *Pst* DC3118 (OD<sub>600nm</sub> = 0.002) with 0.002% Silwet L-77 and bacterial growth was quantified two days post inoculation. For characterizing the defense response during the pre-invasive stage, four-week-old plants were spray inoculated with *Pst* DC3000 (OD<sub>600nm</sub> = 0.2) or *Pst* DC3118 (OD<sub>600nm</sub> = 0.2) with 0.02% Silwet L-77 and pathogen growth was quantified three days post inoculation. For

characterizing the defense response during the pre-invasive stage in plants at an early developmental stage, 2-week-old plants were dip inoculated with *Pst* DC3000 ( $OD_{600nm} = 0.05$ ) or *Pst* DC3118 ( $OD_{600nm} = 0.05$ ) with 0.02% Silwet L-77 and pathogen growth was quantified two days post inoculation. For pathogen biomass quantification by qPCR, four-week-old plants were inoculated with *Pst* DC3000, *Pst* DC3000 *hrcC* or *Pst* DC3118 with  $OD_{600nm} = 0.0002$  (syringe infiltration) or  $OD_{600nm} = 0.2$  with 0.02% Silwet L-77 (spray) and DNA was extracted from leaf tissue at specific time points by grinding tissue in 200  $\mu$ l CTAB Extraction Buffer (2% cetyl trimethylammonium bromide, 100 mM Tris-HCl pH 8, 1.4 M NaCl, 20 mM EDTA, 0.5%  $\beta$ -Mercaptoethanol, 2% polyvinyl pyrrolidone). For qPCR analysis, about 10 ng of template DNA were used and bacterial biomass was measured using *P. syringae*-specific oprF primer pair<sup>40</sup> (S2 Table) using GoTaq qPCR master mix (Promega) in a RealPlex S MasterCycler (Eppendorf).

### ***Gene expression analysis***

Total RNA was extracted from Arabidopsis leaves using TRIzol reagent (Invitrogen) and genomic DNA contamination was removed by DNase I (Ambion) treatment. Reverse transcription was conducted with SuperScript III first-strand RT-PCR kit (Invitrogen), and gene expression was determined using GoTaq qPCR Master Mix (Promega) with transcript-specific primers in a RealPlex S MasterCycler (Eppendorf). Primers used for qRT-PCR are listed in the Supplementary Table 2.

### ***$\beta$ -glucuronidase (GUS) activity quantification***

Transgenic T<sub>3</sub> homozygous lines uORF1-uORF2-GUS (*Ler*), uORF1-uORF2-

GUS (*atgcn2*) and uorf1-uorf2-GUS (*Ler*) were syringe infiltrated with *Psm* ES4326/avrRpm1 (OD<sub>600nm</sub> = 0.1) and tissues were collected at specified time points. Total proteins were extracted with extraction buffer (50 mM NaPO<sub>4</sub> [pH 7.0], 1 mM Na<sub>2</sub>EDTA, 0.1% SDS, 0.1% Triton X-100, protease inhibitor for plant extracts [Sigma] and 10 mM β-mercapethanol). As described previously<sup>3</sup>, GUS activity was quantified by incubating protein extract with 1 mM MUG (4-methylumbelliferyl β-D-glucuronide). The reaction was terminated with 1 M Na<sub>2</sub>CO<sub>3</sub> and fluorescence was measured using microplate Reader (Tecan) with excitation wavelength of 365 nm, an emissions wavelength of 455 nm and a filter wavelength of 430 nm. The relative GUS activity was obtained by normalizing data to Bradford assay.

### ***Protein extraction and immunoblot analysis***

Total proteins were extracted from liquid MS-grown two-week-old seedlings exposed to mock or live pathogen *Pst* DC3000, *Pst* DC3118 or *Pst* DC3000 *hrcC* (OD<sub>600nm</sub> = 0.02) by grinding tissue in 200 µl extraction buffer (10 mM HEPES [pH 7.7], 2 mM EDTA, 150 mM NaCl, 10 mM MgCl<sub>2</sub>, 0.3% Triton X-100, protease inhibitor for plant extracts (Sigma), proteasome inhibitor MG132 (Sigma) and PhoSTOP (Roche)<sup>3</sup>. Protein extracts were separated on 10% SDS-PAGE gel and proteins were transferred onto nitrocellulose membrane (Whatman) with semi-dry transfer system (FisherBiotech). Equal protein loading was confirmed by 0.1% Ponceau S staining. To detect the phosphorylation of eIF2α, membranes were blocked in 5% skimmed milk in TBS-T buffer (10 mM Tris-HCl [pH 7.5], 150 mM NaCl and 0.1% Tween 20) for 1 h at room temperature before incubation with 1:1000 dilution of primary anti-eIF2αS1 antibody (Abcam)

overnight at 4°C. For detection of total eIF2 $\alpha$  protein, polyclonal antibody against peptide (IRRMRMTPQPMKIRAD) was raised in rabbits (Genscript)<sup>18</sup>. Membranes were blocked in 5% skimmed milk in TBS-T buffer overnight at 4°C and incubated with 1:4000 dilution of primary antibody in 2% skimmed milk in TBS-T buffer. After incubation with primary antibodies, membranes were incubated with 1:5000 dilution of secondary anti-rabbit HRP-conjugated antibody (Santa Cruz Biotechnology) in 2% skimmed milk in TBS-T buffer for 1 h at room temperature. Immunoblots were detected with Clarity ECL Substrate (Bio-Rad) for chemiluminescence development.

### ***ABA quantification***

Four-week-old plants were spray inoculated with *Pst* DC3000 or *Pst* DC3118 ( $OD_{600nm} = 0.2$ ) with 0.02% Silwet L-77 and ABA extraction was performed as described previously<sup>41</sup>. ABA was extracted using extraction buffer (10 mM HCl, 1% PVPP in methanol) overnight at 4°C. The tissue extract was neutralized with 1 M NaOH before dried under the SpeedVac (Thermofisher). The dried residues were resuspended in water and ABA concentration was measured using Phytodetek Immunoassay kit for ABA (AG-DIA Inc.).

### ***The Stomatal aperture assay***

To measure the stomatal aperture, epidermal leaf peels of the abaxial side were collected from mature leaves of four-week-old plants. Leaf peels were incubated in MES buffer (25 mM MES [pH 6.15], 10 mM KCl) or MES buffer containing 10  $\mu$ M ABA (Sigma) or 0.5 ng/ $\mu$ l coronatine (Sigma) on the top of a glass slide and observed under

the light microscope at specified time points<sup>42</sup>. Stomatal response to living bacteria was performed by incubating leaf peels in water or water containing *Pst* DC3118 (OD<sub>600nm</sub> = 0.2) and observed at specified time points. Random (in order to avoid personal preference) pictures were taken under the microscope and at least 60 stomata were recorded for each treatment per time point. The stomatal aperture measurement was performed with NIS element software (<https://www.nikoninstruments.com/Products/Software/NIS-Elements-Advanced-Research/NIS-Elements-Viewer>).

### ***Statistics and reproducibility***

Statistical differences were calculated by two-way ANOVA or one-way ANOVA followed by Tukey's test or Bonferroni's test in a GraphPad Prism 8. Statistically significant differences are indicated with \*p < 0.05, \*\*p < 0.01, \*\*\*p < 0.001, and \*\*\*\*p < 0.0001. Raw data used to create graphs are available in Supplementary Data.

### ***Acknowledgements***

The authors wish to acknowledge Dr. Jean-Marc Deragon for the gift of *atgcn2*: AtGCN2 seeds, Dr. Camilla Koerner for valuable suggestions, Lucas Boatwright, Yali Sun and Danish Diwan for technical assistance, and Drs. Jeff Dangl and Shahid Mukhtar for critical reading of the manuscript. This work was supported by NSF-CAREER (IOS-1350244) to KPM.

## References

1. Whitacre, J. M. Biological robustness: paradigms, mechanisms, and systems principles. *Front. Genet.* 3, 67 (2012).
2. Garbutt, C. C., Bangalore, P. V., Kannar, P. & Mukhtar, M. S. Getting to the edge: protein dynamical networks as a new frontier in plant-microbe interactions. *Front. Plant Sci.* 5, 312 (2014).
3. Pajerowska-Mukhtar, K. M. et al. The HSF-like transcription factor TBF1 is a major molecular switch for plant growth-to-defense transition. *Curr. Biol.* 22, 103–112 (2012).
4. Huot, B., Yao, J., Montgomery, B. L. & He, S. Y. Growth-defense tradeoffs in plants: a balancing act to optimize fitness. *Mol. Plant* 7, 1267–1287 (2014).
5. Walls, J., Sinclair, L. & Finlay, D. Nutrient sensing, signal transduction and immune responses. *Semin. Immunol.* 28, 396–407 (2016).
6. Tsalikis, J., Croitoru, D. O., Philpott, D. J. & Girardin, S. E. Nutrient sensing and metabolic stress pathways in innate immunity. *Cell Microbiol.* 15, 1632–1641 (2013).
7. Zhang, Y., Dickinson, J. R., Paul, M. J. & Halford, N. G. Molecular cloning of an *Arabidopsis* homologue of GCN2, a protein kinase involved in coordinated response to amino acid starvation. *Planta* 217, 668–675 (2003).
8. Dong, J., Qiu, H., Garcia-Barrio, M., Anderson, J. & Hinnebusch, A. G. Uncharged tRNA activates GCN2 by displacing the protein kinase moiety from a bipartite tRNA-binding domain. *Mol. Cell* 6, 269–279 (2000).
9. Hao, S. et al. Uncharged tRNA and sensing of amino acid deficiency in mammalian piform cortex. *Science* 307, 1776–1778 (2005).

10. Hinnebusch, A. G. Translational regulation of GCN4 and the general amino acid control of yeast. *Annu. Rev. Microbiol.* 59, 407–450 (2005).
11. Wek, R. C., Jiang, H. Y. & Anthony, T. G. Coping with stress: eIF2 kinases and translational control. *Biochem. Soc. Trans.* 34, 7–11 (2006).
12. Donnelly, N., Gorman, A. M., Gupta, S. & Samali, A. The eIF2 $\alpha$  kinases: their structures and functions. *Cell. Mol. Life Sci.* 70, 3493–3511 (2013).
13. Castilho, B. A. et al. Keeping the eIF2 alpha kinase Gcn2 in check. *Biochim. Biophys. Acta* 1843, 1948–1968 (2014).
14. Immanuel, T. M., Greenwood, D. R. & MacDiarmid, R. M. A critical review of translation initiation factor eIF2 $\alpha$  kinases in plants—regulating protein synthesis during stress. *Funct. Plant Biol.* 39, 717–735 (2012).
15. Lageix, S. et al. Arabidopsis eIF2 $\alpha$  kinase GCN2 is essential for growth in stress conditions and is activated by wounding. *BMC Plant Biol.* 8, 134 (2008).
16. Li, M. W., AuYeung, W. K. & Lam, H. M. The GCN2 homologue in *Arabidopsis thaliana* interacts with uncharged tRNA and uses *Arabidopsis* eIF2 $\alpha$  molecules as direct substrates. *Plant Biol.* 15, 13–18 (2013).
17. Terry, B. C., Liu, X., Murphy, A. M. & Pajerowska-Mukhtar, K. M. *Arabidopsis thaliana* GCN2 is involved in responses to osmotic and heat stresses. *Int. J. Plant Res.* 5, 87–95 (2015).
18. Zhang, Y. et al. GCN2-dependent phosphorylation of eukaryotic translation initiation factor-2 $\alpha$  in *Arabidopsis*. *J. Exp. Bot.* 59, 3131–3141 (2008).
19. Luna, E. et al. Plant perception of  $\beta$ -aminobutyric acid is mediated by an aspartyl-tRNA synthetase. *Nat. Chem. Biol.* 10, 450–456 (2014).

20. Schwarzenbacher, R. E., Luna, E. & Ton, J. The discovery of the BABA receptor: scientific implications and application potential. *Front. Plant Sci.* 5, 304 (2014).
21. Liu, X., Merchant, A., Rockett, K. S., McCormack, M. & Pajerowska-Mukhtar, K. M. Characterization of *Arabidopsis thaliana* GCN2 kinase roles in seed germination and plant development. *Plant Signal. Behav.* 10, e992264 (2015).
22. Korner, C. J., Du, X., Vollmer, M. E. & Pajerowska-Mukhtar, K. M. Endoplasmic reticulum stress signaling in plant immunity—at the crossroad of life and death. *Int. J. Mol. Sci.* 16, 26582–26598 (2015).
23. Zhu, X., Thalor, S. K., Takahashi, Y., Berberich, T. & Kusano, T. An inhibitory effect of the sequence-conserved upstream open-reading frame on the translation of the main open-reading frame of HsfB1 transcripts in *Arabidopsis*. *Plant Cell Environ.* 35, 2014–2030 (2012).
24. Liu, X. et al. *Arabidopsis thaliana* atGCN2 kinase is involved in disease resistance against pathogens with diverse life styles. *Int. J. Phytopathol.* 4, 93–104 (2015).
25. Lozano-Durán, R. et al. The transcriptional regulator BZR1 mediates trade-off between plant innate immunity and growth. *Elife* 2, e00983 (2013).
26. Pieterse, C. M., Van der Does, D., Zamioudis, C., Leon-Reyes, A. & Van Wees, S. C. Hormonal modulation of plant immunity. *Annu. Rev. Cell Dev. Biol.* 28, 489–521 (2012).
27. Pajerowska-Mukhtar, K. M. et al. Natural variation of potato allene oxide synthase 2 causes differential levels of jasmonates and pathogen resistance in *Arabidopsis*. *Planta* 228, 293–306 (2008).

28. Liu, X., Rockett, K. S., Korner, C. J. & Pajerowska-Mukhtar, K. M. Salicylic acid signalling: new insights and prospects at a quarter-century milestone. *Essays Biochem.* 58, 101–113 (2015).
29. Boatwright, J. L. & Pajerowska-Mukhtar, K. Salicylic acid: an old hormone up to new tricks. *Mol. Plant Pathol.* 14, 623–634 (2013).
30. Pajerowska-Mukhtar, K. M., Emerine, D. K. & Mukhtar, M. S. Tell me more: roles of NPRs in plant immunity. *Trends Plant Sci.* 18, 402–411 (2013).
31. Xin, X. F. & He, S. Y. *Pseudomonas syringae* pv. *tomato* DC3000: a model pathogen for probing disease susceptibility and hormone signaling in plants. *Annu. Rev. Phytopathol.* 51, 473–498 (2013).
32. Mukhtar, M. S., McCormack, M. E., Argueso, C. T. & Pajerowska-Mukhtar, K. M. Pathogen tactics to manipulate plant cell death. *Curr. Biol.* 26, R608–R619 (2016).
33. Mohr, T. J. et al. Naturally occurring nonpathogenic isolates of the plant pathogen *Pseudomonas syringae* lack a type III secretion system and effector gene orthologues. *J. Bacteriol.* 190, 2858–2870 (2008).
34. Arnaud, D. & Hwang, I. A sophisticated network of signaling pathways regulates stomatal defenses to bacterial pathogens. *Mol. Plant* 8, 566–581 (2015).
35. Katsir, L., Schilmiller, A. L., Staswick, P. E., He, S. Y. & Howe, G. A. COI1 is a critical component of a receptor for jasmonate and the bacterial virulence factor coronatine. *Proc. Natl Acad. Sci. USA* 105, 7100–7105 (2008).
36. Panchal, S. et al. Coronatine facilitates *Pseudomonas syringae* infection of arabidopsis leaves at night. *Front Plant Sci.* 7, 880 (2016).

37. Ton, J., Flors, V. & Mauch-Mani, B. The multifaceted role of ABA in disease resistance. *Trends Plant Sci.* 14, 310–317 (2009).
38. Mittal, S. & Davis, K. R. Role of the phytotoxin coronatine in the infection of *Arabidopsis thaliana* by *Pseudomonas syringae* pv. *tomato*. *Mol. Plant Microbe Interact.* 8, 165–171 (1995).
39. Dever, T. E. et al. Phosphorylation of initiation factor 2 $\alpha$  by protein kinase GCN2 mediates gene-specific translational control of GCN4 in yeast. *Cell* 68, 585–596 (1992).
40. Sood, R., Porter, A. C., Olsen, D., Cavener, D. R. & Wek, R. C. A mammalian homologue of GCN2 protein kinase important for translational control by phosphorylation of eukaryotic initiation factor-2 $\alpha$ . *Genetics* 154, 787–801 (2000).
41. Vattem, K. M. & Wek, R. C. Reinitiation involving upstream ORFs regulates ATF4 mRNA translation in mammalian cells. *Proc. Natl Acad. Sci. USA* 101, 11269–11274 (2004).
42. Garcia-Barrio, M., Dong, J., Ufano, S. & Hinnebusch, A. G. Association of GCN1–GCN20 regulatory complex with the N-terminus of eIF2 $\alpha$  kinase GCN2 is required for GCN2 activation. *EMBO J.* 19, 1887–1899 (2000).
43. Marton, M. J., De Aldana, C. V., Qiu, H., Chakraburty, K. & Hinnebusch, A. G. Evidence that GCN1 and GCN20, translational regulators of GCN4, function on elongating ribosomes in activation of eIF2alpha kinase GCN2. *Mol. Cell. Biol.* 17, 4474–4489 (1997).
44. de Aldana, C. V., Marton, M. & Hinnebusch, A. GCN20, a novel ATP binding cassette protein, and GCN1 reside in a complex that mediates activation of the eIF-2 alpha kinase GCN2 in amino acid-starved cells. *EMBO J.* 14, 3184 (1995).

45. Izquierdo, Y. et al. Arabidopsis nonresponding to oxylipins locus NOXY7 encodes a yeast GCN1 homolog that mediates noncanonical translation regulation and stress adaptation. *Plant Cell Environ.* 41, 1438–1452 (2018).
46. Monaghan, J. & Li, X. The HEAT repeat protein ILITYHIA is required for plant immunity. *Plant Cell Physiol.* 51, 742–753 (2010).
47. Zeng, W. et al. A genetic screen reveals Arabidopsis stomatal and/or apoplastic defenses against *Pseudomonas syringae* pv. *tomato* DC3000. *PLoS Pathog.* 7, e1002291 (2011).
48. Laurie-Berry, N., Joardar, V., Street, I. H. & Kunkel, B. N. The *Arabidopsis thaliana* JASMONATE INSENSITIVE 1 gene is required for suppression of salicylic acid-dependent defenses during infection by *Pseudomonas syringae*. *Mol. Plant Microbe. Interact.* 19, 789–800 (2006).
49. Lim, C. W., Baek, W., Jung, J., Kim, J. H. & Lee, S. C. Function of ABA in stomatal defense against biotic and drought stresses. *Int. J. Mol. Sci.* 16, 15251–15270 (2015).
50. Melotto, M., Underwood, W., Koczan, J., Nomura, K. & He, S. Y. Plant stomata function in innate immunity against bacterial invasion. *Cell* 126, 969–980 (2006).
51. Zheng, X.-y et al. Coronatine promotes *Pseudomonas syringae* virulence in plants by activating a signaling cascade that inhibits salicylic acid accumulation. *Cell Host Microbe* 11, 587–596 (2012).
52. Katagiri, F., Thilmony, R. & He, S. Y. The *Arabidopsis thaliana-pseudomonas syringae* interaction. *Arab. Book* 1, e0039 (2002).
53. Xu, G. et al. Global translational reprogramming is a fundamental layer of immune regulation in plants. *Nature* 545, 487–490 (2017).

54. Xu, G. et al. uORF-mediated translation allows engineered plant disease resistance without fitness costs. *Nature* 545, 491–494 (2017).
55. Lemaitre, B. & Girardin, S. E. Translation inhibition and metabolic stress pathways in the host response to bacterial pathogens. *Nat. Rev. Microbiol.* 11, 365–369 (2013).
56. Murguia, J. R. & Serrano, R. New functions of protein kinase Gcn2 in yeast and mammals. *IUBMB Life* 64, 971–974 (2012).
57. Ravindran, R. et al. Vaccine activation of the nutrient sensor GCN2 in dendritic cells enhances antigen presentation. *Science* 343, 313–317 (2014).
58. Fischer, K. E. et al. Health effects of long-term rapamycin treatment: the impact on mouse health of enteric rapamycin treatment from four months of age throughout life. *PLoS ONE* 10, e0126644 (2015).
59. Weichhart, T., Hengstschlager, M. & Linke, M. Regulation of innate immune cell function by mTOR. *Nat. Rev. Immunol.* 15, 599–614 (2015).
60. Zhang, C. et al. ATF4 is directly recruited by TLR4 signaling and positively regulates TLR4-triggered cytokine production in human monocytes. *Cell. Mol. Immunol.* 10, 84–94 (2013).
61. Shan, X., Yan, J. & Xie, D. Comparison of phytohormone signaling mechanisms. *Curr. Opin. Plant Biol.* 15, 84–91 (2012).
62. Rubio, S. et al. Triple loss of function of protein phosphatases type 2C leads to partial constitutive response to endogenous abscisic acid. *Plant Physiol.* 150, 1345–1355 (2009).
63. Lim, C. W., Luan, S. & Lee, S. C. A prominent role for RCAR3-mediated ABA signaling in response to *Pseudomonas syringae* pv. *tomato* DC3000 infection in *Arabidopsis*. *Plant Cell Physiol.* 55, 1691–1703 (2014).

64. Jin, L. et al. Direct and indirect targeting of PP2A by conserved bacterial type-III effector proteins. *PLoS Pathog.* 12, e1005609 (2016).
65. de Torres-Zabala, M. et al. *Pseudomonas syringae* pv. *tomato* hijacks the *Arabidopsis* abscisic acid signalling pathway to cause disease. *EMBO J.* 26, 1434–1443 (2007).
66. Guzel Deger, A. et al. Guard cell SLAC1-type anion channels mediate flagellin-induced stomatal closure. *New Phytol.* 208, 162–173 (2015).
67. Kurusu, T. et al. An S-type anion channel SLAC1 is involved in cryptogein-induced ion fluxes and modulates hypersensitive responses in tobacco BY-2 cells. *PLoS ONE* 8, e70623 (2013).
68. Kim, T. H. et al. Chemical genetics reveals negative regulation of abscisic acid signaling by a plant immune response pathway. *Curr. Biol.* 21, 990–997 (2011).
69. Shimazaki, K.-i, Doi, M., Assmann, S. M. & Kinoshita, T. Light regulation of stomatal movement. *Annu. Rev. Plant Biol.* 58, 219–247 (2007).
70. Okamoto, M. et al. High humidity induces abscisic acid 8'-hydroxylase in stomata and vasculature to regulate local and systemic abscisic acid responses in *Arabidopsis*. *Plant Physiol.* 149, 825–834 (2009).
71. Wang, L. et al. The inhibition of protein translation mediated by AtGCN1 is essential for cold tolerance in *Arabidopsis thaliana*. *Plant Cell Environ.* 40, 56–68 (2017).
72. Sattlegger, E. et al. YIH1 is an actin-binding protein that inhibits protein kinase GCN2 and impairs general amino acid control when overexpressed. *J. Biol. Chem.* 279, 29952–29962 (2004).
73. Pereira, C. M. et al. IMPACT, a protein preferentially expressed in the mouse brain, binds GCN1 and inhibits GCN2 activation. *J. Biol. Chem.* 280, 28316–28323 (2005).

74. Basbouss-Serhal, I., Soubigou-Taconnat, L., Bailly, C. & Leymarie, J. Germination potential of dormant and nondormant *Arabidopsis* seeds is driven by distinct recruitment of messenger RNAs to polysomes. *Plant Physiol.* 168, 1049–1065 (2015).
75. Liu, X. et al. Bacterial leaf infiltration assay for fine characterization of plant defense responses using the *Arabidopsis thaliana*-*Pseudomonas syringae* pathosystem. *J. Vis. Exp.* e53364 (2015). <https://doi.org/10.3791/53364>.
76. Ross, A. & Somssich, I. E. A DNA-based real-time PCR assay for robust growth quantification of the bacterial pathogen *Pseudomonas syringae* on *Arabidopsis thaliana*. *Plant Methods* 12, 48 (2016).
77. Arenas-Huertero, F., Arroyo, A., Zhou, L., Sheen, J. & Leon, P. Analysis of *Arabidopsis* glucose insensitive mutants, gin5 and gin6, reveals a central role of the plant hormone ABA in the regulation of plant vegetative development by sugar. *Genes Dev.* 14, 2085–2096 (2000).

## **CHAPTER 3**

### **THE INTERPLAY OF GTP-BINDING PROTEIN AGB1 WITH ER STRESS SENSORS IRE1A AND IRE1B MODULATES ARABIDOPSIS UNFOLDED PROTEIN RESPONSE AND BACTERIAL IMMUNITY**

by

Taiaba Afrin<sup>1</sup>, Caitlin N. Costello<sup>1</sup>, Amber N. Monella<sup>1</sup>, Camilla J. Kørner<sup>1</sup> and Karolina M. Pajerowska-Mukhtar<sup>1</sup>

<sup>1</sup> Department of Biology, University of Alabama at Birmingham, 1300 University Blvd., Birmingham, AL 35294, USA

Published, Plant Signaling & Behavior, Volume 17, 2022 - Issue 1,  
<https://doi.org/10.1080/15592324.2021.2018857>

Copyright ©2022, Taylor & Francis Group, LLC  
by  
Taiaba Afrin  
Used by permission  
Format adapted for dissertation

## Abstract

In eukaryotic cells, the accumulation of unfolded or misfolded proteins in the endoplasmic reticulum (ER) results in ER stress that induces a cascade of reactions called the unfolded protein response (UPR). In Arabidopsis, the most conserved UPR sensor, Inositol-requiring enzyme 1 (IRE1), responds to both abiotic- and biotic-induced ER stress. Guanine nucleotide-binding proteins (G proteins) constitute another universal and conserved family of signal transducers that have been extensively investigated due to their ubiquitous presence and diverse nature of action. Arabidopsis GTP-binding protein  $\beta$ 1 (AGB1) is the only G-protein  $\beta$ -subunit encoded by the Arabidopsis genome that is involved in numerous signaling pathways. Mounting evidence suggests the existence of a crosstalk between IRE1 and G protein signaling during ER stress. AGB1 has previously been shown to control a distinct UPR pathway independently of IRE1 when treated with an ER stress inducer tunicamycin. Our results obtained with combinatorial knockout mutants support the hypothesis that both IRE1 and AGB1 synergistically contribute to ER stress responses chemically induced by dithiothreitol (DTT) as well as to the immune responses against a phytopathogenic bacterium *Pseudomonas syringae* pv. tomato strain DC3000. Our study highlights the crosstalk between the plant UPR transducers under abiotic and biotic stress.

**Keywords:** Unfolded Protein Response, Inositol-Requiring Enzyme 1, GTP-binding Protein B1, *Pseudomonas syringae* pv. tomato DC3000, *Arabidopsis thaliana*

## Introduction

Eukaryotic cells rely on their plasma membrane-localized receptor proteins to sense the extracellular stimuli and send the signals to intracellular components.<sup>1</sup>

Among the receptor proteins, guanine nucleotide-binding proteins (G proteins) are universal signal transduction elements in all eukaryotes that have been extensively investigated due to their ubiquitous presence and diverse nature of action.<sup>2</sup> The G proteins form typically plasma membrane-bound heterotrimeric complexes<sup>3</sup> that function as hubs regulating responses to diverse developmental and environmental cues.<sup>2,4–7</sup>

The canonical G-protein complexes are composed of G $\alpha$ , G $\beta$  and G $\gamma$  subunits<sup>8</sup> and mediate the action of seven transmembrane cell surface receptors known as G protein-coupled receptors.<sup>2,8</sup> Typically, the plant genomes encode one G $\alpha$ , one G $\beta$ , and three to five G $\gamma$  subunits.<sup>2</sup> For example, rice has one G $\alpha$ , one G $\beta$  and five G $\gamma$  subunits<sup>9</sup> while Arabidopsis contains one G $\alpha$  (AtGPA1),<sup>10</sup> three extra-large G $\alpha$ 's (XLG1/XLG2/XLG3),<sup>11,12</sup> one G $\beta$  (AGB1)<sup>13</sup> and three G $\gamma$  (AGG1, AGG2, and AGG3) subunits.<sup>14–16</sup>

It is well established that the plant G proteins play important roles in a multitude of developmental responses to stimuli such as light, nutrients, sugar, and regulation of growth and stomatal density, among others.<sup>2,8,17–22</sup> Moreover, G proteins are implicated in phytohormone signaling, most notably auxin,<sup>18</sup> gibberellic acid,<sup>23,24</sup> brassinosteroids (BR),<sup>23</sup> abscisic acid (ABA),<sup>25</sup> and jasmonic acid.<sup>8</sup> Moreover, G proteins are also extensively involved in plant defense responses. Evidence suggests that AGB1 (G $\beta$ ), AGG1/AGG2 (G $\gamma$ ), and XLG2/XLG3 (extra-large G $\alpha$ ) participate in Arabidopsis innate immune responses for defenses against a broad spectrum of pathogens.<sup>8,26–29</sup> Additional reports indicate that the G proteins also constitute an integral part of

resistance mechanisms against necrotrophic fungal infections<sup>8,26</sup>.

G proteins are primarily associated with the plasma membrane; however, a fraction of the Arabidopsis G $\beta$  subunit, GTP-binding protein  $\beta$ 1 (AGB1), was detected in association with the ER membrane,<sup>30</sup> providing an intriguing connection between G proteins and the ER signaling. The ER, as the largest membrane system of a eukaryotic cell, plays a central and integrative role in the coordination of cellular transport and signaling.<sup>31</sup> The ER coordinates the essential cellular processes such as membrane protein synthesis, folding, post-translational modifications, and peptide delivery to target locations, ensuring the maintenance of proteostasis.<sup>31,32</sup> Biotic and abiotic stress can disrupt these processes, leading to the accumulation of malfolded or unassembled proteins in the ER, forming toxic protein aggregates that cause subsequent ER stress.<sup>33</sup> The onset of ER stress triggers several responses to restore cellular homeostasis. Among those, unfolded protein response (UPR) is a universal form of the ER stress signaling executed by Inositol-Requiring Enzyme 1 (IRE1) and aimed at correcting the aberrant ER conditions and protecting cellular viability.<sup>34-37</sup> IRE1 is an evolutionarily conserved trans-membrane sensor serine/threonine kinase equipped with an N-terminal ER-resident stress-sensing domain and a C-terminal endoribonuclease domain.<sup>37,38</sup> Arabidopsis contains three IRE homologs: IRE1a, IRE1b, and IRE1c.<sup>36,39</sup> IRE1a and IRE1b are the full-length homologs extensively involved in ER stress signaling in response to various biotic and abiotic stimuli<sup>36,39-42</sup> and share considerable amino acid sequence similarity especially within their cytoplasmic tails.<sup>43</sup> Whereas, IRE1c is a truncated variant,<sup>39</sup> which lacks the ER-resident N-terminal domain and plays a crucial role in gametogenesis in the

absence of IRE1b.<sup>39</sup> Upon biotic or abiotic stress, transcription and translation rapidly intensify, which places a burden on the ER protein folding machinery. The luminal domain of IRE1 senses the accumulation of misfolded peptides, leading to IRE1 homooligomerization, trans-autophosphorylation, and culminates in the activation of unconventional splicing of its cognate mRNA substrate *bZIP60* to mediate downstream signal transduction.<sup>42,44</sup>

Mounting evidence suggests the existence of a crosstalk between IRE1 and G protein signaling during ER stress. AGB1 has been reported to be involved in UPR through a pathway parallel to IRE1,<sup>30,40</sup> as evidenced by the heightened sensitivity to chemical ER stress, aggravated short-root phenotypes, and decreased expression of a suite of ER chaperones in the triple mutants *ire1a/ire1b/agb1* when compared to *ire1a/ire1b* or *agb1* alone.<sup>40</sup> Another report further corroborated the *AGB1*'s involvement in the sensitivity to tunicamycin (Tm; a potent inhibitor of N-linked glycosylation) and ER chaperone expression.<sup>30</sup> In addition to its role in the ER stress responses, AGB1 is also implicated in diverse developmental and physiological processes, and the *agb1* mutants display several related phenotypes, such as reduced hypocotyl lengths, shorter siliques,<sup>2,18,45–47</sup> altered leaf and flower shape,<sup>18,47</sup> enhanced cell division in roots and excess lateral roots,<sup>18</sup> higher stomatal density<sup>21</sup> and altered metal ion profiles.<sup>48</sup> Furthermore, AGB1 was shown to physically interact with a group I bZIP protein (VIP1),<sup>49</sup> which is involved in the regulation of extracellular osmolarity and turgor pressure. The loss of AGB1 function additionally caused altered abiotic stress responses, for example, increased drought tolerance,<sup>22</sup> hypersensitivity to salt stress,<sup>50</sup> enhanced programmed cell death,<sup>51</sup> altered responses to

hormones, i.e., BR, ABA, and auxin, as well as altered sugar sensing.<sup>23,45,52–56</sup>

Several studies reported the involvement of AGB1 in plant immunity,<sup>57</sup> demonstrating reduced reactive oxygen species accumulation upon microbial infection,<sup>56,58,59</sup> hypersensitivity to fungal infections by *Alternaria brassicicola*,<sup>3,8</sup> *Botrytis cinerea*,<sup>26</sup> *Plectosphaerella cucumerina*,<sup>26,60</sup> and *Fusarium oxysporum*.<sup>8,26,28</sup> An earlier report also indicated that AGB1 is involved in defenses against hemibiotrophic bacteria *Pseudomonas syringae*<sup>59</sup> in a manner that is independent of salicylic acid (SA) signaling.

Here, we set out to provide more insights into the relationship of AGB1 and IRE1 in ER stress signaling and the mechanisms of resistance to *P. syringae*. We employed a genetic approach using single and combinatorial loss-of-function mutants of AGB1, IRE1a, and IRE1b to assess the differential sensitivity of these genotypes to two established ER stress-inducing chemicals, tunicamycin (Tm) and dithiothreitol (DTT), by measuring plant fresh weight and root elongation rates following chemical exposure. We also quantified the levels of susceptibility to infection with a phytopathogenic bacterium *P. syringae* pv. *tomato* strain DC3000. Our results showed that *Arabidopsis* AGB1 is required for effective ER stress and immune responses, and provided evidence suggesting that AGB1 works in parallel and synergistically with the IRE1 pathway to regulate ER homeostasis.

## Materials and methods

### Plant materials

Ecotype Columbia (Col-0) was used as the control genotype in this study. T-DNA and EMS mutant lines *agb1-2* (CS6535), *ire1a-2* (SALK\_018112), *ire1b-4* (SAIL\_238\_F07)<sup>42</sup> and *npr1-1* (CS3726)<sup>61</sup> was obtained from Arabidopsis Biological Resource Center (ABRC). The phenotypes of rosette leaves in all genotypes are illustrated in Figure 1. Phenotypes of seedlings treated with tm and DTT are displayed in Figure 2a, 3a and 4a. All pictures were taken by NIKON D5600 camera and images were prepared using Adobe Photoshop (Version: 22.4.2).



Figure 1. Representative phenotypes of Arabidopsis plants used in the study. Plants were photographed by NIKON D5600 camera. Images were prepared using Adobe Photoshop (Version: 21.2.4).

### ER stress response assays

Arabidopsis seeds were sterilized with a wash buffer (70% Ethanol and 0.05% Triton) and stratified at 4°C for 3 days on half-strength solid Murashige Skoog (MS)

media plates (Phytotechnology Labs, Overland Park, KS, USA). The MS plates were then transferred to a growth chamber under a 12 h light/12 h dark photoperiod; 40% relative humidity; 21°C and 100 µmol/m<sup>2</sup>/s light intensity. The plants were grown vertically for 7 days, followed by the appropriate chemical ER stress treatment.

For tunicamycin (Tm) sensitivity assays, 7 days old Arabidopsis seedlings were transferred to 12-well plates containing liquid half-strength MS media supplemented with Tm concentration of 0.3 µg/mL (Tocris Bioscience) or mock (DMSO). After 5 days of Tm exposure, the total fresh weight of seedlings was recorded. 15 seedlings were used per biological replication and at least three biological replications were performed.

For dithiothreitol (DTT) sensitivity assays, 7 days old Arabidopsis seedlings were transferred to 12-well plates containing liquid half-strength MS media supplemented with 0.75 mM of DTT (ACROS Organics) or mock (ddH<sub>2</sub>O). After 7 days of DTT exposure, the total fresh weight of seedlings was recorded. An average of 15 seedlings was used per biological replication and at least four biological replications were performed. For root length assays, 7 days old seedlings were transferred to half-strength solid MS media plates with or without 0.75 mM of DTT. After 7 days, the root length was measured using a ruler. An average of 15 seedlings was used per biological replication and at least four biological replications were performed.

### ***Bacterial strain and growth quantification***

For bacterial quantification assays, seedlings were sown in individual pots on sterilized soil (SunGro Horticulture, Super-Fine Germinating Mix) and transferred to a cold room facility for stratification at 4°C for 7–10 days. After stratification, the pots were

transferred to a controlled growth room facility with 12 h light/12 h dark photoperiod; 40% relative humidity; 21°C and 100 µmol/m<sup>2</sup>/s light intensity. 10–15 days old seedlings were transplanted into 72-well flats for growth. 3–4 weeks old rosette leaves were infiltrated with *Pseudomonas syringae* pv. *tomato* DC3000 (*Pst* DC3000) (OD<sub>600</sub> = 0.0002) using needleless syringes and bacterial growth was quantified after 72 hours.<sup>62</sup> 3 leaves per plant, 6 plants per biological replication, and at least three biological replications were performed.

### ***Statistical analyses***

Statistical differences were calculated by two-tailed Student's *t*-test or one-way ANOVA in Microsoft Excel. RStudio (ggplot2) was used to generate the graph in Figure 3 while MS Excel was used to make graphs in Figure 2b, 3b, and 4b. Statistically significant differences are indicated with \*p < .05, \*\*p < .01, \*\*\*p < .001, or \*\*\*\*p < .0001.

## **Results**

### ***Responses to ER stress***

A decade ago, the *Arabidopsis* AGB1 was proposed to operate in an ER stress-responsive pathway that is independent of and parallel to IRE1a/IRE1b.<sup>40</sup> While previous studies reported somewhat conflicting findings on the specific role of AGB1 in ER stress, ranging from enhanced sensitivity to enhanced tolerance,<sup>30,40,63</sup> here we set out to better understand the possible combinatory effects of AGB1 with IRE1 homologs when exposed to different chemical ER stressors. Toward this, we crossed the *agb1-2* mutants with the *ire1a-2/ire1b-4* double mutant plants (further referred to as *ire1a-2/1b-4*) to

obtain the triple mutant *ire1a-2/ire1b-4/agb1-2* (further referred to as *ire1a-2/1b-4/agb1-2*). All of these mutants showed distinguishable morphology from wild-type Col-0 under our growth conditions (Figure 1) and the previously described rounder rosette leaves phenotype of the *agb1-2* plants was also detected under our growth conditions in the *ire1a-2/1b-4/agb1-2* plants.<sup>22</sup> Next, we subjected MS-media grown Col-0, *agb1-2*, *ire1a-2/1b-4* and *ire1a-2/1b-4/agb1-2* seedlings to treatments with 0.3 µg/mL Tm, which we previously determined to be the ideal concentration for the detection of mild defects in the UPR tolerance,<sup>64</sup> and we quantified their total weight after 5 days of exposure. We found that all of the tested genotypes were sensitive to Tm, as indicated by the statistically significant decrease in the relative weight (*P*-value < 0.00001) when compared to their respective mock-treated control groups (Table 1).

**Table 1.** P-values from independent sample (two-tailed) *t*-test for fresh weight data resulting from the Tm treatment experiments.

Comparison of Tm-treated genotypes:	<i>p</i> -value
Col-0 to <i>ire1a-2/1b-4</i>	< 0.00001
Col-0 to <i>agb1-2</i>	< 0.00001
<i>Col-0 to ire1a-2/1b-4/ agb1-2</i>	0.009688
<i>ire1a-2/1b-4 to ire1a-2/1b-4/ agb1-2</i>	0.037884
<i>agb1-2 to ire1a-2/1b-4/ agb1-2</i>	<u>0.14394</u>

We observed that the Tm exposure reduced the weight of the *agb1-2* plants more dramatically than that of Col-0 (Figure 2 a, b), which is in agreement with the previous findings on this specific *agb1* mutant allele.<sup>40,63</sup> We detected an enhanced Tm sensitivity in the *ire1a-2/1b-4* seedlings, which was expected given the pivotal roles of IRE1a and IRE1b in plant ER stress responses, and is also consistent with the earlier reports.<sup>64,65</sup> The

triple mutant *ire1a-2/1b-4/agb1-2* displayed a statistically significant reduction in the fresh weight; however, its Tm sensitivity was not further enhanced compared to the double mutant *ire1a-2/1b-4* seedlings (Figure 2 a, b).

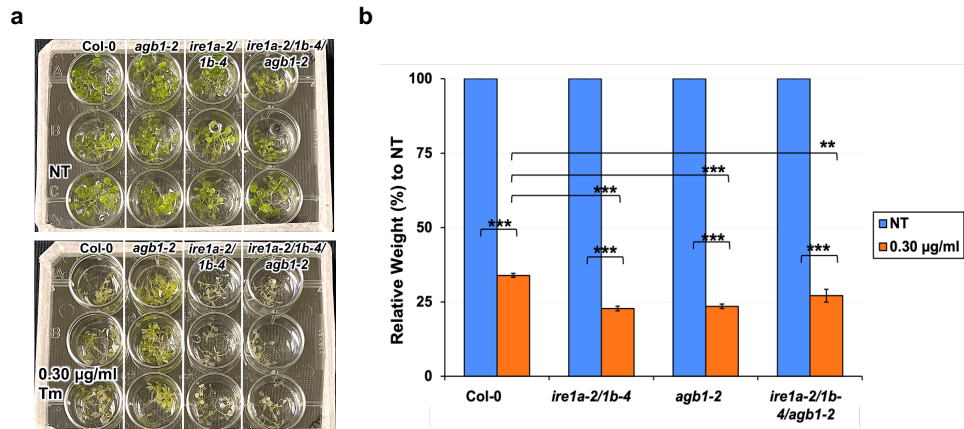


**Figure 2.** Analysis of chemical ER stress sensitivity to 0.3 µg/ml tunicamycin (Tm) on fresh weight of indicated genotypes. Seedlings were grown vertically on solid MS media for 7 days, then transferred to fresh liquid MS media without (NT = no treatment) or with Tm. Five days following Tm exposure, the seedlings were photographed. (a) and total fresh weight of at least 30 plants per biological replication was recorded (b). At least three biological replications were performed. Statistical analyses were performed by two-tailed Student's t-test or one-way ANOVA in Excel. Error bars show mean ± SD ( $n \geq 30$ ). Significant differences are indicated by asterisks (\*\*\*)  $p < .001$ , \*\*  $p < .01$ ). Short solid bars connecting bars represent the comparison of fresh weight between untreated and treated samples for each genotype, while long solid lines represent the comparison of fresh weights of Tm-treated plants between Col-0 and an indicated mutant.

To substantiate our findings with Tm and further test the genetic relationship between AGB1 and IRE1a/IRE1b pathways in *Arabidopsis* chemically-induced ER stress, we exposed the mutants to another ER stress-eliciting chemical, dithiothreitol (DTT), and measured their total fresh weight 7 days following the treatment. We found that all of the tested genotypes were sensitive to 0.75 mM DTT and displayed a statistically significant reduction in their fresh weights as compared to their respective mock-treated control groups (Table 2). In response to treatment, the average fresh weight of the *agb1-2* plants

**Table 2.** P-values from independent sample (two-tailed) *t*-test for fresh weight data resulting from the DTT treatment experiments.

Comparison of DTT-treated genotypes:	<i>p</i> -value
Col-0 to <i>ire1a-2/1b-4</i>	0.000273
Col-0 to <i>agb1-2</i>	0.269186
Col-0 to <i>ire1a-2/1b-4/ agb1-2</i>	< 0.00001
<i>ire1a-2/1b-4</i> to <i>ire1a-2/1b-4/ agb1-2</i>	< 0.00001
<i>agb1-2</i> to <i>ire1a-2/1b-4/ agb1-2</i>	< 0.00001

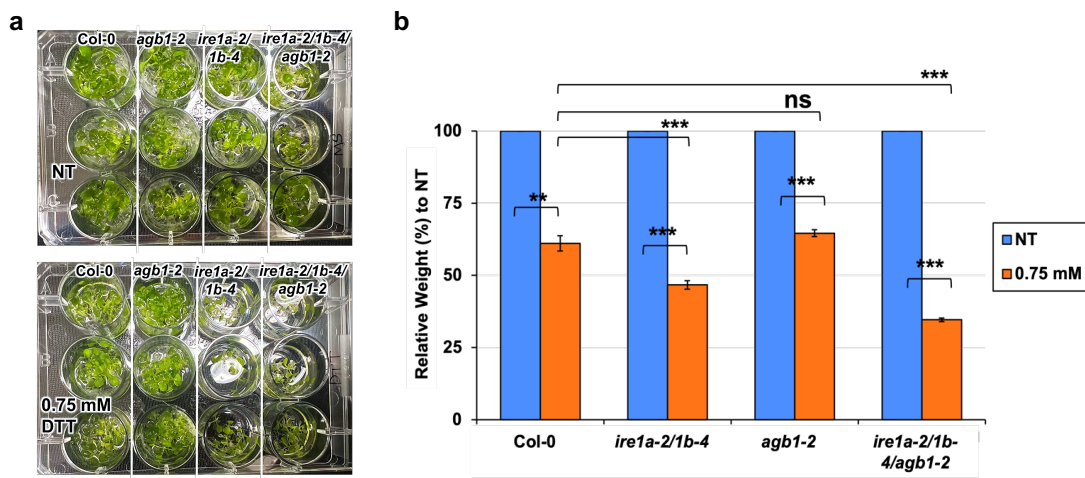


**Figure 3.** Analysis of chemical ER stress sensitivity to 0.75 mM DTT on fresh weight of indicated genotypes. Seedlings were grown vertically on solid MS media for 7 days, then transferred to fresh liquid MS media without (NT = no treatment) or with DTT. Seven days following DTT exposure, the seedlings were photographed (a) and total fresh weight of at least 30 plants per biological replication was recorded (b). At least three biological replications were performed. Statistical analyses were performed by two-tailed Student's *t*-test or one-way ANOVA in Excel. Error bars show mean  $\pm$  SD ( $n \geq 30$ ). Significant differences are indicated by asterisks (\*\* $p < .001$ , \*\* $p < .01$ ), while "ns" indicates no statistically significant differences. Short solid bars connecting bars represent the comparison of fresh weight between untreated and treated samples for each genotype, while long solid lines represent the comparison of fresh weights of DTT-treated plants between Col-0 and an indicated mutant.

was not significantly different when compared to that of Col-0 (Figure 3 a, b). Whereas

*ire1a-2/1b-4* double mutants showed a significantly increased DTT sensitivity, weighing

~30% less than the Col-0 control plants. The DTT-treated triple mutants *ire1a-2/1b-4/agb1-2* displayed a further reduction in their fresh weight compared to all other tested genotypes, indicating a synergistic effect of the IRE1a/IRE1b and AGB1 pathways on the Arabidopsis sensitivity to DTT-triggered chemical ER stress (Figure 3 a, b).

Given that we were able to better observe the genetic interaction between IRE1a/IRE1b and AGB1 using the DTT-induced ER stress treatment, we further investigated the effect of this compound on the inhibition of root elongation. We grew the above-described genotypes vertically on plates supplemented with 0.75 mM DTT and we observed that all of the experimental plants showed marked sensitivity to DTT exposure as reflected by a statistically significant reduction in root length (Figure 4 a, b and Table 3).

**Table 3.** P-values from independent sample (two-tailed) *t*-test for root length data resulting from the DTT treatment experiments.

Comparison of genotypes:	NT to DTT <i>p</i> -value	DTT to DTT <i>p</i> -value
Col-0	< 0.00001	-
<i>ire1a-2/1b-4</i>	< 0.00001	-
<i>agb1-2</i>	< 0.00001	-
<i>ire1a-2/1b-4/ agb1-2</i>	< 0.00001	-
Col-0 to <i>ire1a-2/1b-4</i>	-	0.025996
Col-0 to <i>agb1-2</i>	-	< 0.00001
Col-0 to <i>ire1a-2/1b-4/ agb1-2</i>	-	0.002349
<i>ire1a-2/1b-4 to ire1a-2/1b-4/ agb1-2</i>	-	0.217358
<i>agb1-2 to ire1a-2/1b-4/ agb1-2</i>	-	< 0.00001

When grown under control conditions, *agb1-2* roots grew slightly longer than wild-type, whereas *ire1a-2/1b-4* and *ire1a-2/1b-4/agb1-2* produced roots shorter than

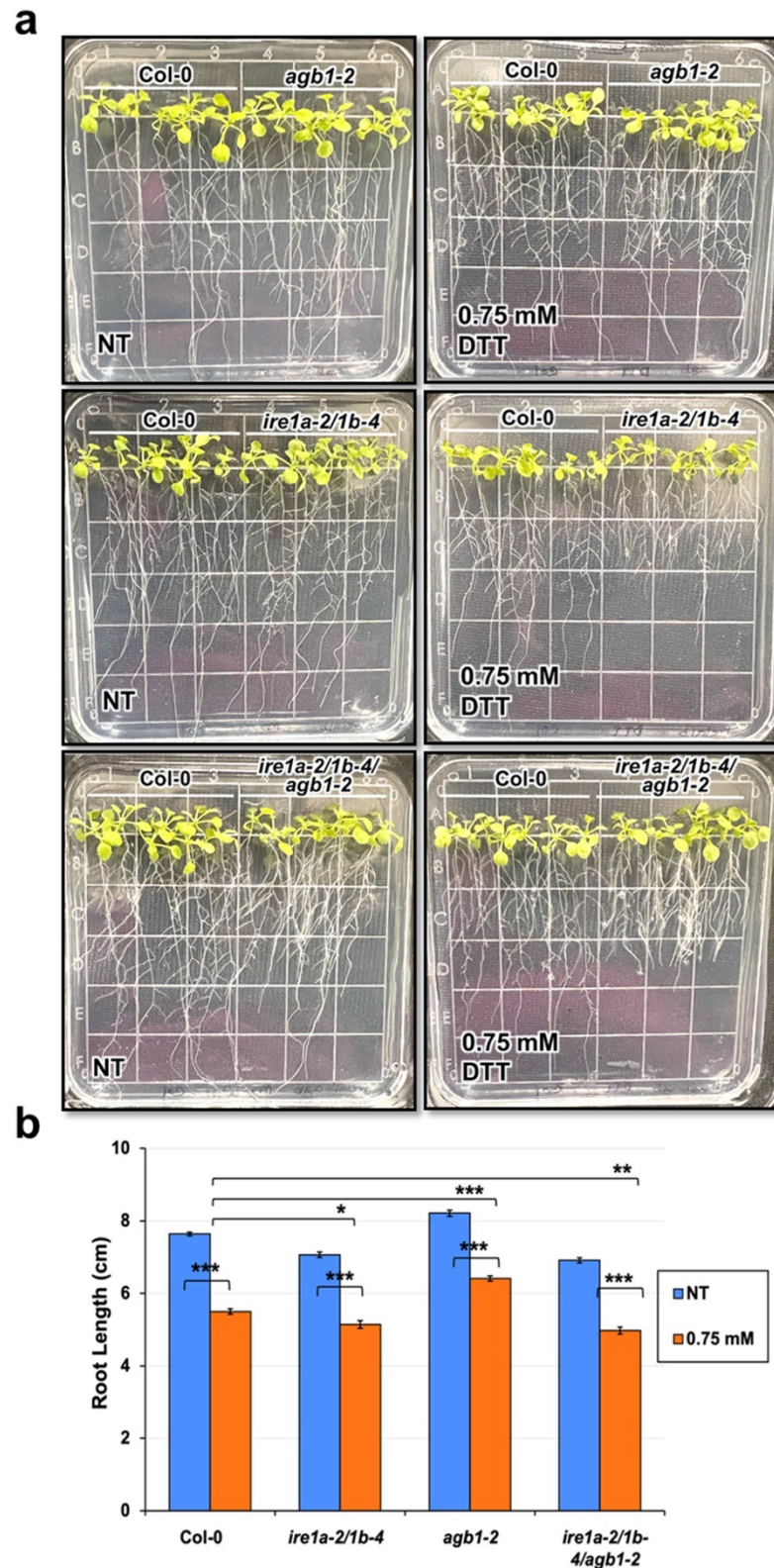


**Figure 4.** Analysis of root length in response to a chemical ER stress triggered by exposure to 0.75 mM DTT of indicated genotypes. Seedlings were grown vertically on solid MS media for 7 days, then transferred to fresh plates containing solid MS media without (NT = no treatment) or with DTT. After 7 days, the seedlings were photographed (a) and root length was measured using a ruler (b). An average of 15 seedlings was used per biological replication and at least four biological replications were performed. Statistical analyses were performed by two-tailed Student's t-test or one-way ANOVA in Excel. Error bars show mean  $\pm$  SD ( $n \geq 30$ ). Significant differences are indicated by asterisks (\*\* $p < .001$ , \*\* $p < .01$ , \* $p < .05$ ). Short solid bars connecting bars represent the comparison of root length between untreated and treated samples for each genotype, while long solid lines represent the comparison of root length of DTT-treated plants between Col-0 and an indicated mutant genotype.

those of Col-0. These findings are consistent with a previous study on these genotypes.<sup>40</sup>

Upon exposure to DTT, the *agb1-2* roots displayed a reduction in length but were still longer than those of Col-0 seedlings. In agreement with the fresh weight DTT assay results, the seedlings of the double mutant *ire1a-2/1b-4* showed a significant DTT sensitivity and produced shorter roots compared to Col-0 (Figure 4 a, b and Table 3). Moreover, we detected a slightly more pronounced DTT sensitivity in the triple mutant *ire1a-2/1b-4/agb1-2*, which was the genotype with the shortest roots following the treatment, despite having comparable root size to the double mutant *ire1a-2/1b-4* when grown in the absence of the chemical ER stress (Figure 4 a, b). This result further substantiates the notion that the DTT-induced chemical ER stress involves a synergistic effect of the IRE1a/IRE1b and AGB1 pathways in Arabidopsis.

### **Responses to bacterial infection with *Pst DC3000***

Earlier reports from our lab indicated that IRE1a and IRE1b play an important role in mediating the basal defense responses and systemic acquired resistance against

*Pseudomonas syringae* infection.<sup>42</sup> On the other hand, evidence exists in support of AGB1's involvement in defense responses against *P. syringae*,<sup>59</sup> although the molecular mechanisms governing its contribution remain to be elucidated. Infection with *P. syringae* is known to cause an increased burden on the cellular translation, protein modifications, and secretion, which can lead to an overwhelmed ER function, accumulation of misfolded peptide aggregates and, in turn, severe ER stress.<sup>66</sup> Given an indication that

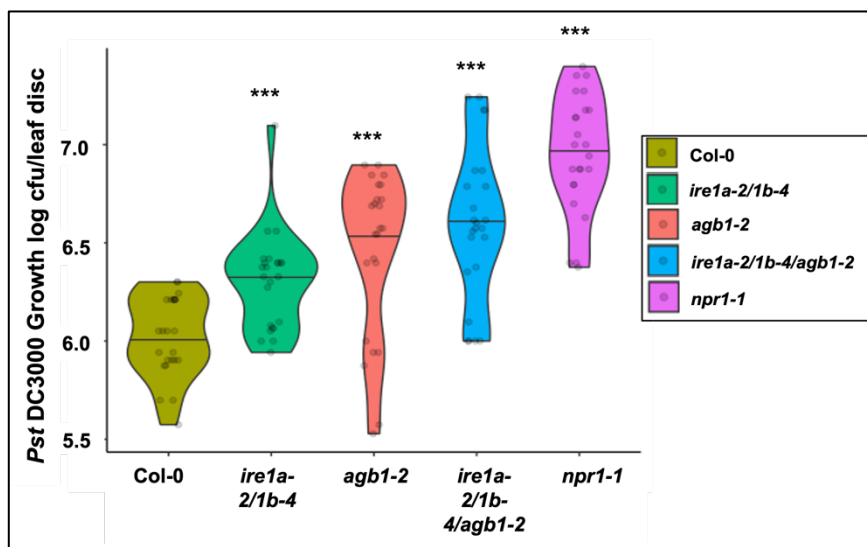


**Figure 5.** Bacterial infection with *Pseudomonas syringae* pv. tomato DC3000. Leaves of 4 weeks old plants of indicated genotypes were syringe infiltrated with the pathogen. *In planta* bacterial growth was quantified at 3 days post inoculation. The violin plots extend from 25th to 75th percentiles and whiskers extend from the minimum to the maximum levels. Light gray dots represent individual data points. Black lines in the middle represent the median. The data was generated from three independent biological replicates. Statistical analyses were performed in MS Excel by One-Way ANOVA. Significant differences in bacterial loads compared to Col-0 are indicated by asterisks (\*\*\*)  $p < .001$ .

IRE1a/IRE1b operate in a signaling pathway independent of AGB1 during UPR signaling, as reported previously<sup>40</sup> and inferred from the results of DTT sensitivity assays described above, we next asked if IRE1a/IRE1b and AGB1 have independent and possibly cumulative contributions to the immune response mounted against a virulent strain of *P.*

*syringae* *Pst* DC3000. Toward this, we subjected the wild type Col-0 (positive control), *agb1-2*, *ire1a-2/1b-4* and *ire1a-2/1b-4/agb1-2* along with the hypersusceptible *npr1-1* mutant to *Pst* DC3000 infection. We used a low bacterial inoculum dose of *Pst* DC3000 (OD<sub>600nm</sub> = 0.0002) to precisely assess the disease phenotypes in the individual genotypes. As expected, the Col-0 plants showed mild disease symptoms and limited pathogen proliferation (Figure 5), while the *npr1-1* exhibited the highest levels of bacterial accumulation, amassing ~31 times more bacterial colonies. The single mutant *agb1-2* and double mutant *ire1a-2/1b-4* displayed significantly enhanced bacterial loads compared to Col-0, which is consistent with earlier reports.<sup>42,59,65</sup> The triple mutant *ire1a-2/1b-4/agb1-2* showed a further increased bacterial susceptibility compared to *ire1a-2/1b-4* and *agb1-2*, supporting 0.7 log (~5 times) more bacterial growth than Col-0 (Figure 5), and further substantiating the hypothesis that the IRE1 and AGB1 likely act non-redundantly and have a cumulative contribution to plant stress responses, including immunity to a bacterial pathogen.

Collectively, our results suggest that AGB1 contributes to both DTT-mediated chemical ER stress as well as pathogen-triggered ER stress in a manner that is distinct from and synergistic with the IRE1-mediated ER stress-responsive pathway in Arabidopsis.

## Discussion

The plant signaling pathways utilize a complex network of interactions to orchestrate biochemical and physiological responses in response to various stresses. To ensure adequate and integrated responses, plants often engage different signaling pathways that are interlinked with each other. In both animals and plants, G proteins

have been well documented to act as hubs interconnecting various cellular signaling pathways.<sup>67–69</sup> Our study showed that the Arabidopsis G protein subunit  $\beta$ 1 (AGB1) cross-talks with the IRE1a and IRE1b homologs to modulate the abiotic and biotic ER stress response mechanisms. While the functions, mechanism of action, and importance of both IRE1a/IRE1b<sup>34–36,40,42,65</sup> and AGB1<sup>2,19,40,47,56,60</sup> in Arabidopsis have been well characterized, the nature of their cooperative roles in UPR remains unclear. Our findings support the notion that AGB1 and IRE1 signaling pathways are at least partially independent and can act synergistically in their response mechanisms, as proposed in an earlier study.<sup>40</sup>

Our study uncovered both commonalities and differences in how Tm and DTT engage AGB1 and IRE1a/b signaling pathways. This finding is not surprising given the distinct modes of action mediated by these two compounds. Tm causes ER stress by interrupting the enzyme GlcNac phosphotransferase, thereby preventing N-linked glycosylation.<sup>70</sup> On the other hand, DTT is a strong reducing agent that inhibits disulfide bond formation during protein folding, which induces acute ER stress.<sup>71</sup> Tm and DTT have been demonstrated to differentially affect the kinetics of ER stress and UPR target gene expression.<sup>72</sup> In our study, seedlings treated with Tm showed enhanced sensitivity to this stressor, as illustrated by a statistically significant decrease in their fresh weights. While the *agb1-2* and *ire1a-2/ib-4* demonstrated heightened sensitivity, the combinatorial triple mutant *ire1a-2/ib-4/agb1-2* did not show further enhanced ER stress phenotypes, possibly because the conditions used by us have already maximized and saturated the responses mediated by the IRE1a/b pathway in the highly sensitized *ire1a-2/ib-4* mutant background. However, treatments with DTT exerted overall a milder degree of

the ER stress than Tm and thus, provided a more sensitive experimental setup to detect the synergistic contributions of both pathways to ER stress responses, as demonstrated by the lowest fresh weights and shortest roots of the triple mutant *ire1a-2/1b-4/agb1-2* seedlings compared to *agb1-2* and *ire1a-2/1b-4*.

The specific dose and duration of the chemical ER stress treatment could be the reason behind some contrasting reports on the AGB1's roles in ER stress. While earlier research using various Tm concentrations supported conclusions ranging from significant sensitivity of *agb1* plants<sup>40,63</sup> to no substantial difference<sup>40</sup> to enhanced resistance,<sup>30</sup> the experimental setup varied between these studies, as did the age of seedlings, the concentration of Tm, duration of exposure to Tm, and the specific *agb1* T-DNA insertion mutant line used. Our conclusion is consistent with the findings of Chen and Brandizzi<sup>40</sup> and Cho et al.,<sup>63</sup> where the *agb1-2* plants were shown to have heightened Tm sensitivity. Moreover, our work provides additional experimental evidence for the role of AGB1 in chemical ER stress responses using a different stressor, DTT, and highlights the synergistic effects of IRE1a/b and AGB1 in this physiological process as previously proposed by Chen and Brandizzi.<sup>40</sup> While the *agb1-2* plants did not show a marked reduction in their fresh weight and root length following DTT exposure, it should be noted that their fresh weights were higher and roots were longer than those of Col-0 under control conditions and we hypothesize that these phenotypes may give the *agb1-2* plants an advantage in withstanding the chemical ER stress. The effect of AGB1's mutation, however, was clearly observed when the *agb1-2* plants were crossed into the highly sensitive *ire1a-2/1b-4* background. Hence, we concluded

that AGB1 works synergistically with IRE1 during UPR induced by DTT to maintain the ER homeostasis.

Previous studies reported the independent contributions of IRE1a/IRE1b<sup>35,36,42,65</sup> and AGB1<sup>2,19,40,47,56,59,60</sup> to plant immune responses. In our study, we provide evidence that both IRE1a/IRE1b and AGB1 are required for initiating the basal defense response against the virulent bacterial pathogen (Figure 5), as the triple mutant *ire1a-2/1b-4/agb1-2* harbored a significantly higher number of bacteria than did the *ire1a-2/1b-4* and *agb1-2* plants. Under the infection conditions tested (inoculation with a low bacterial dose), the *agb1-2* plants showed a more susceptible phenotype than *ire1a-2/1b-4*, which indicates a trend opposite to the findings with DTT. This observation points toward an intriguing possibility that AGB1 may play a prominent role in the alleviation of biotic stress induced UPR. Nonetheless, and consistent with the DTT results, the *ire1a-2/1b-4/agb1-2* triple mutants supported the highest levels of bacterial growth, further confirming the synergistic relationship of these two signaling pathways.

In summary, our study provided evidence of AGB1 contributions to both DTT-mediated chemical ER stress as well as pathogen-triggered ER stress in a manner that is distinct from and synergistic with the IRE1-mediated ER stress-responsive pathway in Arabidopsis. Our study highlights the novel aspects of crosstalk between the plant UPR transducers under abiotic and biotic stress.

### Acknowledgments

The authors wish to thank Danish Diwan and Katrina Sahawneh for providing valuable experimental suggestions.

## References

- 1 Wettschureck, N. & Offermanns, S. Mammalian G proteins and their cell type specific functions. *Physiol Rev* **85**, 1159-1204, doi:10.1152/physrev.00003.2005 (2005).
- 2 Urano, D. & Jones, A. M. Heterotrimeric G protein-coupled signaling in plants. *Annu Rev Plant Biol* **65**, 365-384, doi:10.1146/annurev-arplant-050213-040133 (2014).
- 3 Trusov, Y. *et al.* Heterotrimeric G proteins-mediated resistance to necrotrophic pathogens includes mechanisms independent of salicylic acid-, jasmonic acid/ethylene- and abscisic acid-mediated defense signaling. *Plant J* **58**, 69-81, doi:10.1111/j.1365-313X.2008.03755.x (2009).
- 4 Gilman, A. G. G proteins: transducers of receptor-generated signals. *Annu Rev Biochem* **56**, 615-649, doi:10.1146/annurev.bi.56.070187.003151 (1987).
- 5 Hamm, H. E. The many faces of G protein signaling. *J Biol Chem* **273**, 669-672, doi:10.1074/jbc.273.2.669 (1998).
- 6 Neubig, R. R. & Siderovski, D. P. Regulators of G-protein signalling as new central nervous system drug targets. *Nat Rev Drug Discov* **1**, 187-197, doi:10.1038/nrd747 (2002).
- 7 Pierce, K. L., Premont, R. T. & Lefkowitz, R. J. Seven-transmembrane receptors. *Nat Rev Mol Cell Biol* **3**, 639-650, doi:10.1038/nrm908 (2002).
- 8 Trusov, Y. *et al.* Heterotrimeric G proteins facilitate Arabidopsis resistance to necrotrophic pathogens and are involved in jasmonate signaling. *Plant Physiol* **140**, 210-220, doi:10.1104/pp.105.069625 (2006).
- 9 Trusov, Y., Chakravorty, D. & Botella, J. R. Diversity of heterotrimeric G-protein gamma subunits in plants. *BMC Res Notes* **5**, 608, doi:10.1186/1756-0500-5-608 (2012).

- 10 Ma, H., Yanofsky, M. F. & Meyerowitz, E. M. Molecular cloning and characterization of GPA1, a G protein alpha subunit gene from *Arabidopsis thaliana*. *Proc Natl Acad Sci U S A* **87**, 3821-3825, doi:10.1073/pnas.87.10.3821 (1990).
- 11 Ding, L., Pandey, S. & Assmann, S. M. *Arabidopsis* extra-large G proteins (XLGs) regulate root morphogenesis. *Plant J* **53**, 248-263, doi:10.1111/j.1365-313X.2007.03335.x (2008).
- 12 Zhu, H. *et al.* *Arabidopsis* extra large G-protein 2 (XLG2) interacts with the Gbeta subunit of heterotrimeric G protein and functions in disease resistance. *Mol Plant* **2**, 513-525, doi:10.1093/mp/ssp001 (2009).
- 13 Weiss, C. A., Garnaat, C. W., Mukai, K., Hu, Y. & Ma, H. Isolation of cDNAs encoding guanine nucleotide-binding protein beta-subunit homologues from maize (ZGB1) and *Arabidopsis* (AGB1). *Proc Natl Acad Sci U S A* **91**, 9554-9558, doi:10.1073/pnas.91.20.9554 (1994).
- 14 Mason, M. G. & Botella, J. R. Completing the heterotrimer: isolation and characterization of an *Arabidopsis thaliana* G protein gamma-subunit cDNA. *Proc Natl Acad Sci U S A* **97**, 14784-14788, doi:10.1073/pnas.97.26.14784 (2000).
- 15 Mason, M. G. & Botella, J. R. Isolation of a novel G-protein gamma-subunit from *Arabidopsis thaliana* and its interaction with Gbeta. *Biochim Biophys Acta* **1520**, 147-153, doi:10.1016/s0167-4781(01)00262-7 (2001).
- 16 Chakravorty, D. *et al.* An atypical heterotrimeric G-protein gamma-subunit is involved in guard cell K<sup>(+)</sup>-channel regulation and morphological development in *Arabidopsis thaliana*. *Plant J* **67**, 840-851, doi:10.1111/j.1365-313X.2011.04638.x (2011).

- 17 Jones, A. M., Ecker, J. R. & Chen, J. G. A reevaluation of the role of the heterotrimeric G protein in coupling light responses in Arabidopsis. *Plant Physiol* **131**, 1623-1627, doi:10.1104/pp.102.017624 (2003).
- 18 Ullah, H. *et al.* The beta-subunit of the Arabidopsis G protein negatively regulates auxin-induced cell division and affects multiple developmental processes. *Plant Cell* **15**, 393-409, doi:10.1105/tpc.006148 (2003).
- 19 Chen, Y., Ji, F., Xie, H. & Liang, J. Overexpression of the regulator of G-protein signalling protein enhances ABA-mediated inhibition of root elongation and drought tolerance in Arabidopsis. *J Exp Bot* **57**, 2101-2110, doi:10.1093/jxb/erj167 (2006).
- 20 Grigston, J. C. *et al.* D-Glucose sensing by a plasma membrane regulator of G signaling protein, AtRGS1. *FEBS Lett* **582**, 3577-3584, doi:10.1016/j.febslet.2008.08.038 (2008).
- 21 Zhang, L., Hu, G., Cheng, Y. & Huang, J. Heterotrimeric G protein alpha and beta subunits antagonistically modulate stomatal density in Arabidopsis thaliana. *Dev Biol* **324**, 68-75, doi:10.1016/j.ydbio.2008.09.008 (2008).
- 22 Xu, D. B. *et al.* A G-protein beta subunit, AGB1, negatively regulates the ABA response and drought tolerance by down-regulating AtMPK6-related pathway in Arabidopsis. *PLoS One* **10**, e0116385, doi:10.1371/journal.pone.0116385 (2015).
- 23 Ullah, H., Chen, J. G., Wang, S. & Jones, A. M. Role of a heterotrimeric G protein in regulation of Arabidopsis seed germination. *Plant Physiol* **129**, 897-907, doi:10.1104/pp.005017 (2002).

- 24 Ueguchi-Tanaka, M. *et al.* Rice dwarf mutant d1, which is defective in the alpha subunit of the heterotrimeric G protein, affects gibberellin signal transduction. *Proc Natl Acad Sci U S A* **97**, 11638-11643, doi:10.1073/pnas.97.21.11638 (2000).
- 25 Ritchie, S. & Gilroy, S. Abscisic acid stimulation of phospholipase D in the barley aleurone is G-protein-mediated and localized to the plasma membrane. *Plant Physiol* **124**, 693-702, doi:10.1104/pp.124.2.693 (2000).
- 26 Llorente, F., Alonso-Blanco, C., Sanchez-Rodriguez, C., Jorda, L. & Molina, A. ERECTA receptor-like kinase and heterotrimeric G protein from Arabidopsis are required for resistance to the necrotrophic fungus *Plectosphaerella cucumerina*. *Plant J* **43**, 165-180, doi:10.1111/j.1365-313X.2005.02440.x (2005).
- 27 Trusov, Y. *et al.* Heterotrimeric G protein gamma subunits provide functional selectivity in Gbetagamma dimer signaling in Arabidopsis. *Plant Cell* **19**, 1235-1250, doi:10.1105/tpc.107.050096 (2007).
- 28 Liu, J. *et al.* Heterotrimeric G proteins serve as a converging point in plant defense signaling activated by multiple receptor-like kinases. *Plant Physiol* **161**, 2146-2158, doi:10.1104/pp.112.212431 (2013).
- 29 Maruta, N., Trusov, Y., Brenya, E., Parekh, U. & Botella, J. R. Membrane-localized extra-large G proteins and Gbg of the heterotrimeric G proteins form functional complexes engaged in plant immunity in Arabidopsis. *Plant Physiol* **167**, 1004-1016, doi:10.1104/pp.114.255703 (2015).
- 30 Wang, S., Narendra, S. & Fedoroff, N. Heterotrimeric G protein signaling in the Arabidopsis unfolded protein response. *Proc Natl Acad Sci U S A* **104**, 3817-3822, doi:10.1073/pnas.0611735104 (2007).

- 31 Latham, K. E. Endoplasmic reticulum stress signaling in mammalian oocytes and embryos: life in balance. *Int Rev Cell Mol Biol* **316**, 227-265, doi:10.1016/bs.ircmb.2015.01.005 (2015).
- 32 Michalak, M., Corbett, E. F., Mesaeli, N., Nakamura, K. & Opas, M. Calreticulin: one protein, one gene, many functions. *Biochem J* **344 Pt 2**, 281-292 (1999).
- 33 Schroder, M. & Kaufman, R. J. The mammalian unfolded protein response. *Annu Rev Biochem* **74**, 739-789, doi:10.1146/annurev.biochem.73.011303.074134 (2005).
- 34 Afrin, T., Diwan, D., Sahawneh, K. & Pajerowska-Mukhtar, K. Multilevel regulation of endoplasmic reticulum stress responses in plants: where old roads and new paths meet. *J Exp Bot* **71**, 1659-1667, doi:10.1093/jxb/erz487 (2020).
- 35 Korner, C. J., Du, X., Vollmer, M. E. & Pajerowska-Mukhtar, K. M. Endoplasmic Reticulum Stress Signaling in Plant Immunity--At the Crossroad of Life and Death. *Int J Mol Sci* **16**, 26582-26598, doi:10.3390/ijms161125964 (2015).
- 36 Koizumi, N. *et al.* Molecular characterization of two Arabidopsis Ire1 homologs, endoplasmic reticulum-located transmembrane protein kinases. *Plant Physiol* **127**, 949-962 (2001).
- 37 Back, S. H., Schroder, M., Lee, K., Zhang, K. & Kaufman, R. J. ER stress signaling by regulated splicing: IRE1/HAC1/XBP1. *Methods* **35**, 395-416, doi:10.1016/j.ymeth.2005.03.001 (2005).
- 38 Sidrauski, C. & Walter, P. The transmembrane kinase Ire1p is a site-specific endonuclease that initiates mRNA splicing in the unfolded protein response. *Cell* **90**, 1031-1039, doi:10.1016/s0092-8674(00)80369-4 (1997).

- 39 Pu, Y., Ruberti, C., Angelos, E. R. & Brandizzi, F. AtIRE1C, an unconventional isoform of the UPR master regulator AtIRE1, is functionally associated with AtIRE1B in Arabidopsis gametogenesis. *Plant Direct* **3**, e00187, doi:10.1002/pld3.187 (2019).
- 40 Chen, Y. & Brandizzi, F. AtIRE1A/AtIRE1B and AGB1 independently control two essential unfolded protein response pathways in Arabidopsis. *Plant J* **69**, 266-277, doi:10.1111/j.1365-313X.2011.04788.x (2012).
- 41 Noh, S. J., Kwon, C. S. & Chung, W. I. Characterization of two homologs of Ire1p, a kinase/endoribonuclease in yeast, in Arabidopsis thaliana. *Biochim Biophys Acta* **1575**, 130-134, doi:10.1016/s0167-4781(02)00237-3 (2002).
- 42 Moreno, A. A. *et al.* IRE1/bZIP60-mediated unfolded protein response plays distinct roles in plant immunity and abiotic stress responses. *PLoS One* **7**, e31944, doi:10.1371/journal.pone.0031944 (2012).
- 43 Li, Z. & Howell, S. H. Review: The two faces of IRE1 and their role in protecting plants from stress. *Plant Sci* **303**, 110758, doi:10.1016/j.plantsci.2020.110758 (2021).
- 44 Deng, Y. *et al.* Heat induces the splicing by IRE1 of a mRNA encoding a transcription factor involved in the unfolded protein response in Arabidopsis. *Proc Natl Acad Sci U S A* **108**, 7247-7252, doi:10.1073/pnas.1102117108 (2011).
- 45 Booker, K. S., Schwarz, J., Garrett, M. B. & Jones, A. M. Glucose attenuation of auxin-mediated bimodality in lateral root formation is partly coupled by the heterotrimeric G protein complex. *PLoS One* **5**, doi:10.1371/journal.pone.0012833 (2010).
- 46 Liang, Y., Zhao, X., Jones, A. M. & Gao, Y. G proteins sculpt root architecture in response to nitrogen in rice and Arabidopsis. *Plant Sci* **274**, 129-136, doi:10.1016/j.plantsci.2018.05.019 (2018).

- 47 Lease, K. A. *et al.* A mutant Arabidopsis heterotrimeric G-protein beta subunit affects leaf, flower, and fruit development. *Plant Cell* **13**, 2631-2641, doi:10.1105/tpc.010315 (2001).
- 48 Wu, T. Y. *et al.* Crosstalk between heterotrimeric G protein-coupled signaling pathways and WRKY transcription factors modulating plant responses to suboptimal micronutrient conditions. *J Exp Bot* **71**, 3227-3239, doi:10.1093/jxb/eraa108 (2020).
- 49 Tsugama, D., Liu, S. & Takano, T. A bZIP protein, VIP1, interacts with Arabidopsis heterotrimeric G protein beta subunit, AGB1. *Plant Physiol Biochem* **71**, 240-246, doi:10.1016/j.plaphy.2013.07.024 (2013).
- 50 Yu, Y. & Assmann, S. M. The heterotrimeric G-protein beta subunit, AGB1, plays multiple roles in the Arabidopsis salinity response. *Plant Cell Environ* **38**, 2143-2156, doi:10.1111/pce.12542 (2015).
- 51 Wei, Q. *et al.* Heterotrimeric G-protein is involved in phytochrome A-mediated cell death of Arabidopsis hypocotyls. *Cell Res* **18**, 949-960, doi:10.1038/cr.2008.271 (2008).
- 52 Chen, J. G. *et al.* GCR1 can act independently of heterotrimeric G-protein in response to brassinosteroids and gibberellins in Arabidopsis seed germination. *Plant Physiol* **135**, 907-915, doi:10.1104/pp.104.038992 (2004).
- 53 Pandey, S., Chen, J. G., Jones, A. M. & Assmann, S. M. G-protein complex mutants are hypersensitive to abscisic acid regulation of germination and postgermination development. *Plant Physiol* **141**, 243-256, doi:10.1104/pp.106.079038 (2006).

- 54 Wang, X. Q., Ullah, H., Jones, A. M. & Assmann, S. M. G protein regulation of ion channels and abscisic acid signaling in Arabidopsis guard cells. *Science* **292**, 2070-2072, doi:10.1126/science.1059046 (2001).
- 55 Mudgil, Y. *et al.* Arabidopsis N-MYC DOWNREGULATED-LIKE1, a positive regulator of auxin transport in a G protein-mediated pathway. *Plant Cell* **21**, 3591-3609, doi:10.1105/tpc.109.065557 (2009).
- 56 Jiang, K. *et al.* Dissecting Arabidopsis G $\beta$  signal transduction on the protein surface. *Plant Physiol* **159**, 975-983, doi:10.1104/pp.112.196337 (2012).
- 57 Urano, D., Leong, R., Wu, T. Y. & Jones, A. M. Quantitative morphological phenomics of rice G protein mutants portend autoimmunity. *Dev Biol* **457**, 83-90, doi:10.1016/j.ydbio.2019.09.007 (2020).
- 58 Ishikawa, A. The Arabidopsis G-protein beta-subunit is required for defense response against Agrobacterium tumefaciens. *Biosci Biotechnol Biochem* **73**, 47-52, doi:10.1271/bbb.80449 (2009).
- 59 Torres, M. A., Morales, J., Sanchez-Rodriguez, C., Molina, A. & Dangl, J. L. Functional interplay between Arabidopsis NADPH oxidases and heterotrimeric G protein. *Mol Plant Microbe Interact* **26**, 686-694, doi:10.1094/MPMI-10-12-0236-R (2013).
- 60 Delgado-Cerezo, M. *et al.* Arabidopsis heterotrimeric G-protein regulates cell wall defense and resistance to necrotrophic fungi. *Mol Plant* **5**, 98-114, doi:10.1093/mp/ssr082 (2012).
- 61 Cao, H., Glazebrook, J., Clarke, J. D., Volko, S. & Dong, X. The Arabidopsis NPR1 gene that controls systemic acquired resistance encodes a novel protein containing ankyrin repeats. *Cell* **88**, 57-63, doi:10.1016/s0092-8674(00)81858-9 (1997).

- 62 Liu, X. *et al.* Bacterial Leaf Infiltration Assay for Fine Characterization of Plant Defense Responses using the *Arabidopsis thaliana*-*Pseudomonas syringae* Pathosystem. *J Vis Exp*, doi:10.3791/53364 (2015).
- 63 Cho, Y., Yu, C. Y., Iwasa, T. & Kanehara, K. Heterotrimeric G protein subunits differentially respond to endoplasmic reticulum stress in *Arabidopsis*. *Plant Signal Behav* **10**, e1061162, doi:10.1080/15592324.2015.1061162 (2015).
- 64 McCormack, M. E., Liu, X., Jordan, M. R. & Pajerowska-Mukhtar, K. M. An improved high-throughput screening assay for tunicamycin sensitivity in *Arabidopsis* seedlings. *Front Plant Sci* **6**, 663, doi:10.3389/fpls.2015.00663 (2015).
- 65 Afrin, T., Seok, M., Terry, B. C. & Pajerowska-Mukhtar, K. M. Probing natural variation of IRE1 expression and endoplasmic reticulum stress responses in *Arabidopsis* accessions. *Sci Rep* **10**, 19154, doi:10.1038/s41598-020-76114-1 (2020).
- 66 Pajerowska-Mukhtar, K. M. *et al.* The HSF-like transcription factor TBF1 is a major molecular switch for plant growth-to-defense transition. *Curr Biol* **22**, 103-112, doi:10.1016/j.cub.2011.12.015 (2012).
- 67 Klopfleisch, K. *et al.* *Arabidopsis* G-protein interactome reveals connections to cell wall carbohydrates and morphogenesis. *Mol Syst Biol* **7**, 532, doi:10.1038/msb.2011.66 (2011).
- 68 Pandey, S. Plant receptor-like kinase signaling through heterotrimeric G-proteins. *J Exp Bot* **71**, 1742-1751, doi:10.1093/jxb/eraa016 (2020).
- 69 Azeloglu, E. U. & Iyengar, R. Signaling networks: information flow, computation, and decision making. *Cold Spring Harb Perspect Biol* **7**, a005934, doi:10.1101/cshperspect.a005934 (2015).

- 70 Heifetz, A., Keenan, R. W. & Elbein, A. D. Mechanism of action of tunicamycin on the UDP-GlcNAc:dolichyl-phosphate Glc-NAc-1-phosphate transferase. *Biochemistry* **18**, 2186-2192, doi:10.1021/bi00578a008 (1979).
- 71 Cleland, W. W. Dithiothreitol, a New Protective Reagent for Sh Groups. *Biochemistry* **3**, 480-482, doi:10.1021/bi00892a002 (1964).
- 72 Li, B. *et al.* Differences in endoplasmic reticulum stress signalling kinetics determine cell survival outcome through activation of MKP-1. *Cell Signal* **23**, 35-45, doi:10.1016/j.cellsig.2010.07.019 (2011).

## **CHAPTER 4**

### **PROBING NATURAL VARIATION OF *IRE1* EXPRESSION AND ENDOPLASMIC RETICULUM STRESS RESPONSES IN ARABIDOPSIS ACCESSIONS**

by

Taiaba Afrin<sup>1</sup>, Minye Seok<sup>1</sup>, Brenna C. Terry<sup>1</sup>, Karolina M. Pajerowska-Mukhtar<sup>1\*</sup>

<sup>1</sup> Department of Biology, University of Alabama at Birmingham, 1300 University Blvd.,  
Birmingham, AL 35294, USA

Published, Scientific Reports volume 10, Article number: 19154 (2020),  
<https://doi.org/10.1038/s41598-020-76114-1>

Copyright ©2020, Springer Nature  
by  
Taiaba Afrin  
Used by permission  
Format adapted for dissertation

## **Abstract**

The environmental effects shape genetic changes in the individuals within plant populations, which in turn contribute to the enhanced genetic diversity of the population as a whole. Thus, individuals within the same species can acquire and accumulate genetic differences in their genomes depending on their local environment and evolutionary history.

IRE1 is a universal endoplasmic reticulum (ER) stress sensor that activates an evolutionarily conserved signaling cascade in response to biotic and abiotic stresses. Here, we selected nine different *Arabidopsis* accessions along with the reference ecotype Columbia-0, based on their geographical origins and differential endogenous IRE1 expression under steady-state conditions to investigate the natural variation of ER stress responses. We cloned and analyzed selected upstream regulatory regions of IRE1a and IRE1b, which revealed differential levels of their inducibility. We also subjected these accessions to an array of biotic and abiotic stresses including heat, ER stress-inducing chemical tunicamycin, phytohormone salicylic acid, and pathogen infection. We measured IRE1-mediated splicing of its evolutionarily conserved downstream client as well as transcript accumulation of ER-resident chaperones and co-chaperones. Collectively, our results illustrate the expression polymorphism of a major plant stress receptor and its relationship with molecular and physiological ER stress sensitivity.

## **Introduction**

Because of their sessile nature, plants constantly need to respond to their surrounding environment and adapt themselves to the ever-changing conditions to ensure a suitable balance for growth and survival<sup>1</sup>. Thus, the native habitat imposes on species a pressure to survive and evolve along with environmental changes<sup>2</sup>. The multidimensional climate fluctuations trigger simultaneous genetic variations in the individuals within the plant population, contributing to an increase in the genetic diversity of the population as a whole<sup>3</sup>. Therefore, the individuals of the same species can exhibit distinct variation in their genome sequences depending on their geographical origins and evolutionary history. The genetic variation found in populations from different natural environments demonstrates the extent of local adaptation<sup>4</sup> and allows the discovery of novel genes and alleles as signatures of plants' adaptive responses<sup>5</sup>. As such, studying natural variation can provide important insights into diverse structural and functional features: novel gene and allele identification<sup>6</sup>, cause and effect of phenotypic variation<sup>7</sup>, understanding complex traits and their impact on phenotypes<sup>8</sup>, and selective pressure towards specific traits<sup>8</sup>. These discoveries can also be useful to engineer agronomically important crop plants for better compatibility with the changing climate. *Arabidopsis thaliana* (hereafter Arabidopsis) originates from continental Eurasia and North Africa but is now extensively distributed throughout the world<sup>9</sup>. Its natural habitat is widely diversified, from beaches to the Rocky Mountains, riverbanks to roadsides<sup>4,9,10</sup>. The broad spectrum of Arabidopsis natural habitats is a major contributor to its substantial genetic variation<sup>11</sup>. Arabidopsis natural accessions around the globe show considerable genetic and phenotypic variation in terms of plant development, physiology, and adaptation to biotic as well as abiotic

stresses, manifested through traits such as rosette diameter<sup>12</sup>, plant height<sup>13</sup>, number of lateral branches<sup>13</sup>, leaf shape<sup>12</sup>, flowering time<sup>14</sup>, the structure of inflorescence<sup>15</sup>, seed dormancy<sup>16</sup>, drought resistance<sup>6</sup>, heat tolerance<sup>17</sup>, cold tolerance<sup>18</sup>, salt tolerance<sup>11</sup>, disease resistance<sup>19</sup>, resistance and tolerance to herbivores<sup>20</sup>, and circadian rhythms<sup>21</sup>. Owing to its short life cycle and small, fully sequenced genome, *Arabidopsis* has been at the forefront of plant model systems for the last 35 years<sup>22</sup>. Its worldwide distribution<sup>9,23</sup>, rich genetic resources<sup>9,23</sup>, feasibility to maintain pure lines<sup>9</sup>, adaptive nature<sup>23</sup>, availability of genome-wide single nucleotide polymorphism (SNP)<sup>4,9</sup>, and collections of materials developed by the international community<sup>16</sup> further increased its usefulness as the model plant. The analysis of *Arabidopsis* natural variation has the potential to equip us with a unique understanding of functional, ecological and evolutionary connections and relationships<sup>8</sup>. In 1996, the *Arabidopsis* Genome Initiative (AGI), an international collaborative community, initiated a project to sequence the *Arabidopsis* genome<sup>24</sup> and in 2008 followed up with a large-scale effort known as the “1001 Genome Project” to provide more refined genetic tools to the *Arabidopsis* community<sup>25</sup>. For instance, a comparative study reported that the two most-used and highly related *Arabidopsis* strains, Columbia-0 (Col-0) and Landsberg *erecta* (*Ler*) differ by a total 25,274 SNPs in their coding and non-coding regions<sup>24</sup>, which underscores the abundance of genetic natural variation within *Arabidopsis* accessions.

The endoplasmic reticulum (ER), the largest membrane system in eukaryotic cells, plays crucial roles in a variety of cellular processes, *i.e.* synthesis of membrane proteins, membrane lipids, secretory proteins, protein folding, glycosylation, disulfide bonding, post-translational modifications, and packaging to target location<sup>26,27</sup>. Disturbances

or malfunctions in any of these processes result in the accumulation of malfolded and/or unassembled proteins and subsequently trigger ER stress. The mechanisms of ER stress signalling have been studied extensively in yeast<sup>28</sup>, mammals<sup>27,28</sup>, and plants<sup>29-31</sup>. In plants, ER stress can be established by application of specific treatments, *i.e.* chemicals (tunicamycin; Tm<sup>32,33</sup>, dithiothreitol; DTT<sup>31,34</sup>, salicylic acid; SA<sup>33,35</sup>, L-azetidine-2-carboxylic acid<sup>36</sup>, cyclopiazonic acid; CPA<sup>33</sup>), viral and bacterial pathogens<sup>33,37,38</sup>, heat stress<sup>35,39,40</sup>, and salt stress<sup>41</sup>, as well as during normal growth and developmental process<sup>31,37,42</sup>. ER stress elicits several cellular responses, with the unfolded protein response (UPR) playing the predominant role<sup>32,43</sup>. UPR is a complex eukaryotic signalling pathway that functions to restore cellular homeostasis<sup>28-30</sup>. The key UPR signal activator and ER stress sensor, Inositol-Requiring Enzyme 1 (IRE1), is evolutionarily ancient and highly conserved in eukaryotes<sup>43</sup>. In *Arabidopsis*, two homologues of IRE1, known as *IRE1a* and *IRE1b*, are the critical players in the UPR signalling pathway<sup>32,33,44</sup>. *IRE1a* and *IRE1b* genes share 41% nucleotide sequence similarity and exhibit both overlapping and distinct expression patterns<sup>32,44,45</sup>. While both of these isoforms are expressed throughout the plant under steady-state conditions, *IRE1b* is specifically enriched in embryos and seeds<sup>32,44</sup> and was reported to be essential for functional male fertility<sup>46</sup>. Under stress-induced conditions, however, the two homologues show more profound functional divergence. *IRE1a* plays a predominant role in biotic stresses<sup>33</sup>, while *IRE1b* is critical during abiotic stresses<sup>39</sup>, pointing towards genetic and physiological specialisation and diversification of the two IRE1 isoforms. How the IRE1 homologues were shaped by the evolutionary forces in diverse *Arabidopsis* accessions to mitigate the ER stress is an intriguing question.

Structurally, the IRE1 proteins possess well-conserved serine/threonine protein kinase and endoribonuclease (RNase) domains, which allow IRE1 to perform dual functions<sup>47</sup>. After sensing ER stress, IRE1 dimerises, undergoes trans-autophosphorylation, and transduces downstream UPR signalling. In Arabidopsis, IRE1a and IRE1b recognise splice-site motifs in the transcript of an evolutionarily conserved basic leucine zipper transcription factor *bZIP60* and catalyse an unconventional cytoplasmic mRNA cleavage. This processed (spliced) form of *bZIP60* mRNA undergoes translation, producing an active protein that translocates to the nucleus and transcriptionally regulates an array of UPR-responsive genes to exert a cytoprotective function<sup>31,38,48</sup>. The IRE1/bZIP60 signalling pathway plays a distinct role in mitigating both biotic and abiotic stresses to restore cellular homeostasis<sup>33,49</sup>. This unconventional splicing is referred to as regulated IRE1-dependent splicing (RIDS). Under acute or prolonged ER stress, IRE1 also degrades mRNAs through a site-specific cleavage process termed as regulated-IRE1 dependent RNA decay (RIDD)<sup>50,51</sup>. In Arabidopsis, RIDD mainly targets the mRNAs encoding secreted proteins<sup>52</sup>.

Abiotic and biotic stress factors have been shown to activate the ER stress signalling in plants. Among several environmental stressors, heat has been previously identified as a major factor affecting the vegetative and reproductive growth of plants<sup>53,54</sup>. Heat is also known to be a powerful inducer of UPR in yeast<sup>55</sup>, mammals<sup>56</sup>, and plants<sup>33,35,39,40,57,58</sup>. Upon heat stress, plant cells initiate a cascade of stress responses, including the UPR signalling in the ER<sup>55,56</sup>. The phytohormone salicylic acid (SA) plays a pivotal role in several growth and developmental processes<sup>59,60</sup>, disease resistance signalling<sup>61,62</sup>, and defence responses against biotrophic pathogens<sup>63,64</sup>. Moreover, SA was

previously shown to activate the IRE1/bZIP60 arm of the UPR signalling pathway via *bZIP60* splicing<sup>58,65,66</sup>. Here, we selected 10 representative natural accessions of *Arabidopsis* and studied the contributions of genetic variation of *IRE1a* and *IRE1b* and downstream ER stress responses in the context of biotic and abiotic triggers. We showed that both *IRE1a* and *IRE1b* vary in their expression levels in the set of selected *Arabidopsis* ecotypes, and we demonstrated differential levels of *bZIP60* splicing in diverse ecotypes in response to SA and heat. We also detected varied accumulation levels of UPR chaperons and co-chaperons upon SA treatment. Finally, we evaluated whole-plant tolerance of the accessions to ER stress triggered by heat and Tm as well as disease resistance phenotypes of these accessions upon infection with a bacterial pathogen. Overall, we provided insights into the natural variation of ER stress responses in *Arabidopsis*.

## Results and Discussion

### *Selection of the representative accessions to study genetic variation of *IRE1a* and *IRE1b* expression*

To better understand how the evolutionary forces and natural selection have shaped the regulatory regions of *IRE1a* and *IRE1b* loci in *Arabidopsis*, we studied Col-0 as the reference accession along with nine additional accessions stemming from six different countries (Fig. 1, Table 1). Our selection was based on the values of basal expression levels of *IRE1a* and/or *IRE1b* genes in respective accessions, derived from the Plant eFP browser<sup>67-70</sup>. Specifically, we selected Bla-5, Dra-1 and En-T as accessions that display the highest basal expression of *IRE1a* compared to Col-0, while Is-0 and M7323S were the additional two accessions with the lowest basal *IRE1a* transcript levels (Table

1). We used the same strategy for *IRE1b* and selected M7323S, HR-5, and Fr-2 that exhibited elevated basal expression levels, and MS-0 and Ta-0 that were characterised by diminished basal *IRE1b* transcript accumulation compared to Col-0.

**Table 1:** Selected accessions for *IRE1a* and *IRE1b* genes, characterised in this study. Basal expression log<sub>2</sub> ratios and fold changes (derived from *Arabidopsis* eFP browser) as well as geographical origin, if known, are shown.

Accessions for <i>IRE1a</i>	log <sub>2</sub> Ratio	Fold Change	Country of Origin	Accessions for <i>IRE1b</i>	log <sub>2</sub> Ratio	Fold Change	Country of Origin
<b>Col-0</b>	0.0	1.0	NW Poland	<b>Col-0</b>	0.0	1.0	NW Poland
<b>Bla-5</b>	0.7	1.62	Blanes, Spain	<b>MS-0</b>	-0.32	0.8	Moscow, Russia
<b>Dra-1</b>	0.79	1.73	Drahonin, Czech Republic	<b>M7323S</b>	0.34	1.27	Unknown
<b>En-T</b>	1.12	2.17	Tajikistan	<b>HR-5</b>	0.29	1.22	United Kingdom
<b>Is-0</b>	-0.86	0.55	Isenberg, Germany	<b>Fr-2</b>	0.46	1.38	Frankfurt, Germany
<b>M7323S</b>	-0.81	0.57	Unknown	<b>Ta-0</b>	-0.32	0.8	Tabor, Czech Republic

### *Differential response of *IRE1a* and *IRE1b* genes to heat stress*

We set out to validate the basal expression values obtained from the Plant eFP browser through an independent experiment. In plants, heat is known to be a powerful inducer of UPR<sup>33,35,39,57,58</sup>; thus, we also examined the inducibility of *IRE1a* and *IRE1b* expression following heat treatment to assess whether basal levels coincide with induced transcript accumulation in both *IRE1a*-and *IRE1b*-related groups. Towards this, we exposed our selected natural accessions to a 90-minute-long treatment of elevated temperature (37°C). Following heat stress, we collected foliar tissues and quantified both basal

and induced levels of *IRE1a* or *IRE1b* (Fig. 2a-d). We used an *ire1a-2 ire1b-4* double mutant as a negative control in our experiment (Fig. S1a). Our results indicated that the

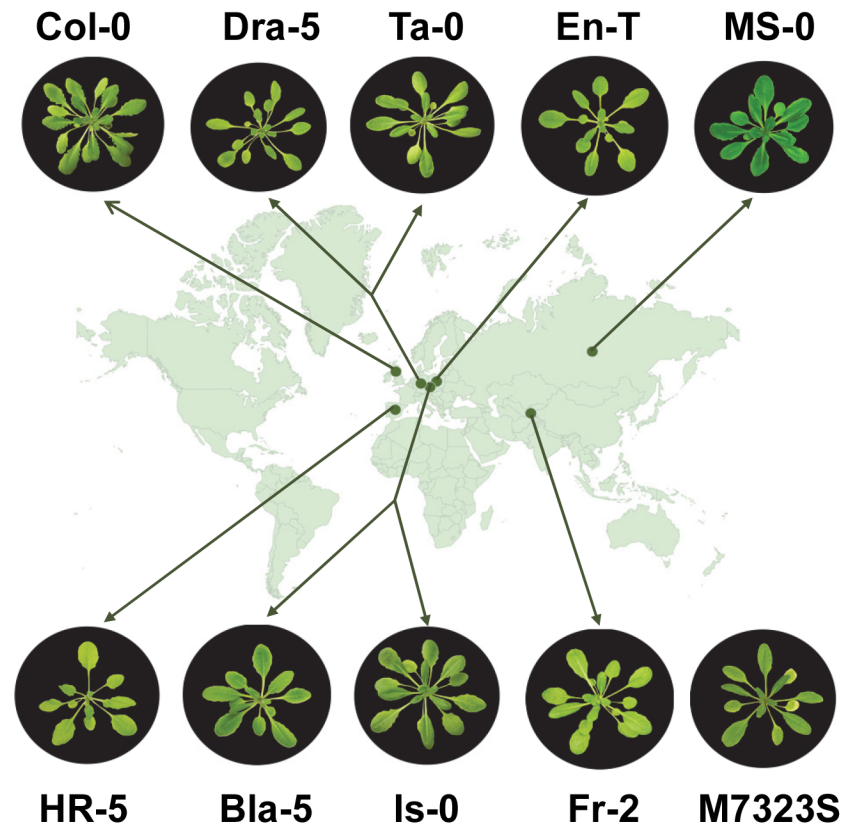


**Figure 1: Geographical distribution and representative phenotypes of selected *Arabidopsis* natural accessions used in this study.** Geographical origins are indicated by green dots on the world map. The origin of M7323S is unknown. 1-month-old plants representative of ecotypes Col-0, Bla-5, Dra-1, En-T, Is-0, MS-0, M7323S, HR-5, Fr-2, and Ta-0 are pictured.

accessions in IRE1a-related group (Bla-5, Dra-1, En-T, Is-0, M7323S) and IRE1b-related group (MS-0, M7323S, HR-5, Fr-2, and Ta-0) showed basal *IRE1a* transcript accumulation levels comparable to the results reported by the plant eFP browser<sup>68</sup> dataset (Fig. 2a, b). Specifically, Bla-5, Dra-1, and En-T plants in the IRE1a-related group exhibited higher basal *IRE1a* transcript levels, whereas Is-0 and M7323S displayed lower basal *IRE1a* accumulation. In the IRE1b-related group, we did not observe any significant

change in the *IRE1a* basal transcript accumulation, consistent with the eFP browser<sup>68</sup> dataset (Fig. 2b). When we analysed heat-induced *IRE1a* transcript levels in the *IRE1a* accession group (Fig. 2a), all ecotypes but Bla-5 significantly induced the *IRE1a* expression with respect to their basal levels. Subsequently, we compared the *IRE1a* induction in these ecotypes with the reference accession Col-0. We demonstrated that three ecotypes

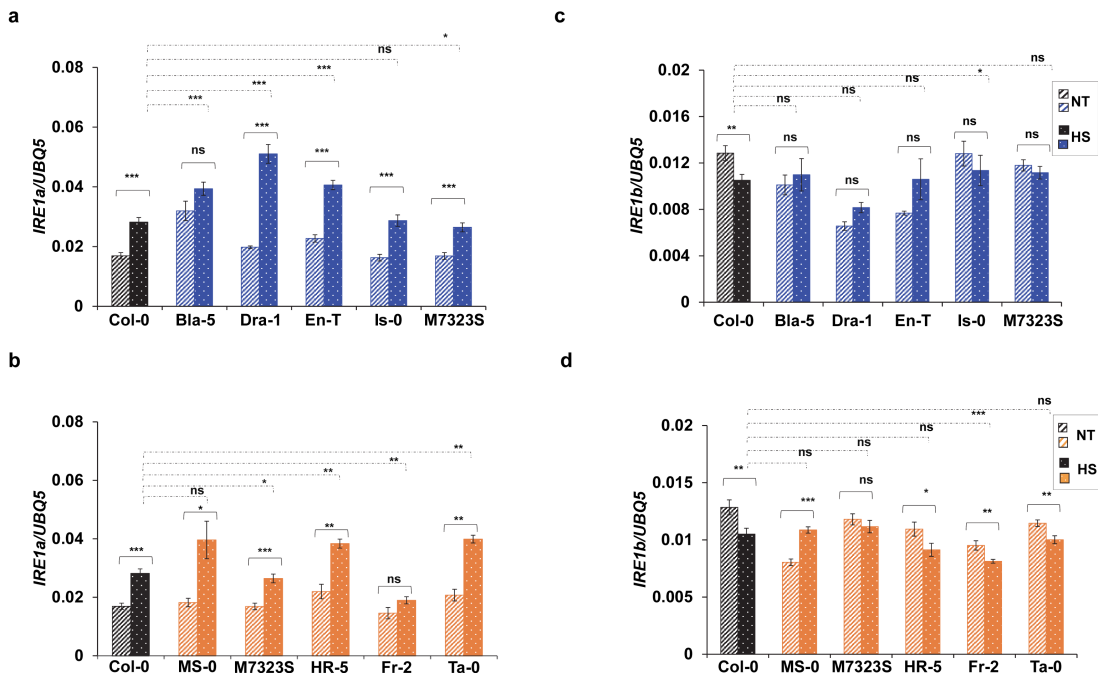


**Figure 2: Analysis of relative *IRE1a* and *IRE1b* expression levels in selected accessions before and after heat stress.** Basal and induced mRNA expression level of *IRE1a* (a, b) or *IRE1b* (c, d) of indicated accessions upon heat stress at 37°C for 90 minutes. Expression levels were measured in leaf tissue of 1-month-old *Arabidopsis* plants via qRT-PCR and were normalised to the housekeeping gene *UBQ5* (Ubiquitin 5). Dashed bars represent basal expression levels, dotted bars correspond to heat-induced expression levels. Treatment groups are represented according to legends. Colours indicate accessions grouping (blue – *IRE1a*-related accessions, orange – *IRE1b*-related accessions, black – reference accession Col-0). Statistical analyses were performed in Excel by One-Way ANOVA. At least three independent biological replicates, each with three technical replicates were performed. Error bars show mean  $\pm$  SD. Significant differences are indicated by asterisks (\*\* p < 0.01, \*\*\* p < 0.001, \* p < 0.05), while “ns” indicates no statistically significant differences. Solid lines connecting bars represent the comparison of basal to heat-induced expression levels for each individual accession, while dashed lines represent the comparison of induced expression levels between Col-0 and an indicated accession.

(Bla-5, Dra-1, and En-T) showed significantly higher *IRE1a* expression levels compared to Col-0, M7323S had a significantly reduced *IRE1a* expression, while the heat-induced *IRE1a* expression in Is-0 was comparable to Col-0. In the IRE1b-related group, *IRE1a* expression was significantly increased in all accessions except Fr-2 when compared to their corresponding controls. We also assayed the heat-induced *IRE1a* transcript compared to reference accession Col-0 and demonstrated a modest but statistically significant increase in the levels of expression in all accessions under study except Ms-0 (Fig. 2b). When comparing fold induction above the basal levels of each accession, the strongest inducers of *IRE1a* were Dra-1, MS-0, and Ta-0 (Fig. S1b, c). Taken together, our data indicate that all of the assayed accessions show an intact ability to induce *IRE1a* following heat stress, and the basal levels are not an accurate predictor of heat inducibility for the *Arabidopsis* *IRE1a* gene (Fig. 2a, b).

Next, we tested *IRE1b* mRNA levels in both *IRE1a*- and *IRE1b*-related accessions. Given that M7323S displayed differential basal levels for both *IRE1a* and *IRE1b*, we also included this ecotype in the *IRE1b*-related category. Overall, *IRE1b* basal and induced expression remained statistically unchanged in the *IRE1a*-related accession group except in the reference accession Col-0, which displayed a subtle but significant reduction in the *IRE1b* mRNA levels (Fig. 2c). By comparing heat-induced *IRE1b* expression levels in the *IRE1a*-accession group with Col-0, we also found no statistically significant differences except for a modest increase in the Is-0 ecotype. Subsequently, we tested the basal and heat-induced *IRE1b* mRNA levels in the *IRE1b*-accession group. While two ecotypes (MS-0 and Ta-0) exhibited expression patterns consistent with the values reported in the plant eFP browser, we noted that the basal expression levels for M7323S,

HR-5, and Fr-2 were different under our experimental conditions (Fig. 2d). Several factors in the experimental set-ups can account for such differences, including the age of plants and light cycle (4 weeks old plants and a 12/12-hour light/dark cycle vs. 4-day-old seedlings and continuous light in our and eFP browser datasets, respectively). After we exposed the *IRE1b* accession group to heat, we found that the expression of *IRE1b*, unlike *IRE1a*, does not increase after heat stress, with one accession, MS-0, being a notable exception (Fig. 2d). The decreased transcript accumulation in Col-0 is also consistent with the data from the plant eFP browser<sup>67</sup>. When compared to the induced levels of *IRE1b* among the *IRE1b*-related ecotypes, we observed a trend of elevated *IRE1b* mRNA levels in Col-0 compared to all five accessions with HR-5, Fr-2, and Ta-0 displaying statistically significant differences (Fig. 2d). Analysing fold induction above the basal levels of each accession, the strongest inducers of *IRE1b* were En-T and MS-0 (Fig. S1d, e). Collectively, we concluded that the *IRE1b* expression levels were not induced upon treatment with heat in the majority of the tested ecotypes.

### ***Single Nucleotide Polymorphisms (SNPs) within the *IRE1a* and *IRE1b* promoter regions***

Our results indicate that the transcriptional control of *IRE1a* and *IRE1b* differs between the two homologues and varies vastly among the natural accessions at both basal and induced levels. To gain more insights into the genetic variation that may be responsible for the observed array of transcriptional dynamics, we sequenced the predicted *IRE1a* and *IRE1b* promoter regions of Col-0 and other accessions classified into *IRE1a*- or *IRE1b*-related groups. We performed multiple sequence alignments of promoter

sequences from these selected accessions and the reference sequences of Col-0. We detected a number of SNPs in transcription factor binding sites across the *IRE1a* promoter regions of Bla-5, Dra-1, and En-T (Table 2, Fig. S2a), which were the top three accessions showing elevated basal *IRE1a* expression levels. Subsequently, we subjected these polymorphic promoter regions to computational predictions of potential binding sites for transcription factors. Our bioinformatics-aided analysis identified DNA binding with one finger (DOF), Myb-related DNA binding proteins (Golden2, ARR, Psr), and Arabidopsis homeobox protein as the potential regulators (Table 2, Fig. S2a). The three accessions selected for higher basal levels of *IRE1a* (Bla-5, Dra-1, and En-T) (Table 1) all share the presence of an SNP at position 7616536 (A->T) in the predicted binding site for Myb-related DNA binding proteins, which is unique to this set of promoters and could be one of the factors contributing to elevated basal levels in those ecotypes. All newly identified promoter sequences have been submitted to NCBI GenBank under accession numbers listed in Table 2. No SNPs were detected in the predicted transcription factor binding sites of *IRE1b* promoter regions, consistent with the previously noted lack of variability in their expression patterns before and after heat treatments.

**Table 2:** SNPs found in *IRE1a* promoter regions across different *Arabidopsis* accessions.

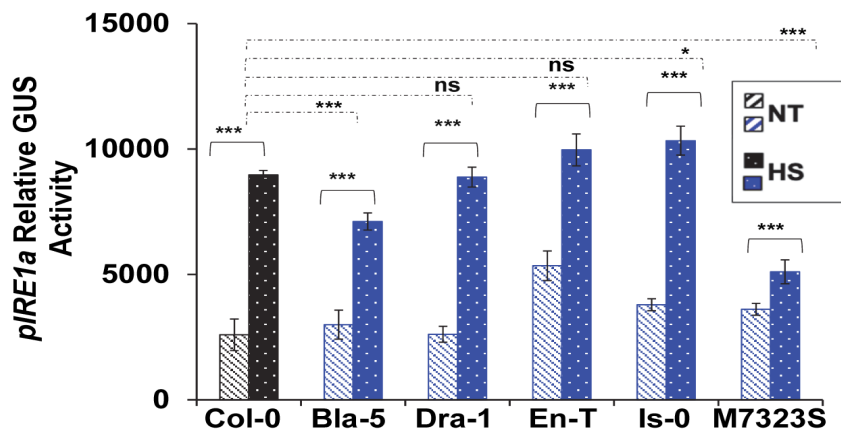
Element Sequence	Promoter position	TF Binding Sites Family Information	SNP Position	Gene Bank ID
acggtataAAAGcgttt	7616364- 7616380	DNA binding with one finger (DOF)	7616379 Bla-5 (G->A)	MT344169
aaaATTAtta	7616531- 7616536	Myb-related DNA binding proteins (Golden2, ARR, Psr)	7616536 Bla-5, Dra-1, En-T (A->T)	MT344169, MT344170, MT344171
ttAGATccgcc	7616480- 7616490	Arabidopsis homeobox protein	7616481 Dra-1, En-T (G->A)	MT344170, MT344171

***Transient expression assays to understand IRE1a and IRE1b expression patterns driven through accession-specific promoter sequences***

To understand the potential contribution of natural variation in the regulation of *IRE1a* and *IRE1b* expression, we employed transient MUG assays. Moreover, this experiment, at last in part, provided an independent experimental method to support our qRT-PCR-based expression data (Fig. 2). Towards this, we cloned sequence-verified promoter fragments corresponding to *IRE1a* and *IRE1b* from their respective accession groups into a plant Gateway expression vector pAM-PAT-GW-GUS. This led to the generation of transcriptional promoter::GUS reporter fusions designated as pAM-PAT-p $\text{IRE1a}^{\text{Col-0}}$ -GUS, pAM-PAT-p $\text{IRE1a}^{\text{Bla-5}}$ -GUS, pAM-PAT-p $\text{IRE1a}^{\text{Dra-1}}$ -GUS, pAM-PAT-p $\text{IRE1a}^{\text{En-1}}$ -GUS, pAM-PAT-p $\text{IRE1a}^{\text{Is-0}}$ -GUS and pAM-PAT-p $\text{IRE1a}^{\text{M7323S}}$ -GUS in *IRE1*-related accession group. Likewise, we generated pAM-PAT-p $\text{IRE1b}^{\text{Col-0}}$ -GUS, pAM-PAT-p $\text{IRE1b}^{\text{MS-0}}$ -GUS, pAM-PAT-p $\text{IRE1b}^{\text{M7323S}}$ -GUS, pAM-PAT-p $\text{IRE1b}^{\text{HR-5}}$ -GUS, pAM-PAT-p $\text{IRE1b}^{\text{Fr-2}}$ -GUS, and pAM-PAT-p $\text{IRE1b}^{\text{Ta-0}}$ -GUS in the *IRE1b*-related accession group category. We transiently expressed these two sets of clones in *Arabidopsis Col-0* leaves using Agrobacterium-mediated transformation over a three-day period followed by induction by heat stress at 37°C for 90 minutes (Fig. 3). We collected the leaf tissues, extracted proteins, and quantified activities of β-glucuronidase (GUS) in each sample via a fluorometric MUG assay<sup>71</sup>. Consistent with our qRT-PCR data, we observed a differential but significant heat-mediated induction of GUS activities driven through the set of *IRE1a* promoters compared to their respective basal levels. It is important to note that the qRT-PCR analyses were performed in the native accession backgrounds, while the MUG assays were done in *Col-0* to avoid any accession-specific heterogeneity in gene

regulatory mechanisms. Intriguingly, pAM-PAT-pIRE1a<sup>Bla-5</sup>-GUS displayed an opposite induction trend in Col-0 background (Fig. 3a) compared to its endogenous *in planta* activity (Fig. 2a). The pIRE1a<sup>Bla-5</sup> sequence contains a unique SNP at nucleotide 7616379 (G->A) (Table 2), which alters a predicted binding site for a DOF transcription factor and might be one of the possible mechanisms explaining the differential inducibility of this promoter variant in the Bla-5 vs. Col-0 backgrounds. pAM-PAT-pIRE1a<sup>Dra-1</sup>-GUS and pAM-PAT-pIRE1a<sup>En-T</sup>-GUS exhibited comparable induction to pAM-PAT-pIRE1a<sup>Col-0</sup>-GUS, indicating that SNP 7616481 (G->A) does not cause elevated basal and/or heat-

**a**



**b**

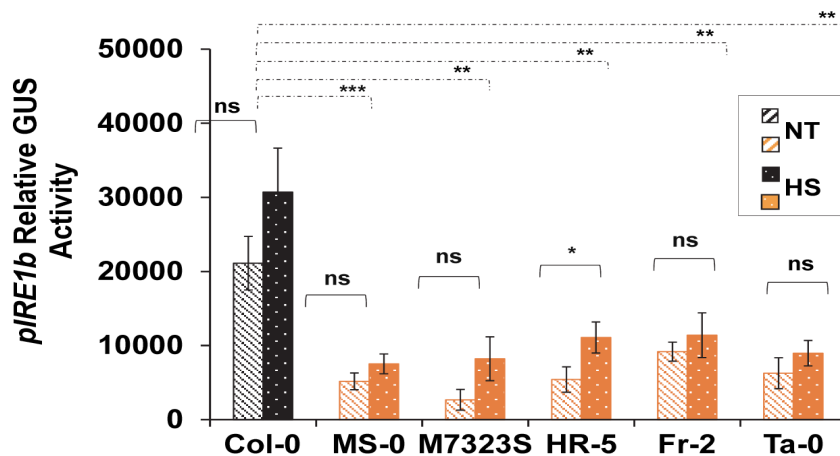


**Figure 3: Transient MUG assay to determine basal and heat-induced activities of IRE1a and IRE1b promoters from selected ecotypes.** Quantification of  $\beta$ -glucuronidase (GUS) activity in Arabidopsis Col-0 leaves transiently expressing transcriptional promoter::GUS reporter fusions corresponding to *IRE1a* (pAM-PAT-pIRE1a<sup>Col-0</sup>-GUS, pAM-PAT-pIRE1a<sup>Bla-5</sup>-GUS, pAM-PAT-pIRE1a<sup>Dra-1</sup>-GUS, pAM-PAT-pIRE1a<sup>En-T</sup>-GUS, pAM-PAT-pIRE1a<sup>Is-0</sup>-GUS and pAM-PAT-pIRE1a<sup>M7323S</sup>-GUS) (**a**) and *IRE1b* (pAM-PAT-pIRE1b<sup>Col-0</sup>-GUS, pAM-PAT-pIRE1b<sup>MS-0</sup>-GUS, pAM-PAT-pIRE1b<sup>M7323S</sup>-GUS, pAM-PAT-pIRE1b<sup>HR-5</sup>-GUS, pAM-PAT-pIRE1b<sup>Fr-2</sup>-GUS and pAM-PAT-pIRE1b<sup>Ta-0</sup>-GUS) (**b**) before and after heat stress at 37°C for 90 minutes. Promoter activities were determined in extracts of plant tissue via fluorometric MUG assay. Statistical analyses were performed in Excel by One-Way ANOVA. At least three independent biological replicates, each with three technical replicates were performed. Error bars show mean  $\pm$  SD. Significant differences are indicated by asterisks (\*\* p<0.001, \*\* p<0.01, \* p<0.05), while “ns” indicates no statistically significant differences. Solid lines connecting bars represent the comparison of basal to heat-induced expression levels for each individual accession, while dashed lines represent the comparison of induced expression levels between Col-0 and an indicated accession.

induced *IRE1a* promoter activity under the tested conditions. Two *pIRE1a* constructs exhibited statistically differential activity levels compared to the *pIRE1a*<sup>Col-0</sup>. While pAM-PAT-pIRE1a<sup>Is-0</sup>-GUS was significantly induced in Col-0 background, pAM-PAT-pIRE1a<sup>M7323S</sup>-GUS showed a reduced activity under the tested conditions (Fig. 3a). Overall, our results suggested that *IRE1a* promoters derived from the accessions under study exhibit differential levels of activity when tested in the reporter-based transient expression assay in Col-0 background but there is no direct correlation of heat-mediated inducibility of *pIRE1a* to the SNPs described above under our experimental conditions (Fig. 3a, Table 2).

Similarly, to our results with *pIRE1a* fragments, we observed a trend of increased reporter accumulation for all *pIRE1b* constructs upon treatment with heat, although we detected a statistically significant ( $p<0.05$ ) expression difference only in pAM-PAT-pIRE1b<sup>HR-5</sup>-GUS, corroborating our qRT-PCR results (Fig. 3b). These data also further

support a minor role of *IRE1b* induction under heat stress conditions. Subsequently, we compared heat-induced *IRE1b* promoter expression differences between Col-0 and the other five ecotypes. While our qRT-PCR data showed significant *IRE1b* transcript differences upon heat treatment in only three accessions (Fig. 2c, d), the MUG assay highlighted significantly increased *IRE1b* promoter::GUS activity in pAM-PAT-p<sub>*IRE1b*</sub><sup>Col-0</sup>-GUS compared to the other five tested reporter constructs (Fig. 3b). These results indicate that the data obtained from the highly sensitive MUG assay is largely in agreement with the qRT-PCR results and further delineate the subtle *IRE1b* expression differences between Col-0 and other ecotypes. Overall, our results confirm that the heat treatment results in a more dramatic transcriptional response in the *IRE1a* expression than it is the case for its homologue, *IRE1b*. A previous study confirmed that *IRE1a* and *IRE1b* have distinct expression patterns in Arabidopsis but both can be detected in leaf tissues, biologically validating our experimental design<sup>32</sup>.

#### ***Arabidopsis* accessions display differential tolerance to heat and Tm-induced ER stresses**

To understand the potential roles of differential *IRE1a* and *IRE1b* transcript levels in different accessions, we subjected a suite of these 10 ecotypes to heat- and Tm-induced whole-plant ER stress assays. Col-0 and *ire1a-2 ire1b-4* double mutant plants were used as controls. Specifically, we exposed Arabidopsis seedlings to 42°C for 2 hours or liquid MS media supplemented with 0, 0.15 µg/mL or 0.3 µg/mL Tm, followed by total weight measurement two (heat) or three (Tm) days later. Overall, we found that all of the accessions displayed a reduction in weight in response to both ER stresses and exhibited

generally consistent trends in their levels of sensitivity to ER stress caused by heat and Tm (Fig. 4a, b). In particular, the Bla-5, En-T, Is-0, MS-0, and Fr-2 accessions showed elevated tolerance to one or both types of ER stresses. In contrast, M7323S and Ta-0 were more susceptible to both ER stress-inducing treatments, while Dra-1 was not statistically different than Col-0 (Fig. 4a, b). Moreover, HR-5 displayed a somewhat divergent response, showing significantly enhanced Tm tolerance but a slight increase in heat sensitivity that was not statistically significant. The *ire1a-2 ire1b-4* double mutants showed dramatic levels of heat and Tm sensitivity, as previously described<sup>46,72</sup>. Consistent with the elevated basal and heat-induced expression levels of *IRE1a* in Bla-5 and En-T (Fig. 2a), we showed that these two ecotypes also displayed increased tolerance to ER stress (Fig. 4a, b). The modest improvement in the heat tolerance of Is-0 seedlings might be explained through IRE1-mediated downstream regulatory steps including bZIP60 splicing (see below) rather than its expression *per se* (Fig. 4c, d). Likewise, MS-0 presented a unique feature, as it is the only accession in the IRE1b-group that was characterised by

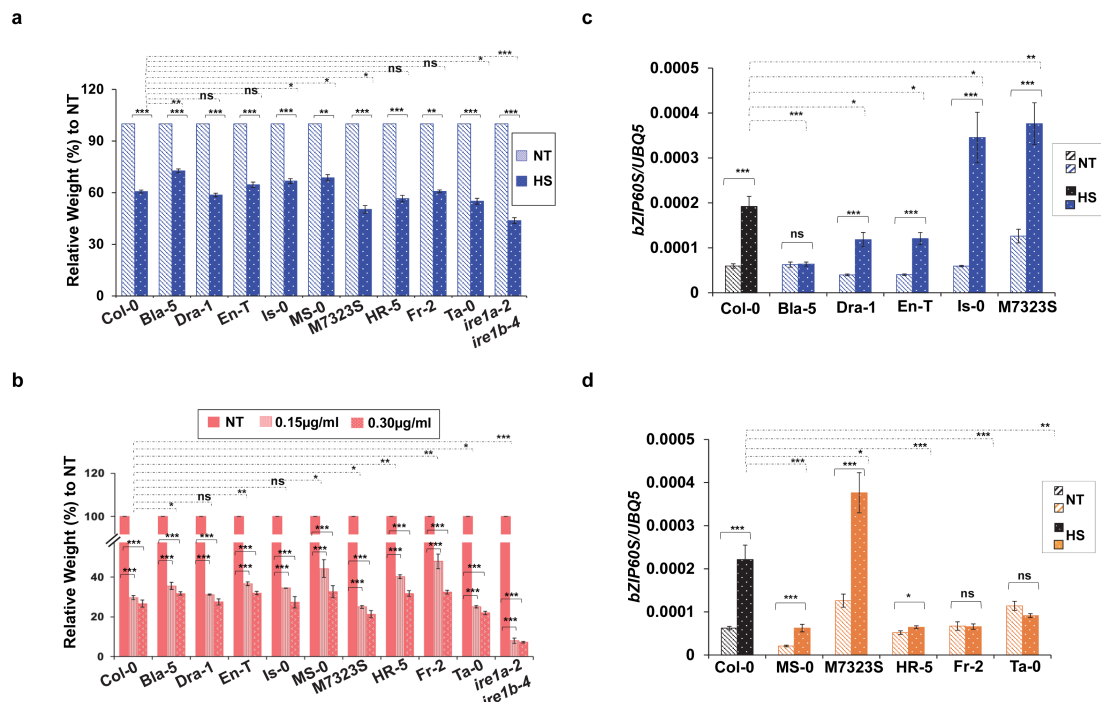


**Figure 4: Analysis of ER stress sensitivity and relative heat-induced mRNA expression levels of spliced *bZIP60* in selected accessions.** (a) Arabidopsis seedlings of indicated ecotypes were grown on solid half-strength MS media for 7 days, and then transferred to liquid half-strength MS media. 9-day-old plants were exposed to 42°C for 2 hours or kept at ambient temperature, and a total fresh weight of 10 plants per biological replication was recorded 2 days later. Three biological replications were performed; (b) 7-day-old Arabidopsis seedlings of indicated ecotypes were transferred to liquid half-strength MS media supplemented with the indicated concentration of Tm or mock. The total fresh weight of 10 plants for each of the three biological replications was recorded 3 days following Tm exposure. Statistical analyses for (a) and (b) were performed by One-Way ANOVA. Error bars show mean ± SD ( $n \geq 30$ ). Significant differences are indicated by asterisks (\*\* $p < 0.001$ , \*\* $p < 0.01$ , \* $p < 0.05$ ), while “ns” indicates no statistically significant differences. Solid lines connecting bars represent the comparison of fresh weight between untreated and treated samples for each individual accession, while dashed lines represent the comparison of fresh weights of stress-treated plants between Col-0 and an indicated accession. Basal and induced spliced *bZIP60* (*bZIP60S*) expression levels were quantified in selected IRE1a-related accessions (c) or IRE1b-related accessions (d) upon heat stress at 37°C for 90 minutes. Expression levels were measured in leaf tissue of 1-month-old Arabidopsis plants via qRT-PCR and were normalised to house-keeping gene *UBQ5* (Ubiquitin 5). Treatment groups are represented according to legends. Dashed bars represent basal expression levels, dotted bars correspond to heat-induced expression levels. Colours indicate accessions grouping (blue – IRE1a-related accessions, orange – IRE1b-related accessions, black – reference accession Col-0). Statistical analyses were performed in Excel by One-Way ANOVA. At least three independent biological replicates, each with three technical replicates were performed. Error bars show mean ± SD. Significant differences are indicated by asterisks (\*\* $p < 0.001$ , \*\* $p < 0.01$ , \* $p < 0.05$ ), while “ns” indicates no statistically significant differences. Solid lines connecting bars represent the comparison of basal to heat-induced expression levels for each individual accession, while dashed lines represent the comparison of induced expression levels between Col-0 and an indicated accession.

increased IRE1b expression levels in response to heat (Fig. 2d). On the other hand, the slight increase in ER stress tolerance demonstrated by Fr-2 could also be attributed to IRE1-independent UPR signalling pathways. Finally, the diminished ER tolerance in M7323S and Ta-0 could potentially be caused by the reduced basal *IRE1b* mRNA levels in the IRE1b-accession group (Fig. 2d and Fig. 4a, b). Overall, we revealed a positive

relationship between *IRE1a* and *IRE1b* expression levels or their downstream signalling activities and observed ER stress tolerance in diverse Arabidopsis ecotypes.

### ***Variation in IRE1-mediated bZIP60 processing upon heat stress***

A hallmark of the UPR activation in Arabidopsis is the induction of *bZIP60* mRNA splicing by *IRE1a* and *IRE1b*. Several studies previously documented a marked increase in the *bZIP60* splicing rate upon exposure to heat in Col-0<sup>33,35,39,58</sup>. It is important to note that the plant eFP browser does not include the transcript data corresponding to *bZIP60* splice variants. Thus, we experimentally tested the efficacy of *bZIP60* splicing in diverse ecotypes in response to heat. Regardless of the *IRE1a* or *IRE1b* expression in different ecotypes, we did not observe major differences in the basal *bZIP60* splicing efficiency when compared to Col-0. However, we did note a relatively lower *bZIP60* splicing activity in En-T, MS-0, and HR-5 (Fig. 4c and d). Subsequently, we investigated the *bZIP60* splicing efficacy under heat-induced conditions. Consistent with our previous study<sup>44</sup>, the reference accession Col-0 showed significant induction of *bZIP60* splicing by heat (Fig. 4c and d), whereas the *ire1a-2 ire1b-4* double mutant was used as a negative control (Fig. S2b). Except for Bla-5, all the other *IRE1a*-related ecotypes including Dra-1, En-T, Is-0, and M7323S showed significantly increased *bZIP60* splicing, indicating a successful activation of the *IRE1* signalling cascade following heat exposure. Subsequently, we measured differences in heat-induced *bZIP60* splicing across different *IRE1a*-related accessions. We demonstrated that the induced *bZIP60* splicing was significantly decreased in Dra-1 and En-T compared to Col-0. On the other hand, Is-0 and M7323S displayed more efficacious *bZIP60* splicing compared to Col-0 (Fig. 4c).

Finally, we discerned that bZIP60 splicing levels did not fully coincide with both basal and induced levels of *IRE1a* expression among the accessions within the IRE1a-related group (Fig. 4c). Intriguingly, we observed an inverse relationship between the induced *IRE1a* mRNA levels and *bZIP60* splicing, indicating possible existence of compensatory mechanisms between transcriptional and translational activation of IRE1a and its downstream signalling.

For the IRE1b-related accessions (Fig. 4d), we detected high levels of *bZIP60* splicing induction in Col-0, MS-0, and M7323S, and a moderate but statistically significant induction in HR-5. While *bZIP60* is a *bona fide* client for both IRE1a and IRE1b during heat stress, we observed some interdependent relationships between *IRE1* expression and *bZIP60* splicing efficiency. MS-0 was the only accession in our study that displayed enhanced *bZIP60* splicing, which is consistent with the increased levels of IRE1b expression following heat in that accession (Fig. 2d) and could provide a mechanistic explanation of this phenotype. M7323S plants, on the other hand, seemed to rely preferentially on the IRE1a transcriptional induction for bZIP60 splicing, as heat induced IRE1a levels were significantly induced in that accession. Finally, the HR-5 ecotype was initially selected to be a high basal IRE1b expressor but turned out to be an under-expressor with a modest induction of *bZIP60* splicing. It is possible that its ability to activate *bZIP60* splicing upon heat could be attributed to the elevated inducibility of *IRE1a* or other factors that operate at the post-translational level to regulate IRE1a/b protein activity.

Intriguingly, we did not detect any heat-induced *bZIP60* splicing in Fr-2 and Ta-0. We first confirmed that our Col-0 specific primers can hybridise to *bZIP60* orthologues

from Fr-2 and Ta-0 by analysing their bZIP60 sequences provided by the 1001 Genomes Project resource<sup>25</sup>; henceforth, we turned to find the answers in the natural history of these two ecotypes. Both accessions originate from Northern and Central Europe (Germany and the Czech Republic), where summers are relatively short and mild, thus prolonged exposure to elevated temperatures (37°C) might not be common in the natural habitat. Therefore, it is possible that the heat-responsive *bZIP60* splicing wasn't shaped by the evolutionary forces in the same way as for several other accessions tested in our experiment. A previous study in mammalian kidney cells demonstrated IRE1's downstream target *Xbp1* is spliced at 40°C but no splicing was detected at 37°C or 43°C, in contrast to robust induction of *Xbp1* splicing in those cells upon treatments with DTT (inhibitor of disulfide bond formation) and thapsigargin (inhibitor of endoplasmic reticulum Ca<sup>2+</sup> ATPase)<sup>56</sup>. These findings suggest that IRE1's downstream splicing is precisely regulated by the temperature, and extreme heat stress may inhibit the ER stress pathway. It is possible that the heat stress of 90 minutes at 37°C was perceived as acute in the *Arabidopsis* Fr-2 and Ta-0 accessions, and resulted in an inhibitory, instead of stimulatory, response. However, given that other accessions from the same geographical regions show intact *bZIP60* splicing ability, more work will be needed to ascertain the mechanistic basis for this observation<sup>39</sup>.

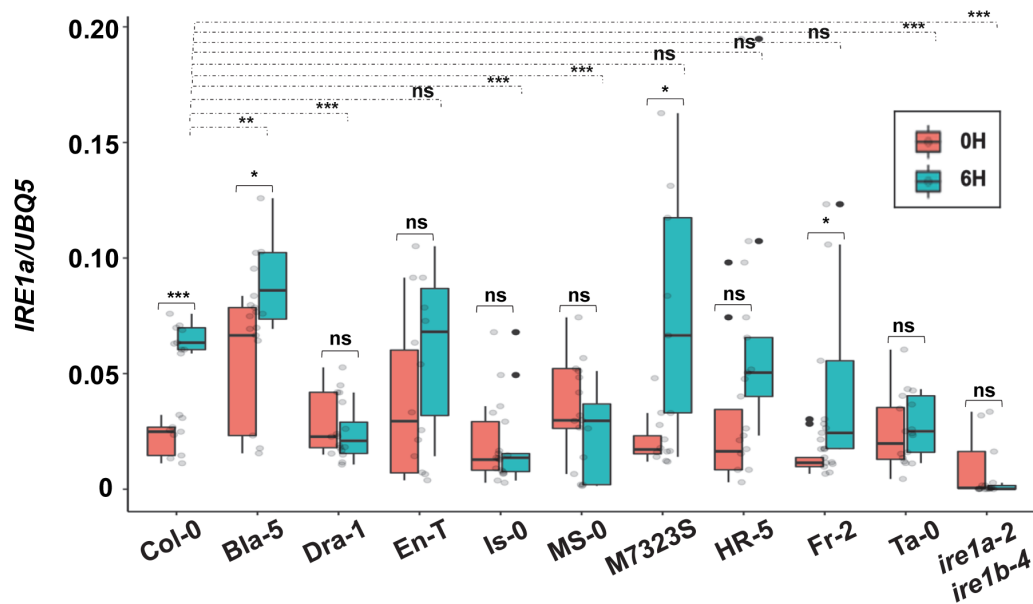
### ***Differences in IRE1-mediated UPR signalling in response to biotic stress***

Given the central role of SA signalling in inducing UPR in *Arabidopsis*, we next set out to assess whether SA exerts differential effects on *IRE1a* and *IRE1b* mRNA levels as well as their downstream UPR signalling activities in our experimental set of

Arabidopsis ecotypes. Four-week-old leaves were sprayed with 0.5mM SA for 6 hours, followed by the quantification of basal and SA-induced transcript abundance for *IRE1a* and *IRE1b* in both IRE1a- and IRE1b-group accessions. As expected, IRE1a expression was significantly induced in the reference Col-0, while no change in mRNA levels was detected in the control *ire1a-2 ire1b-4* double mutant. SA-induced *IRE1a* transcript was found to be elevated only in the Bla-5, M7323S, and Fr-2 ecotypes, while no significant change was observed in the remaining members of the IRE1a- and IRE1b-accession groups (Fig. 5a). By comparing the induced levels of IRE1a with those of Col-0, three accessions, namely Bla-5, M7323S, and Fr-2 exhibited significantly higher expression of *IRE1a*, whereas Dra-1, Is-0 and MS-0 displayed lower, albeit not statistically significant *IRE1a* mRNA abundance (Fig. 5a). Interestingly, Dra-1 showed an opposite regulation of *IRE1a* transcripts when exposed to two diverse ER inducing stressors, heat, and SA, whereas Bla-5 and M7323S consistently displayed the upregulation of *IRE1a* under both biotic and abiotic ER stress conditions (Fig. 2a, b, and 5a). When comparing fold induction above the basal levels of each accession, the strongest inducers of IRE1a were M7323S, Fr-2, Col-0, and HR-5 (Fig. S2c). In agreement with our results indicating the significant reduction of *IRE1b* transcript in response to heat, we also observed a markedly decreased *IRE1b* mRNA levels in SA-treated Col-0 plants, while no difference in the transcript abundance was observed in the control *ire1a-2 ire1b-4* double mutant (Fig. 5b). Similar to the results obtained for heat induced *IRE1b* transcript abundance, no significant change was observed in both IRE1a and IRE1b accession groups (Fig. 5b). By comparing the *IRE1b* induction levels between Col-0 and other ecotypes, however, we observed an overall reduction of *IRE1b* transcript accumulation in our experimental set of

accessions (Fig. 5b). When analysing fold induction above the basal levels of each accession, only En-T noticeably induced the *IRE1b* transcript, Bla-5 showed a minimal increase, and all the remaining accessions downregulated *IRE1b* expression in response to SA (Fig. S2d). It is worth noting that some of the ecotypes displayed very low levels of basal and/or induced *IRE1b* transcript, potentially masking some expression differences

**a**



**b**

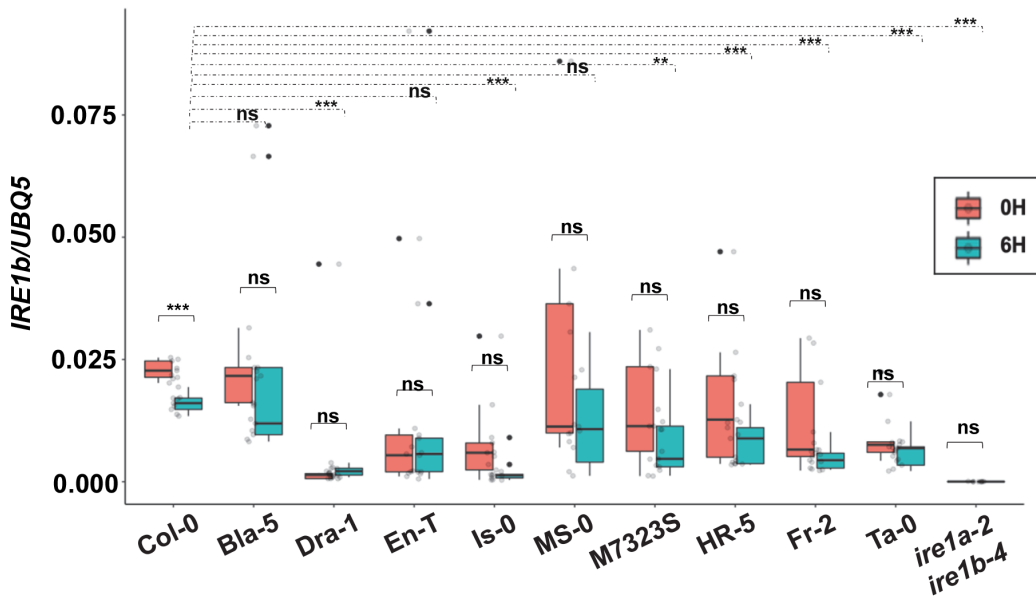


**Figure 5. Quantification of relative mRNA levels of *IRE1a* and *IRE1b* following Salicylic Acid treatment.**

Transcript levels of *IRE1a* (**a**) and *IRE1b* (**b**) were quantified using qRT-PCR in leaf tissues of 1-month-old plants that were treated with 0.5mM SA or H<sub>2</sub>O (mock) for 6 hours. Treatment groups are represented according to legends. All expression levels were normalised to the housekeeping gene *UBQ5* (Ubiquitin 5). The box plots extend from the 25<sup>th</sup> to 75<sup>th</sup> percentiles and the whiskers extend from the minimum to the maximum levels. Light grey dots represent individual data points. Outliers, shown as dark grey dots, were identified by the test statistics of the geom\_boxplot function in ggplot2. Median values were plotted in the boxes with the data generated from three independent biological replicates. Statistical analyses were performed in Excel by one-way ANOVA. Significant differences are indicated by asterisks (\*\* p<0.001, \*\* p<0.01, \* p<0.05), while “ns” indicates no statistically significant differences. Solid lines connecting bars represent the comparison of basal to SA-induced expression levels for each individual accession, while dashed lines represent the comparison of SA-induced expression levels between Col-0 and an indicated accession.

and limiting our ability to reach additional conclusions. Overall, we noted that *IRE1b* expression does not appear to be substantially changed in the majority of the ecotypes under both biotic and abiotic stress conditions (Fig. 2c and d, and Fig. 5b).

We next tested bZIP60 splicing in response to SA treatment. Consistent with our heat-induced splicing experiment (Fig. 4c and d), we did not observe any significant differences in basal *bZIP60* splicing activity in an independent assay (Fig. 6a), indicating the uniformity in our experimental set-up. Subsequently, we examined the efficacy of SA-induced *bZIP60* splicing in the ecotypes under study. The *bZIP60* splicing was markedly induced in the leaf tissue of the reference accession Col-0 treated with 0.5mM SA for 6 hours, while the negative control double mutant *ire1a-2 ire1b-4* did not exhibit any *bZIP60* splicing activity (Fig. 6a). Overall, despite rather low levels of transcript detected in some instances, we observed a significant induction of *bZIP60* splicing in all IRE1a- and IRE1b-related ecotypes except the Bla-5 and Ta-0 accessions. When comparing these results with heat-induced *bZIP60* splicing activity, Fr-2 was the only ecotype that

exhibits a divergent response pattern to SA. Fr-2 did not activate *bZIP60* splicing under heat stress (Fig. 4d) but was capable of splicing *bZIP60* under biotic stress conditions (Fig. 6a), indicating that the ER stress induction in the Fr-2 background is more sensitised towards biotic factors. Moreover, we also observed differences in the amplitude of *bZIP60* splicing induction after SA or heat treatments indicating that individual *Arabidopsis* accessions can differentiate between biotic and abiotic stresses and fine-tune their ER stress responses.

In addition to *bZIP60* splicing, the UPR signalling is also manifested by the production and accumulation of various ER chaperons. Previous studies found a positive relationship of endogenous *BiP* genes expression and UPR response in *Arabidopsis*<sup>31,34,38,48,73</sup>. Luminal Binding Protein (*BiP*) chaperons, also known as HSP70 and GRP78, are very abundant in the ER lumen and thought to bind newly synthesised proteins as they are translocated into the ER, maintain them in a state competent for subsequent folding and oligomerisation, and prevent aggregation of malfolded proteins. *BiP1*, *BiP2* and *BiP3* genes are considered among the most reliable markers for ER stress regulation in plants<sup>31,39,42,45,66,71,74</sup>. *Arabidopsis BiP1* and *BiP2* are nearly identical in sequence, and the primers used in our analysis detect transcripts of both of those genes. Therefore, we tested the induction of *BiP1/2* and *BiP3* upon SA treatment. Except for Ta-0, all of the tested accessions showed significant upregulation of *BiP1/2* and *BiP3* expression (Fig. 6b and S3a). While displaying a statistically significant induction ( $p<0.05$ ), the mRNA of *BiP3* in Ta-0 was accumulated at very low levels. On the other hand, the induction of *BiP1/2* expression in this ecotype was not statistically significant. Moreover, we also observed that Col-0 was the strongest inducer of *BiP3*, while SA-mediated

*BiP1/2* expression reached its highest levels in three accessions, *i.e.*, Col-0, Bla-5, and En-T; notably, the latter two were among the high basal *IRE1a* expressors. The double mutant *ire1a-2 ire1b-4* showed a lack of significant *BiP1/2* and *BiP3* induction (Fig. 6b)<sup>31,39,42,45,66,71,74</sup>.

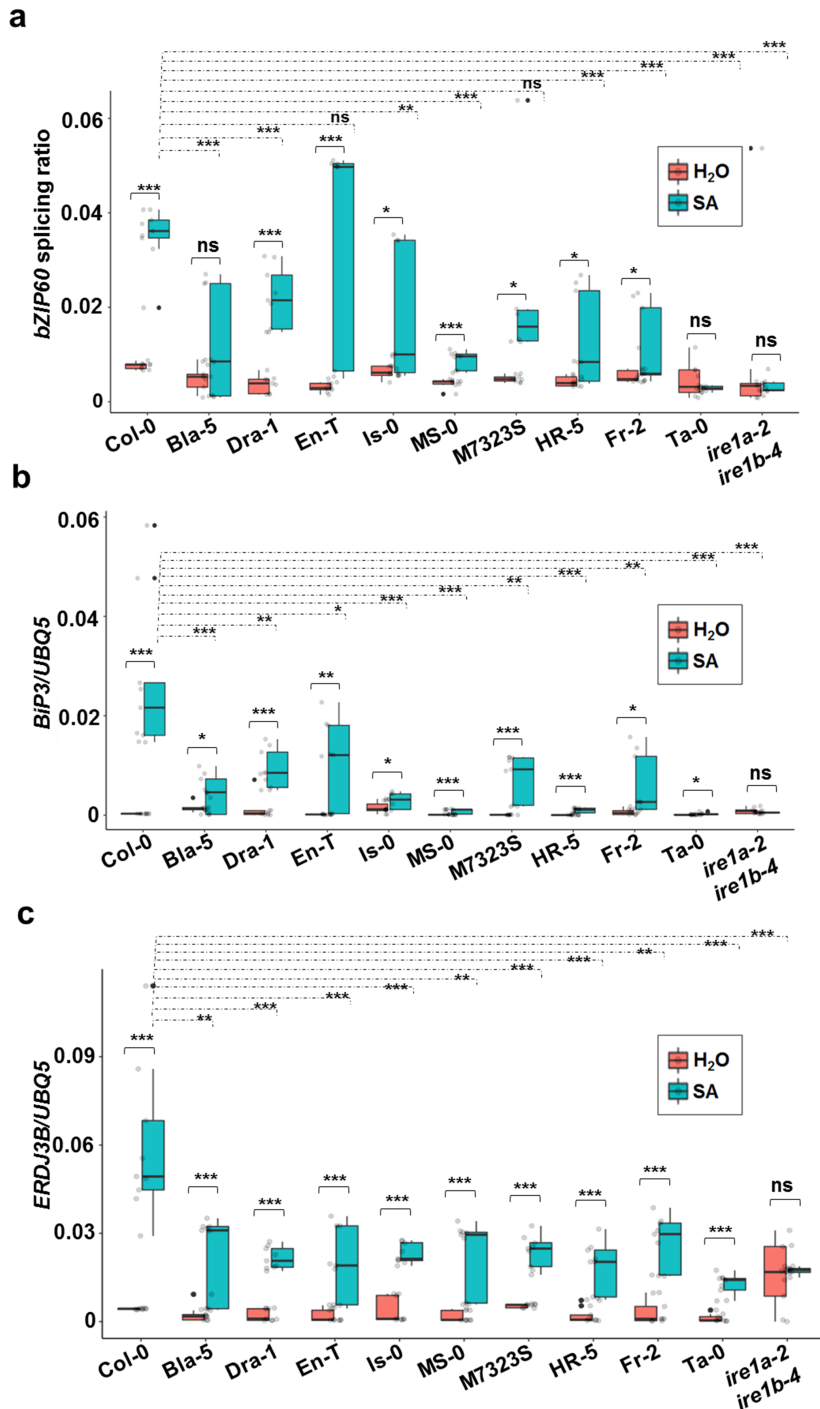


**Figure 6. Quantification of bZIP60 splicing efficacy and relative mRNA levels of ER stress markers *BiP3* and *ERDJ3B*.** (a) Transcript accumulation of spliced and unspliced *bZIP60* was measured using qRT-PCR in leaf tissues of 1-month-old plants that were treated with 0.5mM SA or H<sub>2</sub>O (mock) for 6 hours. AtbZIP60 splicing activity was calculated by normalizing values of spliced *AtbZIP60* to unspliced *AtbZIP60* transcript abundance. Transcript levels of *BiP3* (b) and *ERDJ3B* (c) were quantified using qRT-PCR in leaf tissues of 1-month-old plants that were treated with 0.5mM SA or H<sub>2</sub>O (mock) for 6 hours. Treatment groups are represented according to legends. All expression levels shown in panels a-c were measured in leaf tissues of 1-month-old Arabidopsis plants *via* qRT-PCR and were normalised to the housekeeping gene *UBQ5* (Ubiquitin 5). The box plots extend from the 25<sup>th</sup> to 75<sup>th</sup> percentiles and the whiskers extend from the minimum to the maximum levels. Light grey dots represent individual data points. Outliers, shown as dark grey dots, were identified by the test statistics of the geom\_boxplot function in ggplot2. Median values were plotted in the boxes with the data generated from three independent biological replicates. Statistical analyses were performed in Excel by one-way ANOVA. Significant differences are indicated by asterisks (\*\* p<0.001, \*\* p<0.01, \* p<0.05), while “ns” indicates no statistically significant differences. Solid lines connecting bars represent the comparison of basal to SA-induced expression levels for each individual accession, while dashed lines represent the comparison of SA-induced expression levels between Col-0 and an indicated accession.

Endoplasmic reticulum dnaJ domain-containing proteins 3A and 3B (ERDJ3A and ERDJ3B) are another two molecular co-chaperones that bind to the BiP proteins in mammals and help mediate the protein folding. In Arabidopsis, ERDJ3A is responsible for functional pollen development while ERDJ3B is involved in quality control of ER proteins<sup>75</sup>. Both genes can be used as reliable markers for UPR activity in plants<sup>45,73,74</sup>. *ERDJ3A* and *ERDJ3B* both showed clear patterns of transcriptional induction following SA treatment (Fig. 6c and S3b) in all accessions with the only exception of M7323S, where *ERDJ3A* was not significantly induced after SA exposure (Fig. S3b). Similar to our findings for *BiP* genes expression, the reference accession Col-0 displayed the highest levels of *ERDJ3A* and *ERDJ3B* induction across all ecotypes tested. The double mutant *ire1a-2 ire1b-4* showed a lack of significant *ERDJ3B* induction but was able to

modestly upregulate *ERDJ3A*, indicating that these two highly related chaperones have distinct transcriptional regulatory mechanisms.

In addition to BiP and ERDJ3 family members, Stromal-Derived Factor 2 (SDF2) represents another important diagnostic ER stress marker<sup>76,77</sup>. *SDF2* is a BTH (an SA analogue)-dependent gene<sup>78</sup> and SDF2 protein can form complexes with ERDJ3B and the BiP proteins to facilitate proper ER homeostasis during PAMP triggered immunity<sup>77</sup>. Consistent with our findings for other ER stress markers, we observed a trend of induction in all *Arabidopsis* accessions tested (Fig. S3c). Bla-5 and M7323S showed the highest levels of *SDF2* induction, along with Col-0 and En-T. Ta-0 was distinguished by the lowest levels of *SDF2* transcript, and *ire1a-2 ire1b-4* double mutant showed a lack of significant *SDF2* induction. On a general note, as it was the case for the *IRE1b* expression (Fig. 5b), several ecotypes accumulated very low levels of several ER chaperone transcripts, potentially obscuring additional conclusions about the SA-mediated transcriptional regulation of those genes. Taken together, we noted differential levels of bZIP60 splicing as well as a pronounced induction of downstream UPR chaperons and co-chaperons following SA treatment in the selected natural accessions, indicating that the UPR machinery in different *Arabidopsis* ecotypes has evolved to cope with versatile surrounding environments.

### ***Response to infection with the bacterial pathogen *Pseudomonas syringae****

We previously reported that IRE1a and IRE1b are implicated in plant immune responses to a bacterial leaf pathogen, *Pseudomonas syringae*, including basal defence and establishment of systemic acquired resistance<sup>33</sup>. Through a systematic genetic analysis

using a suite of single and double *ire1* mutants, we previously discovered that IRE1a plays a more prominent role in mediating Arabidopsis defences against *P. syringae* than IRE1b, but both homologues exhibit some degree of functional redundancy and consequently *ire1a ire1b* double mutants display a more profound immune phenotype than the *ire1a* single mutants<sup>33</sup>. We hypothesised that the accessions showing higher basal and/or induced levels of *IRE1a*, *IRE1b*, SA-mediated *bZIP60* splicing, and ER-associated marker genes expression might be better equipped to fight off an infection with virulent *P. syringae* bacteria strain DC3000 (hereafter, *Pst* DC3000). To test this hypothesis, we subjected Col-0, nine natural accessions, and a hypersusceptible *npr1-1* mutant<sup>79,80</sup> (negative control) to a series of bacterial infection assays<sup>81</sup>. The *Pst* DC3000 bacteria were pressure-infiltrated into the leaves followed by quantification of the bacterial growth three days later<sup>81</sup>. As expected, the *npr1-1* plants showed a susceptible phenotype with the highest bacterial loads (Fig. 7). Accessions Bla-5, Dra-1, MS-0, M7323S, and Ta-0 showed lower bacterial growth levels compared to Col-0, indicating their relative resistance to *Pst* DC3000, whereas En-T, Is-0, and HR-5 displayed a similar trend that was not, however, statistically significant. Among all ecotypes tested, Fr-2 was the only one accession that amassed slightly higher, although not statistically significant, pathogen loads when compared to Col-0 (Fig. 7). Double mutant *ire1a-2 ire1b-4* displayed significant susceptibility compared to Col-0, as reported previously<sup>33</sup> (Fig. S4).

While the plant immune response is a complex process that engages numerous signalling pathways, we detected some parallels between pathogen resistance and expression of *IRE1* genes and downstream ER stress markers. Our initial hypothesis has proven correct for several accessions. For example, Dra-1, the accession with the highest basal

*IRE1a* levels, showed increased heat-induced *IRE1a* expression, increased *bZIP60* splicing after the heat and SA treatments, and strong SA-mediated inducibility of *BiP1/2*,

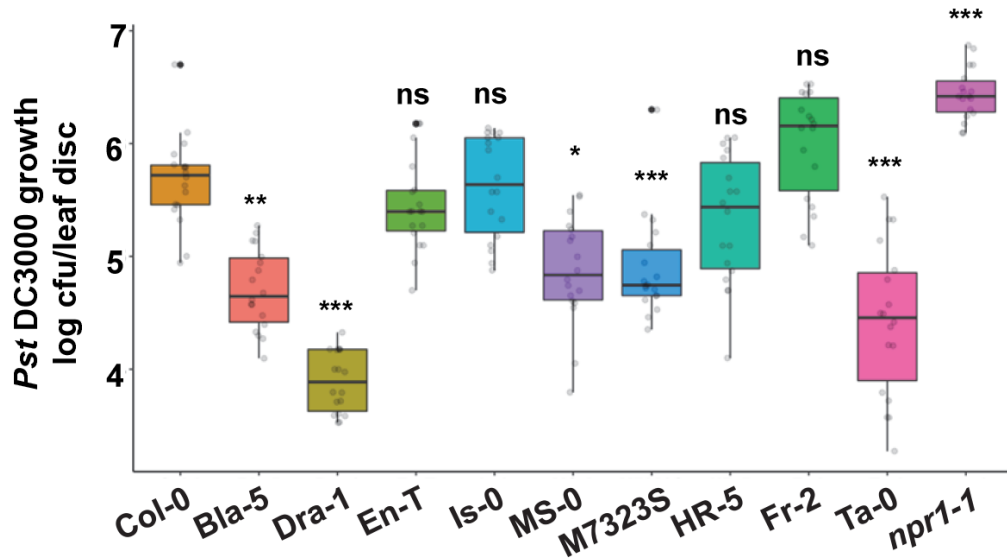


**Figure 7. Natural variation of resistance to *Pseudomonas syringae* pv. tomato DC3000 among selected *Arabidopsis* accessions.** Leaves of 4 weeks old plants were syringe infiltrated with *Pseudomonas syringae* pv. tomato strain DC3000 (*Pst* DC3000). *In planta* bacterial growth was quantified at 3 days post-inoculation. The box plots extend from 25<sup>th</sup> to 75<sup>th</sup> percentiles and whiskers extend from the minimum to the maximum levels. Light grey dots represent individual data points. Outliers, shown as dark grey dots, were identified by the test statistics of the geom\_boxplot function in ggplot2. Median values were plotted in the boxes with the data generated from three independent biological replicates. Statistical analyses were performed in Excel by One-Way ANOVA. Significant differences are indicated by asterisks (\*\* p<0.01, \*\*\* p<0.001), while “ns” indicates no statistically significant differences. Black asterisks are representing the comparison of resistance or susceptibility of respective accession compared to Col-0.

*BiP3*, *ERDJ3A*, *ERDJ3B*, and *SDF2*. *Dra-5* was also the most resistant accession in our study and accumulated bacterial loads ~100 times lower than those of *Col-0*. Another resistant ecotype *HR-5* (high basal *IRE1b* accession) showed reduced sensitivity to Tm, high levels of *bZIP60* splicing after the heat and SA treatments, and strong SA-mediated inducibility of *BiP1/2*, *BiP3*, *ERDJ3A*, *ERDJ3B*, and *SDF2*. Analogous conclusions can

be drawn for Bla-5 (high basal *IRE1a* accession), which displayed a similar data trend with the exception of the *bZIP60* splicing, which was not significantly induced. Interestingly, MS-0 and M7323S are two accessions that were selected as low *IRE1a* and/or *IRE1b* expressors yet displayed increased *bZIP60* splicing after the heat and SA treatments and substantial SA-mediated inducibility of almost all tested ER markers. This increased induction of *bZIP60* splicing and ER markers are consistent with enhanced disease resistance phenotypes of MS-0 and M7323S. On the other hand, Ta-0 is an accession that we initially selected based on reduced basal *IRE1b* transcript levels. Predictably, in our expression studies, we observed a complete lack of *bZIP60* inducibility and very low overall levels of the ER markers expression, as well as increased sensitivity to both heat and Tm. Yet, despite its poor ER-associated transcriptional signature, Ta-0 showed surprisingly low levels of *Pst* DC3000 growth, ranking as the second most resistant accession in our analysis. This finding points towards the likely existence of compensatory mechanisms, where other defence-related pathways might have been hyperactive to fend off the pathogens in their local environment while the induction of UPR machinery is impaired. In conclusion, our phytopathology analyses provided several lines of evidence for an interrelation between the relative fitness of the ER signalling pathways and overall immunity to *Pst* DC3000 infection.

***Euclidean clustering analysis reveals integrative transcriptional and phenotypic pattern.***

To integrate our findings and uncover novel patterns and relationships between the ecotypes, we next performed Euclidean clustering analysis of the transcriptional and

phenotypic responses in our panel of accessions (Fig. 8). Is-0, Fr-2 and Col-0 ecotypes share common geographical origins: Is-0 originates from Isenberg, Germany, Fr-2 stems from the neighbouring city of Frankfurt, Germany, and Col-0, often incorrectly attributed

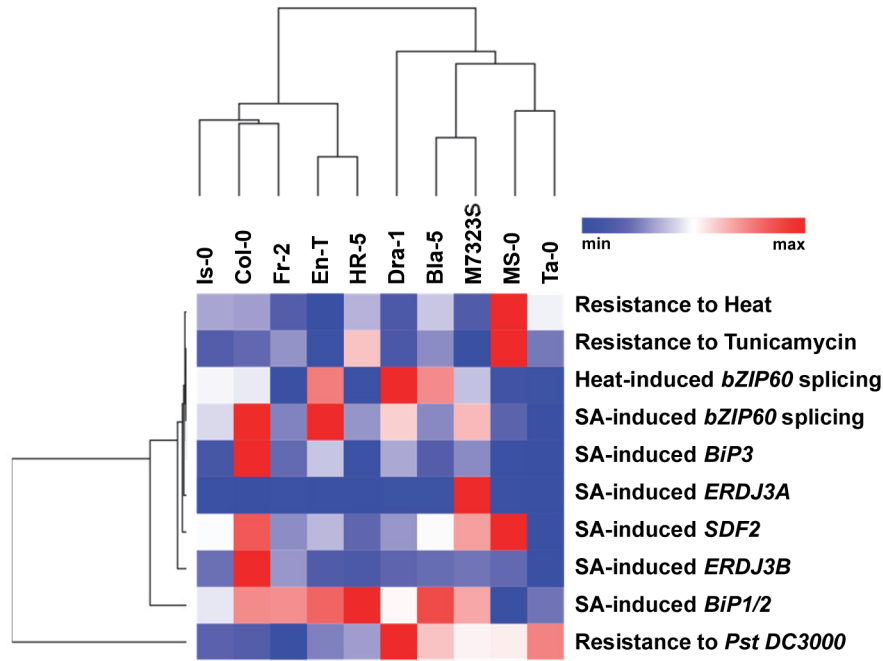


**Figure 8: Heat map comparisons of differential gene expression, whole-plant ER stress sensitivity, and pathology phenotypes of selected *Arabidopsis* accessions.** Responses of the selected accessions to different treatments were integrated into a heat map. Euclidean distance was used as a metric for KMeans and hierarchical clustering. In hierarchical clustering, the average was the linkage method. Accession names and treatments are indicated. Colours from red to blue indicate high to low expression/trait intensity.

to Columbia, Missouri, USA, actually originates from north-western Poland<sup>82</sup>. These three accessions clustered together in our analysis, demonstrating predominantly consistent trends of stress-induced transcriptional responses, and similar levels of susceptibility to bacterial disease. MS-0 of Moscow, Russia, and Ta-0, hailing from Tabor, Czech Republic, both low basal expressors of *IRE1b*, clustered in a separate group distinguished by low amplitudes of transcriptional ER stress responses but high levels of bacterial

resistance, indicating that *Arabidopsis* immunity to *Pst* DC3000 can be variably tied to UPR signalling depending on the specific genetic background. It is worth noting that MS-0 showed a positive relationship between high *SDF2* transcript levels and enhanced tolerance to heat and Tm, which distinguished it as the only ecotype with such phenotypic features. Interestingly, our analysis also uncovered an interrelation between the efficacy of *bZIP60* splicing and expression of *BiP3* (Fig. 6), which is consistent with the notion that *BiP3* itself has been shown to be one of the main transcriptional targets of active *bZIP60* transcription factor<sup>83</sup>. This relationship is further reinforced by a positive feedback loop as an active *bZIP60* is also able to activate its own expression through an ERSE (ER response element)-like element presents in its promoter<sup>48</sup>. Expression trends of *BiP1/2* were independent of other markers, which is not unexpected since *BiP1* and *BiP2* are strongly and ubiquitously expressed, and weakly regulated by *bZIP60*<sup>31</sup>. *ERDJ3A*, which has been previously shown to be a heat- and *bZIP60*-independent ER stress marker<sup>84</sup>, showed expression patterns that clustered together with multiple ER chaperones following the immune stressor SA treatment. This observation is consistent with the presence of SA-inducible heat shock-like *translocon1* (*TL1*) *cis*-regulatory elements in *ERDJ3A* promoter<sup>71,84</sup> and indicates that additional transcriptional regulators, such as TBF1<sup>71</sup>, might operate to bridge the UPR signalling with SA-mediated immune responses. In support of this hypothesis, TBF1 was previously shown to regulate SA-induced expression of *BiP2* via *TL1* motifs<sup>71</sup>. Given the complexity of the plant immune response, it is predictable that the levels of bacterial resistance don't show an absolute concurrence with any specific ER stress marker(s) in our analysis; however, these results prove valuable to provide

interesting insights into the ecological and evolutionary relationship between the UPR and immunity to *Pst* DC3000.

## Conclusion

The genetic variation found in populations from different natural environments demonstrates the extent of local adaptation and helps gain insights into the molecular underpinnings of plant adaptive responses. This study characterised the ER stress responses in a panel of 10 natural *Arabidopsis* accessions and uncovered a number of variations in their UPR signatures following exposure to biotic and abiotic stress factors. Our work suggests that both *Arabidopsis IRE1* homologues, as well as their downstream signalling components, are subject to variation imposed by the evolutionary forces both at the genomic and gene regulation levels. We provided new insights into the natural diversity of a ubiquitous and evolutionarily conserved cellular stress signalling pathway, and our discoveries can form a foundation to engineer climate-resilient crop plants, a necessity for a sustainable future.

## Materials and Methods

### ***Plant Material and Growth Conditions:***

The seeds of selected *A. thaliana* accessions listed in Table 1 were ordered from the *Arabidopsis* Biological Resource Center (ABRC, Ohio State University, Columbus, OH, USA). All the seeds were sown on sterilised soil (SunGro Horticulture, Super-Fine Germinating Mix) in individual pots. The seeds were stratified for seven days in a cold room facility at 4°C. The pots were then transferred to a controlled growth room facility

(12h light/12h dark photoperiod; 21°C; 100 µmol/m<sup>2</sup>/s light intensity and 40% relative humidity). 10-15 days old seedlings were then transplanted into 72-well flats for growth (1 month) and subsequent experimentation.

### ***Selection of Accessions:***

The accessions (Table 1) were selected based on *IRE1a* and *IRE1b* expression patterns in Arabidopsis eFP (electronic Fluorescent Pictograph) browser, available at <http://www.bar.utoronto.ca/>. Logarithmic fold-change values were provided by ePLANT, with relative logarithmic values above 0.7 and below -0.8. The accessions that showed the highest extent of variation, characterised by the highest and lowest expression values for *IRE1a* and *IRE1b* were selected.

### ***Heat Stress Assays and Salicylic Acid Treatments:***

1-month-old Arabidopsis plants grown in soil were exposed to heat stress at 37°C for 90 minutes in an incubator, then leaf tissue was sampled. For phytohormone treatment, aerial parts of 1-month-old soil-grown Arabidopsis plants were sprayed with 0.5mM SA, covered with a dome for 2 hours, and leaf samples were collected after 6 hours post-treatment. At least three leaves derived from three independent plants were collected for each ecotype/treatment/time point combination.

### ***ER Stress Assays:***

Seeds from different Arabidopsis accessions were washed with 70% Ethanol and 0.05% Triton and then stratified at 4°C for 3 days on half-strength solid Murashige Skoog

(MS) media plates (Phytotechnology Labs, Overland Park, KS, USA). After stratification, MS plates were transferred to growth chambers (12h light/12h dark photoperiod; 21°C; 100  $\mu$ mol/m<sup>2</sup>/s light intensity and 40% relative humidity). 0.15 $\mu$ g/mL or 0.30  $\mu$ g/mL of Tunicamycin (Tm) (Tocris Bioscience; 3516/10) were used as a chemical ER stressor. 7 days old seedlings were transferred to liquid half-strength MS media with or without the appropriate concentration of Tm. The total fresh weight of 10 plants for each biological replications was recorded 3 days following Tm exposure. For heat stress, *Arabidopsis* seedlings were grown on solid half-strength MS media for 7 days and then transferred to liquid half-strength MS media. 9 days old *Arabidopsis* plants were exposed to 42°C for 2 hours and the total weight was recorded 2 days later.

#### ***mRNA Quantification and bZIP60 splicing:***

Gene expression analysis was conducted as described previously<sup>85</sup>. In brief, leaf tissue from 1-month-old plants was collected at designated time points. At least three leaves derived from three independent plants were collected for each genotype/ treatment/ time point combination. Trizol reagent (Invitrogen) was used to extract total RNA and DNase I (Ambion) was applied to remove DNA contaminants. 10 $\mu$ g of total RNA were reverse transcribed using SuperScript III first-strand RT-PCR kit (Invitrogen), and quantitative gene expression analysis was determined using GoTaq qPCR Master Mix (Promega) with transcript-specific primers in a RealPlex S MasterCycler (Eppendorf). The Ct values were normalised to ubiquitin 5 (*UBQ5*) gene. bZIP60 splicing assays were performed as described in Moreno et al.<sup>33</sup>. Briefly, we used a common forward primer and a pair of reverse primers that specifically hybridise to either the unspliced or spliced

variants of cDNA originated from bZIP60 mRNA, respectively. This allows for the detection of two specific qRT-PCR products corresponding to unspliced and spliced bZIP60 variants (Fig. S5). Primers used for qRT-PCR are listed in Table S1.

#### ***Preparation of promoter::GUS constructs:***

DNA extraction was performed from 1 month old plants with 200 µl CTAB extraction buffer (2% cetyl-trimethyl ammonium bromide, 100 mM tris [pH 8.0], 20 mM EDTA pH [8.0], 1.4M NaCl, 0.5% β-Mercaptoethanol, 2% polyvinyl pyrrolidone). The promoter region of *IRE1a* (~1.267 kb) and *IRE1b* (~1.477 kb) from different accessions were amplified from genomic DNA by PCR using Phusion Polymerase (Thermo Scientific) with attB-flanked primers (Table S1). The PCR products were cloned into pDONR207 Gateway vector *via* BP reactions (Invitrogen). After confirming the entry clones through PCR and Sanger sequencing (primers listed in Table S1), destination clones were constructed by LR reactions with binary Gateway vector pAM-PAT-GW-GUS and confirmed through PCR and Sanger sequencing. The plant expression vector pAM-PAT-35S-GW-GUS was a gift from Drs. Nico Dissmeyer and Imre Somssich (Addgene plasmid # 80678; <http://n2t.net/addgene:80678>; RRID: Addgene\_80678). The resulting pAM-PAT-promoter-GUS constructs were transformed into *Agrobacterium tumefaciens* (strain GV3101) for transient expression assays.

#### ***IRE1a and IRE1b promoter analyses:***

We analysed the obtained promoter sequences using 4Peaks software (<https://ucleabytes.com/4peaks/index.html>). The confirmed sequences were aligned with the

*IRE1a* or *IRE1b* promoter sequence of the reference accession Col-0 using MultAlin website (<http://multalin.toulouse.inra.fr/multalin/>) (Fig. S2). The promoter sequences from Col-0 were used to predict putative transcription factor binding sites using the software MatInspector ([https://www.genomatix.de/online\\_help/help\\_matinspector/matin-spector\\_help.html](https://www.genomatix.de/online_help/help_matinspector/matin-spector_help.html)) and the website PlantRegMap (<http://plantregmap.gao-lab.org>). The predicted TF target sequences were matched with the SNPs identified from MultAlin website. The newly identified TF binding sites with SNPs have been submitted to NCBI GenBank under the following accession numbers: MT344169, MT344170, and MT344171.

***Quantitative GUS assay:***

1-month-old Col-0 plants were agroinfiltrated with a needleless syringe as described previously<sup>86</sup>. Three days post-inoculation, the plants were exposed to heat stress in an incubator at 37°C for 90 minutes. Immediately following the heat stress, the tissues were collected and ground under liquid nitrogen. Total proteins from the harvested tissue were extracted with extraction buffer (50 mM NaPO<sub>4</sub> [pH 7.0], 1mM Na<sub>2</sub>EDTA, 0.1% SDS, 0.1% Triton X-100, protease inhibitor for plant extracts [Sigma], and 10 mM β-mercapethanol) as described previously<sup>71</sup>. Followed by centrifugation (10 min, 4,000 × g, 4°C) the supernatants were collected, and protein concentration was quantified using Bradford Reagent (Sigma). The extracted proteins were incubated with 1 mM MUG (4-methylumbelliferyl β-D-glucuronide) to quantify GUS activity. 1 M Na<sub>2</sub>CO<sub>3</sub> was used as a stop buffer to terminate the reaction and fluorescence was measured with a microplate reader (Tecan) with an excitation wavelength of 365 nm, an emission wavelength of

455 nm and a filter wavelength of 430 nm. The relative MUG values were obtained by normalizing data to the Bradford assay. The experimental procedures were adjusted based on a previously published protocol<sup>87</sup>.

***Bacterial strains and bacterial growth quantification:***

*Pseudomonas syringae* pv. tomato DC3000 (*Pst* DC3000) was used for pathogen infection and quantification assay. 1-month-old soil-grown plants were syringe-infiltrated with *Pst* DC3000 (OD<sub>600</sub>=0.0002). 3 leaves/plant, 6 plants/replication, and at least three independent biological replications were performed. Bacterial growth was quantified three days of post inoculation as described previously<sup>81</sup>.

***Heat map and Euclidean clustering analysis:***

The heat map was generated using the website Morpheus ([https://soft-ware.broadinstitute.org/morpheus/](https://software.broadinstitute.org/morpheus/)). Euclidean distance was used as a metric for KMeans and Hierarchical clustering. In hierarchical clustering, the average was the linkage method. Colors from red to blue indicate high to low expression/trait intensity.

***Statistical Analysis:***

Statistical differences were calculated by one-way ANOVA in Excel and R. ggplot2 was used to make graphs shown in figures 5, 6, and 7, and supplemental figures 3 and 4. Statistically significant differences are indicated with \*p < 0.05, \*\*p < 0.01, \*\*\*p < 0.001, and \*\*\*\*p < 0.0001.

### **Acknowledgments**

We thank Dr. Shahid Mukhtar for editing and critically reading the manuscript, and Mr. Bharat Mishra for assistance with bioinformatics-aided promoter analyses.

## Reference:

- 1 Claeys, H. & Inze, D. The agony of choice: how plants balance growth and survival under water-limiting conditions. *Plant Physiol* **162**, 1768-1779, doi:10.1104/pp.113.220921 (2013).
- 2 Aitken, S. N., Yeaman, S., Holliday, J. A., Wang, T. & Curtis-McLane, S. Adaptation, migration or extirpation: climate change outcomes for tree populations. *Evol Appl* **1**, 95-111, doi:10.1111/j.1752-4571.2007.00013.x (2008).
- 3 Jump, A. S. & Penuelas, J. Running to stand still: adaptation and the response of plants to rapid climate change. *Ecology letters* **8**, 1010-1020 (2005).
- 4 Fournier-Level, A. *et al.* A map of local adaptation in *Arabidopsis thaliana*. *Science* **334**, 86-89, doi:10.1126/science.1209271 (2011).
- 5 Alonso-Blanco, C. & Koornneef, M. Naturally occurring variation in *Arabidopsis*: an underexploited resource for plant genetics. *Trends Plant Sci* **5**, 22-29, doi:10.1016/s1360-1385(99)01510-1 (2000).
- 6 Bouchabke, O. *et al.* Natural variation in *Arabidopsis thaliana* as a tool for highlighting differential drought responses. *PLoS One* **3**, e1705, doi:10.1371/journal.pone.0001705 (2008).
- 7 Shindo, C., Bernasconi, G. & Hardtke, C. S. Natural genetic variation in *Arabidopsis*: tools, traits and prospects for evolutionary ecology. *Ann Bot* **99**, 1043-1054, doi:10.1093/aob/mcl281 (2007).
- 8 Koornneef, M., Alonso-Blanco, C. & Vreugdenhil, D. Naturally occurring genetic variation in *Arabidopsis thaliana*. *Annu Rev Plant Biol* **55**, 141-172, doi:10.1146/annurev.arplant.55.031903.141605 (2004).
- 9 Horton, M. W. *et al.* Genome-wide patterns of genetic variation in worldwide *Arabidopsis thaliana* accessions from the RegMap panel. *Nat Genet* **44**, 212-216, doi:10.1038/ng.1042 (2012).
- 10 Hoffmann, M. H. Biogeography of *Arabidopsis thaliana* (L.) Heynh. (Brassicaceae). *Journal of Biogeography* **29**, 125-134 (2002).
- 11 Katori, T. *et al.* Dissecting the genetic control of natural variation in salt tolerance of *Arabidopsis thaliana* accessions. *J Exp Bot* **61**, 1125-1138, doi:10.1093/jxb/erp376 (2010).
- 12 Pérez-Pérez, J. M., Serrano-Cartagena, J. & Micol, J. L. Genetic analysis of natural variations in the architecture of *Arabidopsis thaliana* vegetative leaves. *Genetics* **162**, 893-915 (2002).
- 13 Pigliucci, M. & Schlichting, C. D. Reaction norms of *Arabidopsis* (Brassicaceae). III. Response to nutrients in 26 populations from a worldwide collection. *American Journal of Botany* **82**, 1117-1125 (1995).
- 14 Koornneef, M., Alonso-Blanco, C., Peeters, A. J. & Soppe, W. Genetic Control of Flowering Time in *Arabidopsis*. *Annu Rev Plant Physiol Plant Mol Biol* **49**, 345-370, doi:10.1146/annurev.arplant.49.1.345 (1998).
- 15 Ungerer, M. C., Halldorsdottir, S. S., Modliszewski, J. L., Mackay, T. F. & Purugganan, M. D. Quantitative trait loci for inflorescence development in *Arabidopsis thaliana*. *Genetics* **160**, 1133-1151 (2002).

- 16 Alonso-Blanco, C., Bentsink, L., Hanhart, C. J., Blankestijn-de Vries, H. & Koornneef, M. Analysis of natural allelic variation at seed dormancy loci of *Arabidopsis thaliana*. *Genetics* **164**, 711-729 (2003).
- 17 Langridge, J. & Griffing, B. A study of high temperature lesions in *Arabidopsis thaliana*. *Australian Journal of Biological Sciences* **12**, 117-135 (1959).
- 18 Thomashow, M. *Arabidopsis thaliana* as a model for studying mechanisms of plant cold tolerance. *Arabidopsis*, 807-834 (1994).
- 19 Adam, L. *et al.* Comparison of *Erysiphe cichoracearum* and *E. cruciferarum* and a survey of 360 *Arabidopsis thaliana* accessions for resistance to these two powdery mildew pathogens. *Mol Plant Microbe Interact* **12**, 1031-1043, doi:10.1094/MPMI.1999.12.12.1031 (1999).
- 20 Weinig, C., Stinchcombe, J. R. & Schmitt, J. QTL architecture of resistance and tolerance traits in *Arabidopsis thaliana* in natural environments. *Mol Ecol* **12**, 1153-1163, doi:10.1046/j.1365-294x.2003.01787.x (2003).
- 21 Swarup, K. *et al.* Natural allelic variation identifies new genes in the *Arabidopsis* circadian system. *Plant J* **20**, 67-77, doi:10.1046/j.1365-313x.1999.00577.x (1999).
- 22 Koornneef, M. & Meinke, D. The development of *Arabidopsis* as a model plant. *The Plant Journal* **61**, 909-921 (2010).
- 23 Mitchell-Olds, T. *Arabidopsis thaliana* and its wild relatives: a model system for ecology and evolution. *Trends in Ecology & Evolution* **16**, 693-700 (2001).
- 24 Arabidopsis Genome, I. Analysis of the genome sequence of the flowering plant *Arabidopsis thaliana*. *Nature* **408**, 796-815, doi:10.1038/35048692 (2000).
- 25 Genomes Consortium. Electronic address, m. n. g. o. a. a. & Genomes, C. 1,135 Genomes Reveal the Global Pattern of Polymorphism in *Arabidopsis thaliana*. *Cell* **166**, 481-491, doi:10.1016/j.cell.2016.05.063 (2016).
- 26 Michalak, M., Corbett, E. F., Mesaeli, N., Nakamura, K. & Opas, M. Calreticulin: one protein, one gene, many functions. *Biochem J* **344 Pt 2**, 281-292 (1999).
- 27 Latham, K. E. Endoplasmic reticulum stress signaling in mammalian oocytes and embryos: life in balance. *Int Rev Cell Mol Biol* **316**, 227-265, doi:10.1016/bs.ircmb.2015.01.005 (2015).
- 28 Wu, H., Ng, B. S. & Thibault, G. Endoplasmic reticulum stress response in yeast and humans. *Biosci Rep* **34**, doi:10.1042/BSR20140058 (2014).
- 29 Afrin, T., Diwan, D., Sahawneh, K. & Pajerowska-Mukhtar, K. Multilevel regulation of endoplasmic reticulum stress responses in plants: where old roads and new paths meet. *J Exp Bot* **71**, 1659-1667, doi:10.1093/jxb/erz487 (2020).
- 30 Korner, C. J., Du, X., Vollmer, M. E. & Pajerowska-Mukhtar, K. M. Endoplasmic Reticulum Stress Signaling in Plant Immunity--At the Crossroad of Life and Death. *Int J Mol Sci* **16**, 26582-26598, doi:10.3390/ijms161125964 (2015).
- 31 Iwata, Y., Fedoroff, N. V. & Koizumi, N. *Arabidopsis bZIP60* is a proteolysis-activated transcription factor involved in the endoplasmic reticulum stress response. *Plant Cell* **20**, 3107-3121, doi:10.1105/tpc.108.061002 (2008).

- 32 Koizumi, N. *et al.* Molecular characterization of two *Arabidopsis* Ire1 homologs, endoplasmic reticulum-located transmembrane protein kinases. *Plant Physiol* **127**, 949-962 (2001).
- 33 Moreno, A. A. *et al.* IRE1/bZIP60-mediated unfolded protein response plays distinct roles in plant immunity and abiotic stress responses. *PLoS One* **7**, e31944, doi:10.1371/journal.pone.0031944 (2012).
- 34 Martinez, I. M. & Chrispeels, M. J. Genomic analysis of the unfolded protein response in *Arabidopsis* shows its connection to important cellular processes. *Plant Cell* **15**, 561-576, doi:10.1105/tpc.007609 (2003).
- 35 Lu, S. J. *et al.* Conservation of IRE1-regulated bZIP74 mRNA unconventional splicing in rice (*Oryza sativa* L.) involved in ER stress responses. *Mol Plant* **5**, 504-514, doi:10.1093/mp/ssr115 (2012).
- 36 Irsigler, A. S. *et al.* Expression profiling on soybean leaves reveals integration of ER- and osmotic-stress pathways. *BMC Genomics* **8**, 431, doi:10.1186/1471-2164-8-431 (2007).
- 37 Vitale, A. & Ceriotti, A. Protein quality control mechanisms and protein storage in the endoplasmic reticulum. A conflict of interests? *Plant Physiol* **136**, 3420-3426, doi:10.1104/pp.104.050351 (2004).
- 38 Ye, C., Dickman, M. B., Whitham, S. A., Payton, M. & Verchot, J. The unfolded protein response is triggered by a plant viral movement protein. *Plant Physiol* **156**, 741-755, doi:10.1104/pp.111.174110 (2011).
- 39 Deng, Y. *et al.* Heat induces the splicing by IRE1 of a mRNA encoding a transcription factor involved in the unfolded protein response in *Arabidopsis*. *Proc Natl Acad Sci U S A* **108**, 7247-7252, doi:10.1073/pnas.1102117108 (2011).
- 40 Zhang, S. S. *et al.* Tissue-Specific Transcriptomics Reveals an Important Role of the Unfolded Protein Response in Maintaining Fertility upon Heat Stress in *Arabidopsis*. *Plant Cell* **29**, 1007-1023, doi:10.1105/tpc.16.00916 (2017).
- 41 Lee, S. C., Choi, H. W., Hwang, I. S., Choi, D. S. & Hwang, B. K. Functional roles of the pepper pathogen-induced bZIP transcription factor, CAbZIP1, in enhanced resistance to pathogen infection and environmental stresses. *Planta* **224**, 1209-1225, doi:10.1007/s00425-006-0302-4 (2006).
- 42 Deng, Y., Srivastava, R. & Howell, S. H. Protein kinase and ribonuclease domains of IRE1 confer stress tolerance, vegetative growth, and reproductive development in *Arabidopsis*. *Proc Natl Acad Sci U S A* **110**, 19633-19638, doi:10.1073/pnas.1314749110 (2013).
- 43 Back, S. H., Schroder, M., Lee, K., Zhang, K. & Kaufman, R. J. ER stress signaling by regulated splicing: IRE1/HAC1/XBP1. *Methods* **35**, 395-416, doi:10.1016/j.ymeth.2005.03.001 (2005).
- 44 Noh, S. J., Kwon, C. S. & Chung, W. I. Characterization of two homologs of Ire1p, a kinase/endoribonuclease in yeast, in *Arabidopsis thaliana*. *Biochim Biophys Acta* **1575**, 130-134, doi:10.1016/s0167-4781(02)00237-3 (2002).
- 45 Chen, Y. & Brandizzi, F. AtIRE1A/AtIRE1B and AGB1 independently control two essential unfolded protein response pathways in *Arabidopsis*. *Plant J* **69**, 266-277, doi:10.1111/j.1365-313X.2011.04788.x (2012).

- 46 Deng, Y. *et al.* IRE1, a component of the unfolded protein response signaling pathway, protects pollen development in Arabidopsis from heat stress. *Plant J* **88**, 193-204, doi:10.1111/tpj.13239 (2016).
- 47 Sidrauski, C. & Walter, P. The transmembrane kinase Ire1p is a site-specific endonuclease that initiates mRNA splicing in the unfolded protein response. *Cell* **90**, 1031-1039, doi:10.1016/s0092-8674(00)80369-4 (1997).
- 48 Iwata, Y. & Koizumi, N. An Arabidopsis transcription factor, AtbZIP60, regulates the endoplasmic reticulum stress response in a manner unique to plants. *Proc Natl Acad Sci U S A* **102**, 5280-5285, doi:10.1073/pnas.0408941102 (2005).
- 49 Nagashima, Y. *et al.* Arabidopsis IRE1 catalyses unconventional splicing of bZIP60 mRNA to produce the active transcription factor. *Sci Rep* **1**, 29, doi:10.1038/srep00029 (2011).
- 50 Hollien, J. *et al.* Regulated Ire1-dependent decay of messenger RNAs in mammalian cells. *J Cell Biol* **186**, 323-331, doi:10.1083/jcb.200903014 (2009).
- 51 Maurel, M., Chevet, E., Tavernier, J. & Gerlo, S. Getting RIDD of RNA: IRE1 in cell fate regulation. *Trends Biochem Sci* **39**, 245-254, doi:10.1016/j.tibs.2014.02.008 (2014).
- 52 Mishiba, K. *et al.* Defects in IRE1 enhance cell death and fail to degrade mRNAs encoding secretory pathway proteins in the Arabidopsis unfolded protein response. *Proc Natl Acad Sci U S A* **110**, 5713-5718, doi:10.1073/pnas.1219047110 (2013).
- 53 Barnabas, B., Jager, K. & Feher, A. The effect of drought and heat stress on reproductive processes in cereals. *Plant Cell Environ* **31**, 11-38, doi:10.1111/j.1365-3040.2007.01727.x (2008).
- 54 Zinn, K. E., Tunc-Ozdemir, M. & Harper, J. F. Temperature stress and plant sexual reproduction: uncovering the weakest links. *J Exp Bot* **61**, 1959-1968, doi:10.1093/jxb/erq053 (2010).
- 55 Liu, Y. & Chang, A. Heat shock response relieves ER stress. *EMBO J* **27**, 1049-1059, doi:10.1038/emboj.2008.42 (2008).
- 56 Xu, X., Gupta, S., Hu, W., McGrath, B. C. & Cavener, D. R. Hyperthermia induces the ER stress pathway. *PLoS One* **6**, e23740, doi:10.1371/journal.pone.0023740 (2011).
- 57 Gao, H., Brandizzi, F., Benning, C. & Larkin, R. M. A membrane-tethered transcription factor defines a branch of the heat stress response in Arabidopsis thaliana. *Proc Natl Acad Sci U S A* **105**, 16398-16403, doi:10.1073/pnas.0808463105 (2008).
- 58 Parra-Rojas, J., Moreno, A. A., Mitina, I. & Orellana, A. The dynamic of the splicing of bZIP60 and the proteins encoded by the spliced and unspliced mRNAs reveals some unique features during the activation of UPR in Arabidopsis thaliana. *PLoS One* **10**, e0122936, doi:10.1371/journal.pone.0122936 (2015).
- 59 Liu, X., Rockett, K. S., Kørner, C. J. & Pajerowska-Mukhtar, K. M. Salicylic acid signalling: new insights and prospects at a quarter-century milestone. *Essays in biochemistry* **58**, 101-113 (2015).

- 60 Boatwright, J. L. & Pajerowska-Mukhtar, K. Salicylic acid: an old hormone up to new tricks. *Molecular plant pathology* **14**, 623-634 (2013).
- 61 Vlot, A. C., Dempsey, D. A. & Klessig, D. F. Salicylic Acid, a multifaceted hormone to combat disease. *Annu Rev Phytopathol* **47**, 177-206, doi:10.1146/annurev.phyto.050908.135202 (2009).
- 62 Delaney, T. P., Friedrich, L. & Ryals, J. A. Arabidopsis signal transduction mutant defective in chemically and biologically induced disease resistance. *Proc Natl Acad Sci U S A* **92**, 6602-6606, doi:10.1073/pnas.92.14.6602 (1995).
- 63 Alhoraibi, H., Bigeard, J., Rayapuram, N., Colcombet, J. & Hirt, H. Plant Immunity: The MTI-ETI Model and Beyond. *Curr Issues Mol Biol* **30**, 39-58, doi:10.21775/cimb.030.039 (2019).
- 64 Mukhtar, M. S., McCormack, M. E., Argueso, C. T. & Pajerowska-Mukhtar, K. M. Pathogen Tactics to Manipulate Plant Cell Death. *Curr Biol* **26**, R608-R619, doi:10.1016/j.cub.2016.02.051 (2016).
- 65 Hayashi, S., Wakasa, Y. & Takaiwa, F. Functional integration between defence and IRE1-mediated ER stress response in rice. *Sci Rep* **2**, 670, doi:10.1038/srep00670 (2012).
- 66 Nagashima, Y., Iwata, Y., Ashida, M., Mishiba, K. & Koizumi, N. Exogenous salicylic acid activates two signaling arms of the unfolded protein response in Arabidopsis. *Plant Cell Physiol* **55**, 1772-1778, doi:10.1093/pcp/pcu108 (2014).
- 67 Kilian, J. *et al.* The AtGenExpress global stress expression data set: protocols, evaluation and model data analysis of UV-B light, drought and cold stress responses. *Plant J* **50**, 347-363, doi:10.1111/j.1365-313X.2007.03052.x (2007).
- 68 Lempe, J. *et al.* Diversity of flowering responses in wild *Arabidopsis thaliana* strains. *PLoS Genet* **1**, 109-118, doi:10.1371/journal.pgen.0010006 (2005).
- 69 Waese, J. *et al.* ePlant: Visualizing and Exploring Multiple Levels of Data for Hypothesis Generation in Plant Biology. *Plant Cell* **29**, 1806-1821, doi:10.1105/tpc.17.00073 (2017).
- 70 Winter, D. *et al.* An "Electronic Fluorescent Pictograph" browser for exploring and analyzing large-scale biological data sets. *PLoS One* **2**, e718, doi:10.1371/journal.pone.0000718 (2007).
- 71 Pajerowska-Mukhtar, K. M. *et al.* The HSF-like transcription factor TBF1 is a major molecular switch for plant growth-to-defense transition. *Curr Biol* **22**, 103-112, doi:10.1016/j.cub.2011.12.015 (2012).
- 72 McCormack, M. E., Liu, X., Jordan, M. R. & Pajerowska-Mukhtar, K. M. An improved high-throughput screening assay for tunicamycin sensitivity in *Arabidopsis* seedlings. *Front Plant Sci* **6**, 663, doi:10.3389/fpls.2015.00663 (2015).
- 73 Ohta, M. *et al.* Analysis of rice ER-resident J-proteins reveals diversity and functional differentiation of the ER-resident Hsp70 system in plants. *J Exp Bot* **64**, 5429-5441, doi:10.1093/jxb/ert312 (2013).
- 74 Hong, Z. H., Qing, T., Schubert, D., Kleinmanns, J. A. & Liu, J. X. BLISTER-regulated vegetative growth is dependent on the protein kinase domain of ER stress

- modulator IRE1A in *Arabidopsis thaliana*. *PLoS Genet* **15**, e1008563, doi:10.1371/journal.pgen.1008563 (2019).
- 75 Yamamoto, M. *et al.* ERdj3B-Mediated Quality Control Maintains Anther Development at High Temperatures. *Plant Physiol* **182**, 1979-1990, doi:10.1104/pp.19.01356 (2020).
- 76 Schott, A. *et al.* *Arabidopsis stromal-derived Factor2 (SDF2)* is a crucial target of the unfolded protein response in the endoplasmic reticulum. *J Biol Chem* **285**, 18113-18121, doi:10.1074/jbc.M110.117176 (2010).
- 77 Nekrasov, V. *et al.* Control of the pattern-recognition receptor EFR by an ER protein complex in plant immunity. *EMBO J* **28**, 3428-3438, doi:10.1038/emboj.2009.262 (2009).
- 78 Wang, D., Amornsiripanitch, N. & Dong, X. A genomic approach to identify regulatory nodes in the transcriptional network of systemic acquired resistance in plants. *PLoS Pathog* **2**, e123, doi:10.1371/journal.ppat.0020123 (2006).
- 79 Pajerowska-Mukhtar, K. M., Emerine, D. K. & Mukhtar, M. S. Tell me more: roles of NPRs in plant immunity. *Trends Plant Sci* **18**, 402-411, doi:10.1016/j.tplants.2013.04.004 (2013).
- 80 Sun, Y., Detchemendy, T. W., Pajerowska-Mukhtar, K. M. & Mukhtar, M. S. NPR1 in JazzSet with Pathogen Effectors. *Trends Plant Sci* **23**, 469-472, doi:10.1016/j.tplants.2018.04.007 (2018).
- 81 Liu, X. *et al.* Bacterial Leaf Infiltration Assay for Fine Characterization of Plant Defense Responses using the *Arabidopsis thaliana*-*Pseudomonas syringae* Pathosystem. *J Vis Exp*, doi:10.3791/53364 (2015).
- 82 Koornneef, M. & Meinke, D. The development of *Arabidopsis* as a model plant. *Plant J* **61**, 909-921, doi:10.1111/j.1365-313X.2009.04086.x (2010).
- 83 Noh, S. J., Kwon, C. S., Oh, D. H., Moon, J. S. & Chung, W. I. Expression of an evolutionarily distinct novel BiP gene during the unfolded protein response in *Arabidopsis thaliana*. *Gene* **311**, 81-91, doi:10.1016/s0378-1119(03)00559-6 (2003).
- 84 Howell, S. H. When is the unfolded protein response not the unfolded protein response? *Plant Sci* **260**, 139-143, doi:10.1016/j.plantsci.2017.03.014 (2017).
- 85 Liu, X., Afrin, T. & Pajerowska-Mukhtar, K. M. *Arabidopsis GCN2 kinase contributes to ABA homeostasis and stomatal immunity*. *Communications biology* **2**, 302, doi:10.1038/s42003-019-0544-x (2019).
- 86 Mangano, S., Gonzalez, C. D. & Petruccelli, S. in *Arabidopsis Protocols* (eds Jose J. Sanchez-Serrano & Julio Salinas) 165-173 (Humana Press, 2014).
- 87 Jefferson, R. A., Kavanagh, T. A. & Bevan, M. W. GUS fusions: beta-glucuronidase as a sensitive and versatile gene fusion marker in higher plants. *The EMBO journal* **6**, 3901-3907 (1987).

## **CHAPTER 5**

### **ELUCIDATING THE ROLE OF NATURAL ANTISENSE RNA LOCI AS PRO-SURVIVAL TO PRO-DEATH MOLECULAR SWITCH IN THE IRE1A SIGNALING PATHWAY IN ARABIDOPSIS THALIANA**

by

Taiaba Afrin<sup>1</sup>, Karolina M. Pajerowska-Mukhtar<sup>1</sup>

<sup>1</sup> Department of Biology, University of Alabama at Birmingham, 1300 University Blvd.,  
Birmingham, AL 35294, USA

Manuscript in Preparation

## Abstract

In eukaryotic cells, both biotic and abiotic stress can disrupt the proper functioning of the endoplasmic reticulum (ER), leading to a response known as the unfolded protein response (UPR). This response aims to mitigate ER stress and is initiated by a highly conserved UPR sensor called Inositol-Requiring Enzyme 1 (IRE1). IRE1 activates a pro-survival pathway to protect the cell. However, when the stress conditions become extreme or chronic, the cells undergoing UPR may switch from pro-survival to pro-death signaling to avoid unfavorable circumstances for the overall well-being of the organism. The specific mechanisms responsible for attenuating the pro-survival branch of IRE1a signaling still need to be better understood in plants. In the model plant *Arabidopsis thaliana* (henceforth: Arabidopsis), it has been observed that during ER stress, IRE1a directly cleaves the mRNA of a transcription factor called bZIP60 (basic leucine zipper 60). This cleavage leads to the production of an active form of bZIP60, activating genes involved in cellular protection. To investigate the regulatory mechanisms governing bZIP60 expression during the immune response in plants, we conducted a study using the plant bacterial pathogen *Pseudomonas syringae* pv. tomato (*Pst* DC3000) as a biotic inducer of ER stress. Our findings revealed the involvement of a novel microRNA called miR5658 in targeting bZIP60 for degradation. Further experiments using reporter-based assays confirmed that the binding sequence of miR5658 on bZIP60 mRNA was necessary for its degradation. Additionally, T-DNA mutants lacking miR5658 showed increased stability of the bZIP60 transcript. Our results indicate that in response to triggering cell death stimuli, miR5658 target bZIP60 mRNA, effectively turning off the pro-survival pathway mediated by IRE1a, thereby tipping the

scales towards a pro-death signaling cascade. These findings provide insights into the intricate regulatory network controlling cell fate during ER stress and plant immune responses.

## **Introduction**

Because of plants' autotrophic nature, they are a very appealing food source for many exploitative herbivorous species like microbes, insects, and higher animals (Zhang et al., 2017). Thus, their survival and health rely on their ability to identify and imply appropriate defensive strategies against those exploitative species. Hence, plants have evolved multilayer defense systems to thrive in nature. Unlike animals, plants have a unique, innate immune system, where every cell expresses innate immune receptors to identify invasion signals (Jones & Dangl, 2006). Plants have cell surface localized pattern recognition receptors (PRRs) to identify the pathogen/microbe-associated molecular pattern (PAMPs/MAMPs) or host-derived damage-associated molecular pattern (DAMPs) and execute defense responses (Jones & Dangl, 2006; Zipfel & Felix, 2005). The successful recognition leads to pattern-triggered immunity (PTI), the very first line of defense responses of plants against almost all microbial pathogens (Chisholm et al., 2006; Dangl & Jones, 2001; Jones & Dangl, 2006). Some pathogens evolved to encode effector molecules as pathogenic virulence to delay or impede and/or restrain PTI, resulting in effector-triggered susceptibility (ETS). In contrast, plants also evolved resistance (*R*) genes to specifically detect effectors, triggering a rapid and higher amplitude of defense responses leading to effector-triggered immunity (ETI) (Chisholm et al., 2006; Dangl & Jones, 2001; Jones & Dangl, 2006). The recognition of pathogen effectors by *R* genes triggers a hypersensitive response (HR) in most cases (Dangl & Jones, 2001) through programmed cell death (PCD), production of reactive oxygen species (ROS), antimicrobial compound synthesis at the infected tissue (Dangl & Jones,

2001; Lam, 2004; Nimchuk et al., 2003). In many instances, there is no distinct difference in-between PTI and ETI (Thomma et al., 2011), and ETI is referred to as amplified PTI (Jones & Dangl, 2006). Hence, the plant immune system is a unique surveillance system that detects intrusions and employs defense responses (Gust et al., 2017). Usually, PTI-mediated PCD appears after several days of infection, while ETI-triggered HR PCD happens within hours of infection (Lam, 2004).

Among different phytohormones that modulate HR cell death under diverse environmental situations, salicylic acid (SA) is a well-described regulator of systemic acquired resistance (SAR) (Alvarez, 2000). During an immune response, endogenous SA serves crucial functions in controlling HR and cell death. Several studies confirmed that elevated SA levels are required to establish local and systemic resistance (Ding & Ding, 2020). Non-expressor of pathogenesis-related gene 1 (NPR1) gene is the master regulator of defense gene expressions and plant immunity and is highly conserved in plant species (Chern et al., 2001; Mou et al., 2003). NPR1 transduces SA signaling by activating downstream PR genes and positively regulates SAR (Pajerowska-Mukhtar et al., 2013). Following exposure to SA, NPR1 can stimulate its expression ; this triggers a co-regulatory mechanism where both transcription and post-transcriptional regulation of NPR1 come into play (Ding & Ding, 2020). Unlike NPR1, both NPR3 and NPR4 act as inhibitors of plant defense mechanisms (Zhang et al., 2006). The double mutant plants *npr3npr4* exhibit increased expression of PR genes and enhanced basal resistance (Fu et al., 2012; Zhang et al., 2006). Due to their strong affinities with SA, NPR3 and NPR4 have been previously identified as SA receptors (Ding et al., 2018; Fu et al., 2012). NPR proteins can regulate immunity by interacting with other hormone regulatory pathways

and reprogramming a huge gene expression network (van Butselaar & Van den Ackerveken, 2020). NPR1 interacts with members of the bZIP transcription factor family to trigger defense responses after entering the nucleus (Fan & Dong, 2002).

The endoplasmic reticulum (ER) is integral to multiple cellular stress response pathways. ER is a protein folding machinery in eukaryotic cells as it is the maturation site of secretory and membrane proteins. When the protein folding and assembly are perturbed in ER, the unfolded and misfolded protein accumulates in ER and causes ER stress. ER stress triggers response mechanisms termed unfolded protein response (UPR) to maintain cellular homeostasis (Afrin, Diwan, et al., 2020; Afrin, Seok, et al., 2020; Verchot & Pajerowska-Mukhtar, 2021). Among three pathways, IRE1 is an ER transmembrane resident stress sensor widely conserved in eukaryotes (Afrin, Seok, et al., 2020; Koizumi et al., 2001). IRE1 is a type-1 membrane protein. In plants, IRE1 mediates transcriptional activation of genes encoding ER chaperones and folding enzymes through unconventional splicing of bZIP60 mRNA (Iwata et al., 2008; Mishiba et al., 2013; Moreno et al., 2012; Nagashima et al., 2011). The spliced bZIP60 travels to the nucleus, acts as a transcription factor, and activates cytoprotective genes (Afrin, Seok, et al., 2020; Iwata et al., 2008; Moreno et al., 2012; Nagashima et al., 2011). IRE1 can also mediate the bulk mRNA degradation to reduce the nascent protein load through the regulated IRE1-dependent decay (RIDD) (Hollien et al., 2009; Mishiba et al., 2013).

Throughout their evolution, plants have been continually subjected to extreme biotic and abiotic stress, which they managed thanks to developing intricate molecular mechanisms. These complex mechanisms evolved largely to help plants to survive and sustain in extreme environmental conditions. Non-protein coding DNA contributes

equally to this complex adaptation process compared to protein-coding DNA. The non-protein coding DNA (also known as "junk" DNA) transcribes a substantial amount of the transcriptional unit identified as non-coding RNAs (ncRNAs). It functions in various regulatory processes (Urquiaga et al., 2020). Long non coding RNA (lncRNA, >200 nucleotides) is a type of regulatory ncRNA (Ponting et al., 2009). Long non-coding natural anti-sense transcripts (lncNATs) are a category of lncRNAs that overlap with one or more exons of a distinct transcript but are located on the reverse strand. The lncRNA's mode of action varies widely; they can interact with other genes, hormones, proteins and ncRNAs; act as precursors of miRNAs siRNAs; act as target mimicry of other miRNAs; or can be co-induces with other neighboring defensive genes (Seo et al., 2017; Sun et al., 2020; Wang et al., 2015; Xin et al., 2011; Yu et al., 2020; Zhu et al., 2014). Few recent studies implicate the significant importance of lncRNA and lncNAT in plants' defense response mechanisms (Kumar & Chakraborty, 2021; Wang et al., 2015).

Among other lncRNAs, NATs play critical roles in gene expression regulation and are mainly involved with various abiotic and biotic stress response mechanisms in many species, for example, *Homo sapiens*, *Mus musculus*, *Saccharomyces cerevisiae*, *Plasmodium falciparum*, *Oryza*, *Zea mays*, *Triticum*, *Brassica rapa*, *Arabidopsis* (Borsani et al., 2005; He et al., 2008; Katayama et al., 2005; Liu et al., 2012; Lu et al., 2012; Oono et al., 2017; Siegel et al., 2014; H. Wang et al., 2014; Xu et al., 2017; Yassour et al., 2010; Yu et al., 2013). lncNAT can regulate the expression level of sense transcript (Marquardt et al., 2014; Sun et al., 2013). Depending on the nature of NATs' effect on sense transcript, NATs can be categorized into two: concordant (NAT and sense transcripts express coordinately), discordant (NAT and sense transcript have opposite

expression patterns) (Jabnoune et al., 2013; Swiezewski et al., 2009; H. Wang et al., 2014). For example, the *Arabidopsis* cold-assisted intronic non-coding RNA (COOLAIR) represses the Flowering locus C (FLC) sense transcript by altering histone marks (Swiezewski et al., 2009); a cis-NAT in rice boosts the translation of its cognate sense mRNA in order to maintain phosphate homeostasis and plant fitness (Jabnoune et al., 2013). Due to their wide range, the general biological functions and regulatory mechanisms are elusive. Researchers have demonstrated that NATs utilize a variety of ways to regulate the transcriptional or post-transcriptional expression of sense transcripts, for example, translation initiation (Wilusz et al., 2009), mRNA stability (Faghihi et al., 2008), transcription termination (Georg et al., 2009), DNA methylation (Lewis et al., 2004), histone methylation (Zhao et al., 2018), translational enhancement (Deforges et al., 2019; Jabnoune et al., 2013), RNA interference (Prescott & Proudfoot, 2002), gene silencing (Katiyar-Agarwal et al., 2006), RNA masking induced alternative splicing (Hastings et al., 1997), RNA editing (Peters et al., 2003).

Many NATs have been identified in plants, i.e., 7-9% of all transcripts are overlapped as cis-NATs (Lu et al., 2012). In *Arabidopsis*, ~88% of cis-NATs pairs are paired as protein-coding genes and non-protein coding transcripts (Okamoto et al., 2010). These cis NATs may form a complex regulatory network, but the current understanding of their role and function is minimal. Several studies in the model plant *Arabidopsis* found NAT's crucial involvement in developmental processes, for instance, during germination (Fedak et al., 2016), flowering (Csorba et al., 2014), and gametophyte development (Wunderlich et al., 2014). NATs are also associated with stress response mechanisms in different plants, e.g., in *Arabidopsis* during salt tolerance (Borsani et al.,

2005; Yu et al., 2013), cold acclimation (Kindgren et al., 2018); in rice phosphate starvation (Jabnoune et al., 2013) and leaf blade flattening (X. Liu et al., 2018), in tomato oomycete resistance (Cui et al., 2017). Along with these direct function, they can act as precursors of siRNA (Yu et al., 2013) and miRNA (Lu et al., 2008).

Plant miRNAs pair with their targets nearly perfectly and can cause mRNA cleavage. miRNAs are small lncRNA with an average 22 nucleotide length. Most reported miRNAs interact with their target mRNA at 3'UTR (untranslated region) (Ha & Kim, 2014). However, they have also been reported to interact with 5' UTR, coding regions and the promotor region (Broughton et al., 2016). Through interaction, miRNAs can suppress or activate gene expression depending on the condition (Ha & Kim, 2014; Vasudevan, 2012). Several recent articles proved the shuttling of miRNA into different subcellular compartments to control transcription and translation rates (Makarova et al., 2016). miRNAs can move from one cell to another through plasmodesmata and for systemic long-distance through the vasculature, and can therefore act as mobile signaling molecules (Li et al., 2021; Molnar et al., 2011). miRNAs are not only mobile within the plant but can also move between plants and interacting organisms (Betti et al., 2021; Zhang et al., 2016).

miRNAs have been reported to regulate plants' developmental (Guo et al., 2005; Wang et al., 2005), biotic (Hajdarpasic & Ruggenthaler, 2012; Varallyay et al., 2010), and abiotic stress responses (Gao et al., 2010; Guan et al., 2014; Phillips et al., 2007; Song et al., 2013; Xie et al., 2015; Zhang, 2015). Several miRNAs have been reported in mammalian systems intertwined with ER stress-responsive pathways. For example, miR-211 has been reported as a key regulator of PERK-ATF4-mediated pro-survival signaling

during mammalian ER stress responses (Chitnis et al., 2012). A number of miRNAs have been reported to play a role in modulating the IRE1 $\alpha$ -XBP1 pathway. For example, miR-214 (Duan et al., 2012), miR-30-c-2\* (Byrd et al., 2012), miR-34c-5p (Bartoszewska et al., 2019), miR-665 (Li et al., 2017) regulate XBP1 expression under different circumstances; miR-1291 can directly target IRE1 $\alpha$  within its 5'-UTR in hepatoma cells, leading to overexpression of the pro-oncogenic protein glypicn-3 (Maurel et al., 2013).

Although miRNA-regulated gene expression has been reported for different kinds of stress, the involvement of miRNA in ER stress response mechanisms in plants, particularly in Arabidopsis, has yet to be adequately investigated. This study demonstrated the regulatory roles of novel miRNA miR5658 during the transition from pro-survival to pro-death molecular switch. Functional analysis indicated that miR5658 regulates cell death during acute ER stress (caused by *Pst* DC3000 AvrRpm1) by controlling bZIP60 expression. We also showed that the sense transcript of miR5658 precursor cis-NAT does not interfere with cell death regulation. Instead, the sense transcript concordantly supports cis-NAT in this regulation. This finding provides insight into the function of cis-NATS in miRNA-guided call death during acute ER stress.

## Results

### ***Identification and analysis of novel miRNAs that can target bZIP60 transcript:***

miRNAs are well-established key regulators of different stress-responsive mechanisms in mammalian and plant systems. As there are already identified miRNAs that regulate the IRE1 $\alpha$ -XBP1 mediated pathway during ER stress, we sought to identify miRNAs that can regulate the IRE1a-bZIP60 mediated pathway in Arabidopsis. To

identify the miRNAs that can target bZIP60 (spliced or unspliced form), we first performed a prediction analysis using miRBase website (<https://mirbase.org>). Using sequence analysis of bZIP60 and mature miRNAs, we have predicted three microRNAs that can target bZIP60 (Table 1). We then confirmed the prediction using psRNATarget: A Plant small RNA Target Analysis Server (<https://www.zhaolab.org/psRNATarget/>) website. Among them, miR5658 and miR414 target bZIP60 at exon 1 and miR397b target at exon 2 of bZIP60 (supplemental figure 1). Using RNAfold WebServer (<http://rna.tbi.univie.ac.at/cgi-bin/RNAWebSuite/RNAfold.cgi>), the predicted secondary structures of microRNA are presented in Table 1.

**Table 1: Predicted miRNAs that can target both spliced and unspliced bZIP60 transcript.** The prediction was performed using “miRBase: the microRNA database” (<https://mirbase.org>). E value, alignment, and target location were adapted from the miRBase prediction. The secondary structure was predicted using “RNAfold WebServer” (<http://rna.tbi.univie.ac.at/cgi-bin/RNAWebSuite/RNAfold.cgi>).

## **Differential expression levels of predicted miRNAs in response to biotic stress:**

To complement our knowledge of miRBase predictions, we quantified the expression levels of predicted miRNAs. We exposed the wild-type Col-0 with pathogen

*Pst* DC3000 AvrRpm1 for up to 6 hours and quantified the expression of miRNAs using the stem-loop qRT-PCR technique. The analysis revealed that all three are detectable in Arabidopsis leaves without stress. After six hours, all three miRNAs' expression levels increased significantly ( $p<0.0001$ ). miR414 has the lowest induced expression, while miR5658 has the highest induced expression (figure 1a). While comparing the induced expression, miR5658 induced significantly highly ( $p<0.0001$ ) compared to miR414 and miR397b. The findings illustrate that miR5658 outperforms itself in transcript accumulation. miR5658 and miR414 possess considerably overlapping target sites on bZIP60, suggesting they may be in competition for targeting bZIP60. Thus, miR5658 asserts its dominance over miR414 in targeting bZIP60 (Supplemental figure 1). We opted for miR5658 for this investigation to discover the most crucial regulator of cell death during biotic stress.

***The expression of endogenous miR5658 increases concurrently with the duration of biotic stress-triggered cell death:***

To strengthen our prediction and better characterize the novel miR5658, we sought a deeper understanding of the accumulation rate of transcripts over time. We collected samples at 0 hours, 2 hours, 4 hours, and 6 hours after exposing wild-type Col-0 to *Pst* DC3000 AvrRpm1. For the assessment, a specialized TaqMan assay was utilized. This TaqMan assay is highly specific for mature miR5658, excluding the possibility of having a false-positive assessment of the miR precursor. This assay uses a stem-loop primer specific to miR5658 during reverse transcription. Figure 1b demonstrates that the accumulation of miR5658 transcripts was triggered at 2 hours and substantially increased

compared to our control group at 6 hours. As these results corroborate our initial hypothesis, we continued examining the correlation between miR5658 and bZIP60

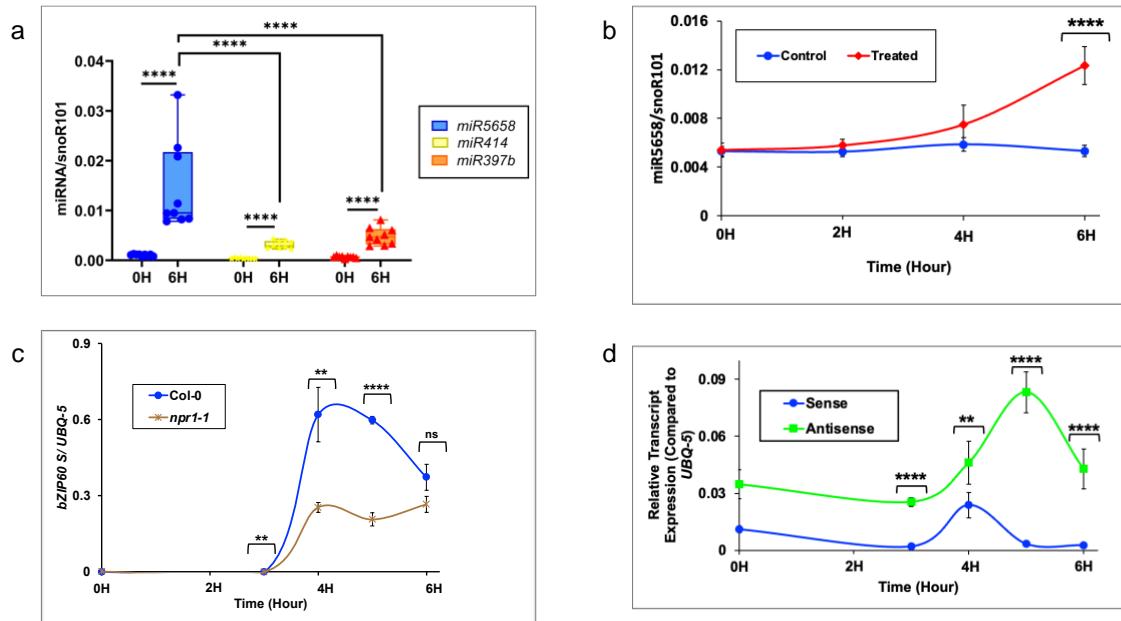


**Figure 1: The analysis of relative miRNA expression level.** (a) Basal and induced expression of miR5658, miR414, miR397b upon exposure to *Pst* DC3000 avrRPM1 for 0 and 6 hours. Expression levels were measured via stem-loop qRT-PCR and transcript levels were normalized to reference small RNA, snoR101 (a small nucleolar RNA). Statistical analyses were performed in GraphPad Prism 9 by Two-Way ANOVA followed by Tukey's multiple comparison test. (b) The expression of miR5658 over a time course upon exposure to *Pst* DC3000 avrRPM1 for 0, 2, 4 and 6 hours. Expression levels were measured via miR5658 specific TaqMan qPCR assay and transcript levels were normalized to a reference small RNA, snoR101. Statistical analyses were performed in GraphPad Prism9 by Two-Way ANOVA followed by Tukey's multiple comparison test. (c) Basal and induced expression of bZIP60 in Col-0 and *npr1-1* genotype upon exposure to *Pst* DC3000 avrRPM1 for 0, 3, 4, 5 and 6 hours. Expression levels were measured via real-time RT-qPCR assay and transcript levels were normalized to a reference gene (Ubiquitin-5). Statistical analyses were performed in Excel by two-tailed student t-test. (d) Basal and induced expression of sense and antisense transcript upon exposure to *Pst* DC3000 avrRPM1 for 0, 3, 4, 5 and 6 hours. Expression levels were measured via strand specific real-time RT-qPCR assay and transcript levels were normalized to a reference gene (Ubiquitin-5). Statistical analyses were performed in GraphPad Prism9 by Multiple Mann-Whitney test. At least three biological replicates with three technical replicates were performed. Significant differences are indicated by asterisks (\*\*\*\* p < 0.0001, \*\*\* p < 0.001, \*\* p < 0.01, \* p < 0.05).

expression.

***miR5658 and spliced bZIP60 transcript accumulation showed a reciprocal relation during cell death triggering stimuli:***

bZIP60 transcript consists of two exons and one intron (supplemental figures 2 and 3). After unconventional splicing of bZIP60 by IRE1 at exon 2, bZIP60 becomes an active, nuclear-localized TF. As our predicted miRNAs also target different locations of the bZIP60 sequence, we investigated if the IRE1 splicing and miRNA target locations overlap. miR5658 and miR414 target at exon 1 of bZIP60 (supplemental figure 1), so these two are excluded from the investigation. Even though miR397b targets exon 2, it does not overlap with the IRE1 splicing site (supplemental figure 1). Hence targeting of our predicted miRNAs is independent of IRE1's splicing. Spliced and unspliced bZIP60 are vulnerable to degradation/repression by all three miRNAs. To better understand the relationship between miR5658 and spliced bZIP60 expression, we subjected our positive control wild type Col-0 and negative control immune-compromised *npr1-1* to pathogen Pst DC3000 AvrRpm1 from 0 to 6 hours to assess the expression through qRT-PCR. The data demonstrate that the expression of spliced bZIP60 in genotype Col-0 started to induce highly at 3 hours, peaked at 4 hours, and decreased at 5 and 6 hours (figure 1c). In the *npr1-1* mutant the expression was higher at 4 hours and remained similar at 5 and 6 hours. Spliced bZIP60 levels in Col-0 were statistically significantly higher than in *npr1-1* at 3, 4, and 5 hours. The increased expression of miR5658 (figure 1b) coincides with the decreased expression of bZIP60 (figure 1c) in wild-type Col-0. Based on this evidence, we can hypothesize that miR5658 is the crucial regulator and acts as a molecular switch from cell survival to cell death during acute biotic stress.

***Antisense transcript dominates at expression over sense transcript during cell death triggering stimuli:***

Next, we proceeded to characterize the miR5658 and after analyzing the transcripts reported in the TAIR 11 database (<https://www.arabidopsis.org/index.jsp>) we identified a lncNAT that serves as a precursor of miR5658. The antisense lncNAT (AT4G39838: 2077 bp) ~95% overlaps with the sense transcript (AT4G39840: 1097 bp) (supplemental figure 4)—the miR5658 precursor region in lncNAT overlaps at the sense transcript exon. To compare the transcript accumulation of lncNAT and sense transcripts, we exposed wild-type Col-0 plants to the pathogen *Pst* DC3000 AvrRpm1 for up to 6 hours and quantified their expression using strand-specific tag-based qRT-PCR (figure 1d). The data suggest that the lncNAT and sense transcript were expressed at all the time points (0, 3, 4, 5, and 6 hours) we analyzed. The lncNAT was expressed significantly higher at 3, 4, 5, and 6 hours when compared to the sense strand. At 4 hours, the sense transcript expression was relatively elevated, whereas, at all other times, it was extremely low and flat. The lncNAT transcript expression was highest at 5 hours compared to the other time points.

***Characteristics of sense and antisense mutant lines:***

As sense transcript (AT4G39840) is predicted to encode a protein and antisense transcript (AT4G39838) is predicted to transcribe the miR5658, we obtained mutant plants that we designated *srcl* (stress response component-like protein, AT4G39840), which contain T-DNA insertion in the sole bZIP60 exon and thus should abolish the

expression of sense protein as well as antisense transcript production (figure 2a). We also generated *NAT<sub>SRCL</sub>* (natural antisense transcript of stress response component like protein, AT4G39838) mutant lines, which have T-DNA insertion in the precursor region of miR5658 and are predicted to eliminate the antisense transcript production (figure 2a). We tested the mutant lines' transcript production through quantification of transcripts by using a tag-based qRT-PCR before and after cell death inducing abiotic stressor *Pst* DC3000 AvrRpm1 for up to 6 hours. Figure 2b demonstrates that the expression of miR5658 precursor producing antisense strand is statistically significantly higher after 6 hours in our positive control wild type Col-0 treated with *Pst* DC3000 AvrRpm1. In comparison, the mutant lines *srcl* and *NAT<sub>SRCL</sub>* did not show significant changes in antisense transcript production even after exposure to *Pst* DC3000 AvrRpm1 (figure 2b). Our negative control *npr1-1* also showed unchanged transcript production upon biotic stressor exposure.

***Mutant lines srcl and NAT<sub>SRCL</sub> are extremely sensitive to prolonged ER stress.***

Upon verifying that the mutant lines (*NAT<sub>SRCL</sub>*, *srcl*) do not express antisense transcripts (figure 2b), we investigated whether these lines demonstrated any changes in their ER stress responses. Quantification of total fresh weight and chlorosis triggered by chemically induced ER stress are two well-established hallmarks of UPR in Arabidopsis (McCormack et al., 2015). We exposed our positive control wild type Col-0, mutant line *NAT<sub>SRCL</sub>*, *srcl*, and our negative control mutants *npr1-1* and *bzip60* (figure 2c, 2d and 2e) to ER stress caused by chemical tunicamycin that is an inhibitor of N-linked glycosylation and causes ER stress by impeding the folding of glycosylated proteins.

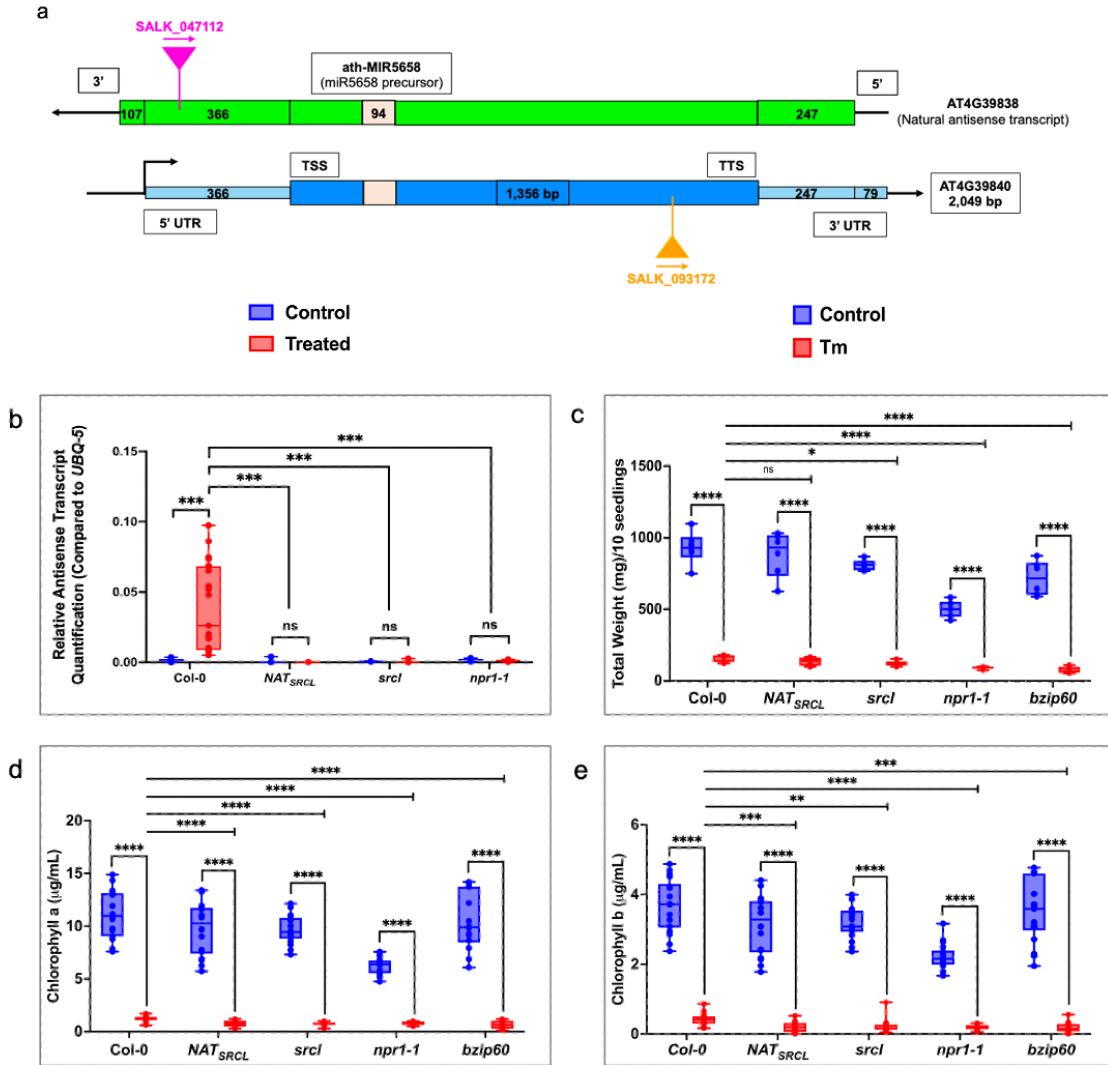


**Figure 2: Characterization of *NAT<sub>SRCL</sub>* and *srcl* mutants:** (a) Schematic of miR5658 precursor NAT (antisense) and its sense transcript with the T-DNA insertion location. (b) Total weight (mg/10 seedlings) of different 5 days old plants upon exposure to Tunicamycin for 3 days and recovery of 3 days. Statistical analyses were performed in GraphPad Prism9 by multiple Mann-Whitney test. (c) and (d) Chlorophyll a ( $\mu\text{g}/\text{ml}$ ) and chlorophyll b ( $\mu\text{g}/\text{ml}$ ) of different 5 days old plants upon exposure to Tunicamycin for 3 days and recovery of 3 days. Statistical analyses were performed in GraphPad Prism9 by multiple Mann-Whitney test.

First, we wanted to investigate if the total plant growth rate is impacted by a prolonged Tm exposure. Towards this, we exposed the seedlings to  $0.3 \mu\text{g}/\text{mL}$  Tm (Tocris Bioscience) supplemented  $\frac{1}{2}$  MS for three days and recovered them for three more days in  $\frac{1}{2}$  MS media. Figure 2c demonstrates that all the mutants, along with our positive

control wild type Col-0, were severely affected, and the total weights were reduced statistically significantly by the Tm-induced ER stress. The NAT mutant line *NAT<sub>SRCL</sub>* was severely impacted by Tm stress, but when compared with Tm stressed wild type Col-0 to Tm stressed *NAT<sub>SRCL</sub>*, the impact is not statistically significant. This might be due to the fact that prolonged ER stress could be overwhelming the miR5658 in Col-0, making it potentially unable to cope with the immense amount of ER stress. On the contrary, the total weight of sense mutant line *srcl* plants was statistically significantly impacted compared to Tm-stressed Col-0, which indicates that the sense transcript may be associated with prolonged ER stress management. The negative control mutants, *npr1-1*, *bzip60*, were severely, and statistically significantly, affected by the Tm stress compared to Col-0. Collectively, the mutant lines were deficient in ER stress recovery compared to our positive control wild-type Col-0.

Next, we investigated the amount of seedling chlorosis because Tm mediated ER stress by quantifying chlorophyll a and chlorophyll b content. Chlorophyll a content in mutant line *NAT<sub>SRCL</sub>* and *srcl* reduced statistically significantly compared to wild-type Col-0 (figure 2d). Negative control mutants *npr1-1* and *bzip60* also showed significant chlorosis compared to Col-0, even compared to *NAT<sub>SRCL</sub>* and *srcl* (figure 2d). The mutant line *NAT<sub>SRCL</sub>* and *srcl* showed significant chlorosis in terms of Chlorophyll b when compared to Col-0 (figure 2e). Negative control mutants *npr1-1* and *bzip60* again showed significant chlorophyll b reduction compared to Col-0 (figure 2e). However, chlorosis of chlorophyll a was higher in all mutant lines compared to the wild type (figure 2d and 2e).

***Mutation in the miR5658 targeted seed region in bZIP60 blocks the miR5658 targeting and increase bZIP60 expression:***

Next, we sought to better comprehend the possible relationship between miR5658 and the bZIP60 transcript. To directly test the miR5658's ability to degrade bZIP60 mRNA during cell death, we mutated the miR seed binding region of wild-type bZIP60 (supplemental figure 5). We hypothesized that the wild-type bZIP60 mRNA will be degraded by miR5658 while the mutated bZIP60 variant will be able to escape the miR5658-mediated degradation. The seed region of miR5658 is complementary to a total of four codons on bZIP60 mRNA corresponding to aspartic acids (GATGATGATGAC), making it a one-of-a-kind binding site. In order to create a synonymous point mutation, we can only change Thymine (T) into Cytosine (C). However, miRNA possesses the capacity to generate a bulge through imperfect base-pairing, which can inhibit the translation of the target transcript. This, in turn, makes it challenging to create synonymous point mutations that will block miR5658 binding to bZIP60. To verify that miR5658 binding is indeed being blocked, we used a combination of two point mutations and two sets of mutated *bZIP60* (designated M1 and M2). We used site-directed mutagenesis to mutate wild-type *bZIP60* into M1 and M2. The mutations in the pDONR207 constructs were confirmed by Sanger sequencing. Next, we generated plant expression constructs carrying 35S promoter followed by WT/M1/M2 *bZIP60* transcript fused with GUS (2x35S::WT *bZIP60*-GUS; 2x35S::M1 *bZIP60*-GUS; 2x35S::M2 *bZIP60*-GUS) (supplemental figure 5), incorporated them into *Agrobacterium tumefaciens* and infiltrated the resulting Agrobacteria into different genotypes of 4-5 weeks old Arabidopsis. At that point, the GUS expression pattern was evaluated using a

transient MUG assay. Our results demonstrated that wild-type Col-0, sense mutant *srcl*, and negative control mutant *bzip60* showed significantly higher mutated *bZIP60* expression compared to wild-type *bZIP60*, whereas the miR5658 mutant line *NAT<sub>SRCL</sub>* had significantly lower expression of mutated *bZIP60* than wild type *bZIP60* (figure 3a). Another control mutant *npr1-1* showed unchanged and significantly higher *bZIP60* expression (both in wild type and mutated) compared to any other genotype (figure 3b). The reduced expression of mutated M2 *bZIP60* in *NAT<sub>SRCL</sub>* was a somewhat unexpected finding; thus, we set out to investigate the reason behind this result. We noted that miR5658 and miR414 have overlapping seed regions (supplemental 1).

To corroborate the transient MUG assay results we performed a histochemical GUS assay with the genotypes Col-0, *NAT<sub>SRCL</sub>*, *srcl*, *bzip60* and *npr1-1* harboring WT *bZIP60* (2x35S::WT *bZIP60-GUS*), M1 *bZIP60* (2x35S::M1 *bZIP60-GUS*) and M2 *bZIP60* (2x35S::M2 *bZIP60-GUS*), respectively. Figure 3c demonstrates that Col-0 plants harboring M2 *bZIP60-GUS* showed a remarkable increase in GUS expression compared to WT *bZIP60*. The *NAT<sub>SRCL</sub>* expressing WT *bZIP60* showed higher *bZIP60-GUS* accumulation than M2 *bZIP60*, which complements the MUG assay data. The sense mutant line *srcl* harboring M2 *bZIP60-GUS* had significantly higher  $\beta$ -glucuronidase activity, indicating higher expression of *bZIP60-GUS* compared to WT *bZIP60*. Another control mutant *bzip60* harboring M2 *bZIP60-GUS* showed comparatively higher GUS levels than WT *bZIP60*. Meanwhile, the negative control mutant *npr1-1* showed similar GUS expression regardless of the harbored construct: WT *bZIP60* or M2 *bZIP60*. Based on the accumulated data, it can be concluded that miR5658 can directly bind to WT *bZIP60* mRNA, thereby inhibiting its translation or inducing its degradation.

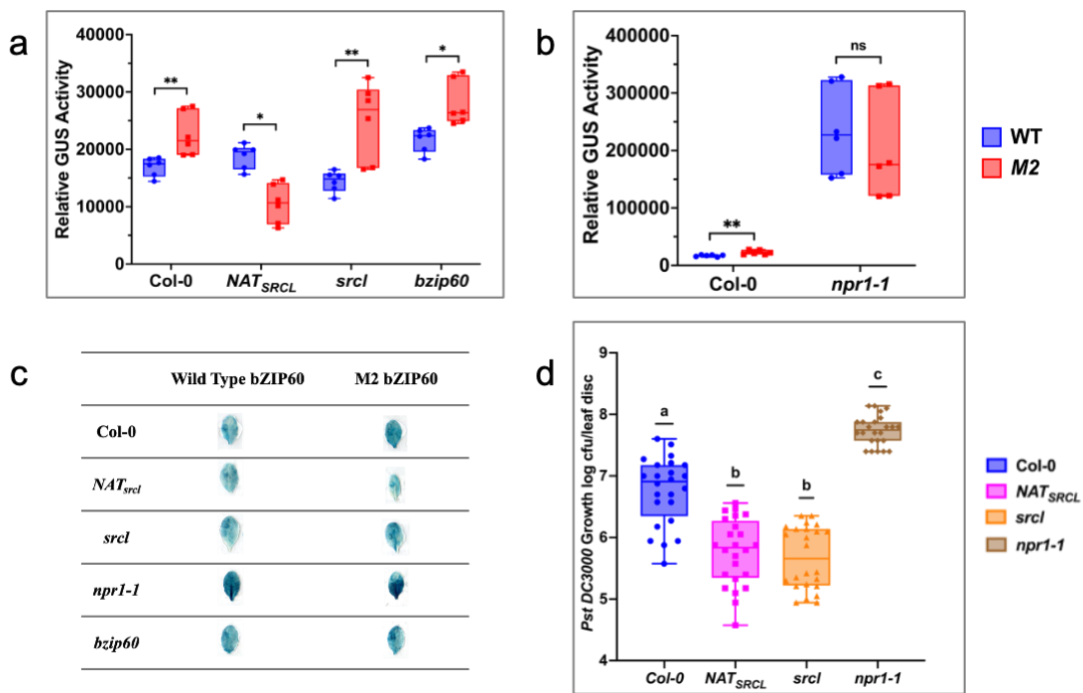


**Figure 3: Transient activity of mutated bZIP60 and pathogenic resistance:** (A) and (B) Transient MUG assay to determine the wild type and mutant bZIP60 expression in presence/absence of miR5658. Quantification of  $\beta$ -glucuronidase (GUS) activity in Arabidopsis Col-0, NAT<sub>SRC</sub>L, srcl, npr1-1 and bZIP60 leaves transiently expressing transcriptional 35S::WT bZIP60-GUS and 35S::M2 bZIP60-GUS reporter. Statistical analyses were performed in Excel by two-tailed student t-test. (C) Histochemical GUS assay in Col-0, NAT<sub>SRC</sub>L, srcl, npr1-1 and bZIP60 leaves transiently expressing transcriptional 35S::WT bZIP60-GUS and 35S::M2 bZIP60-GUS reporter. (D) Enhanced disease resistance of different genotypes upon exposure to *Pst* DC3000. Bacterial populations were quantified at 2 dpi. Statistical analyses were performed in Excel by One-Way ANOVA followed by Tukey's multiple comparison test. Treatment groups are represented according to legends. 4-5 weeks old plants were used to perform the experiment. At least three biological replicates with three technical replicates were performed. Significant differences are indicated by asterisks (\*\*\*\* p<0.0001, \*\*\* p<0.001, \*\* p<0.01, \* p<0.05) or by letters (a/b/c) for different groups.

**Antisense and sense mutant lines are more resistant towards biotic stress inducing**

**pathogen *Pseudomonas syringae*:**

We next aimed to study the possible involvement of miR5658 and its sense transcript in the pathogen resistance mechanisms. We pressure-infiltrated *Pst* DC3000

into the leaves of the wild-type control Col-0, mutant lines *NAT<sub>SRCL</sub>*, *srcl* and hypersusceptible *npr1-1* followed by bacterial growth quantification three days post infiltration (Liu et al., 2015). The miR5658 mutant line *NAT<sub>SRCL</sub>* demonstrated more than a half log lower bacterial growth than the wild-type Col-0 (figure 3d). The sense transcript mutant line *srcl* showed about one log lower bacterial growth compared to Col-0. Accumulating lower bacterial loads, the mutant lines showed heightened resistance against pathogen infection compared to Col-0. As the miR5658 and/or its sense transcript is absent in these mutants, we posit that their pro-survival pathway is active longer than in Col-0, which helps the plants to defend more effectively against the *Pst* infection. The negative control *npr1-1* showed the highest amount of bacterial growth, as it was expected given the well-documented hyper susceptibility phenotype of *npr1-1*.

***miR5658 and its sense transcript regulate HR mediated cell death:***

After obtaining direct evidence that miR5658 can bind to *bZIP60*, next, we sought to comprehend the pivotal regulatory role of miR5658 in the progression of cell death. To investigate the function of miR5658 in HR-mediated cell death, we challenged the miR5658 mutant line *NAT<sub>SRCL</sub>*, sense mutant line *srcl*, Col-0, and *npr1-1* with the pathogen *Pst* DC3000 harboring an avirulent effector AvrRpm1. The levels of cell death upon pathogen infection were quantified by electrolyte leakage measurement. As the dying cells release electrolytes, the amount of leaked electrolytes is directly proportional to the number of dying infected plant cells. The mutant *NAT<sub>SRCL</sub>* suppressed the extent of cell death caused by the avirulent pathogen *Pst* DC3000 AvrRpm1 (figure 4a). The sense mutant *srcl* also suppressed the cell death progression compared to the positive control

Col-0 and negative control *npr1-1*. Both *NAT<sub>SRCL</sub>* and *src1* mutant showed different cell death patterns compared to the controls, which were delayed and of a lower amplitude. The wild-type Col-0 showed steep progression of cell death every 30 minutes, and arrived at the plateau around seven hours after *Pst* DC3000 AvrRpm1 exposure. In the case of *npr1-1*, the cell death plateaued around six hours and 30 minutes. The *NAT<sub>SRCL</sub>* and *src1* plants showed slower progression and lower conductivity readings than the control genotypes. . Consistent with our hypothesis detailed above, as the mutant lines are

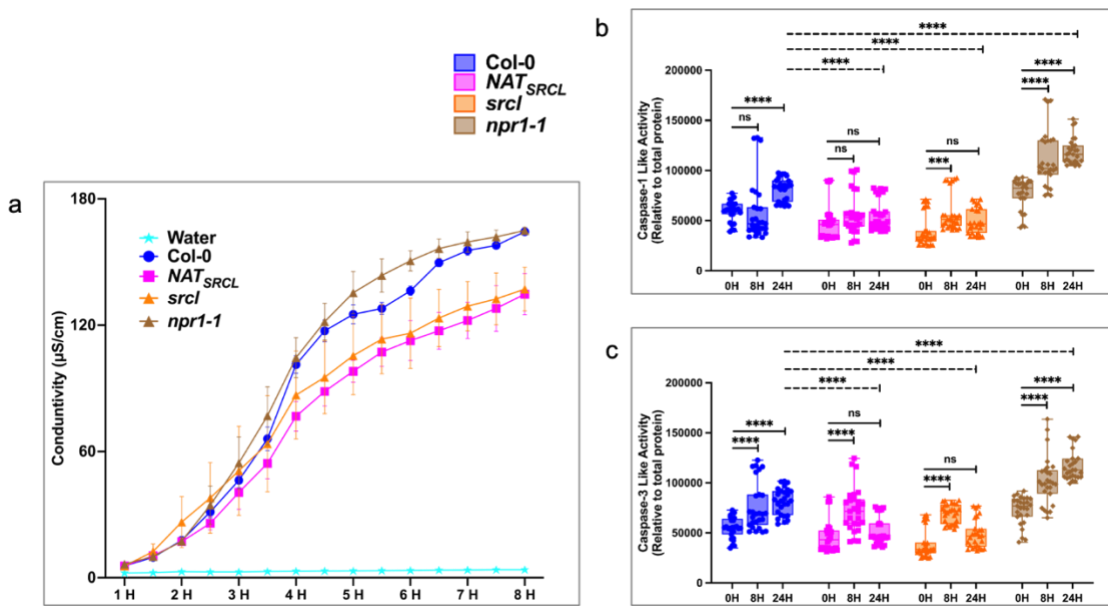


**Figure 4: Cell Death Analysis of control and mutant lines.** (A) Electrolyte leakage from Col-0, *NAT<sub>SRCL</sub>*, *src1* and *npr1-1* after bacterial inoculation. 4-5 weeks old Arabidopsis leaves were syringe-infiltrated with *Pst* DC3000 avrRPM1. Conductivity measurements of electrolytes leakage from dying cell were recorded from 1 to 8 hour after inoculation. (B) and (C) The levels of Caspase-1 and Caspase-3-like activity in the total protein content at 0, 8 and 24 hours were measured in Col-0 *NAT<sub>SRCL</sub>*, *src1* and *npr1-1* Arabidopsis plants following bacterial inoculation. Syringe infiltration of *Pst* DC3000 avrRPM1 was performed on 4-5-week-old Arabidopsis leaves. Statistical analyses were performed in GraphPad Prism9 by multiple Mann-Whitney test. At least three biological replicates with three technical replicates were performed. Significant differences are indicated by asterisks (\*\*\*\* p<0.0001, \*\*\* p<0.001, \*\* p<0.01, \* p<0.05) or by letters (a/b/c) for different

deficient in the miR5658 production, their IRE1/bZIP60 mediated survival pathway is still active, delaying cell death. Collectively, these data demonstrate that miR5658 and its sense transcript play a significant role in regulating HR-mediated cell death following a bacterial pathogen infection.

There is evidence that in HR-mediated cell death during ER stress, caspase-like activities are involved in plants. To substantiate the electrolyte leakage data, next, we aimed to quantitate protease activity in dying cells (Lam & Pozo, 2000; Woltering, 2004; Zuppini et al., 2004). Towards this, we exposed the wild type control Col-0, miR5658 mutant line *NAT<sub>SRCL</sub>*, sense mutant line *srcl*, and hypersensitive mutant *npr1-1* to the pathogen *Pst* DC3000 AvrRpm1 for eight hours and 24 hours. Arabidopsis, like many other plant species, does not have true caspases identified within its genome. However, it possesses vacuolar processing enzymes (VPEs) that exhibit similar properties to animal caspases. These VPEs are capable of carrying out proteolysis and play a crucial role in regulating pathways associated with PCD. Taking advantage of this, we employed a tetrapeptide sequence substrate (Ac-YVAD-MCA) based on caspase-1 cleavage site for the quantification of caspase-1-like protease activity in Arabidopsis (Hatsugai et al., 2015; Lam, 2005). In the Col-0, caspase-1-like activity remains unchanged at eight hours while getting highly statistically significantly induced at 24 hours (figure 4b). miR5658 mutant line *NAT<sub>SRCL</sub>* showed unchanged caspase-1-like activity for eight and 24 hours. Sense mutant line *srcl* showed increased caspase-1-like activity at eight hours, but unchanged activity at 24 hours. Our hypersensitive control mutant *npr1-1* showed increased caspase-1-like activity at eight and 24 hours. The wild-type Col-0 showed

significantly higher caspase-1-like activity at 24 hours compared to *NAT<sub>SRCL</sub>* and *srcl*; while Col-0 has lower caspase-1-like activity than *npr1-1* mutant.

Papain-like cysteine proteases (PLCPs) represent an additional group of proteases that play a significant role in PCD (H. Liu et al., 2018). Among them, cathepsin B demonstrates caspase-3-like (Ac-DEVD-MCA) activity (Rotari & Gallois, 2016). This activity is achieved by inhibiting caspase-3 inhibitors, resulting in the downregulation of PCD (Rotari & Gallois, 2016). Both cathepsin B and VPEs function independently but in parallel to execute PCD (Cai et al., 2018). In the context of caspase-3-like activity, the wild-type Col-0 exhibits a significant induction of activity at both 8 hours and 24 hours (figure 4c). miR5658 mutant line *NAT<sub>SRCL</sub>* showed induced caspase-3-like activity at eight hours, which goes down at 24 hours. Sense mutant line *srcl* showed increased caspase-3 like activity at eight hours but unchanged at 24 hours. Our hypersensitive control mutant *npr1-1* has increased caspase-1 like activity at eight and 24 hours. The wild type Col-0 showed significantly higher caspase-3-like activity at 24 hours compared to *NAT<sub>SRCL</sub>*, *srcl*; while Col-0 has lower caspase-1 like activity compared to control mutant *npr1-1*.

In the *NAT<sub>SRCL</sub>* line, which lacks miR5658, as well as in the sense mutant line *srcl*, the protease-like activity is significantly reduced. Interestingly, the sense mutant line *srcl* displayed comparable caspase-1/caspase-3-like activity to *NAT<sub>SRCL</sub>*, possibly due to the cognate mode of expression of the sense transcripts. This observation further supports the notion that the slower cell death progression in these lines occurs during HR-induced cell death.

**Differential expression of IRE1a, bZIP60 and cell death markers upon cell death induction:**

Subsequently, we set out to investigate the differential expression level of IRE1a as a response to cell death triggering stimuli by challenging the different genotypes (Col-0, miR5658 mutant line *NAT<sub>SRC</sub>L*, sense mutant line *srcl*, *npr1-1*, and *bzip60*) with *Pst* DC3000 AvrRpm1. We collected the samples at 0, 3, 4, 5 and 6 hours and quantified IRE1a expression levels through qRT-PCR. At three hours, the IRE1a in *NAT<sub>SRC</sub>L* was induced statistically significantly higher compared to Col-0 and the induction level continued to increase at six hours (figure 5a). It indicates that, due to miR5658 absence in *NAT<sub>SRC</sub>L*, these plants display an induced IRE1a signaling state, which in turn is activating the pro-survival pathway and resisting cell death. The sense transcript mutant *srcl* induced a similar level of IRE1a compared with Col-0 at three hours, but at six hours, significantly higher amount of IRE1a was detected in the *srcl* plants. At six hours, the *NAT<sub>SRC</sub>L* and *srcl* produced similar level of IRE1a, which corroborates their concordant mode of function. The *npr1-1* mutant showed a significantly reduced level of IRE1a expression compared to Col-0. Similarly, the *bzip60* mutant plants also showed reduced IRE1a expression throughout the assayed time points.

Next, we quantified the expression level of *bZIP60*, another crucial gene in the po-survival pathway. As *bZIP60* goes through unconventional splicing by IRE1, we quantified both unspliced (US) and spliced (S) *bZIP60* upon cell death triggering stimuli. The *NAT<sub>SRC</sub>L* induced a statistically significantly higher amount of unspliced *bZIP60* at four hours, but at six hours, that trend was reversed as we recorded significantly lower *bZIP60* amount compared to wild-type Col-0 (figure 5b). At the same time, *NAT<sub>SRC</sub>L*

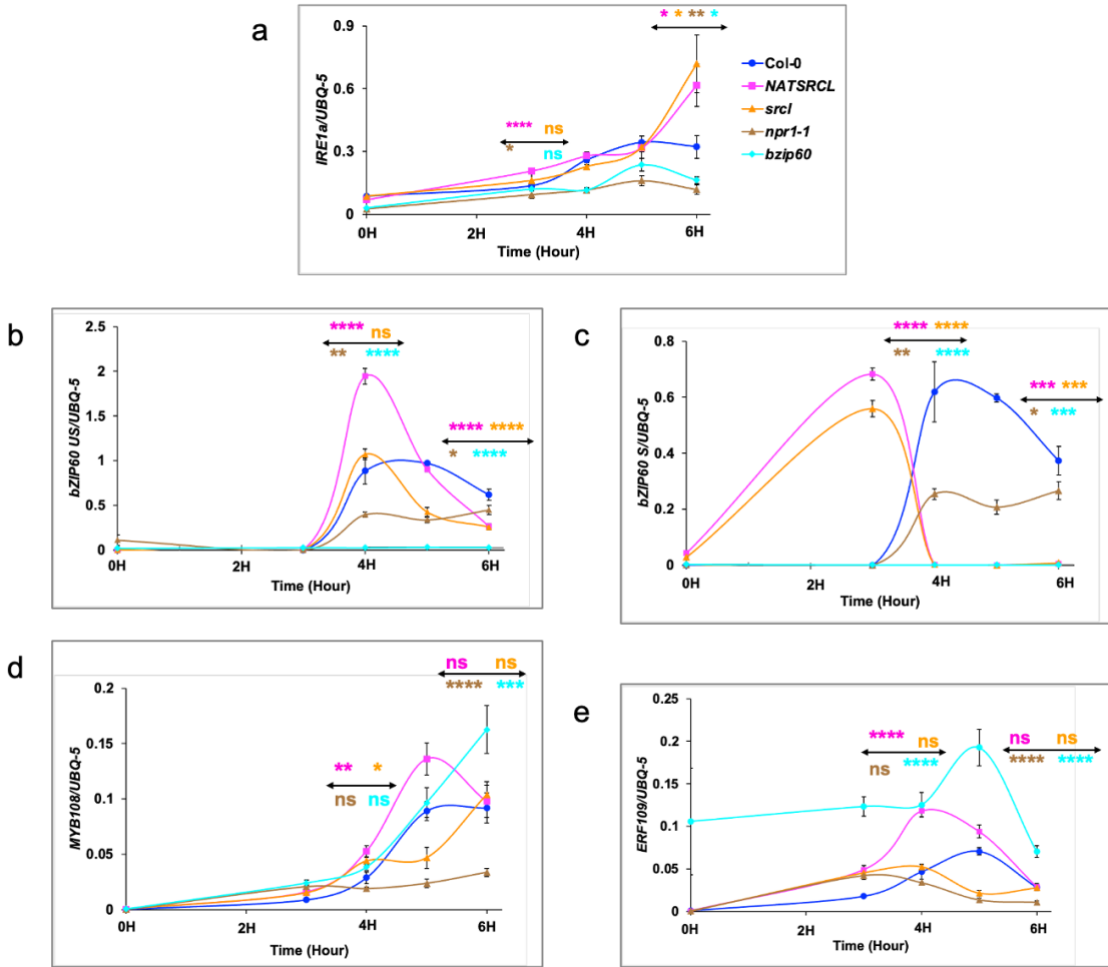


**Figure 5: Upstream and downstream signaling markers quantification:** The expression quantification of (A) IRE1a, (B) bZIP60 unspliced, (C) bZIP60 Spliced, (D) MYB108 and (E) ERF109 in Col-0, *NATSRCL*, *srcl*, *npr1-1* and *bZIP60* leaves upon exposure to *Pst* DC3000 avrRPM1 for 0, 3, 4, 5 and 6 hours. Expression levels were measured via qRT-PCR and transcript levels were normalized to reference gene (Ubiquitin-5). Statistical analyses were performed in Excel by two tailed student t-tests. Treatment groups are represented according to legends. 4-5 weeks old plants were used to perform the experiment. At least three biological replicates with three technical replicates were performed. Significant differences are indicated by asterisks (\*\*\*\* p<0.0001, \*\*\* p<0.001, \*\* p<0.01, \* p<0.05).

showed the highest spliced *bZIP60* at three hours, which began to decline at four hours and subsequent time points (figure 5c). *NATSRCL* showed the highest amount of IRE1a at three hours (figure 5a), which could explain the highest amount of spliced bZIP60 at that time point, resulting in the sustained activation of the pro-survival pathway. The *srcl*

plants showed a higher amount of unspliced bZIP60 at four hours (figure 5b), while at three hours, they had a higher amount of spliced bZIP60 (figure 5c), compared to Col-0. They also expressed more IRE1a at three hours (figure 5a). Even though the *srcl* plants showed a higher amount of IRE1a and subsequently spliced bZIP60, their expression of these transcripts was lower than *NAT<sub>SRCL</sub>*, which could indicate that the antisense transcript supports the function of miR5658. The *npr1-1* mutant showed a lower level of both unspliced and spliced bZIP60 (figure 5b and 5c) along with IRE1a (figure 5a). As expected, the null *bzip60* mutant showed minimal or zero expression throughout the time (figure 5b and 5c).

After correlating the expression of IRE1a and bZIP60, next we aimed to quantify the progression of cell death using two representative marker genes, , *MYB domain protein 108 (MYB108)* and *ethylene response factor 109 (EEF109)*. MYB108 is an essential player in programmed cell death and is a negative regulator of cell death (Cui et al., 2013; Cui et al., 2022; Mengiste et al., 2003). The time course expression of MYB108 indicates that the *NAT<sub>SRCL</sub>* is triggering cell death stress signaling earlier and is more robust than Col-0 to activate/sustain the pro-survival pathway and slow the cell death rate. While the sense mutant *srcl* showed an initially lower MYB108 expression, it reached the levels comparable to Col-0 and *NAT<sub>SRCL</sub>* at six hours (figure 5d). The *npr1-1* mutant showed the lowest expression of MYB108 throughout the time points (figure 5d). The *bzip60* plants showed a consistent increase in the expression of MYB108, peaking at six hours.

The second marker gene, *ERF109* delays PCD by regulating PCD-inhibitor genes and helping plants adapt to salt stress (Bahieldin et al., 2016; Bahieldin et al., 2018). We

quantified the expression of ERF109 in our experimental genotypes and demonstrated that *NAT<sub>SRCL</sub>* showed statistically significantly higher expression of ERF109 at four hours, which began to decrease at five and six hours, reaching the levels comparable to wild type Col-0 (figure 5e). The sense mutant *srcl* showed *ERF109* expression levels that were similar to Col-0 at four hours, followed by a decrease that was sustained at 5 and 6 hours post inoculation. The *npr1-1* plants showed a lower level of *ERF109* throughout the assayed time points, while the *bzip60* mutant showed the highest expression of *ERF109* throughout the time points. It is plausible that the higher accumulation of *ERF109* in *NAT<sub>SRCL</sub>* delayed the cell death and sustained the pro-survival pathway in this miR5658 deficient line , while the *bzip60* mutant over-accumulated *ERF109* to delay the cell death due to the absence of a functional *bZIP60* transcript in these plants

## Discussion

Maintaining cellular homeostasis is crucial for eukaryotic cells during normal developmental processes and stress periods alike. Specifically, maintaining ER homeostasis is vital for plants' growth, development, and overall survival. Within the three distinct pathways, IRE1 is evolutionarily the oldest and most conserved branch of UPR in eukaryotes that maintains ER homeostasis (Howell, 2013). Numerous investigations in the mammalian system have demonstrated that miRNA-mediated regulation shapes the ER stress and that ER stress reciprocally governs the expression of miRNAs (Mesitov et al., 2017). Several mammalian miRNAs (miR-214, miR-30-c-2\*, miR-34c-5p, miR-665, miR-1291) have been discovered to be directly involved with the regulation of IRE1 and XBP1 (Bartoszewska et al., 2019; Byrd et al., 2012; Duan et al.,

2012; Li et al., 2017; Maurel et al., 2013). However, in Arabidopsis, there are no detailed studies to date to shed light on the regulatory roles of miRNA during ER stress response. Prokaryotic and eukaryotic organisms both encode lncRNAs, which serve important regulatory functions. Nevertheless, the roles and functions of lncRNAs in the ER stress response of Arabidopsis remain largely unexplored and have not been extensively studied thus far. The present study aims to investigate the role of a specific miRNA (miR5658) derived from a novel lncNAT in changing the response of the IRE1/bZIP60 pathway from pro-survival to pro-death during acute ER stress induced by a biotic stressor in Arabidopsis.

Through bioinformatics analysis, we investigated the potential miRNAs that can target the *bZIP60* mRNA and regulate IRE1/*bZIP60* mediated pro-survival pathway. We identified three miRNAs (miR5658, miR414, miR397b) that can target the *bZIP60* transcript (Table 1). All three of them originate from distinct lncRNAs. The miR414 family is highly conserved across plant systems and has five homologs, two of which are from *Arabidopsis thaliana*, and three from *Oryza sativa* (Pani et al., 2011). miR414 has been reported to negatively regulate the heat shock protein 90.1 (AtHSP90.1) during the early proteotoxic stress conditions (Kim et al., 2019). Two members of the highly conserved miR397 family, miR397a and miR397b, are located on chromosome IV; there is just one nucleotide that separates miR397a and miR397b. (Abdel-Ghany & Pilon, 2008). miR397b is reported to regulate flowering in Arabidopsis and is proposed to play crucial roles in enhancing the overall fitness of plants (Feng et al., 2020), while its rice homolog OsmiR397 has been reported to be involved with the regulation of seed size, grain yield, and early flowering (C. Y. Wang et al., 2014; Zhang et al., 2013). The third

candidate microRNA, miR5658, has been found on *A. thaliana*, *Brassica rapa*, eggplant, and *Cannabis sativa*. *L* (Breakfield et al., 2012; Hajieghrari et al., 2017; Kapadia et al., 2023; Selvaraj et al., 2015; Yang et al., 2019). In *Cannabis sativa*. *L* five members of miR5658 have been identified and predicted to target important transcription factor (TF) groups (MYB and GRAS family), BAK1-interacting receptor-like kinase 1, serine/threonine protein phosphatase, dof zinc finger protein, and nucleotide-binding site-leucine-rich repeat (NBS-LRR) domain (Selvaraj et al., 2015). All these targets are associated with plant development, metabolism, hormonal signaling, membrane receptors and channels regulation, transcriptional regulation, HR, and apoptosis (Selvaraj et al., 2015). miR5658 has been documented to directly stimulate the expression of the AT3G25290 gene by specifically targeting its promoter region (Yang et al., 2019). In eggplant, miR5658 has been reported for its negative roles to the host immunity suppression against the wilt-causing pathogen *Ralstonia solanacearum* (Kapadia et al., 2023). While miR5658 has not been studied in detail yet, it originates from a NAT (lncNAT), a type of lncRNA. After analyzing the differential expression level of miR5658, miR414, and miR397b, we focused on miR5658 as it showed the exceptionally highest level of induced expression. Furthermore, miR5658 has been predicted to participate in cell death-related processes such as HR and apoptosis, and was also demonstrated to play a role in modulating the host immune response in other plant systems (Kapadia et al., 2023; Selvaraj et al., 2015). After carefully evaluating the expression of lncNAT transcript, miR5658, and bZIP60 (figure 1b, 1c, and 1d), we concluded that the miR5658 and *bZIP60* mRNA levels showed an inverse relationship, which supported our primary hypothesis.

The lncNAT's primary and most well-understood function is the regulation of target gene expression, among its broad spectrum of roles (Morris & Mattick, 2014; Werner & Sayer, 2009). Therefore, we proceeded to examine the role of miR5658 in two T-DNA insertional mutant strains, *NAT<sub>SRCL</sub>*, and the sense transcript mutant line *src1* under varying conditions of abiotic and biotic stress. The *NAT<sub>SRCL</sub>* mutant exhibits enhanced tolerance to prolonged ER stress induced by Tm, whereas the sense transcript *src1* displays sensitivity to prolonged Tm-mediated ER stress (figure 2c, 2d, and 2e).

To further substantiate the existing evidence, our transient MUG and GUS assay results demonstrated that the mutation in bZIP60 hinders the binding and functional activity of miR5658 (figure 3a, 3c). Surprisingly, the transient expression of bZIP60-GUS in the miR5658 mutant *NAT<sub>SRCL</sub>* is lower than expected, possibly indicating a binding competition between miR5658 and miR414 (figure 3a). Therefore, we hypothesize that miR414 may possibly compete with miR5658 for binding to the seed region of *bZIP60*. As miR414 has significantly lower transcript accumulation than miR5658, it is plausible that, under wild-type conditions, it is the limiting factor preventing it from exerting a major regulatory effect on the bZIP60 transcript accumulation. However, in mutated M1 *bZIP60*, when the seed region of miR5658 is mutated, and its binding is blocked, miR414 seizes this opportunity to bind to the mutated bZIP60, resulting in reduced expression (supplemental figure 6). Additional evidence in support of this hypothesis comes from our bioinformatics analysis of binding prediction through the miRBase website, which confirmed that miR414 displays a strong binding affinity to the mutated M1 *bZIP60* variant. In the context of pathogen resistance, the mutant lines *NAT<sub>SRCL</sub>* and *src1* demonstrated enhanced resistance, indicating that the

presence of miR5658 has an adverse impact on host resistance (3d). A previous investigation conducted on eggplant documented a similar role for miR5658. (Kapadia et al., 2023). The resistance observed against virulent *Pst* DC3000 highlights the involvement of miR5658 in regulating hypersensitive cell death.

Multiple studies have documented the generation of an "oxidative burst" occurring during the early and late stages of plant-pathogen interactions. Furthermore, these studies have highlighted the involvement of reactive oxygen species (ROS) in regulating of cell death responses and signaling pathways. Moreover, the disturbance of cytosolic ionic homeostasis is identified as a pivotal event in HR-mediated cell death. (Clarke et al., 2000; Clough et al., 2000; Devoto et al., 1999; Lam, 2004; Mittler et al., 1995). Our findings revealed a reduction in leaked ions during HR-mediated cell death within the mutant lines *NAT<sub>SRCL</sub>* and *srcl*, indicating an elevated resistance level to *Pst* DC3000 avrRMP1 in these mutants (figure 4a). Further, caspases are a class of intracellular proteases that play a crucial role in initiating various signaling cascades involved in programmed cell death, cell proliferation, and inflammation. Despite the absence of established caspases in plant genome sequencing data (Uren et al., 2000), the occurrence of caspase-like proteolytic activity has been observed in plant cell death processes associated with hypersensitive response (HR) and disease (Bonneau et al., 2008; Sueldo & van der Hoorn, 2017). Our findings demonstrate that *NAT<sub>SRCL</sub>* exhibits minimal caspase-1 and caspase-3-like activity at eight and 24 hours. Similarly, *srcl* displays minimal activity at eight hours, which further declined at 24 hours (figure 4b and 4c). This evidence supports the conclusion that miR5658, in conjunction with its sense

transcript, promotes the transition from a pro-survival to a pro-death signaling pathway during immune cell death in Arabidopsis.

To investigate the interplay between *IRE1a*, *bZIP60*, miR5658, and downstream signaling genes, we quantified their expression levels over a time course ranging from zero to six hours. In the miR5658 mutant line *NAT<sub>SRCL</sub>*, we observed elevated expression of *IRE1a* at three hours, which coincided with the highest level of *bZIP60* splicing at three hours, and a significantly increased expression of downstream cell death indicator signaling genes *MYB108* and *ERF109* (figure 5a, 5b, 5c, 5d and 5e). In the sense transcript mutant *srcl*, we observed higher expression of *IRE1a* at three hours and increased *bZIP60* splicing at three hours. Additionally, there was a modest increase in the expression of downstream signaling genes *MYB108* and *ERF109*, although the differences were not statistically significant. Taken together, these data suggest that the absence of miR5658 in the mutant line *NAT<sub>SRCL</sub>* results in extended duration of the pro-survival pathway compared to the wild-type Col-0 plants.

Furthermore, we assessed the expression of *IRE1b* to investigate any potential relationship it may have with miR5658; however, we observed consistently low/minimal levels of *IRE1b* expression across different genotypes from zero to six hours. These findings suggest no direct relationship between miR5658 expression and *IRE1b* transcript accumulation. To investigate the possibility of miR5658 targeting the promoter region of *IRE1a*, we conducted prediction analyses using miRBase and psRNATarget online tools. The analysis revealed that miR5658 can potentially target the promoter region of *IRE1a*,

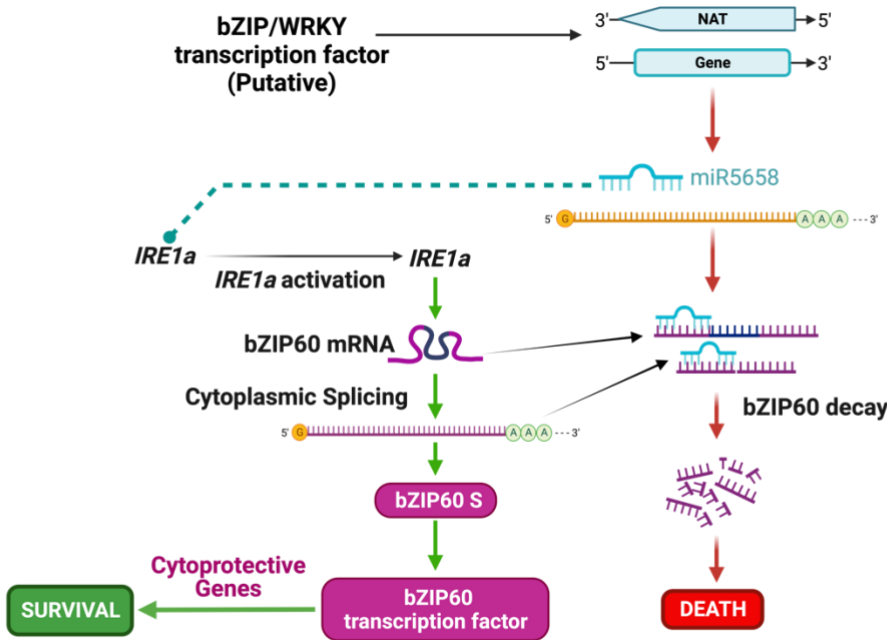


**Figure 6: The proposed model for miR5658 expression and activity.**

with a predicted binding site located precisely around 38 base pairs upstream of the transcription start site. Based on a previous study by Yang et al. (2019) demonstrating the regulatory role of miR5658 in gene expression through targeting the promoter region, it is plausible that miR5658 may have the ability to modulate the expression of *IRE1a* under yet-to-be determined scenarios. Interestingly, the bZIP and WRKY family have been identified as cognate regulators of a potential *cis*-regulatory element of a miR5658 homolog in Cannabis, as predicted by computational analyses (Selvaraj et al., 2015). Collectively, these findings suggest that members of the bZIP/WRKY family, such as the ER stress-implicated factors bZIP17 and bZIP28, may play a role in regulating the expression of miR5658 in response to ER stress conditions. Consequently, miR5658 can modulate the mRNA levels of transcription factor *bZIP60*, leading to a signaling state transition from the pro-survival to the pro-death pathway in *Arabidopsis* immune

response to *Pst* DC3000 avrRPM1 (figure 6). Additionally, future research will address whether miR5658 may also be involved in regulating the expression of *IRE1a* under specific conditions.

## Conclusion

In conclusion, we identified three miRNAs - miR5658, miR414, and miR397b, which are all derived from lncRNAs and target bZIP60 under severe ER stress conditions. Of these, our research found the most influential regulatory role for miR5658. The precursor of miR5658, lncNAT, and its associated sense transcript work in tandem during severe ER stress. miR5658 serves a critical function in the Hypersensitive Response (HR)-induced cell death, potentially targeting IRE1a and modulating its expression at the transcriptional level. Taken together, our findings suggest that miR5658 governs the IRE1a/bZIP60 mediated pro-survival pathway during intense ER stress induced by the biotic stressor *Pst* DC3000 avrRPM1.

## Materials and Methods

### ***Plant Material and Growth Conditions:***

In this study, the wild-type Columbia-0 accession of *Arabidopsis thaliana* (L.), specifically was utilized. The *NAT<sub>SRC</sub>L* and *srcl* T-DNA insertion lines with the accession code SALK\_047112 and SALK\_093172, respectively, were obtained from the Arabidopsis Biological Resource Center (ABRC, the Ohio State University, Columbus, OH, USA). Every seed was planted individually in pots containing sterilized soil (SunGro Horticulture, Super-Fine Germinating Mix). The seeds were stratified in a cold room

facility at 4°C for seven days. Subsequently, the pots were relocated to a controlled growth room facility with specific conditions including a 12-hour light and 12-hour dark photoperiod, a temperature of 21°C, a light intensity of 100 µmol/m<sup>2</sup>/s, and a relative humidity of 40%. Seedlings aged between 10 and 15 days were then transferred into 72-well flats for growth over a period of one month, during which subsequent experimentation took place.

***miRNA Expression Analysis:***

Stem-loop RT-PCR was employed to analyze the expression of miR5658, miR414, and miR397b. Total RNA extraction was carried out using the previously described method (Liu et al., 2019). Following that, the stem-loop RT-PCR analysis protocol was adapted from Chen et al. (2005)(Chen et al., 2005). Briefly, leaf tissue was collected from one-month-old plants at specific time points for the designated genotype, treatment, and time point combinations. At least three leaves were obtained from three independent plants for each combination. Total RNA was extracted using Trizol reagent from Invitrogen, and DNase I from Ambion was utilized to eliminate DNA contaminants. For reverse transcription, 3.33 µg of total RNA was utilized and transcribed using the SuperScript III first-strand RT-PCR kit from Invitrogen. Quantitative gene expression analysis was conducted using GoTaq qPCR Master Mix from Promega, along with miRNA-specific primers, in a RealPlex S MasterCycler (Eppendorf). To ensure equal RNA input, *snoR101*, a small nucleolar RNA, was employed as the internal control in this study. The Cycle Threshold (Ct) values were normalized to the expression of snoR101 to account for variations in RNA input. The bZIP60 splicing assays were

conducted following the methodology described in Moreno et al.(Moreno et al., 2012). In summary, a shared forward primer was utilized alongside a set of reverse primers designed to selectively bind to either the unspliced or spliced forms of the cDNA derived from bZIP60 mRNA. This approach facilitated the identification of two distinct qRT-PCR products representing the unspliced and spliced variants of bZIP60 (supplemental figure 3). The primer sequences utilized for qRT-PCR analysis can be found in Supplementary Table 1.

***TaqMan Assay for miR5658 Expression Analysis:***

The expression of miR5658 was quantified using a specific TaqMan assay designed for miR5658. Total RNA extraction and DNase I treatment were carried out following the aforementioned protocol (Liu et al., 2019). The protocol used in this assay was adapted from Fisher Scientific. In brief, the reverse transcription master mix consisted of the following components: 0.15 µL of 100 mM dNTP mix, 4.16 µL of nuclease-free water, 1.00 µL of MultiScribe reverse transcriptase, 1.50 µL of 10X reverse transcriptase buffer, 0.19 µL of Rnase inhibitor, and 3 µL of the corresponding RT primer provided. For the RT reaction, 5 µL of RNA was added to 10 µL of the RT master mix. The qPCR master mix was prepared by combining 7.67 µL of nuclease-free water, 1.00 µL of TaqMan microRNA assay (20X), 10.00 µL of TaqMan 2X universal PCR master mix, and 1.33 µL of the RT reaction product. Means and standard errors were calculated based on three replicate measurements per genotype.

**Sense and antisense transcript quantification:**

To quantify the sense and antisense transcript, we used strand specific tag-based RT-PCR. Total RNA extraction and DNase I treatment were performed in accordance with the previously described protocol (Liu et al., 2019). The procedure for synthesizing cDNA involves a reaction that includes the following components: 3 $\mu$ M transcript-specific tagged primer, 1  $\mu$ g RNA, 5X first strand buffer, 0.1M DTT, 10mM dNTP, superscript III reverse transcriptase (200U/l), RNase inhibitor (40U/l) and nuclease-free water. Following the reverse transcription (RT) reaction, exonuclease (20U) was applied to deactivate any unbound reverse transcription primers. The mixture for quantitative PCR (qPCR) includes the products of reverse transcription, both forward and reverse primers, the GoTaq qPCR Master Mix sourced from Promega, and nuclease-free water. The Ct values were adjusted to correspond to the *ubiquitin 5 (UBQ5)* gene. The primer sequences utilized for qRT-PCR analysis can be found in Supplementary Table 1.

**Assays for measuring ER stress Analysis:**

Seeds from various *Arabidopsis* strains underwent a cleansing process using 70% Ethanol and 0.05% Triton. Following this, they were placed on half-strength solid Murashige Skoog (MS) (Phytotechnology Labs, Overland Park, KS, USA) media plates and stratified at 4 °C for 3 days. Upon completion of the stratification process, the MS plates were moved to growth chambers for growth for 5 days. These chambers were maintained under specific conditions: a 12-hour light/12-hour dark cycle, a consistent temperature of 21 °C, a light intensity of 100  $\mu$ mol/m<sup>2</sup>/s, and a relative humidity of 40%. Tunicamycin (Tocris Bioscience 3516/10) was employed at a concentration of 0.30

$\mu\text{g/mL}$  as a chemical inducer of ER stress. Five-day-old seedlings were transitioned to a liquid half-strength MS medium, either with or without the appropriate concentration of Tm. They were then left to this medium for a duration of three days. After a three-day period, the seedlings were relocated to a fresh MS medium devoid of Tunicamycin, allowing them to recover from the ER stress over another three days. The total fresh weight of 10 plants, covering three biological replicates with two technical replicates for each biological replicate, was documented. Upon completion of the survival assay, chlorophyll was isolated using 100% methanol. The levels were then quantified using a Tecan microplate reader at wavelengths of 652 nm for Chlorophyll a and 665 nm for Chlorophyll b.

***Preparation of 35S::WT/M1/M2 bZIP60-GUS constructs:***

DNA was extracted from 4-5 weeks old wild type Col-0 plants using 200  $\mu\text{l}$  of CTAB extraction buffer. This buffer was composed of 2% cetyl-trimethyl ammonium bromide (CTAB), 100 mM Tris (pH 8.0), 20 mM EDTA (pH 8.0), 1.4 M NaCl, 0.5%  $\beta$ -Mercaptoethanol, and 2% polyvinyl pyrrolidone. The Coding DNA (CD) region of bZIP60 (spanning 888 base pairs) was amplified from the genomic DNA of the wild type Col-0 using PCR. The amplification was carried out using Phusion Polymerase (Thermo Scientific) and primers flanked by attB sites (Table S1). The PCR products were incorporated into the *pDONR207* Gateway vector using BP reactions (Invitrogen). The entry clones were then verified using PCR and Sanger sequencing, with the specific primers outlined in Table S1. The *pDONR207* vector was subsequently employed to introduce M1 and M2 mutations at the miR5658 seed region to block binding, utilizing

the technique of site-directed mutagenesis. The introduced mutations were verified using PCR and Sanger sequencing. Destination clones were assembled using LR reactions with the plant expression vector pMDC10 (C-GUS) (Addgene plasmid #118,492). These clones were then verified through PCR and Sanger sequencing. The resulting constructs, denoted as 2x35S::bZIP60 (WT/M1/M2)-GUS, were introduced into *Agrobacterium tumefaciens* (strain GV3101) to perform subsequent transient expression assays.

***Quantitative and qualitative GUS assay:***

Plants of different genotypes, aged between 4-5 weeks, were subjected to agroinfiltration using a needleless syringe, following a previously described article (Mangano et al., 2014). Three days after inoculation, the plant tissues were harvested and ground under liquid nitrogen. The total proteins were extracted from the collected tissue using an extraction buffer. This buffer was composed of 50 mM NaPO<sub>4</sub> (pH = 7.0), 1 mM Na<sub>2</sub>EDTA, 0.1% SDS, 0.1% Triton X-100, a protease inhibitor for plant extracts (Sigma), and 10 mM β-mercaptoethanol, following a method described earlier (Pajerowska-Mukhtar et al., 2012). After a centrifugation step (10 minutes at 4000×g and 4 °C), the supernatants were collected, and the protein concentration was determined using Bradford Reagent (Sigma). The proteins extracted were then incubated with 1 mM MUG (4-methylumbelliferyl β-D-glucuronide) to measure GUS activity. To halt the reaction, a stop buffer composed of 1 M Na<sub>2</sub>CO<sub>3</sub> was used. The resulting fluorescence was quantified using a microplate reader (Tecan), using an excitation wavelength of 365 nm, an emission wavelength of 455 nm, and a filter wavelength of 430 nm. The relative MUG values were calculated by adjusting the data according to the Bradford assay

results. The methodology for these experimental procedures was adapted from a previously published protocol (Jefferson et al., 1987).

For the histochemical assay, leaf tissues were harvested at 3 days post-inoculation. Following this, a staining solution was introduced into the leaves through vacuum infiltration. This staining solution was composed of 100 mM NaPO<sub>4</sub> (with a pH of 7.0), 10 mM Na<sub>2</sub>EDTA, 0.1% Triton X-100, 1 mM K<sub>3</sub>Fe(CN)<sub>6</sub>, 2 mM X-Gluc (50 mg/ml) in dimethylformamide (DMF) and nuclease-free water. Subsequently, the leaf tissues were immersed in the staining solution, covered with aluminum foil, and incubated at 37°C for a duration of 24-48 hours. Following incubation, the leaves were removed from the staining solution and sequentially washed with increasing concentrations of ethanol (ranging from 30% to 80%) every hour to effectively eliminate the chlorophyll. The samples were photographically documented using a scanner.

***Bacterial strains and plant resistance quantification:***

The bacterium *Pseudomonas syringae* pv. tomato DC3000 (*Pst* DC3000) was used for the pathogen infection and quantification assays. Soil grown 4-5 weeks old plants were infiltrated using a needleless syringe with *Pst* DC3000 (OD<sub>600</sub> = 0.001) to test the enhanced disease resistance (EDR). For each replication, three leaves per plant were used, with a total of six plants. At least three independent biological replicates were performed. Two days post-inoculation, bacterial growth was quantified following a previously described protocol (Liu et al., 2015).

***Assay for measuring cell death through ion leakage:***

Soil-grown 4-5 weeks old plants were infiltrated with *Pst* DC3000 avrRPM1 at ( $OD_{600} = 0.01$ ). Using a needless syringe, three leaves per plant were infiltrated for the procedure. Using a hole puncher, leaf discs were collected and promptly transferred into a beaker containing deionized water. Following a 30-minute period, the leaf discs were relocated into Falcon tubes, each containing 15ml of sterile deionized water per 15 leaf discs and the conductivity was then determined using a conductivity meter (Fisher, cat: 13-636-AP85) every 30 minutes for 8 hours of post-inoculation.

***Assay for measuring cell death through Caspase Assay:***

To measure the caspase activity 4-5 weeks old plants were syringe infiltrated with *Pst* DC3000 avrRPM1 at  $OD_{600} = 0.01$ . In the assay, three leaves per plant were used, with three plants per biological replication. At least three biological replications were performed in total. Leaf samples were collected eight- and 24-hours post-inoculation. The proteins were extracted from collected samples using a extraction buffer composed of: 50mM HEPES (pH 7.5), 5% glycerol, 1mM EDTA, 1mM DTT, 1mM PMSF, 0.1% Triton and 50mM NaCl. The extracted proteins underwent centrifugation, after which the supernatants were collected and diluted using assay buffer. The diluted proteins were then combined with stock substrate buffer of synthetic caspases and the plate was incubated at 30°C. Caspase activity was measured at 360<sub>nm</sub> excitation and 465<sub>nm</sub> emission using a plate reader. Protein concentrations were determined using a Bradford assay. Synthetic Caspase-1 (Ac-YVAD-MCA) (Peptide Institute, catalog #3161-v) and caspase-

3 (Ac-DEVD-MCA) (Peptide Institute, catalog #3171-v) substrates were used to quantify the caspase-like activity.

***Statistical analysis:***

Statistical analysis was performed using one-way ANOVA and two-tailed t-test in either Excel or GraphPad Prism to determine significant differences. The graphs presented in Figures 1a, 2b, 2c, 2d, 2e, 3a, 3b, 3d, 4b and 4c were generated using GraphPad Prism. Statistically significant differences are denoted by asterisks: \* for  $p < 0.05$ , \*\* for  $p < 0.01$ , \*\*\* for  $p < 0.001$ , and \*\*\*\* for  $p < 0.0001$ .

## References

- Abdel-Ghany, S. E., & Pilon, M. (2008). MicroRNA-mediated systemic down-regulation of copper protein expression in response to low copper availability in Arabidopsis. *Journal of Biological Chemistry*, 283(23), 15932-15945.
- Afrin, T., Diwan, D., Sahawneh, K., & Pajerowska-Mukhtar, K. (2020). Multilevel regulation of endoplasmic reticulum stress responses in plants: where old roads and new paths meet. *J Exp Bot*, 71(5), 1659-1667.  
<https://doi.org/10.1093/jxb/erz487>
- Afrin, T., Seok, M., Terry, B. C., & Pajerowska-Mukhtar, K. M. (2020). Probing natural variation of IRE1 expression and endoplasmic reticulum stress responses in Arabidopsis accessions. *Sci Rep*, 10(1), 19154. <https://doi.org/10.1038/s41598-020-76114-1>
- Alvarez, M. E. (2000). Salicylic acid in the machinery of hypersensitive cell death and disease resistance. *Plant Mol Biol*, 44(3), 429-442.  
<https://doi.org/10.1023/a:1026561029533>
- Bahieldin, A., Atef, A., Edris, S., Gadalla, N. O., Ali, H. M., Hassan, S. M., Al-Kordy, M. A., Ramadan, A. M., Makki, R. M., Al-Hajar, A. S., & El-Domyati, F. M. (2016). Ethylene responsive transcription factor ERF109 retards PCD and improves salt tolerance in plant. *BMC Plant Biol*, 16(1), 216. <https://doi.org/10.1186/s12870-016-0908-z>
- Bahieldin, A., Atef, A., Edris, S., Gadalla, N. O., Ramadan, A. M., Hassan, S. M., Al Attas, S. G., Al-Kordy, M. A., Al-Hajar, A. S. M., Sabir, J. S. M., Nasr, M. E., Osman, G. H., & El-Domyati, F. M. (2018). Multifunctional activities of ERF109 as affected by salt stress in Arabidopsis. *Sci Rep*, 8(1), 6403. <https://doi.org/10.1038/s41598-018-24452-6>
- Bartoszewska, S., Cabaj, A., Dabrowski, M., Collawn, J. F., & Bartoszewski, R. (2019). miR-34c-5p modulates X-box-binding protein 1 (XBP1) expression during the adaptive phase of the unfolded protein response. *FASEB J*, 33(10), 11541-11554. <https://doi.org/10.1096/fj.201900600RR>
- Betti, F., Ladera-Carmona, M. J., Weits, D. A., Ferri, G., Iacopino, S., Novi, G., Svezia, B., Kunkowska, A. B., Santaniello, A., Piaggesi, A., Loreti, E., & Perata, P. (2021). Exogenous miRNAs induce post-transcriptional gene silencing in plants. *Nat Plants*, 7(10), 1379-1388. <https://doi.org/10.1038/s41477-021-01005-w>
- Bonneau, L., Ge, Y., Drury, G. E., & Gallois, P. (2008). What happened to plant caspases? *Journal of experimental botany*, 59(3), 491-499.
- Borsani, O., Zhu, J., Verslues, P. E., Sunkar, R., & Zhu, J. K. (2005). Endogenous siRNAs derived from a pair of natural cis-antisense transcripts regulate salt tolerance in Arabidopsis. *Cell*, 123(7), 1279-1291. <https://doi.org/10.1016/j.cell.2005.11.035>
- Breakfield, N. W., Corcoran, D. L., Petricka, J. J., Shen, J., Sae-Seaw, J., Rubio-Somoza, I., Weigel, D., Ohler, U., & Benfey, P. N. (2012). High-resolution experimental and

- computational profiling of tissue-specific known and novel miRNAs in Arabidopsis. *Genome Res*, 22(1), 163-176.  
<https://doi.org/10.1101/gr.123547.111>
- Broughton, J. P., Lovci, M. T., Huang, J. L., Yeo, G. W., & Pasquinelli, A. E. (2016). Pairing beyond the Seed Supports MicroRNA Targeting Specificity. *Mol Cell*, 64(2), 320-333. <https://doi.org/10.1016/j.molcel.2016.09.004>
- Byrd, A. E., Aragon, I. V., & Brewer, J. W. (2012). MicroRNA-30c-2\* limits expression of proadaptive factor XBP1 in the unfolded protein response. *J Cell Biol*, 196(6), 689-698. <https://doi.org/10.1083/jcb.201201077>
- Cai, Y. M., Yu, J., Ge, Y., Mironov, A., & Gallois, P. (2018). Two proteases with caspase-3-like activity, cathepsin B and proteasome, antagonistically control ER-stress-induced programmed cell death in Arabidopsis. *New Phytologist*, 218(3), 1143-1155.
- Chen, C., Ridzon, D. A., Broomer, A. J., Zhou, Z., Lee, D. H., Nguyen, J. T., Barbisin, M., Xu, N. L., Mahuvakar, V. R., Andersen, M. R., Lao, K. Q., Livak, K. J., & Guegler, K. J. (2005). Real-time quantification of microRNAs by stem-loop RT-PCR. *Nucleic Acids Research*, 33(20), e179-e179. <https://doi.org/10.1093/nar/gni178>
- Chern, M. S., Fitzgerald, H. A., Yadav, R. C., Canlas, P. E., Dong, X., & Ronald, P. C. (2001). Evidence for a disease-resistance pathway in rice similar to the NPR1-mediated signaling pathway in Arabidopsis. *Plant J*, 27(2), 101-113.  
<https://doi.org/10.1046/j.1365-313x.2001.01070.x>
- Chisholm, S. T., Coaker, G., Day, B., & Staskawicz, B. J. (2006). Host-microbe interactions: shaping the evolution of the plant immune response. *Cell*, 124(4), 803-814.  
<https://doi.org/10.1016/j.cell.2006.02.008>
- Chitnis, N. S., Pytel, D., Bobrovnikova-Marjon, E., Pant, D., Zheng, H., Maas, N. L., Frederick, B., Kushner, J. A., Chodosh, L. A., Koumenis, C., Fuchs, S. Y., & Diehl, J. A. (2012). miR-211 is a prosurvival microRNA that regulates chop expression in a PERK-dependent manner. *Mol Cell*, 48(3), 353-364.  
<https://doi.org/10.1016/j.molcel.2012.08.025>
- Clarke, A., Desikan, R., Hurst, R. D., Hancock, J. T., & Neill, S. J. (2000). NO way back: nitric oxide and programmed cell death in Arabidopsis thaliana suspension cultures. *Plant J*, 24(5), 667-677. <https://doi.org/10.1046/j.1365-313x.2000.00911.x>
- Clough, S. J., Fengler, K. A., Yu, I. C., Lippok, B., Smith, R. K., Jr., & Bent, A. F. (2000). The Arabidopsis dnd1 "defense, no death" gene encodes a mutated cyclic nucleotide-gated ion channel. *Proc Natl Acad Sci U S A*, 97(16), 9323-9328.  
<https://doi.org/10.1073/pnas.150005697>
- Csorba, T., Questa, J. I., Sun, Q., & Dean, C. (2014). Antisense COOLAIR mediates the coordinated switching of chromatin states at FLC during vernalization. *Proc Natl Acad Sci U S A*, 111(45), 16160-16165. <https://doi.org/10.1073/pnas.1419030111>
- Cui, F., Brosche, M., Sipari, N., Tang, S., & Overmyer, K. (2013). Regulation of ABA dependent wound induced spreading cell death by MYB108. *New Phytol*, 200(3), 634-640. <https://doi.org/10.1111/nph.12456>

- Cui, F., Li, X., Wu, W., Luo, W., Wu, Y., Brosché, M., & Overmyer, K. (2022). Ectopic expression of BOTRYTIS SUSCEPTIBLE1 reveals its function as a positive regulator of wound-induced cell death and plant susceptibility to Botrytis. *The Plant Cell*, 34(10), 4105-4116. <https://doi.org/10.1093/plcell/koac206>
- Cui, J., Luan, Y., Jiang, N., Bao, H., & Meng, J. (2017). Comparative transcriptome analysis between resistant and susceptible tomato allows the identification of lncRNA16397 conferring resistance to Phytophthora infestans by co-expressing glutaredoxin. *Plant J*, 89(3), 577-589. <https://doi.org/10.1111/tpj.13408>
- Dangl, J. L., & Jones, J. D. (2001). Plant pathogens and integrated defence responses to infection. *Nature*, 411(6839), 826-833. <https://doi.org/10.1038/35081161>
- Deforges, J., Reis, R. S., Jacquet, P., Sheppard, S., Gadekar, V. P., Hart-Smith, G., Tanzer, A., Hofacker, I. L., Iseli, C., Xenarios, I., & Poirier, Y. (2019). Control of Cognate Sense mRNA Translation by cis-Natural Antisense RNAs. *Plant Physiol*, 180(1), 305-322. <https://doi.org/10.1104/pp.19.00043>
- Devoto, A., Piffanelli, P., Nilsson, I., Wallin, E., Panstruga, R., von Heijne, G., & Schulze-Lefert, P. (1999). Topology, subcellular localization, and sequence diversity of the Mlo family in plants. *J Biol Chem*, 274(49), 34993-35004. <https://doi.org/10.1074/jbc.274.49.34993>
- Ding, P., & Ding, Y. (2020). Stories of Salicylic Acid: A Plant Defense Hormone. *Trends Plant Sci*, 25(6), 549-565. <https://doi.org/10.1016/j.tplants.2020.01.004>
- Ding, Y., Sun, T., Ao, K., Peng, Y., Zhang, Y., Li, X., & Zhang, Y. (2018). Opposite roles of salicylic acid receptors NPR1 and NPR3/NPR4 in transcriptional regulation of plant immunity. *Cell*, 173(6), 1454-1467. e1415.
- Duan, Q., Wang, X., Gong, W., Ni, L., Chen, C., He, X., Chen, F., Yang, L., Wang, P., & Wang, D. W. (2012). ER stress negatively modulates the expression of the miR-199a/214 cluster to regulates tumor survival and progression in human hepatocellular cancer. *PLoS One*, 7(2), e31518. <https://doi.org/10.1371/journal.pone.0031518>
- Faghihi, M. A., Modarresi, F., Khalil, A. M., Wood, D. E., Sahagan, B. G., Morgan, T. E., Finch, C. E., St Laurent, G., 3rd, Kenny, P. J., & Wahlestedt, C. (2008). Expression of a noncoding RNA is elevated in Alzheimer's disease and drives rapid feed-forward regulation of beta-secretase. *Nat Med*, 14(7), 723-730. <https://doi.org/10.1038/nm1784>
- Fan, W., & Dong, X. (2002). In vivo interaction between NPR1 and transcription factor TGA2 leads to salicylic acid-mediated gene activation in Arabidopsis. *Plant Cell*, 14(6), 1377-1389. <https://doi.org/10.1105/tpc.001628>
- Fedak, H., Palusinska, M., Krzyczmonik, K., Brzezniak, L., Yatusevich, R., Pietras, Z., Kaczanowski, S., & Swiezewski, S. (2016). Control of seed dormancy in Arabidopsis by a cis-acting noncoding antisense transcript. *Proc Natl Acad Sci U S A*, 113(48), E7846-E7855. <https://doi.org/10.1073/pnas.1608827113>
- Feng, Y. Z., Yu, Y., Zhou, Y. F., Yang, Y. W., Lei, M. Q., Lian, J. P., He, H., Zhang, Y. C., Huang, W., & Chen, Y. Q. (2020). A Natural Variant of miR397 Mediates a Feedback Loop in Circadian Rhythm. *Plant Physiol*, 182(1), 204-214. <https://doi.org/10.1104/pp.19.00710>

- Fu, Z. Q., Yan, S., Saleh, A., Wang, W., Ruble, J., Oka, N., Mohan, R., Spoel, S. H., Tada, Y., & Zheng, N. (2012). NPR3 and NPR4 are receptors for the immune signal salicylic acid in plants. *Nature*, 486(7402), 228-232.
- Gao, P., Bai, X., Yang, L., Lv, D., Li, Y., Cai, H., Ji, W., Guo, D., & Zhu, Y. (2010). Over-expression of osa-MIR396c decreases salt and alkali stress tolerance. *Planta*, 231(5), 991-1001. <https://doi.org/10.1007/s00425-010-1104-2>
- Georg, J., Voss, B., Scholz, I., Mitschke, J., Wilde, A., & Hess, W. R. (2009). Evidence for a major role of antisense RNAs in cyanobacterial gene regulation. *Mol Syst Biol*, 5, 305. <https://doi.org/10.1038/msb.2009.63>
- Guan, X., Pang, M., Nah, G., Shi, X., Ye, W., Stelly, D. M., & Chen, Z. J. (2014). miR828 and miR858 regulate homoeologous MYB2 gene functions in Arabidopsis trichome and cotton fibre development. *Nat Commun*, 5, 3050. <https://doi.org/10.1038/ncomms4050>
- Guo, H. S., Xie, Q., Fei, J. F., & Chua, N. H. (2005). MicroRNA directs mRNA cleavage of the transcription factor NAC1 to downregulate auxin signals for arabidopsis lateral root development. *Plant Cell*, 17(5), 1376-1386. <https://doi.org/10.1105/tpc.105.030841>
- Gust, A. A., Pruitt, R., & Nurnberger, T. (2017). Sensing Danger: Key to Activating Plant Immunity. *Trends Plant Sci*, 22(9), 779-791. <https://doi.org/10.1016/j.tplants.2017.07.005>
- Ha, M., & Kim, V. N. (2014). Regulation of microRNA biogenesis. *Nat Rev Mol Cell Biol*, 15(8), 509-524. <https://doi.org/10.1038/nrm3838>
- Hajdarpasic, A., & Ruggenthaler, P. (2012). Analysis of miRNA expression under stress in Arabidopsis thaliana. *Bosn J Basic Med Sci*, 12(3), 169-176. <https://doi.org/10.17305/bjbm.2012.2471>
- Hajieghrari, B., Farrokhi, N., Goliae, B., & Kavousi, K. (2017). Computational identification of MicroRNAs and their transcript target (s) in field mustard (*Brassica rapa* L.). *Iranian Journal of Biotechnology*, 15(1), 22.
- Hastings, M. L., Milcarek, C., Martincic, K., Peterson, M. L., & Munroe, S. H. (1997). Expression of the thyroid hormone receptor gene, erbAalpha, in B lymphocytes: alternative mRNA processing is independent of differentiation but correlates with antisense RNA levels. *Nucleic Acids Res*, 25(21), 4296-4300. <https://doi.org/10.1093/nar/25.21.4296>
- Hatsugai, N., Yamada, K., Goto-Yamada, S., & Hara-Nishimura, I. (2015). Vacuolar processing enzyme in plant programmed cell death. *Frontiers in plant science*, 6, 234.
- He, Y., Vogelstein, B., Velculescu, V. E., Papadopoulos, N., & Kinzler, K. W. (2008). The antisense transcriptomes of human cells. *Science*, 322(5909), 1855-1857.
- Hollien, J., Lin, J. H., Li, H., Stevens, N., Walter, P., & Weissman, J. S. (2009). Regulated Ire1-dependent decay of messenger RNAs in mammalian cells. *J Cell Biol*, 186(3), 323-331. <https://doi.org/10.1083/jcb.200903014>
- Howell, S. H. (2013). Endoplasmic reticulum stress responses in plants. *Annu Rev Plant Biol*, 64, 477-499. <https://doi.org/10.1146/annurev-arplant-050312-120053>

- Iwata, Y., Fedoroff, N. V., & Koizumi, N. (2008). Arabidopsis bZIP60 is a proteolysis-activated transcription factor involved in the endoplasmic reticulum stress response. *Plant Cell*, 20(11), 3107-3121. <https://doi.org/10.1105/tpc.108.061002>
- Jabnoune, M., Secco, D., Lecampion, C., Robaglia, C., Shu, Q., & Poirier, Y. (2013). A rice cis-natural antisense RNA acts as a translational enhancer for its cognate mRNA and contributes to phosphate homeostasis and plant fitness. *The Plant Cell*, 25(10), 4166-4182.
- Jefferson, R. A., Kavanagh, T. A., & Bevan, M. W. (1987). GUS fusions: beta-glucuronidase as a sensitive and versatile gene fusion marker in higher plants. *The EMBO journal*, 6(13), 3901-3907.
- Jones, J. D., & Dangl, J. L. (2006). The plant immune system. *Nature*, 444(7117), 323-329. <https://doi.org/10.1038/nature05286>
- Kapadia, C., Datta, R., Mahammad, S. M., Tomar, R. S., Kheni, J. K., & Ercisli, S. (2023). Genome-Wide Identification, Quantification, and Validation of Differentially Expressed miRNAs in Eggplant (*Solanum melongena* L.) Based on Their Response to *Ralstonia solanacearum* Infection. *ACS Omega*, 8(2), 2648-2657. <https://doi.org/10.1021/acsomega.2c07097>
- Katayama, S., Tomaru, Y., Kasukawa, T., Waki, K., Nakanishi, M., Nakamura, M., Nishida, H., Yap, C., Suzuki, M., & Kawai, J. (2005). Antisense transcription in the mammalian transcriptome. *Science*, 309(5740), 1564-1566.
- Katiyar-Agarwal, S., Morgan, R., Dahlbeck, D., Borsani, O., Villegas, A., Jr., Zhu, J. K., Staskawicz, B. J., & Jin, H. (2006). A pathogen-inducible endogenous siRNA in plant immunity. *Proc Natl Acad Sci U S A*, 103(47), 18002-18007. <https://doi.org/10.1073/pnas.0608258103>
- Kim, J. H., Oh, T. R., Cho, S. K., Yang, S. W., & Kim, W. T. (2019). Inverse Correlation Between MPSR1 E3 Ubiquitin Ligase and HSP90.1 Balances Cytoplasmic Protein Quality Control. *Plant Physiol*, 180(2), 1230-1240. <https://doi.org/10.1104/pp.18.01582>
- Kindgren, P., Ard, R., Ivanov, M., & Marquardt, S. (2018). Transcriptional read-through of the long non-coding RNA SVALKA governs plant cold acclimation. *Nat Commun*, 9(1), 4561. <https://doi.org/10.1038/s41467-018-07010-6>
- Koizumi, N., Martinez, I. M., Kimata, Y., Kohno, K., Sano, H., & Chrispeels, M. J. (2001). Molecular characterization of two *Arabidopsis* Ire1 homologs, endoplasmic reticulum-located transmembrane protein kinases. *Plant Physiol*, 127(3), 949-962. <https://www.ncbi.nlm.nih.gov/pubmed/11706177>
- Kumar, K., & Chakraborty, S. (2021). Roles of long non-coding RNAs in plant virus interactions. *Journal of Plant Biochemistry and Biotechnology*, 30(4), 684-697. <https://doi.org/10.1007/s13562-021-00697-7>
- Lam, E. (2004). Controlled cell death, plant survival and development. *Nat Rev Mol Cell Biol*, 5(4), 305-315. <https://doi.org/10.1038/nrm1358>
- Lam, E. (2005). Vacuolar proteases livening up programmed cell death. *Trends in cell biology*, 15(3), 124-127.
- Lam, E., & Pozo, O. d. (2000). Caspase-like protease involvement in the control of plant cell death. *Plant molecular biology*, 44, 417-428.

- Lewis, A., Mitsuya, K., Umlauf, D., Smith, P., Dean, W., Walter, J., Higgins, M., Feil, R., & Reik, W. (2004). Imprinting on distal chromosome 7 in the placenta involves repressive histone methylation independent of DNA methylation. *Nat Genet*, 36(12), 1291-1295. <https://doi.org/10.1038/ng1468>
- Li, M., Zhang, S., Qiu, Y., He, Y., Chen, B., Mao, R., Cui, Y., Zeng, Z., & Chen, M. (2017). Upregulation of miR-665 promotes apoptosis and colitis in inflammatory bowel disease by repressing the endoplasmic reticulum stress components XBP1 and ORMDL3. *Cell Death Dis*, 8(3), e2699. <https://doi.org/10.1038/cddis.2017.76>
- Li, S., Wang, X., Xu, W., Liu, T., Cai, C., Chen, L., Clark, C. B., & Ma, J. (2021). Unidirectional movement of small RNAs from shoots to roots in interspecific heterografts. *Nat Plants*, 7(1), 50-59. <https://doi.org/10.1038/s41477-020-00829-2>
- Liu, H., Hu, M., Wang, Q., Cheng, L., & Zhang, Z. (2018). Role of papain-like cysteine proteases in plant development. *Frontiers in Plant Science*, 9, 1717.
- Liu, J., Jung, C., Xu, J., Wang, H., Deng, S., Bernad, L., Arenas-Huertero, C., & Chua, N. H. (2012). Genome-wide analysis uncovers regulation of long intergenic noncoding RNAs in Arabidopsis. *Plant Cell*, 24(11), 4333-4345. <https://doi.org/10.1105/tpc.112.102855>
- Liu, X., Afrin, T., & Pajerowska-Mukhtar, K. M. (2019). Arabidopsis GCN2 kinase contributes to ABA homeostasis and stomatal immunity. *Commun Biol*, 2, 302. <https://doi.org/10.1038/s42003-019-0544-x>
- Liu, X., Li, D., Zhang, D., Yin, D., Zhao, Y., Ji, C., Zhao, X., Li, X., He, Q., Chen, R., Hu, S., & Zhu, L. (2018). A novel antisense long noncoding RNA, TWISTED LEAF, maintains leaf blade flattening by regulating its associated sense R2R3-MYB gene in rice. *New Phytol*, 218(2), 774-788. <https://doi.org/10.1111/nph.15023>
- Liu, X., Sun, Y., Korner, C. J., Du, X., Vollmer, M. E., & Pajerowska-Mukhtar, K. M. (2015). Bacterial Leaf Infiltration Assay for Fine Characterization of Plant Defense Responses using the Arabidopsis thaliana-Pseudomonas syringae Pathosystem. *J Vis Exp*(104). <https://doi.org/10.3791/53364>
- Lu, C., Jeong, D. H., Kulkarni, K., Pillay, M., Nobuta, K., German, R., Thatcher, S. R., Maher, C., Zhang, L., Ware, D., Liu, B., Cao, X., Meyers, B. C., & Green, P. J. (2008). Genome-wide analysis for discovery of rice microRNAs reveals natural antisense microRNAs (nat-miRNAs). *Proc Natl Acad Sci U S A*, 105(12), 4951-4956. <https://doi.org/10.1073/pnas.0708743105>
- Lu, T., Zhu, C., Lu, G., Guo, Y., Zhou, Y., Zhang, Z., Zhao, Y., Li, W., Lu, Y., Tang, W., Feng, Q., & Han, B. (2012). Strand-specific RNA-seq reveals widespread occurrence of novel cis-natural antisense transcripts in rice. *BMC Genomics*, 13, 721. <https://doi.org/10.1186/1471-2164-13-721>
- Makarova, J. A., Shkurnikov, M. U., Wicklein, D., Lange, T., Samatov, T. R., Turchinovich, A. A., & Tonevitsky, A. G. (2016). Intracellular and extracellular microRNA: An update on localization and biological role. *Prog Histochem Cytochem*, 51(3-4), 33-49. <https://doi.org/10.1016/j.proghi.2016.06.001>

- Mangano, S., Gonzalez, C. D., & Petruccelli, S. (2014). Agrobacterium tumefaciens-mediated transient transformation of *Arabidopsis thaliana* leaves. *Arabidopsis Protocols*, 165-173.
- Marquardt, S., Raitskin, O., Wu, Z., Liu, F., Sun, Q., & Dean, C. (2014). Functional consequences of splicing of the antisense transcript COOLAIR on FLC transcription. *Mol Cell*, 54(1), 156-165.  
<https://doi.org/10.1016/j.molcel.2014.03.026>
- Maurel, M., Dejeans, N., Taouji, S., Chevet, E., & Grosset, C. F. (2013). MicroRNA-1291-mediated silencing of IRE1alpha enhances Glycan-3 expression. *RNA*, 19(6), 778-788. <https://doi.org/10.1261/rna.036483.112>
- McCormack, M. E., Liu, X., Jordan, M. R., & Pajerowska-Mukhtar, K. M. (2015). An improved high-throughput screening assay for tunicamycin sensitivity in *Arabidopsis* seedlings. *Frontiers in Plant Science*, 6, 663.
- Mengiste, T., Chen, X., Salmeron, J., & Dietrich, R. (2003). The BOTRYTIS SUSCEPTIBLE1 Gene Encodes an R2R3MYB Transcription Factor Protein That Is Required for Biotic and Abiotic Stress Responses in *Arabidopsis*. *The Plant Cell*, 15(11), 2551-2565. <https://doi.org/10.1105/tpc.014167>
- Mesitov, M. V., Soldatov, R. A., Zaichenko, D. M., Malakho, S. G., Klementyeva, T. S., Sokolovskaya, A. A., Kubatiev, A. A., Mironov, A. A., & Moskovtsev, A. A. (2017). Differential processing of small RNAs during endoplasmic reticulum stress. *Sci Rep*, 7, 46080. <https://doi.org/10.1038/srep46080>
- Mishiba, K., Nagashima, Y., Suzuki, E., Hayashi, N., Ogata, Y., Shimada, Y., & Koizumi, N. (2013). Defects in IRE1 enhance cell death and fail to degrade mRNAs encoding secretory pathway proteins in the *Arabidopsis* unfolded protein response. *Proc Natl Acad Sci U S A*, 110(14), 5713-5718.  
<https://doi.org/10.1073/pnas.1219047110>
- Mittler, R., Shulaev, V., & Lam, E. (1995). Coordinated Activation of Programmed Cell Death and Defense Mechanisms in Transgenic Tobacco Plants Expressing a Bacterial Proton Pump. *Plant Cell*, 7(1), 29-42. <https://doi.org/10.1105/tpc.7.1.29>
- Molnar, A., Melnyk, C., & Baulcombe, D. C. (2011). Silencing signals in plants: a long journey for small RNAs. *Genome Biol*, 12(1), 215. <https://doi.org/10.1186/gb-2010-11-12-219>
- Moreno, A. A., Mukhtar, M. S., Blanco, F., Boatwright, J. L., Moreno, I., Jordan, M. R., Chen, Y., Brandizzi, F., Dong, X., Orellana, A., & Pajerowska-Mukhtar, K. M. (2012). IRE1/bZIP60-mediated unfolded protein response plays distinct roles in plant immunity and abiotic stress responses. *PLoS One*, 7(2), e31944.  
<https://doi.org/10.1371/journal.pone.0031944>
- Morris, K. V., & Mattick, J. S. (2014). The rise of regulatory RNA. *Nat Rev Genet*, 15(6), 423-437. <https://doi.org/10.1038/nrg3722>
- Mou, Z., Fan, W., & Dong, X. (2003). Inducers of plant systemic acquired resistance regulate NPR1 function through redox changes. *Cell*, 113(7), 935-944.  
[https://doi.org/10.1016/s0092-8674\(03\)00429-x](https://doi.org/10.1016/s0092-8674(03)00429-x)

- Nagashima, Y., Mishiba, K., Suzuki, E., Shimada, Y., Iwata, Y., & Koizumi, N. (2011). Arabidopsis IRE1 catalyses unconventional splicing of bZIP60 mRNA to produce the active transcription factor. *Sci Rep*, 1, 29. <https://doi.org/10.1038/srep00029>
- Nimchuk, Z., Eulgem, T., Holt, B. F., 3rd, & Dangl, J. L. (2003). Recognition and response in the plant immune system. *Annu Rev Genet*, 37, 579-609. <https://doi.org/10.1146/annurev.genet.37.110801.142628>
- Okamoto, M., Tatematsu, K., Matsui, A., Morosawa, T., Ishida, J., Tanaka, M., Endo, T. A., Mochizuki, Y., Toyoda, T., Kamiya, Y., Shinozaki, K., Nambara, E., & Seki, M. (2010). Genome-wide analysis of endogenous abscisic acid-mediated transcription in dry and imbibed seeds of Arabidopsis using tiling arrays. *Plant J*, 62(1), 39-51. <https://doi.org/10.1111/j.1365-313X.2010.04135.x>
- Oono, Y., Yazawa, T., Kanamori, H., Sasaki, H., Mori, S., & Matsumoto, T. (2017). Genome-wide analysis of rice cis-natural antisense transcription under cadmium exposure using strand-specific RNA-Seq. *BMC Genomics*, 18(1), 761. <https://doi.org/10.1186/s12864-017-4108-5>
- Pajerowska-Mukhtar, K. M., Emerine, D. K., & Mukhtar, M. S. (2013). Tell me more: roles of NPRs in plant immunity. *Trends Plant Sci*, 18(7), 402-411. <https://doi.org/10.1016/j.tplants.2013.04.004>
- Pajerowska-Mukhtar, K. M., Wang, W., Tada, Y., Oka, N., Tucker, C. L., Fonseca, J. P., & Dong, X. (2012). The HSF-like transcription factor TBF1 is a major molecular switch for plant growth-to-defense transition. *Current Biology*, 22(2), 103-112.
- Pani, A., Mahapatra, R. K., Behera, N., & Naik, P. K. (2011). Computational identification of sweet wormwood (*Artemisia annua*) microRNA and their mRNA targets. *Genomics Proteomics Bioinformatics*, 9(6), 200-210. [https://doi.org/10.1016/S1672-0229\(11\)60023-5](https://doi.org/10.1016/S1672-0229(11)60023-5)
- Peters, N. T., Rohrbach, J. A., Zalewski, B. A., Byrkett, C. M., & Vaughn, J. C. (2003). RNA editing and regulation of Drosophila 4f-rnp expression by sas-10 antisense readthrough mRNA transcripts. *RNA*, 9(6), 698-710. <https://doi.org/10.1261/rna.2120703>
- Phillips, J. R., Dalmay, T., & Bartels, D. (2007). The role of small RNAs in abiotic stress. *FEBS Lett*, 581(19), 3592-3597. <https://doi.org/10.1016/j.febslet.2007.04.007>
- Ponting, C. P., Oliver, P. L., & Reik, W. (2009). Evolution and functions of long noncoding RNAs. *Cell*, 136(4), 629-641. <https://doi.org/10.1016/j.cell.2009.02.006>
- Prescott, E. M., & Proudfoot, N. J. (2002). Transcriptional collision between convergent genes in budding yeast. *Proc Natl Acad Sci U S A*, 99(13), 8796-8801. <https://doi.org/10.1073/pnas.132270899>
- Rotari, V., & Gallois, P. (2016). Inhibition of cathepsin B by caspase-3 inhibitors blocks programmed cell death in Arabidopsis. *Cell death and differentiation*, 23(9), 1493-1501.
- Selvaraj, G., Kumar, A., Jakse, J., & Matousek, J. (2015). Computational Prediction, Target Identification and Experimental Validation of miRNAs from Expressed Sequence Tags in Cannabis sativa. *L. Research & Reviews: Journal of Botanical Sciences*.

- Seo, J. S., Sun, H. X., Park, B. S., Huang, C. H., Yeh, S. D., Jung, C., & Chua, N. H. (2017). ELF18-INDUCED LONG-NONCODING RNA Associates with Mediator to Enhance Expression of Innate Immune Response Genes in Arabidopsis. *Plant Cell*, 29(5), 1024-1038. <https://doi.org/10.1105/tpc.16.00886>
- Siegel, T. N., Hon, C. C., Zhang, Q., Lopez-Rubio, J. J., Scheidig-Benatar, C., Martins, R. M., Sismeiro, O., Coppee, J. Y., & Scherf, A. (2014). Strand-specific RNA-Seq reveals widespread and developmentally regulated transcription of natural antisense transcripts in Plasmodium falciparum. *BMC Genomics*, 15(1), 150. <https://doi.org/10.1186/1471-2164-15-150>
- Song, J. B., Gao, S., Sun, D., Li, H., Shu, X. X., & Yang, Z. M. (2013). miR394 and LCR are involved in Arabidopsis salt and drought stress responses in an abscisic acid-dependent manner. *BMC Plant Biol*, 13, 210. <https://doi.org/10.1186/1471-2229-13-210>
- Sueldo, D. J., & van der Hoorn, R. A. L. (2017). Plant life needs cell death, but does plant cell death need Cys proteases? *FEBS J*, 284(10), 1577-1585. <https://doi.org/10.1111/febs.14034>
- Sun, Q., Csorba, T., Skourtis-Stathaki, K., Proudfoot, N. J., & Dean, C. (2013). R-loop stabilization represses antisense transcription at the Arabidopsis FLC locus. *Science*, 340(6132), 619-621. <https://doi.org/10.1126/science.1234848>
- Sun, Y., Zhang, H., Fan, M., He, Y., & Guo, P. (2020). Genome-wide identification of long non-coding RNAs and circular RNAs reveal their ceRNA networks in response to cucumber green mottle mosaic virus infection in watermelon. *Arch Virol*, 165(5), 1177-1190. <https://doi.org/10.1007/s00705-020-04589-4>
- Swiezewski, S., Liu, F., Magusin, A., & Dean, C. (2009). Cold-induced silencing by long antisense transcripts of an Arabidopsis Polycomb target. *Nature*, 462(7274), 799-802. <https://doi.org/10.1038/nature08618>
- Thomma, B. P., Nurnberger, T., & Joosten, M. H. (2011). Of PAMPs and effectors: the blurred PTI-ETI dichotomy. *Plant Cell*, 23(1), 4-15. <https://doi.org/10.1105/tpc.110.082602>
- Urquiaga, M. C. O., Thiebaut, F., Hemerly, A. S., & Ferreira, P. C. G. (2020). From Trash to Luxury: The Potential Role of Plant LncRNA in DNA Methylation During Abiotic Stress. *Front Plant Sci*, 11, 603246. <https://doi.org/10.3389/fpls.2020.603246>
- van Butselaar, T., & Van den Ackerveken, G. (2020). Salicylic Acid Steers the Growth-Immunity Tradeoff. *Trends Plant Sci*, 25(6), 566-576. <https://doi.org/10.1016/j.tplants.2020.02.002>
- Varallyay, E., Valoczi, A., Agyi, A., Burgyan, J., & Havelda, Z. (2010). Plant virus-mediated induction of miR168 is associated with repression of ARGONAUTE1 accumulation. *EMBO J*, 29(20), 3507-3519. <https://doi.org/10.1038/emboj.2010.215>
- Vasudevan, S. (2012). Posttranscriptional upregulation by microRNAs. *Wiley Interdiscip Rev RNA*, 3(3), 311-330. <https://doi.org/10.1002/wrna.121>
- Verchot, J., & Pajerowska-Mukhtar, K. M. (2021). UPR signaling at the nexus of plant viral, bacterial, and fungal defenses. *Curr Opin Virol*, 47, 9-17. <https://doi.org/10.1016/j.coviro.2020.11.001>

- Wang, C. Y., Zhang, S., Yu, Y., Luo, Y. C., Liu, Q., Ju, C., Zhang, Y. C., Qu, L. H., Lucas, W. J., Wang, X., & Chen, Y. Q. (2014). MiR397b regulates both lignin content and seed number in Arabidopsis via modulating a laccase involved in lignin biosynthesis. *Plant Biotechnol J*, 12(8), 1132-1142. <https://doi.org/10.1111/pbi.12222>
- Wang, H., Chung, P. J., Liu, J., Jang, I. C., Kean, M. J., Xu, J., & Chua, N. H. (2014). Genome-wide identification of long noncoding natural antisense transcripts and their responses to light in Arabidopsis. *Genome Res*, 24(3), 444-453. <https://doi.org/10.1101/gr.165555.113>
- Wang, J., Yu, W., Yang, Y., Li, X., Chen, T., Liu, T., Ma, N., Yang, X., Liu, R., & Zhang, B. (2015). Genome-wide analysis of tomato long non-coding RNAs and identification as endogenous target mimic for microRNA in response to TYLCV infection. *Sci Rep*, 5, 16946. <https://doi.org/10.1038/srep16946>
- Wang, J. W., Wang, L. J., Mao, Y. B., Cai, W. J., Xue, H. W., & Chen, X. Y. (2005). Control of root cap formation by MicroRNA-targeted auxin response factors in Arabidopsis. *Plant Cell*, 17(8), 2204-2216. <https://doi.org/10.1105/tpc.105.033076>
- Werner, A., & Sayer, J. A. (2009). Naturally occurring antisense RNA: function and mechanisms of action. *Curr Opin Nephrol Hypertens*, 18(4), 343-349. <https://doi.org/10.1097/MNH.0b013e32832cb982>
- Wilusz, J. E., Sunwoo, H., & Spector, D. L. (2009). Long noncoding RNAs: functional surprises from the RNA world. *Genes Dev*, 23(13), 1494-1504. <https://doi.org/10.1101/gad.1800909>
- Woltering, E. J. (2004). Death proteases come alive. *Trends in Plant Science*, 9(10), 469-472.
- Wunderlich, M., Gross-Hardt, R., & Schoffl, F. (2014). Heat shock factor HSF2a involved in gametophyte development of Arabidopsis thaliana and its expression is controlled by a heat-inducible long non-coding antisense RNA. *Plant Mol Biol*, 85(6), 541-550. <https://doi.org/10.1007/s11103-014-0202-0>
- Xie, F., Jones, D. C., Wang, Q., Sun, R., & Zhang, B. (2015). Small RNA sequencing identifies miRNA roles in ovule and fibre development. *Plant Biotechnol J*, 13(3), 355-369. <https://doi.org/10.1111/pbi.12296>
- Xin, M., Wang, Y., Yao, Y., Song, N., Hu, Z., Qin, D., Xie, C., Peng, H., Ni, Z., & Sun, Q. (2011). Identification and characterization of wheat long non-protein coding RNAs responsive to powdery mildew infection and heat stress by using microarray analysis and SBS sequencing. *BMC Plant Biol*, 11, 61. <https://doi.org/10.1186/1471-2229-11-61>
- Xu, J., Wang, Q., Freeling, M., Zhang, X., Xu, Y., Mao, Y., Tang, X., Wu, F., Lan, H., Cao, M., Rong, T., Lisch, D., & Lu, Y. (2017). Natural antisense transcripts are significantly involved in regulation of drought stress in maize. *Nucleic Acids Res*, 45(9), 5126-5141. <https://doi.org/10.1093/nar/gkx085>
- Yang, G., Li, Y., Wu, B., Zhang, K., Gao, L., & Zheng, C. (2019). MicroRNAs transcriptionally regulate promoter activity in Arabidopsis thaliana. *J Integr Plant Biol*, 61(11), 1128-1133. <https://doi.org/10.1111/jipb.12775>

- Yassour, M., Pfiffner, J., Levin, J. Z., Adiconis, X., Gnirke, A., Nusbaum, C., Thompson, D. A., Friedman, N., & Regev, A. (2010). Strand-specific RNA sequencing reveals extensive regulated long antisense transcripts that are conserved across yeast species. *Genome Biol*, 11(8), R87. <https://doi.org/10.1186/gb-2010-11-8-r87>
- Yu, X., Yang, J., Li, X., Liu, X., Sun, C., Wu, F., & He, Y. (2013). Global analysis of cis-natural antisense transcripts and their heat-responsive nat-siRNAs in *Brassica rapa*. *BMC Plant Biol*, 13, 208. <https://doi.org/10.1186/1471-2229-13-208>
- Yu, Y., Zhou, Y. F., Feng, Y. Z., He, H., Lian, J. P., Yang, Y. W., Lei, M. Q., Zhang, Y. C., & Chen, Y. Q. (2020). Transcriptional landscape of pathogen-responsive lncRNAs in rice unveils the role of ALEX1 in jasmonate pathway and disease resistance. *Plant Biotechnol J*, 18(3), 679-690. <https://doi.org/10.1111/pbi.13234>
- Zhang, B. (2015). MicroRNA: a new target for improving plant tolerance to abiotic stress. *J Exp Bot*, 66(7), 1749-1761. <https://doi.org/10.1093/jxb/erv013>
- Zhang, T., Zhao, Y. L., Zhao, J. H., Wang, S., Jin, Y., Chen, Z. Q., Fang, Y. Y., Hua, C. L., Ding, S. W., & Guo, H. S. (2016). Cotton plants export microRNAs to inhibit virulence gene expression in a fungal pathogen. *Nat Plants*, 2(10), 16153. <https://doi.org/10.1038/nplants.2016.153>
- Zhang, W., Corwin, J. A., Copeland, D., Feusier, J., Eshbaugh, R., Chen, F., Atwell, S., & Kliebenstein, D. J. (2017). Plastic Transcriptomes Stabilize Immunity to Pathogen Diversity: The Jasmonic Acid and Salicylic Acid Networks within the *Arabidopsis*/Botrytis Pathosystem. *Plant Cell*, 29(11), 2727-2752. <https://doi.org/10.1105/tpc.17.00348>
- Zhang, Y., Cheng, Y. T., Qu, N., Zhao, Q., Bi, D., & Li, X. (2006). Negative regulation of defense responses in *Arabidopsis* by two NPR1 paralogs. *The Plant Journal*, 48(5), 647-656.
- Zhang, Y. C., Yu, Y., Wang, C. Y., Li, Z. Y., Liu, Q., Xu, J., Liao, J. Y., Wang, X. J., Qu, L. H., Chen, F., Xin, P., Yan, C., Chu, J., Li, H. Q., & Chen, Y. Q. (2013). Overexpression of microRNA OsmiR397 improves rice yield by increasing grain size and promoting panicle branching. *Nat Biotechnol*, 31(9), 848-852. <https://doi.org/10.1038/nbt.2646>
- Zhao, X., Li, J., Lian, B., Gu, H., Li, Y., & Qi, Y. (2018). Global identification of *Arabidopsis* lncRNAs reveals the regulation of MAF4 by a natural antisense RNA. *Nat Commun*, 9(1), 5056. <https://doi.org/10.1038/s41467-018-07500-7>
- Zhu, Q. H., Stephen, S., Taylor, J., Helliwell, C. A., & Wang, M. B. (2014). Long noncoding RNAs responsive to *Fusarium oxysporum* infection in *Arabidopsis thaliana*. *New Phytol*, 201(2), 574-584. <https://doi.org/10.1111/nph.12537>
- Zipfel, C., & Felix, G. (2005). Plants and animals: a different taste for microbes? *Curr Opin Plant Biol*, 8(4), 353-360. <https://doi.org/10.1016/j.pbi.2005.05.004>
- Zuppini, A., Navazio, L., & Mariani, P. (2004). Endoplasmic reticulum stress-induced programmed cell death in soybean cells. *Journal of cell science*, 117(12), 2591-2598.

## **Discussions and Future Directions**

The ER is a crucial organelle in eukaryotic cells that plays a vital role in protein synthesis, folding, and modification (Mori, 2000; Stefano et al., 2015). However, the ER is prone to stress caused by various factors, including nutrient deprivation, oxidative stress, pathogen infection, and even by usual growth/developmental demands of plants (Afrin, Diwan, et al., 2020; Korner et al., 2015; Moreno et al., 2012). ER stress triggers the UPR that aims to restore ER homeostasis by reducing protein synthesis, increasing protein folding capacity, and degrading misfolded proteins (Walter & Ron, 2011). The UPR is a complex and dynamic process that involves multiple signaling pathways and transcription factors. In Chapter One, I discussed the recent advances in understanding the UPR in plants, including the signaling pathways, transcriptional regulation, and crosstalk with other stress response pathways. In the mammalian system, the UPR is mitigated by three ER transmembrane sensors: IRE1, ATF6, and PERK. These sensors detect the accumulation of unfolded or misfolded proteins in the ER lumen and activate downstream signaling pathways to restore ER homeostasis. IRE1 is the most conserved and well-studied UPR sensor in plants, a bifunctional protein that possesses both kinase and endoribonuclease activities. Upon activation, IRE1 splices the mRNA of bZIP60, a transcription factor that regulates the expression of ER chaperones and folding enzymes (Deng et al., 2011; Moreno et al., 2012). IRE1 also degrades mRNAs encoding secretory

pathway proteins, thereby reducing the load of newly synthesized proteins entering the ER through RIDD (Hollien & Weissman, 2006). Recent studies have shown that IRE1 can activate other signaling pathways, including autophagy and programmed cell death, in response to ER stress (Bao et al., 2018; Mishiba et al., 2013).

ATF6 in the mammalian system is another ER transmembrane sensor that is activated by ER stress (Walter & Ron, 2011). In plants, ER membrane-associated TFs AtbZIP17 and AtbZIP28 exhibit a significant level of conservation with ATF6; get activated upon cleavage from the membrane due to ER stress (Hillary & FitzGerald, 2018; Howell, 2013; Liu et al., 2007). PERK is the third ER transmembrane sensor in mammals that is activated by ER stress. Upon activation, PERK phosphorylates eIF2 $\alpha$ , a translation initiation factor, which reduces global protein synthesis and promotes the translation of specific mRNAs, including ATF4 (Rutkowski & Kaufman, 2003). AtGCN2 has been demonstrated to regulate abscisic acid (ABA) homeostasis and stomatal immunity in plants (Liu et al., 2019). It also controls the translation of a transcription factor, TBF1, through the upstream open reading frame (uORF) reinitiation, a mechanism similar to that observed in mammalian ATF4 and yeast GCN4 (Liu et al., 2019; Pajerowska-Mukhtar et al., 2012).

The study described in Chapter Two provides significant insights into the role of AtGCN2, a protein kinase in Arabidopsis, in regulating of ABA homeostasis and stomatal immunity. The research reveals that AtGCN2 is an immune regulator that triggers eIF2 $\alpha$ -mediated down-stream signaling events. It is suggested that AtGCN2 might be directly or indirectly implicated in the translational control of TBF1, leading to the repression of ABA signaling components upon pathogen infection (Figure 1d-1f).

AtGCN2 can target TBF1, which can regulate the plant hormone ABA (known to play a role in plant defense responses) during the preinvasive stage of pathogen infection (figure 2d-2g). In addition, the induction of AtGCN2 expression leads to the activation of the eIF2 $\alpha$  kinase GCN2, which in turn leads to the phosphorylation of eIF2 $\alpha$  and the subsequent inhibition of translation initiation (figure 2h-2k). The research further demonstrates the opposing roles of AtGCN2 in regulating ABA accumulation and signaling. It is found that AtGCN2 promotes ABA accumulation, which is a crucial factor in plant response to environmental stress, including pathogen attack. However, AtGCN2 also negatively affects ABA signaling components, suggesting a complex interplay in the plant's immune response. Moreover, the study highlights the potential role of AtGCN2 in COR-mediated stomatal reopening, a hallmark of virulent bacterial infection. It is proposed that AtGCN2 serves as an upstream regulator of this process, adding to the understanding of hormonal interplay during preinvasive immunity. The study offers a model in which the induction of AtGCN2 expression and subsequent activation of GCN2 leads to the selective translation of mRNAs containing uORFs, leading to the downregulation of genes involved in plant defense responses. This model is supported by the authors' finding that the induction of AtGCN2 expression upon pathogen infection leads to the downregulation of the transcription factors MYC2, ANAC019, and ANAC055, which are known to play a role in plant defense responses (figure 3a-3h). AtGCN2 has also been demonstrated to play a role in the coronatine (COR)-mediated stomata reopening, subsequently controlling bacteria entry into the leaf.

TBF1, a master transcriptional regulator, is regulated translationally through uORFs (Pajerowska-Mukhtar et al., 2012). Chapter Two established that the AtGCN2-

eIF2 $\alpha$  pathway is responsible for reinitiating translation on TBF1 mRNA. Pathogen stress triggers the AtGCN2-dependent phosphorylation of eIF2 $\alpha$ , subsequently leading to translation reinitiation at the main open reading frame (mORF) of TBF1. We have also highlighted the significant role of AtGCN2 in regulating stomatal immunity during the pre-invasive stage of pathogen infection. Therefore, it would be intriguing to investigate if additional genes containing uORFs are translationally regulated by the AtGCN2-eIF2 $\alpha$  pathway during stomatal immunity. In conclusion, the research underscores the importance of AtGCN2 in regulating ABA homeostasis and stomatal immunity in Arabidopsis. The findings open up new avenues: for further research into the molecular mechanisms of plant immunity and the potential applications in enhancing plant resistance to pathogens to the development of new strategies for crop protection, which could have important implications for global food security. However, the complete mechanism governing these phenomena still needs to be improved, indicating the need for more in-depth studies in the future. This study has immense importance in understanding the intricate regulatory network of UPR.

A complex network of transcription factors and signaling pathways tightly regulates the UPR. Recent studies have identified several transcription factors (bZIP28, bZIP60, and WRKY17) that regulate the expression of UPR genes in plants (Arraño-Salinas et al., 2018). I discussed the bZIP28 and bZIP60 earlier. WRKY17 is a transcription factor that represses the expression of bZIP28, thereby regulating the UPR in response to pathogen infection (Arraño-Salinas et al., 2018). The UPR is a complex and dynamic process that involves multiple signaling pathways and transcription factors. Recent studies have shed light on the molecular mechanisms underlying the UPR in

plants, including the signaling pathways, transcriptional regulation, and crosstalk with other stress response pathways. The UPR plays a crucial role in plant growth, development, and stress tolerance, and its manipulation holds great promise for improving crop yield and quality. Further research is needed to fully understand the UPR and its interactions with other stress response pathways. This will pave the way for developing of novel strategies to enhance plant stress tolerance and productivity.

AtAGB1, the sole G-protein β-subunit encoded by the *Arabidopsis* genome, has been shown to work in tandem with AtIRE1a and AtIRE1b to regulate two distinct UPR pathways (Chen & Brandizzi, 2012). In Chapter Three, I explored the role of GTP-binding protein AGB1 in regulating of the unfolded protein response (UPR) and bacterial immunity in *Arabidopsis*. The study found that AGB1 interacts with the ER stress sensors IRE1a and IRE1b to modulate the UPR and bacterial immunity in *Arabidopsis*. Bacterial immunity is the ability of plants to defend themselves against bacterial pathogens. Bacterial pathogens can cause plant disease by secreting virulence factors that manipulate plant signaling pathways. The plant immune system recognizes these virulence factors and activates defense responses to prevent pathogen's spread. The plant immune system is regulated by a complex network of signaling pathways that involve GTP-binding proteins. GTP-binding proteins are a family of proteins that are involved in a wide range of cellular processes, including signal transduction, protein synthesis, and vesicle trafficking (Latham, 2015; Liu et al., 2013; Llorente et al., 2005; Trusov et al., 2006; Urano & Jones, 2014). GTP-binding proteins are divided into three families: small GTPases, heterotrimeric G proteins, and monomeric G proteins. Heterotrimeric G proteins are composed of three subunits: alpha, beta, and gamma. Heterotrimeric G

proteins are involved in signal transduction pathways that regulate plant growth, development, and stress responses (Jones et al., 2003; Llorente et al., 2005; Trusov et al., 2006; Ullah et al., 2003; Urano & Jones, 2014; Zhang et al., 2008).

The study found that AGB1 interacts with IRE1a and IRE1b to regulate the splicing of bZIP60 mRNA and the expression of UPR target genes. Our research uncovered a synergistic interaction between AGB1 and IRE1a/IRE1b in response to ER stress induced by DTT and Tm (figure 2-figure 4). This research study offers fresh insights into regulating the unfolded protein response (UPR) and bacterial immunity in plants. The study demonstrates that AGB1 plays a crucial role in this regulation by interacting with IRE1a and IRE1b (figure 5). To summarize, this study offers novel perspectives on the regulation of the unfolded protein response (UPR) and bacterial immunity in plants. It highlights the significant role of AGB1 in governing the UPR and bacterial immunity through its interaction with IRE1a and IRE1b. These findings hold implications for the field of plant biology and agriculture and lay the groundwork for further investigations in this domain. While numerous studies have shed light on the various functions of AGB1, more in-depth research is needed to elucidate the interplay between AGB1 and IRE1a/IRE1b/IRE1c under a range of biotic and abiotic ER stressors.

The fourth Chapter provides a comprehensive understanding of the role of IRE1 in plant stress responses, which is crucial for developing strategies to improve plant stress tolerance. This study explored the natural variation of IRE1 expression and ER stress responses in different *Arabidopsis* accessions. Our findings revealed that IRE1 expression levels and the ability to induce UPR under heat stress varied among different *Arabidopsis* accessions. The study highlights the importance of different IRE1 accessions during heat

stress response in Arabidopsis (figure 2, figure 3, and figure 4). The heat shock response is a vital mechanism for plant survival during high-temperature conditions, and the discovery of IRE1's involvement in this process is highly significant. This finding is further reinforced by comparing basal and heat-induced conditions' expression levels for each accession.

The study also highlighted the role of IRE1 accessions in plant immunity. The UPR, mediated by IRE1, is activated during pathogen infection, suggesting a link between ER stress responses and plant defense mechanisms. The findings of this study further support this link, demonstrating that IRE1 expression levels can influence the plant's response to pathogen infection. The research also delves into the role of salicylic acid in plant immunity and stress responses (figure 5). Salicylic acid is a multifaceted hormone that combats disease, and its interaction with the unfolded protein response in Arabidopsis is a noteworthy aspect of the study. The study also mentions the role of the ER stress modulator IRE1a in plant growth and defense transition, indicating the multifaceted role of IRE1 in plant physiology (figure 6 and figure 7). The research also brings to light the role of the UPR in the ER, a crucial aspect of plant cell survival under stress conditions. Our findings underscore that alterations solely in the promoter regions of various accessions can significantly influence the responses to ER stress. While the study examined nine key accessions in response to heat and bacterial-induced ER stress, other ER stressors need detailed investigation. There is a pressing need for an in-depth bioinformatics analysis of the IRE1 promoter regions of different accessions. The study be supplemented with direct evidence of transcription factor binding to the single nucleotide polymorphisms (SNPs) within these promoter regions when challenged with ER stressors. While the primary

regulatory functions of IRE1 have been identified, the UPR possesses a highly complex regulatory network. Therefore, the interaction between IRE1 from different accessions and other regulatory components of the UPR warrants further investigation. In conclusion, the study provides valuable insights into the role of IRE1 and the unfolded protein response in plant stress responses. It highlights the potential of exploiting natural variation in IRE1 expression for improving plant stress tolerance and disease resistance. These findings can be instrumental in developing strategies to improve plant stress tolerance, which is crucial in changing environmental conditions.

As discussed earlier, IRE1 acts to cleave mRNA (through RIDS) or bulk mRNAs (RIDD) as a response to mitigate ER stress, the extent of which is dependent on the level of ER stress present. In mammalian systems, RIDD plays a crucial role in the transition between the pro-survival and pro-death functions of IRE1 (Abdullah & Ravanan, 2018). The splicing of bZIP60 by IRE1 primarily promotes pro-survival by activating genes that help mitigate ER stress (Moreno et al., 2012). However, RIDD can influence cell fate, depending on the specific mRNAs that are degraded. In the fifth Chapter, we aimed to investigate the role of a specific microRNA (miR5658) derived from a novel lncNAT in shifting the response of the IRE1/bZIP60 pathway from pro-survival to pro-death during acute ER stress induced by a biotic stressor in *Arabidopsis*. ER stress is shaped by miRNA-mediated regulations, and ER stress additionally governs the expression of miRNAs. Several miRNAs have been discovered to be directly involved with the regulation of IRE1 and XBP1 in the mammalian system (Bartoszewska et al., 2019; Byrd et al., 2012; Duan et al., 2012; Li et al., 2017; Maurel et al., 2013). Nonetheless, a comprehensive

investigation of miRNA's regulatory functions during the ER stress response in Arabidopsis is currently lacking.

Through bioinformatics analysis, we explored potential microRNAs (miRNAs) that could target bZIP60 and regulate the pro-survival pathway mediated by IRE1/bZIP60. We identified three distinct miRNAs (miR5658, miR414, miR397b) capable of targeting the bZIP60 transcript (refer to Table 1). Interestingly, these miRNAs originate from a different long non-coding RNA (lncRNA). The miR414 family, which is highly conserved across the plant system, consists of five homologs, two of which originate from lncNATs. Similarly, miR397b, also conserved across the plant system, has two homologs, one derived from a lncNAT. In contrast, miR5658 is a newly identified miRNA with only one homolog, which is also sourced from a lncNAT.

The miR5658 mutant line *NAT<sub>SRCL</sub>* and the sense transcript mutant line *srcl* showed significant chlorosis in terms of Chlorophyll b when compared to Col-0. Negative control mutants *npr1-1* and *bzip60* again showed significant chlorophyll b reduction compared to Col-0. Nevertheless, chlorosis of chlorophyll a was higher in all mutant lines compared to the wild type (figure 2). Mutation in the miR5658 targeted seed region in bZIP60 blocks the miR5658 targeting and increases bZIP60 expression (figure 3a-c). We highlighted the regulatory roles of the novel microRNA, miR5658, during the transition from pro-survival to pro-death signaling. Our functional analysis suggested that miR5658 governs cell death during acute ER stress (induced by Pst DC3000 avrRPM1) by modulating bZIP60 expression (figure 4 and 5). Furthermore, we demonstrated that the sense transcript of the miR5658 precursor cis-NAT does not interfere with cell death regulation. Instead, it works in harmony with the cis-NAT to support this regulation. This

finding provides valuable insights into cis-NATs' involvement in mediating miRNA-guided cell death during acute ER stress. In conclusion, our study provides a novel insight into the function of miR5658 and its role in regulating the IRE1/bZIP60 pathway during acute ER stress. The findings of this study could open new avenues for understanding the complex regulatory networks involved in plant stress responses. They could be used to develop strategies for improving plant stress tolerance. However, further studies are needed to fully elucidate the molecular mechanisms underlying the IRE1/bZIP60 pathway regulation by miR5658 and other miRNAs.

Our prediction analysis based on miRbase and psRNATarget website showed that miR5658 could target the promoter region of IRE1a. As previously described by Yang et al. (2019) that miR5658 can regulate gene expression by targeting its promoter region. Does miR5658 upregulate or downregulate IRE1a expression? When does miR5658 target IRE1a? Does miR5658 alter its target between bZIP60 and IRE1a, or the reverse, depending on the level of ER stress? Does miR5658 target other upstream/downstream genes to facilitate the UPR responses? As miR5658 and miR414 has almost overlapping target sequence, do they work synergistically or compete for their target? As the precursor of miR5658 is a lncNAT, is there any regulatory function of that lncNAT in maintaining ER homeostasis? What role does the sense transcript of lncNAT play, and how does it contribute to the function of lncNAT? Do the other two long non-coding RNAs (precursors of miR414 and miR397b) have any additional roles in the regulation of ER stress? While we examined the transition from pro-survival to pro-death using a biotic ER stress inducer, does the same transition occur under abiotic and chemical stress conditions? In the mammalian system, numerous lncRNAs and miRNAs regulate the

ATF6 and PERK pathways. What miRNAs regulate the bZIP17/bZIP28 and GCN2 pathways in response to endoplasmic reticulum (ER) stress? Addressing these questions is crucial for a more comprehensive understanding of how cells manage ER stress conditions and reestablish cellular homeostasis.

Furthermore, exploring of the roles of lncRNAs in ER stress regulation could shed light on the complex UPR interplay. The studies could lead to the discovery of novel regulatory mechanisms and potential targets for genetic manipulation to enhance stress tolerance. In conclusion, answering these questions could significantly advance our understanding of the complex molecular mechanisms underpinning cellular stress responses and homeostasis restoration, with potential applications in both plant and broader cell biology.

## References

- Abdullah, A., & Ravanant, P. (2018). The unknown face of IRE1 $\alpha$ —Beyond ER stress. *European journal of cell biology*, 97(5), 359-368.
- Afrin, T., Costello, C. N., Monella, A. N., Kørner, C. J., & Pajerowska-Mukhtar, K. M. (2022). The interplay of GTP-binding protein AGB1 with ER stress sensors IRE1a and IRE1b modulates Arabidopsis unfolded protein response and bacterial immunity. *Plant Signaling & Behavior*, 17(1), 2018857.
- Afrin, T., Diwan, D., Sahawneh, K., & Pajerowska-Mukhtar, K. (2020). Multilevel regulation of endoplasmic reticulum stress responses in plants: where old roads and new paths meet. *J Exp Bot*, 71(5), 1659-1667.  
<https://doi.org/10.1093/jxb/erz487>
- Afrin, T., Seok, M., Terry, B. C., & Pajerowska-Mukhtar, K. M. (2020). Probing natural variation of IRE1 expression and endoplasmic reticulum stress responses in Arabidopsis accessions. *Sci Rep*, 10(1), 19154. <https://doi.org/10.1038/s41598-020-76114-1>
- Alvarez, M. E. (2000). Salicylic acid in the machinery of hypersensitive cell death and disease resistance. *Plant Mol Biol*, 44(3), 429-442.  
<https://doi.org/10.1023/a:1026561029533>
- Arraño-Salinas, P., Domínguez-Figueroa, J., Herrera-Vásquez, A., Zavala, D., Medina, J., Vicente-Carabajosa, J., Meneses, C., Canessa, P., Moreno, A. A., & Blanco-Herrera, F. (2018). WRKY7,-11 and -17 transcription factors are modulators of the bZIP28 branch of the unfolded protein response during PAMP-triggered immunity in *Arabidopsis thaliana*. *Plant Science*, 277, 242-250.
- Ausubel, F. M. (2005). Are innate immune signaling pathways in plants and animals conserved? *Nature immunology*, 6(10), 973-979.
- Axtell, M. J., & Staskawicz, B. J. (2003). Initiation of RPS2-specified disease resistance in *Arabidopsis* is coupled to the AvrRpt2-directed elimination of RIN4. *Cell*, 112(3), 369-377.
- Bao, Y., & Howell, S. H. (2017). The unfolded protein response supports plant development and defense as well as responses to abiotic stress. *Frontiers in plant science*, 8, 344.
- Bao, Y., Pu, Y., Yu, X., Gregory, B. D., Srivastava, R., Howell, S. H., & Bassham, D. C. (2018). IRE1B degrades RNAs encoding proteins that interfere with the induction

- of autophagy by ER stress in *Arabidopsis thaliana*. *Autophagy*, 14(9), 1562-1573. <https://doi.org/10.1080/15548627.2018.1462426>
- Bartoszewska, S., Cabaj, A., Dabrowski, M., Collawn, J. F., & Bartoszewski, R. (2019). miR-34c-5p modulates X-box-binding protein 1 (XBP1) expression during the adaptive phase of the unfolded protein response. *FASEB J*, 33(10), 11541-11554. <https://doi.org/10.1096/fj.201900600RR>
- Bonneau, L., Ge, Y., Drury, G. E., & Gallois, P. (2008). What happened to plant caspases? *Journal of experimental botany*, 59(3), 491-499.
- Borsani, O., Zhu, J., Verslues, P. E., Sunkar, R., & Zhu, J. K. (2005). Endogenous siRNAs derived from a pair of natural cis-antisense transcripts regulate salt tolerance in *Arabidopsis*. *Cell*, 123(7), 1279-1291. <https://doi.org/10.1016/j.cell.2005.11.035>
- Bozhkov, P. V., & Lam, E. (2011). Green death: revealing programmed cell death in plants. *Cell Death Differ*, 18(8), 1239-1240. <https://doi.org/10.1038/cdd.2011.86>
- Braakman, I., Helenius, J., & Helenius, A. (1992). Manipulating disulfide bond formation and protein folding in the endoplasmic reticulum. *The EMBO journal*, 11(5), 1717-1722.
- Byrd, A. E., Aragon, I. V., & Brewer, J. W. (2012). MicroRNA-30c-2\* limits expression of proadaptive factor XBP1 in the unfolded protein response. *J Cell Biol*, 196(6), 689-698. <https://doi.org/10.1083/jcb.201201077>
- Cai, Y.-M., Yu, J., & Gallois, P. (2014). Endoplasmic reticulum stress-induced PCD and caspase-like activities involved. *Frontiers in Plant Science*, 5, 41.
- Chen, J., Mohan, R., Zhang, Y., Li, M., Chen, H., Palmer, I. A., Chang, M., Qi, G., Spoel, S. H., Mengiste, T., Wang, D., Liu, F., & Fu, Z. Q. (2019). NPR1 Promotes Its Own and Target Gene Expression in Plant Defense by Recruiting CDK8. *Plant Physiol*, 181(1), 289-304. <https://doi.org/10.1104/pp.19.00124>
- Chen, Y., & Brandizzi, F. (2012). AtIRE1A/AtIRE1B and AGB1 independently control two essential unfolded protein response pathways in *Arabidopsis*. *The Plant Journal*, 69(2), 266-277.
- Chen, Y., & Brandizzi, F. (2013). IRE1: ER stress sensor and cell fate executor. *Trends in cell biology*, 23(11), 547-555.
- Chern, M. S., Fitzgerald, H. A., Yadav, R. C., Canlas, P. E., Dong, X., & Ronald, P. C. (2001). Evidence for a disease-resistance pathway in rice similar to the NPR1-mediated signaling pathway in *Arabidopsis*. *Plant J*, 27(2), 101-113. <https://doi.org/10.1046/j.1365-313x.2001.01070.x>
- Chisholm, S. T., Coaker, G., Day, B., & Staskawicz, B. J. (2006). Host-microbe interactions: shaping the evolution of the plant immune response. *Cell*, 124(4), 803-814. <https://doi.org/10.1016/j.cell.2006.02.008>
- Chung, E.-H., Da Cunha, L., Wu, A.-J., Gao, Z., Cherkis, K., Afzal, A. J., Mackey, D., & Dangl, J. L. (2011). Specific threonine phosphorylation of a host target by two unrelated type III effectors activates a host innate immune receptor in plants. *Cell host & microbe*, 9(2), 125-136.
- Clarke, A., Desikan, R., Hurst, R. D., Hancock, J. T., & Neill, S. J. (2000). NO way back: nitric oxide and programmed cell death in *Arabidopsis thaliana* suspension

- cultures. *Plant J*, 24(5), 667-677. <https://doi.org/10.1046/j.1365-313x.2000.00911.x>
- Clough, S. J., Fengler, K. A., Yu, I. C., Lippok, B., Smith, R. K., Jr., & Bent, A. F. (2000). The *Arabidopsis dnd1* "defense, no death" gene encodes a mutated cyclic nucleotide-gated ion channel. *Proc Natl Acad Sci U S A*, 97(16), 9323-9328. <https://doi.org/10.1073/pnas.150005697>
- Coll, N. S., Smidler, A., Puigvert, M., Popa, C., Valls, M., & Dangl, J. L. (2014). The plant metacaspase AtMC1 in pathogen-triggered programmed cell death and aging: functional linkage with autophagy. *Cell Death & Differentiation*, 21(9), 1399-1408.
- Cook, D. E., Mesarich, C. H., & Thomma, B. P. (2015). Understanding plant immunity as a surveillance system to detect invasion. *Annual review of phytopathology*, 53, 541-563.
- Csorba, T., Questa, J. I., Sun, Q., & Dean, C. (2014). Antisense COOLAIR mediates the coordinated switching of chromatin states at FLC during vernalization. *Proc Natl Acad Sci U S A*, 111(45), 16160-16165. <https://doi.org/10.1073/pnas.1419030111>
- Cui, J., Luan, Y., Jiang, N., Bao, H., & Meng, J. (2017). Comparative transcriptome analysis between resistant and susceptible tomato allows the identification of lncRNA16397 conferring resistance to Phytophthora infestans by co-expressing glutaredoxin. *Plant J*, 89(3), 577-589. <https://doi.org/10.1111/tpj.13408>
- Dangl, J. L., Horvath, D. M., & Staskawicz, B. J. (2013). Pivoting the plant immune system from dissection to deployment. *Science*, 341(6147), 746-751. <https://doi.org/10.1126/science.1236011>
- Dangl, J. L., & Jones, J. D. (2001). Plant pathogens and integrated defence responses to infection. *Nature*, 411(6839), 826-833. <https://doi.org/10.1038/35081161>
- Deforges, J., Reis, R. S., Jacquet, P., Sheppard, S., Gadekar, V. P., Hart-Smith, G., Tanzer, A., Hofacker, I. L., Iseli, C., Xenarios, I., & Poirier, Y. (2019). Control of Cognate Sense mRNA Translation by cis-Natural Antisense RNAs. *Plant Physiol*, 180(1), 305-322. <https://doi.org/10.1104/pp.19.00043>
- Deng, Y., Humbert, S., Liu, J. X., Srivastava, R., Rothstein, S. J., & Howell, S. H. (2011). Heat induces the splicing by IRE1 of a mRNA encoding a transcription factor involved in the unfolded protein response in *Arabidopsis*. *Proc Natl Acad Sci U S A*, 108(17), 7247-7252. <https://doi.org/10.1073/pnas.1102117108>
- Deng, Y., Srivastava, R., & Howell, S. H. (2013). Endoplasmic reticulum (ER) stress response and its physiological roles in plants. *International journal of molecular sciences*, 14(4), 8188-8212.
- Deng, Y., Srivastava, R., & Howell, S. H. (2013). Protein kinase and ribonuclease domains of IRE1 confer stress tolerance, vegetative growth, and reproductive development in *Arabidopsis*. *Proc Natl Acad Sci U S A*, 110(48), 19633-19638. <https://doi.org/10.1073/pnas.1314749110>
- Deslandes, L., Olivier, J., Peeters, N., Feng, D. X., Khounlotham, M., Boucher, C., Somssich, I., Genin, S., & Marco, Y. (2003). Physical interaction between RRS1-R, a protein conferring resistance to bacterial wilt, and PopP2, a type III effector

- targeted to the plant nucleus. *Proceedings of the National Academy of Sciences*, 100(13), 8024-8029.
- Devadas, S. K., & Raina, R. (2002). Preexisting systemic acquired resistance suppresses hypersensitive response-associated cell death in *Arabidopsis hrl1* mutant. *Plant Physiol*, 128(4), 1234-1244. <https://doi.org/10.1104/pp.010941>
- Devoto, A., Piffanelli, P., Nilsson, I., Wallin, E., Panstruga, R., von Heijne, G., & Schulze-Lefert, P. (1999). Topology, subcellular localization, and sequence diversity of the Mlo family in plants. *J Biol Chem*, 274(49), 34993-35004. <https://doi.org/10.1074/jbc.274.49.34993>
- Ding, P., & Ding, Y. (2020). Stories of Salicylic Acid: A Plant Defense Hormone. *Trends Plant Sci*, 25(6), 549-565. <https://doi.org/10.1016/j.tplants.2020.01.004>
- Doblas, V. G., Amorim-Silva, V., Posé, D., Rosado, A., Esteban, A., Arró, M., Azevedo, H., Bombarely, A., Borsani, O., & Valpuesta, V. (2013). The SUD1 gene encodes a putative E3 ubiquitin ligase and is a positive regulator of 3-hydroxy-3-methylglutaryl coenzyme a reductase activity in *Arabidopsis*. *The Plant Cell*, 25(2), 728-743.
- Dong, X. (2004). NPR1, all things considered. *Current opinion in plant biology*, 7(5), 547-552.
- Duan, Q., Wang, X., Gong, W., Ni, L., Chen, C., He, X., Chen, F., Yang, L., Wang, P., & Wang, D. W. (2012). ER stress negatively modulates the expression of the miR-199a/214 cluster to regulates tumor survival and progression in human hepatocellular cancer. *PLoS One*, 7(2), e31518. <https://doi.org/10.1371/journal.pone.0031518>
- Edinger, A. L., & Thompson, C. B. (2004). Death by design: apoptosis, necrosis and autophagy. *Curr Opin Cell Biol*, 16(6), 663-669. <https://doi.org/10.1016/j.ceb.2004.09.011>
- Ellgaard, L., & Helenius, A. (2003). Quality control in the endoplasmic reticulum. *Nature reviews Molecular cell biology*, 4(3), 181-191.
- Faghihi, M. A., Modarresi, F., Khalil, A. M., Wood, D. E., Sahagan, B. G., Morgan, T. E., Finch, C. E., St Laurent, G., 3rd, Kenny, P. J., & Wahlestedt, C. (2008). Expression of a noncoding RNA is elevated in Alzheimer's disease and drives rapid feed-forward regulation of beta-secretase. *Nat Med*, 14(7), 723-730. <https://doi.org/10.1038/nm1784>
- Fan, W., & Dong, X. (2002). In vivo interaction between NPR1 and transcription factor TGA2 leads to salicylic acid-mediated gene activation in *Arabidopsis*. *Plant Cell*, 14(6), 1377-1389. <https://doi.org/10.1105/tpc.001628>
- Fan, Y., Yang, J., Mathioni, S. M., Yu, J., Shen, J., Yang, X., Wang, L., Zhang, Q., Cai, Z., Xu, C., Li, X., Xiao, J., Meyers, B. C., & Zhang, Q. (2016). PMS1T, producing phased small-interfering RNAs, regulates photoperiod-sensitive male sterility in rice. *Proc Natl Acad Sci U S A*, 113(52), 15144-15149. <https://doi.org/10.1073/pnas.1619159114>
- Faus, I., Zabalza, A., Santiago, J., Nebauer, S. G., Royuela, M., Serrano, R., & Gadea, J. (2015). Protein kinase GCN2 mediates responses to glyphosate in *Arabidopsis*. *BMC plant biology*, 15(1), 1-12.

- Fedak, H., Palusinska, M., Krzyczmonik, K., Brzezniak, L., Yatusevich, R., Pietras, Z., Kaczanowski, S., & Swiezewski, S. (2016). Control of seed dormancy in Arabidopsis by a cis-acting noncoding antisense transcript. *Proc Natl Acad Sci U S A*, 113(48), E7846-E7855. <https://doi.org/10.1073/pnas.1608827113>
- Fu, Z. Q., & Dong, X. (2013). Systemic acquired resistance: turning local infection into global defense. *Annual review of plant biology*, 64, 839-863.
- Georg, J., Voss, B., Scholz, I., Mitschke, J., Wilde, A., & Hess, W. R. (2009). Evidence for a major role of antisense RNAs in cyanobacterial gene regulation. *Mol Syst Biol*, 5, 305. <https://doi.org/10.1038/msb.2009.63>
- Glazebrook, J. (2005). Contrasting mechanisms of defense against biotrophic and necrotrophic pathogens. *Annu. Rev. Phytopathol.*, 43, 205-227.
- Göhre, V., Spallek, T., Häweker, H., Mersmann, S., Mentzel, T., Boller, T., de Torres, M., Mansfield, J. W., & Robatzek, S. (2008). Plant pattern-recognition receptor FLS2 is directed for degradation by the bacterial ubiquitin ligase AvrPtoB. *Current biology*, 18(23), 1824-1832.
- Gómez-Gómez, L., & Boller, T. (2000). FLS2: an LRR receptor-like kinase involved in the perception of the bacterial elicitor flagellin in Arabidopsis. *Molecular cell*, 5(6), 1003-1011.
- Grant, M. R., & Jones, J. D. (2009). Hormone (dis) harmony moulds plant health and disease. *Science*, 324(5928), 750-752.
- Gust, A. A., Pruitt, R., & Nurnberger, T. (2017). Sensing Danger: Key to Activating Plant Immunity. *Trends Plant Sci*, 22(9), 779-791.  
<https://doi.org/10.1016/j.tplants.2017.07.005>
- Hastings, M. L., Milcarek, C., Martincic, K., Peterson, M. L., & Munroe, S. H. (1997). Expression of the thyroid hormone receptor gene, erbAalpha, in B lymphocytes: alternative mRNA processing is independent of differentiation but correlates with antisense RNA levels. *Nucleic Acids Res*, 25(21), 4296-4300.  
<https://doi.org/10.1093/nar/25.21.4296>
- He, Y., Vogelstein, B., Velculescu, V. E., Papadopoulos, N., & Kinzler, K. W. (2008). The antisense transcriptomes of human cells. *Science*, 322(5909), 1855-1857.
- Helenius, A., & Aebi, M. (2004). Roles of N-linked glycans in the endoplasmic reticulum. *Annual review of biochemistry*, 73(1), 1019-1049.
- Henriquez-Valencia, C., Moreno, A. A., Sandoval-Ibañez, O., Mitina, I., Blanco-Herrera, F., Cifuentes-Esquivel, N., & Orellana, A. (2015). bZIP17 and bZIP60 regulate the expression of BiP3 and other salt stress responsive genes in an UPR-independent manner in *Arabidopsis thaliana*. *Journal of cellular biochemistry*, 116(8), 1638-1645.
- Hetz, C. (2012). The unfolded protein response: controlling cell fate decisions under ER stress and beyond. *Nature reviews Molecular cell biology*, 13(2), 89-102.
- Hillary, R. F., & FitzGerald, U. (2018). A lifetime of stress: ATF6 in development and homeostasis. *J Biomed Sci*, 25(1), 48. <https://doi.org/10.1186/s12929-018-0453-1>
- Hofius, D., Schultz-Larsen, T., Joensen, J., Tsitsigiannis, D. I., Petersen, N. H., Mattsson, O., Jorgensen, L. B., Jones, J. D., Mundy, J., & Petersen, M. (2009). Autophagic

- components contribute to hypersensitive cell death in Arabidopsis. *Cell*, 137(4), 773-783. <https://doi.org/10.1016/j.cell.2009.02.036>
- Hollien, J., & Weissman, J. S. (2006). Decay of endoplasmic reticulum-localized mRNAs during the unfolded protein response. *Science*, 313(5783), 104-107. <https://doi.org/10.1126/science.1129631>
- Howell, S. H. (2013). Endoplasmic reticulum stress responses in plants. *Annual review of plant biology*, 64, 477-499.
- Irsigler, A. S., Costa, M. D., Zhang, P., Reis, P. A., Dewey, R. E., Boston, R. S., & Fontes, E. P. (2007). Expression profiling on soybean leaves reveals integration of ER- and osmotic-stress pathways. *BMC Genomics*, 8, 431. <https://doi.org/10.1186/1471-2164-8-431>
- Iwata, Y., Fedoroff, N. V., & Koizumi, N. (2008). Arabidopsis bZIP60 is a proteolysis-activated transcription factor involved in the endoplasmic reticulum stress response. *Plant Cell*, 20(11), 3107-3121. <https://doi.org/10.1105/tpc.108.061002>
- Iwata, Y., & Koizumi, N. (2005). Unfolded protein response followed by induction of cell death in cultured tobacco cells treated with tunicamycin. *Planta*, 220, 804-807.
- Jabnoune, M., Secco, D., Lecampion, C., Robaglia, C., Shu, Q., & Poirier, Y. (2013). A rice cis-natural antisense RNA acts as a translational enhancer for its cognate mRNA and contributes to phosphate homeostasis and plant fitness. *The Plant Cell*, 25(10), 4166-4182.
- Jones, A. M., Ecker, J. R., & Chen, J. G. (2003). A reevaluation of the role of the heterotrimeric G protein in coupling light responses in Arabidopsis. *Plant Physiol*, 131(4), 1623-1627. <https://doi.org/10.1104/pp.102.017624>
- Jones, J. D., & Dangl, J. L. (2006). The plant immune system. *Nature*, 444(7117), 323-329. <https://doi.org/10.1038/nature05286>
- Kamauchi, S., Nakatani, H., Nakano, C., & Urade, R. (2005). Gene expression in response to endoplasmic reticulum stress in Arabidopsis thaliana. *The FEBS journal*, 272(13), 3461-3476.
- Katayama, S., Tomaru, Y., Kasukawa, T., Waki, K., Nakanishi, M., Nakamura, M., Nishida, H., Yap, C., Suzuki, M., & Kawai, J. (2005). Antisense transcription in the mammalian transcriptome. *Science*, 309(5740), 1564-1566.
- Katiyar-Agarwal, S., Morgan, R., Dahlbeck, D., Borsani, O., Villegas, A., Jr., Zhu, J. K., Staskawicz, B. J., & Jin, H. (2006). A pathogen-inducible endogenous siRNA in plant immunity. *Proc Natl Acad Sci U S A*, 103(47), 18002-18007. <https://doi.org/10.1073/pnas.0608258103>
- Kaufman, R. J., Scheuner, D., Schröder, M., Shen, X., Lee, K., Liu, C. Y., & Arnold, S. M. (2002). The unfolded protein response in nutrient sensing and differentiation. *Nature reviews Molecular cell biology*, 3(6), 411-421.
- Kim, J.-S., Yamaguchi-Shinozaki, K., & Shinozaki, K. (2018). ER-anchored transcription factors bZIP17 and bZIP28 regulate root elongation. *Plant physiology*, 176(3), 2221-2230.
- Kim, M. G., Da Cunha, L., McFall, A. J., Belkhadir, Y., DebRoy, S., Dangl, J. L., & Mackey, D. (2005). Two *Pseudomonas syringae* type III effectors inhibit RIN4-regulated basal defense in Arabidopsis. *Cell*, 121(5), 749-759.

- Kindgren, P., Ard, R., Ivanov, M., & Marquardt, S. (2018). Transcriptional read-through of the long non-coding RNA SVALKA governs plant cold acclimation. *Nat Commun*, 9(1), 4561. <https://doi.org/10.1038/s41467-018-07010-6>
- Kinkema, M., Fan, W., & Dong, X. (2000). Nuclear localization of NPR1 is required for activation of PR gene expression. *Plant Cell*, 12(12), 2339-2350. <https://doi.org/10.1105/tpc.12.12.2339>
- Koizumi, N., Martinez, I. M., Kimata, Y., Kohno, K., Sano, H., & Chrispeels, M. J. (2001). Molecular characterization of two *Arabidopsis* Ire1 homologs, endoplasmic reticulum-located transmembrane protein kinases. *Plant Physiol*, 127(3), 949-962. <https://www.ncbi.nlm.nih.gov/pubmed/11706177>
- Korner, C. J., Du, X., Vollmer, M. E., & Pajerowska-Mukhtar, K. M. (2015). Endoplasmic Reticulum Stress Signaling in Plant Immunity--At the Crossroad of Life and Death. *Int J Mol Sci*, 16(11), 26582-26598. <https://doi.org/10.3390/ijms161125964>
- Kumar, K., & Chakraborty, S. (2021). Roles of long non-coding RNAs in plant virus interactions. *Journal of Plant Biochemistry and Biotechnology*, 30(4), 684-697. <https://doi.org/10.1007/s13562-021-00697-7>
- Kung, J. T., Colognori, D., & Lee, J. T. (2013). Long noncoding RNAs: past, present, and future. *Genetics*, 193(3), 651-669. <https://doi.org/10.1534/genetics.112.146704>
- Lageix, S., Lanet, E., Pouch-Pélissier, M.-N., Espagnol, M.-C., Robaglia, C., Deragon, J.-M., & Pélassier, T. (2008). Arabidopsis eIF2 $\alpha$  kinase GCN2 is essential for growth in stress conditions and is activated by wounding. *BMC plant biology*, 8(1), 1-9.
- Lai, Y.-S., Stefano, G., Zemelis-Durfee, S., Ruberti, C., Gibbons, L., & Brandizzi, F. (2018). Systemic signaling contributes to the unfolded protein response of the plant endoplasmic reticulum. *Nature Communications*, 9(1), 3918.
- Lam, E. (2004). Controlled cell death, plant survival and development. *Nat Rev Mol Cell Biol*, 5(4), 305-315. <https://doi.org/10.1038/nrm1358>
- Lam, E., Kato, N., & Lawton, M. (2001). Programmed cell death, mitochondria and the plant hypersensitive response. *Nature*, 411(6839), 848-853. <https://doi.org/10.1038/35081184>
- Latham, K. E. (2015). Endoplasmic reticulum stress signaling in mammalian oocytes and embryos: life in balance. *Int Rev Cell Mol Biol*, 316, 227-265. <https://doi.org/10.1016/bs.ircmb.2015.01.005>
- Lee, S. C., Choi, H. W., Hwang, I. S., Choi, D. S., & Hwang, B. K. (2006). Functional roles of the pepper pathogen-induced bZIP transcription factor, CAbZIP1, in enhanced resistance to pathogen infection and environmental stresses. *Planta*, 224(5), 1209-1225. <https://doi.org/10.1007/s00425-006-0302-4>
- Lewis, A., Mitsuya, K., Umlauf, D., Smith, P., Dean, W., Walter, J., Higgins, M., Feil, R., & Reik, W. (2004). Imprinting on distal chromosome 7 in the placenta involves repressive histone methylation independent of DNA methylation. *Nat Genet*, 36(12), 1291-1295. <https://doi.org/10.1038/ng1468>
- Li, M., Zhang, S., Qiu, Y., He, Y., Chen, B., Mao, R., Cui, Y., Zeng, Z., & Chen, M. (2017). Upregulation of miR-665 promotes apoptosis and colitis in inflammatory bowel disease by repressing the endoplasmic reticulum stress components XBP1 and ORMDL3. *Cell Death Dis*, 8(3), e2699. <https://doi.org/10.1038/cddis.2017.76>

- Li, N., Zhang, S.-j., Zhao, Q., Long, Y., Guo, H., Jia, H.-f., Yang, Y.-x., Zhang, H.-y., Ye, X.-f., & Zhang, S.-t. (2018). Overexpression of tobacco GCN2 stimulates multiple physiological changes associated with stress tolerance. *Frontiers in Plant Science*, 9, 725.
- Li, Y., Humbert, S., & Howell, S. H. (2012). ZmbZIP60 mRNA is spliced in maize in response to ER stress. *BMC Research Notes*, 5, 1-11.
- Liu, J., Ding, P., Sun, T., Nitta, Y., Dong, O., Huang, X., Yang, W., Li, X., Botella, J. R., & Zhang, Y. (2013). Heterotrimeric G proteins serve as a converging point in plant defense signaling activated by multiple receptor-like kinases. *Plant Physiol*, 161(4), 2146-2158. <https://doi.org/10.1104/pp.112.212431>
- Liu, J., Jung, C., Xu, J., Wang, H., Deng, S., Bernad, L., Arenas-Huertero, C., & Chua, N. H. (2012). Genome-wide analysis uncovers regulation of long intergenic noncoding RNAs in Arabidopsis. *Plant Cell*, 24(11), 4333-4345. <https://doi.org/10.1105/tpc.112.102855>
- Liu, J.-X., & Howell, S. H. (2010). bZIP28 and NF-Y transcription factors are activated by ER stress and assemble into a transcriptional complex to regulate stress response genes in Arabidopsis. *The Plant Cell*, 22(3), 782-796.
- Liu, J. X., Srivastava, R., Che, P., & Howell, S. H. (2007). Salt stress responses in Arabidopsis utilize a signal transduction pathway related to endoplasmic reticulum stress signaling. *The Plant Journal*, 51(5), 897-909.
- Liu, X., Afrin, T., & Pajerowska-Mukhtar, K. M. (2019). Arabidopsis GCN2 kinase contributes to ABA homeostasis and stomatal immunity. *Commun Biol*, 2, 302. <https://doi.org/10.1038/s42003-019-0544-x>
- Liu, X., Kørner, C. J., Hajdu, D., Guo, T., Ramonell, K. M., Argueso, C. T., & Pajerowska-Mukhtar, K. M. (2015). Arabidopsis thaliana atGCN2 kinase is involved in disease resistance against pathogens with diverse life styles. *International Journal of Phytopathology*, 4(2), 93-104.
- Liu, X., Li, D., Zhang, D., Yin, D., Zhao, Y., Ji, C., Zhao, X., Li, X., He, Q., Chen, R., Hu, S., & Zhu, L. (2018). A novel antisense long noncoding RNA, TWISTED LEAF, maintains leaf blade flattening by regulating its associated sense R2R3-MYB gene in rice. *New Phytol*, 218(2), 774-788. <https://doi.org/10.1111/nph.15023>
- Liu, Y., & Li, J. (2014). Endoplasmic reticulum-mediated protein quality control in Arabidopsis. *Frontiers in Plant Science*, 5, 162.
- Liu, Y., Schiff, M., Czymbek, K., Talloczy, Z., Levine, B., & Dinesh-Kumar, S. P. (2005). Autophagy regulates programmed cell death during the plant innate immune response. *Cell*, 121(4), 567-577. <https://doi.org/10.1016/j.cell.2005.03.007>
- Llorente, F., Alonso-Blanco, C., Sanchez-Rodriguez, C., Jordà, L., & Molina, A. (2005). ERECTA receptor-like kinase and heterotrimeric G protein from Arabidopsis are required for resistance to the necrotrophic fungus *Plectosphaerella cucumerina*. *Plant J*, 43(2), 165-180. <https://doi.org/10.1111/j.1365-313X.2005.02440.x>
- Lu, C., Jeong, D. H., Kulkarni, K., Pillay, M., Nobuta, K., German, R., Thatcher, S. R., Maher, C., Zhang, L., Ware, D., Liu, B., Cao, X., Meyers, B. C., & Green, P. J. (2008). Genome-wide analysis for discovery of rice microRNAs reveals natural

- antisense microRNAs (nat-miRNAs). *Proc Natl Acad Sci U S A*, 105(12), 4951-4956. <https://doi.org/10.1073/pnas.0708743105>
- Lu, S. J., Yang, Z. T., Sun, L., Sun, L., Song, Z. T., & Liu, J. X. (2012). Conservation of IRE1-regulated bZIP74 mRNA unconventional splicing in rice (*Oryza sativa* L.) involved in ER stress responses. *Mol Plant*, 5(2), 504-514.  
<https://doi.org/10.1093/mp/ssr115>
- Lu, T., Zhu, C., Lu, G., Guo, Y., Zhou, Y., Zhang, Z., Zhao, Y., Li, W., Lu, Y., Tang, W., Feng, Q., & Han, B. (2012). Strand-specific RNA-seq reveals widespread occurrence of novel cis-natural antisense transcripts in rice. *BMC Genomics*, 13, 721.  
<https://doi.org/10.1186/1471-2164-13-721>
- Mackey, D., Belkhadir, Y., Alonso, J. M., Ecker, J. R., & Dangl, J. L. (2003). Arabidopsis RIN4 is a target of the type III virulence effector AvrRpt2 and modulates RPS2-mediated resistance. *Cell*, 112(3), 379-389.
- Mackey, D., Holt, B. F., Wiig, A., & Dangl, J. L. (2002). RIN4 interacts with *Pseudomonas syringae* type III effector molecules and is required for RPM1-mediated resistance in Arabidopsis. *Cell*, 108(6), 743-754.
- Marquardt, S., Raitskin, O., Wu, Z., Liu, F., Sun, Q., & Dean, C. (2014). Functional consequences of splicing of the antisense transcript COOLAIR on FLC transcription. *Mol Cell*, 54(1), 156-165.  
<https://doi.org/10.1016/j.molcel.2014.03.026>
- Martinez, I. M., & Chrispeels, M. J. (2003). Genomic analysis of the unfolded protein response in Arabidopsis shows its connection to important cellular processes. *Plant Cell*, 15(2), 561-576. <https://doi.org/10.1105/tpc.007609>
- Mattick, J. S., & Makunin, I. V. (2006). Non-coding RNA. *Hum Mol Genet*, 15 Spec No 1, R17-29. <https://doi.org/10.1093/hmg/ddl046>
- Mattick, J. S., & Rinn, J. L. (2015). Discovery and annotation of long noncoding RNAs. *Nat Struct Mol Biol*, 22(1), 5-7. <https://doi.org/10.1038/nsmb.2942>
- Maurel, M., Chevet, E., Tavernier, J., & Gerlo, S. (2014). Getting RIDD of RNA: IRE1 in cell fate regulation. *Trends in biochemical sciences*, 39(5), 245-254.
- Maurel, M., Dejeans, N., Taouji, S., Chevet, E., & Grosset, C. F. (2013). MicroRNA-1291-mediated silencing of IRE1alpha enhances Glypican-3 expression. *RNA*, 19(6), 778-788. <https://doi.org/10.1261/rna.036483.112>
- McHale, L., Tan, X., Koehl, P., & Michelmore, R. W. (2006). Plant NBS-LRR proteins: adaptable guards. *Genome Biol*, 7(4), 212. <https://doi.org/10.1186/gb-2006-7-4-212>
- Minina, E. A., Coll, N. S., Tuominen, H., & Bozhkov, P. V. (2017). Metacaspases versus caspases in development and cell fate regulation. *Cell Death Differ*, 24(8), 1314-1325. <https://doi.org/10.1038/cdd.2017.18>
- Minina, E. A., Staal, J., Alvarez, V. E., Berges, J. A., Berman-Frank, I., Beyaert, R., Bidle, K. D., Bornancin, F., Casanova, M., Cazzulo, J. J., Choi, C. J., Coll, N. S., Dixit, V. M., Dolinar, M., Fasel, N., Funk, C., Gallois, P., Gevaert, K., Gutierrez-Beltran, E., . . . Bozhkov, P. V. (2020). Classification and Nomenclature of Metacaspases and Paracaspases: No More Confusion with Caspases. *Mol Cell*, 77(5), 927-929.  
<https://doi.org/10.1016/j.molcel.2019.12.020>

- Mishiba, K.-i., Iwata, Y., Mochizuki, T., Matsumura, A., Nishioka, N., Hirata, R., & Koizumi, N. (2019). Unfolded protein-independent IRE1 activation contributes to multifaceted developmental processes in Arabidopsis. *Life science alliance*, 2(5).
- Mishiba, K.-i., Nagashima, Y., Suzuki, E., Hayashi, N., Ogata, Y., Shimada, Y., & Koizumi, N. (2013). Defects in IRE1 enhance cell death and fail to degrade mRNAs encoding secretory pathway proteins in the Arabidopsis unfolded protein response. *Proceedings of the National Academy of Sciences*, 110(14), 5713-5718.
- Mishina, T. E., & Zeier, J. (2007). Pathogen-associated molecular pattern recognition rather than development of tissue necrosis contributes to bacterial induction of systemic acquired resistance in Arabidopsis. *The Plant Journal*, 50(3), 500-513.
- Mittler, R., Shulaev, V., & Lam, E. (1995). Coordinated Activation of Programmed Cell Death and Defense Mechanisms in Transgenic Tobacco Plants Expressing a Bacterial Proton Pump. *Plant Cell*, 7(1), 29-42. <https://doi.org/10.1105/tpc.7.1.29>
- Monaghan, J., & Li, X. (2010). The HEAT repeat protein ILITYHIA is required for plant immunity. *Plant and cell physiology*, 51(5), 742-753.
- Moore, J. W., Loake, G. J., & Spoel, S. H. (2011). Transcription dynamics in plant immunity. *The Plant Cell*, 23(8), 2809-2820.
- Moreno, A. A., Mukhtar, M. S., Blanco, F., Boatwright, J. L., Moreno, I., Jordan, M. R., Chen, Y., Brandizzi, F., Dong, X., Orellana, A., & Pajerowska-Mukhtar, K. M. (2012). IRE1/bZIP60-mediated unfolded protein response plays distinct roles in plant immunity and abiotic stress responses. *PLoS One*, 7(2), e31944. <https://doi.org/10.1371/journal.pone.0031944>
- Mori, K. (2000). Tripartite management of unfolded proteins in the endoplasmic reticulum. *Cell*, 101(5), 451-454.
- Mou, Z., Fan, W., & Dong, X. (2003). Inducers of plant systemic acquired resistance regulate NPR1 function through redox changes. *Cell*, 113(7), 935-944. [https://doi.org/10.1016/s0092-8674\(03\)00429-x](https://doi.org/10.1016/s0092-8674(03)00429-x)
- Necsulea, A., Soumillon, M., Warnefors, M., Liechti, A., Daish, T., Zeller, U., Baker, J. C., Grutzner, F., & Kaessmann, H. (2014). The evolution of lncRNA repertoires and expression patterns in tetrapods. *Nature*, 505(7485), 635-640. <https://doi.org/10.1038/nature12943>
- Nimchuk, Z., Eulgem, T., Holt, B. F., 3rd, & Dangl, J. L. (2003). Recognition and response in the plant immune system. *Annu Rev Genet*, 37, 579-609. <https://doi.org/10.1146/annurev.genet.37.110801.142628>
- Okamoto, M., Tatematsu, K., Matsui, A., Morosawa, T., Ishida, J., Tanaka, M., Endo, T. A., Mochizuki, Y., Toyoda, T., Kamiya, Y., Shinozaki, K., Nambara, E., & Seki, M. (2010). Genome-wide analysis of endogenous abscisic acid-mediated transcription in dry and imbibed seeds of Arabidopsis using tiling arrays. *Plant J*, 62(1), 39-51. <https://doi.org/10.1111/j.1365-313X.2010.04135.x>
- Oono, Y., Yazawa, T., Kanamori, H., Sasaki, H., Mori, S., & Matsumoto, T. (2017). Genome-wide analysis of rice cis-natural antisense transcription under cadmium exposure using strand-specific RNA-Seq. *BMC Genomics*, 18(1), 761. <https://doi.org/10.1186/s12864-017-4108-5>

- Pajerowska-Mukhtar, K. M., Emerine, D. K., & Mukhtar, M. S. (2013). Tell me more: roles of NPRs in plant immunity. *Trends Plant Sci*, 18(7), 402-411.  
<https://doi.org/10.1016/j.tplants.2013.04.004>
- Pajerowska-Mukhtar, K. M., Wang, W., Tada, Y., Oka, N., Tucker, C. L., Fonseca, J. P., & Dong, X. (2012). The HSF-like transcription factor TBF1 is a major molecular switch for plant growth-to-defense transition. *Current Biology*, 22(2), 103-112.
- Patel, S., & Dinesh-Kumar, S. P. (2008). Arabidopsis ATG6 is required to limit the pathogen-associated cell death response. *Autophagy*, 4(1), 20-27.  
<https://doi.org/10.4161/auto.5056>
- Peters, N. T., Rohrbach, J. A., Zalewski, B. A., Byrkett, C. M., & Vaughn, J. C. (2003). RNA editing and regulation of Drosophila 4f-rnp expression by sas-10 antisense readthrough mRNA transcripts. *RNA*, 9(6), 698-710.  
<https://doi.org/10.1261/rna.2120703>
- Pollier, J., Moses, T., González-Guzmán, M., De Geyter, N., Lippens, S., Bossche, R. V., Marhavý, P., Kremer, A., Morreel, K., & Guérin, C. J. (2013). The protein quality control system manages plant defence compound synthesis. *Nature*, 504(7478), 148-152.
- Ponting, C. P., Oliver, P. L., & Reik, W. (2009). Evolution and functions of long noncoding RNAs. *Cell*, 136(4), 629-641. <https://doi.org/10.1016/j.cell.2009.02.006>
- Prescott, E. M., & Proudfoot, N. J. (2002). Transcriptional collision between convergent genes in budding yeast. *Proc Natl Acad Sci U S A*, 99(13), 8796-8801.  
<https://doi.org/10.1073/pnas.132270899>
- Rai, M. I., Alam, M., Lightfoot, D. A., Gurha, P., & Afzal, A. J. (2019). Classification and experimental identification of plant long non-coding RNAs. *Genomics*, 111(5), 997-1005. <https://doi.org/10.1016/j.ygeno.2018.04.014>
- Rasmussen, S., Barah, P., Suarez-Rodriguez, M. C., Bressendorff, S., Friis, P., Costantino, P., Bones, A. M., Nielsen, H. B., & Mundy, J. (2013). Transcriptome responses to combinations of stresses in Arabidopsis. *Plant physiology*, 161(4), 1783-1794.
- Rutkowski, D. T., & Kaufman, R. J. (2003). All roads lead to ATF4. *Developmental cell*, 4(4), 442-444.
- Salvesen, G. S., Hempel, A., & Coll, N. S. (2016). Protease signaling in animal and plant-regulated cell death. *FEBS J*, 283(14), 2577-2598.  
<https://doi.org/10.1111/febs.13616>
- Schröder, M., & Kaufman, R. J. (2005). The mammalian unfolded protein response. *Annu. Rev. Biochem.*, 74, 739-789.
- Seo, J. S., Sun, H. X., Park, B. S., Huang, C. H., Yeh, S. D., Jung, C., & Chua, N. H. (2017). ELF18-INDUCED LONG-NONCODING RNA Associates with Mediator to Enhance Expression of Innate Immune Response Genes in Arabidopsis. *Plant Cell*, 29(5), 1024-1038. <https://doi.org/10.1105/tpc.16.00886>
- Shafiq, S., Li, J., & Sun, Q. (2016). Functions of plants long non-coding RNAs. *Biochim Biophys Acta*, 1859(1), 155-162. <https://doi.org/10.1016/j.bbagr.2015.06.009>
- Siegel, T. N., Hon, C. C., Zhang, Q., Lopez-Rubio, J. J., Scheidig-Benatar, C., Martins, R. M., Sismeiro, O., Coppee, J. Y., & Scherf, A. (2014). Strand-specific RNA-Seq reveals widespread and developmentally regulated transcription of natural antisense

- transcripts in *Plasmodium falciparum*. *BMC Genomics*, 15(1), 150.  
<https://doi.org/10.1186/1471-2164-15-150>
- Silva, P. A., Silva, J. C. F., Caetano, H. D., Machado, J. P. B., Mendes, G. C., Reis, P. A., Brustolini, O. J., Dal-Bianco, M., & Fontes, E. P. (2015). Comprehensive analysis of the endoplasmic reticulum stress response in the soybean genome: conserved and plant-specific features. *BMC Genomics*, 16, 1-20.
- Sitia, R., & Braakman, I. (2003). Quality control in the endoplasmic reticulum protein factory. *Nature*, 426(6968), 891-894.
- Spoel, S. H., Mou, Z., Tada, Y., Spivey, N. W., Genschik, P., & Dong, X. (2009). Proteasome-mediated turnover of the transcription coactivator NPR1 plays dual roles in regulating plant immunity. *Cell*, 137(5), 860-872.
- Srivastava, R., Deng, Y., & Howell, S. H. (2014). Stress sensing in plants by an ER stress sensor/transducer, bZIP28. *Frontiers in Plant Science*, 5, 59.
- Srivastava, R., Deng, Y., Shah, S., Rao, A. G., & Howell, S. H. (2013). BINDING PROTEIN is a master regulator of the endoplasmic reticulum stress sensor/transducer bZIP28 in Arabidopsis. *The Plant Cell*, 25(4), 1416-1429.
- Stefano, G., Renna, L., Lai, Y., Slabaugh, E., Mannino, N., Buono, R. A., Otegui, M. S., & Brandizzi, F. (2015). ER network homeostasis is critical for plant endosome streaming and endocytosis. *Cell Discovery*, 1(1), 1-16.
- Sueldo, D. J., & van der Hoorn, R. A. L. (2017). Plant life needs cell death, but does plant cell death need Cys proteases? *FEBS J*, 284(10), 1577-1585.  
<https://doi.org/10.1111/febs.14034>
- Sun, Q., Csorba, T., Skourtis-Stathaki, K., Proudfoot, N. J., & Dean, C. (2013). R-loop stabilization represses antisense transcription at the Arabidopsis FLC locus. *Science*, 340(6132), 619-621. <https://doi.org/10.1126/science.1234848>
- Sun, X., Zheng, H., Li, J., Liu, L., Zhang, X., & Sui, N. (2020). Comparative Transcriptome Analysis Reveals New lncRNAs Responding to Salt Stress in Sweet Sorghum. *Front Bioeng Biotechnol*, 8, 331. <https://doi.org/10.3389/fbioe.2020.00331>
- Sun, Y., Zhang, H., Fan, M., He, Y., & Guo, P. (2020). Genome-wide identification of long non-coding RNAs and circular RNAs reveal their ceRNA networks in response to cucumber green mottle mosaic virus infection in watermelon. *Arch Virol*, 165(5), 1177-1190. <https://doi.org/10.1007/s00705-020-04589-4>
- Swiezewski, S., Liu, F., Magusin, A., & Dean, C. (2009). Cold-induced silencing by long antisense transcripts of an Arabidopsis Polycomb target. *Nature*, 462(7274), 799-802. <https://doi.org/10.1038/nature08618>
- Thomma, B. P., Nurnberger, T., & Joosten, M. H. (2011). Of PAMPs and effectors: the blurred PTI-ETI dichotomy. *Plant Cell*, 23(1), 4-15.  
<https://doi.org/10.1105/tpc.110.082602>
- Trusov, Y., Rookes, J. E., Chakravorty, D., Armour, D., Schenk, P. M., & Botella, J. R. (2006). Heterotrimeric G proteins facilitate Arabidopsis resistance to necrotrophic pathogens and are involved in jasmonate signaling. *Plant Physiol*, 140(1), 210-220. <https://doi.org/10.1104/pp.105.069625>

- Tsiatsiani, L., Van Breusegem, F., Gallois, P., Zavialov, A., Lam, E., & Bozhkov, P. V. (2011). Metacaspases. *Cell Death Differ*, 18(8), 1279-1288.  
<https://doi.org/10.1038/cdd.2011.66>
- Ullah, H., Chen, J. G., Temple, B., Boyes, D. C., Alonso, J. M., Davis, K. R., Ecker, J. R., & Jones, A. M. (2003). The beta-subunit of the Arabidopsis G protein negatively regulates auxin-induced cell division and affects multiple developmental processes. *Plant Cell*, 15(2), 393-409. <https://doi.org/10.1105/tpc.006148>
- Urano, D., & Jones, A. M. (2014). Heterotrimeric G protein-coupled signaling in plants. *Annu Rev Plant Biol*, 65, 365-384. <https://doi.org/10.1146/annurev-arplant-050213-040133>
- Uren, A. G., O'Rourke, K., Aravind, L. A., Pisabarro, M. T., Seshagiri, S., Koonin, E. V., & Dixit, V. M. (2000). Identification of paracaspases and metacaspases: two ancient families of caspase-like proteins, one of which plays a key role in MALT lymphoma. *Mol Cell*, 6(4), 961-967. [https://doi.org/10.1016/s1097-2765\(00\)00094-0](https://doi.org/10.1016/s1097-2765(00)00094-0)
- Urquiaga, M. C. O., Thiebaut, F., Hemerly, A. S., & Ferreira, P. C. G. (2020). From Trash to Luxury: The Potential Role of Plant LncRNA in DNA Methylation During Abiotic Stress. *Front Plant Sci*, 11, 603246. <https://doi.org/10.3389/fpls.2020.603246>
- van Butselaar, T., & Van den Ackerveken, G. (2020). Salicylic Acid Steers the Growth-Immunity Tradeoff. *Trends Plant Sci*, 25(6), 566-576.  
<https://doi.org/10.1016/j.tplants.2020.02.002>
- Vercammen, D., Declercq, W., Vandenameele, P., & Van Breusegem, F. (2007). Are metacaspases caspases? *J Cell Biol*, 179(3), 375-380.  
<https://doi.org/10.1083/jcb.200705193>
- Verchot, J., & Pajerowska-Mukhtar, K. M. (2021). UPR signaling at the nexus of plant viral, bacterial, and fungal defenses. *Current Opinion in Virology*, 47, 9-17.
- Vitale, A., & Ceriotti, A. (2004). Protein quality control mechanisms and protein storage in the endoplasmic reticulum. A conflict of interests? *Plant Physiol*, 136(3), 3420-3426. <https://doi.org/10.1104/pp.104.050351>
- Vitale, A., & Denecke, J. (1999). The endoplasmic reticulum—gateway of the secretory pathway. *The Plant Cell*, 11(4), 615-628.
- Wakasa, Y., Hayashi, S., Ozawa, K., & Takaiwa, F. (2012). Multiple roles of the ER stress sensor IRE1 demonstrated by gene targeting in rice. *Scientific Reports*, 2(1), 1-6.
- Walter, P., & Ron, D. (2011). The unfolded protein response: from stress pathway to homeostatic regulation. *Science*, 334(6059), 1081-1086.
- Wang, D., Weaver, N. D., Kesarwani, M., & Dong, X. (2005). Induction of protein secretory pathway is required for systemic acquired resistance. *Science*, 308(5724), 1036-1040.
- Wang, H., Chung, P. J., Liu, J., Jang, I. C., Kean, M. J., Xu, J., & Chua, N. H. (2014). Genome-wide identification of long noncoding natural antisense transcripts and their responses to light in Arabidopsis. *Genome Res*, 24(3), 444-453.  
<https://doi.org/10.1101/gr.165555.113>
- Wang, J., Yu, W., Yang, Y., Li, X., Chen, T., Liu, T., Ma, N., Yang, X., Liu, R., & Zhang, B. (2015). Genome-wide analysis of tomato long non-coding RNAs and

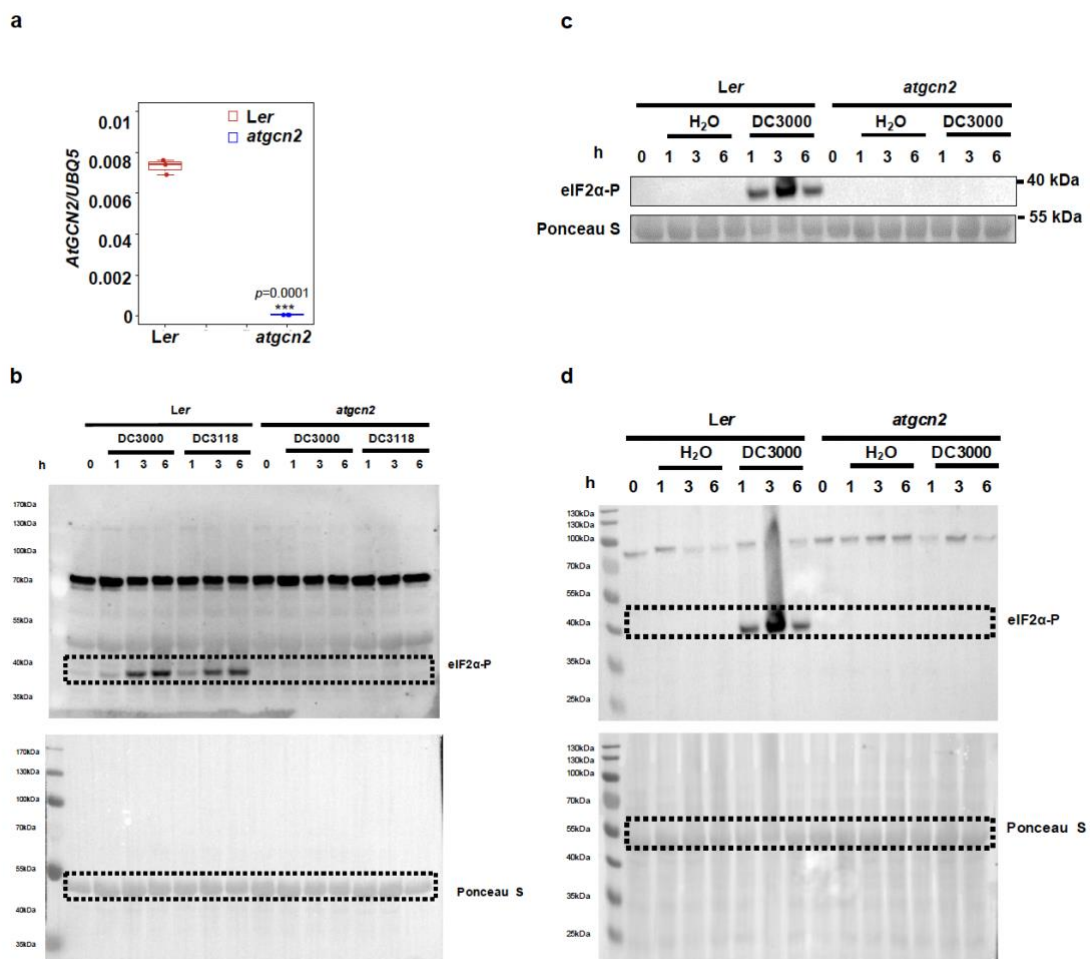
- identification as endogenous target mimic for microRNA in response to TYLCV infection. *Sci Rep*, 5, 16946. <https://doi.org/10.1038/srep16946>
- Wang, Y., Fan, X., Lin, F., He, G., Terzaghi, W., Zhu, D., & Deng, X. W. (2014). Arabidopsis noncoding RNA mediates control of photomorphogenesis by red light. *Proc Natl Acad Sci U S A*, 111(28), 10359-10364. <https://doi.org/10.1073/pnas.1409457111>
- Wang, Y., Li, J., Hou, S., Wang, X., Li, Y., Ren, D., Chen, S., Tang, X., & Zhou, J.-M. (2010). A *Pseudomonas syringae* ADP-ribosyltransferase inhibits Arabidopsis mitogen-activated protein kinase kinases. *The Plant Cell*, 22(6), 2033-2044.
- Wang, Z., Liu, Y., Li, L., Li, D., Zhang, Q., Guo, Y., Wang, S., Zhong, C., & Huang, H. (2017). Whole transcriptome sequencing of *Pseudomonas syringae* pv. actinidiae-infected kiwifruit plants reveals species-specific interaction between long non-coding RNA and coding genes. *Sci Rep*, 7(1), 4910. <https://doi.org/10.1038/s41598-017-05377-y>
- Williams, B., Verchot, J., & Dickman, M. B. (2014). When supply does not meet demand-ER stress and plant programmed cell death. *Frontiers in plant science*, 5, 211.
- Wilusz, J. E., Sunwoo, H., & Spector, D. L. (2009). Long noncoding RNAs: functional surprises from the RNA world. *Genes Dev*, 23(13), 1494-1504. <https://doi.org/10.1101/gad.1800909>
- Wu, H., Ng, B. S., & Thibault, G. (2014). Endoplasmic reticulum stress response in yeast and humans. *Biosci Rep*, 34(4). <https://doi.org/10.1042/BSR20140058>
- Wunderlich, M., Gross-Hardt, R., & Schoffl, F. (2014). Heat shock factor HSFB2a involved in gametophyte development of *Arabidopsis thaliana* and its expression is controlled by a heat-inducible long non-coding antisense RNA. *Plant Mol Biol*, 85(6), 541-550. <https://doi.org/10.1007/s11103-014-0202-0>
- Xiang, T., Zong, N., Zou, Y., Wu, Y., Zhang, J., Xing, W., Li, Y., Tang, X., Zhu, L., & Chai, J. (2008). *Pseudomonas syringae* effector AvrPto blocks innate immunity by targeting receptor kinases. *Current biology*, 18(1), 74-80.
- Xin, M., Wang, Y., Yao, Y., Song, N., Hu, Z., Qin, D., Xie, C., Peng, H., Ni, Z., & Sun, Q. (2011). Identification and characterization of wheat long non-protein coding RNAs responsive to powdery mildew infection and heat stress by using microarray analysis and SBS sequencing. *BMC Plant Biol*, 11, 61. <https://doi.org/10.1186/1471-2229-11-61>
- Xu, C., Bailly-Maitre, B., & Reed, J. C. (2005). Endoplasmic reticulum stress: cell life and death decisions. *The Journal of clinical investigation*, 115(10), 2656-2664.
- Xu, J., Wang, Q., Freeling, M., Zhang, X., Xu, Y., Mao, Y., Tang, X., Wu, F., Lan, H., Cao, M., Rong, T., Lisch, D., & Lu, Y. (2017). Natural antisense transcripts are significantly involved in regulation of drought stress in maize. *Nucleic Acids Res*, 45(9), 5126-5141. <https://doi.org/10.1093/nar/gkx085>
- Xu, Z., Song, N., Ma, L., & Wu, J. (2019). IRE1-bZIP60 pathway is required for Nicotiana attenuata resistance to fungal pathogen *Alternaria alternata*. *Frontiers in Plant Science*, 10, 263.
- Yassour, M., Pfiffner, J., Levin, J. Z., Adiconis, X., Gnirke, A., Nusbaum, C., Thompson, D. A., Friedman, N., & Regev, A. (2010). Strand-specific RNA sequencing reveals

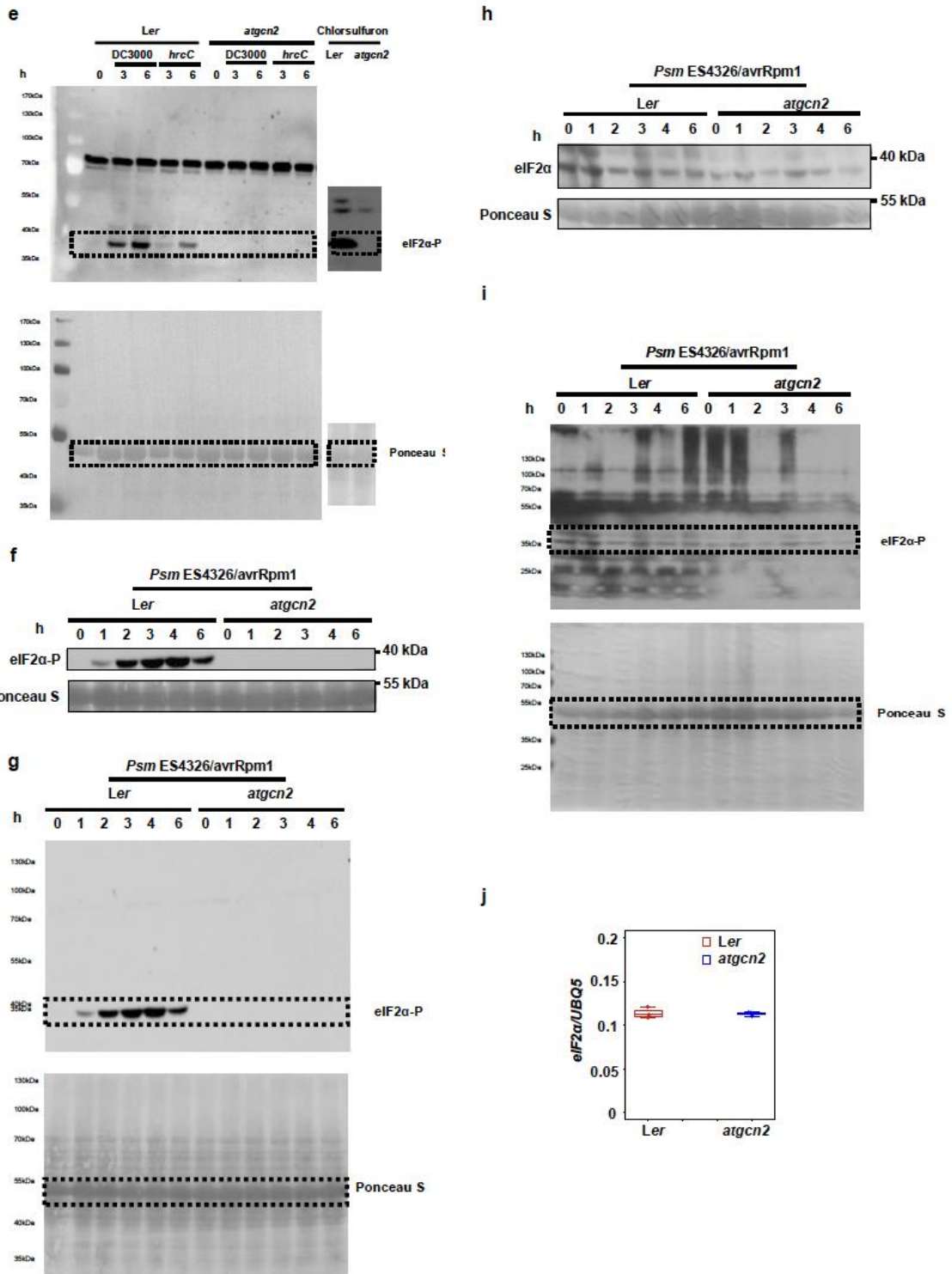
- extensive regulated long antisense transcripts that are conserved across yeast species. *Genome Biol*, 11(8), R87. <https://doi.org/10.1186/gb-2010-11-8-r87>
- Ye, C., Dickman, M. B., Whitham, S. A., Payton, M., & Verchot, J. (2011). The unfolded protein response is triggered by a plant viral movement protein. *Plant Physiol*, 156(2), 741-755. <https://doi.org/10.1104/pp.111.174110>
- Yu, X., Yang, J., Li, X., Liu, X., Sun, C., Wu, F., & He, Y. (2013). Global analysis of cis-natural antisense transcripts and their heat-responsive nat-siRNAs in *Brassica rapa*. *BMC Plant Biol*, 13, 208. <https://doi.org/10.1186/1471-2229-13-208>
- Yu, Y., Zhou, Y. F., Feng, Y. Z., He, H., Lian, J. P., Yang, Y. W., Lei, M. Q., Zhang, Y. C., & Chen, Y. Q. (2020). Transcriptional landscape of pathogen-responsive lncRNAs in rice unveils the role of ALEX1 in jasmonate pathway and disease resistance. *Plant Biotechnol J*, 18(3), 679-690. <https://doi.org/10.1111/pbi.13234>
- Zhang, H., Chen, X., Wang, C., Xu, Z., Wang, Y., Liu, X., Kang, Z., & Ji, W. (2013). Long non-coding genes implicated in response to stripe rust pathogen stress in wheat (*Triticum aestivum* L.). *Mol Biol Rep*, 40(11), 6245-6253. <https://doi.org/10.1007/s11033-013-2736-7>
- Zhang, H., Hu, W., Hao, J., Lv, S., Wang, C., Tong, W., Wang, Y., Wang, Y., Liu, X., & Ji, W. (2016). Genome-wide identification and functional prediction of novel and fungi-responsive lincRNAs in *Triticum aestivum*. *BMC Genomics*, 17, 238. <https://doi.org/10.1186/s12864-016-2570-0>
- Zhang, J., Shao, F., Li, Y., Cui, H., Chen, L., Li, H., Zou, Y., Long, C., Lan, L., & Chai, J. (2007). A *Pseudomonas syringae* effector inactivates MAPKs to suppress PAMP-induced immunity in plants. *Cell host & microbe*, 1(3), 175-185.
- Zhang, L., Hu, G., Cheng, Y., & Huang, J. (2008). Heterotrimeric G protein alpha and beta subunits antagonistically modulate stomatal density in *Arabidopsis thaliana*. *Dev Biol*, 324(1), 68-75. <https://doi.org/10.1016/j.ydbio.2008.09.008>
- Zhang, S. S., Yang, H., Ding, L., Song, Z. T., Ma, H., Chang, F., & Liu, J. X. (2017). Tissue-Specific Transcriptomics Reveals an Important Role of the Unfolded Protein Response in Maintaining Fertility upon Heat Stress in *Arabidopsis*. *Plant Cell*, 29(5), 1007-1023. <https://doi.org/10.1105/tpc.16.00916>
- Zhang, W., Corwin, J. A., Copeland, D., Feusier, J., Eshbaugh, R., Chen, F., Atwell, S., & Kliebenstein, D. J. (2017). Plastic Transcriptomes Stabilize Immunity to Pathogen Diversity: The Jasmonic Acid and Salicylic Acid Networks within the *Arabidopsis*/Botrytis Pathosystem. *Plant Cell*, 29(11), 2727-2752. <https://doi.org/10.1105/tpc.17.00348>
- Zhao, L., Wang, J., Li, Y., Song, T., Wu, Y., Fang, S., Bu, D., Li, H., Sun, L., Pei, D., Zheng, Y., Huang, J., Xu, M., Chen, R., Zhao, Y., & He, S. (2021). NONCODEV6: an updated database dedicated to long non-coding RNA annotation in both animals and plants. *Nucleic Acids Res*, 49(D1), D165-D171. <https://doi.org/10.1093/nar/gkaa1046>
- Zhao, X., Li, J., Lian, B., Gu, H., Li, Y., & Qi, Y. (2018). Global identification of *Arabidopsis* lncRNAs reveals the regulation of MAF4 by a natural antisense RNA. *Nat Commun*, 9(1), 5056. <https://doi.org/10.1038/s41467-018-07500-7>

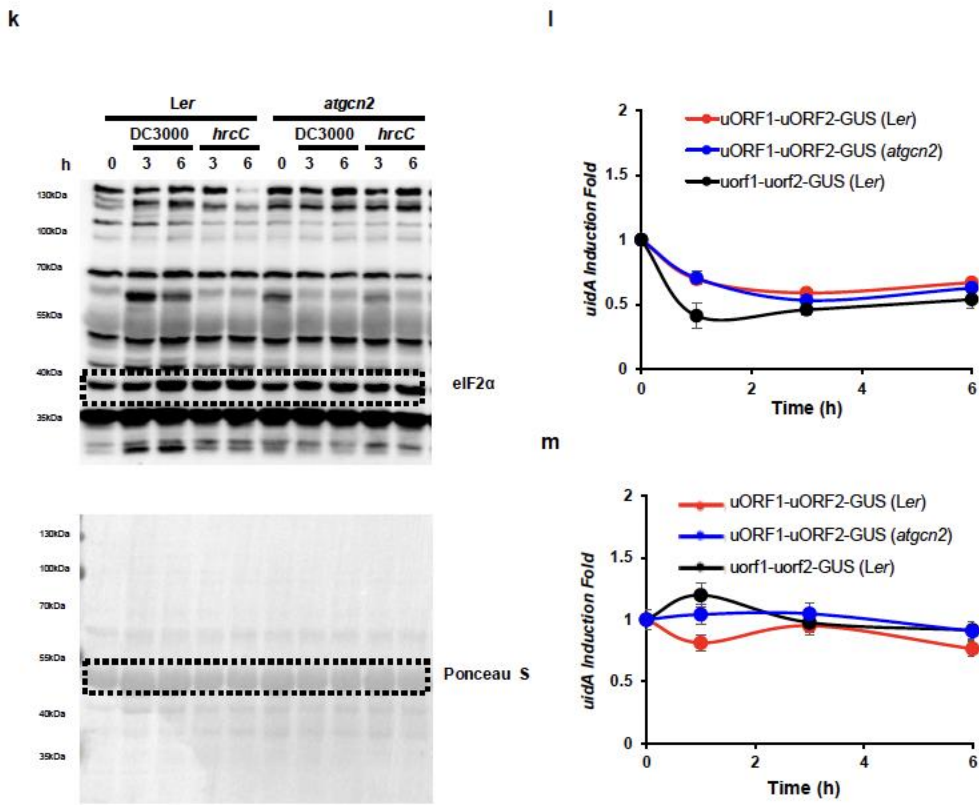
- Zhu, Q. H., Stephen, S., Taylor, J., Helliwell, C. A., & Wang, M. B. (2014). Long noncoding RNAs responsive to *Fusarium oxysporum* infection in *Arabidopsis thaliana*. *New Phytol*, 201(2), 574-584. <https://doi.org/10.1111/nph.12537>
- Zipfel, C. (2014). Plant pattern-recognition receptors. *Trends Immunol*, 35(7), 345-351. <https://doi.org/10.1016/j.it.2014.05.004>
- Zipfel, C., Kunze, G., Chinchilla, D., Caniard, A., Jones, J. D., Boller, T., & Felix, G. (2006). Perception of the bacterial PAMP EF-Tu by the receptor EFR restricts Agrobacterium-mediated transformation. *Cell*, 125(4), 749-760.
- Zuppini, A., Navazio, L., & Mariani, P. (2004). Endoplasmic reticulum stress-induced programmed cell death in soybean cells. *Journal of cell science*, 117(12), 2591-2598.

**APPENDIX A**  
**SUPPLEMENTAL FIGURES**

CHAPTER 2 ARABIDOPSIS GCN2 KINASE CONTRIBUTES TO ABA  
HOMEOSTASIS AND STOMATAL IMMUNITY



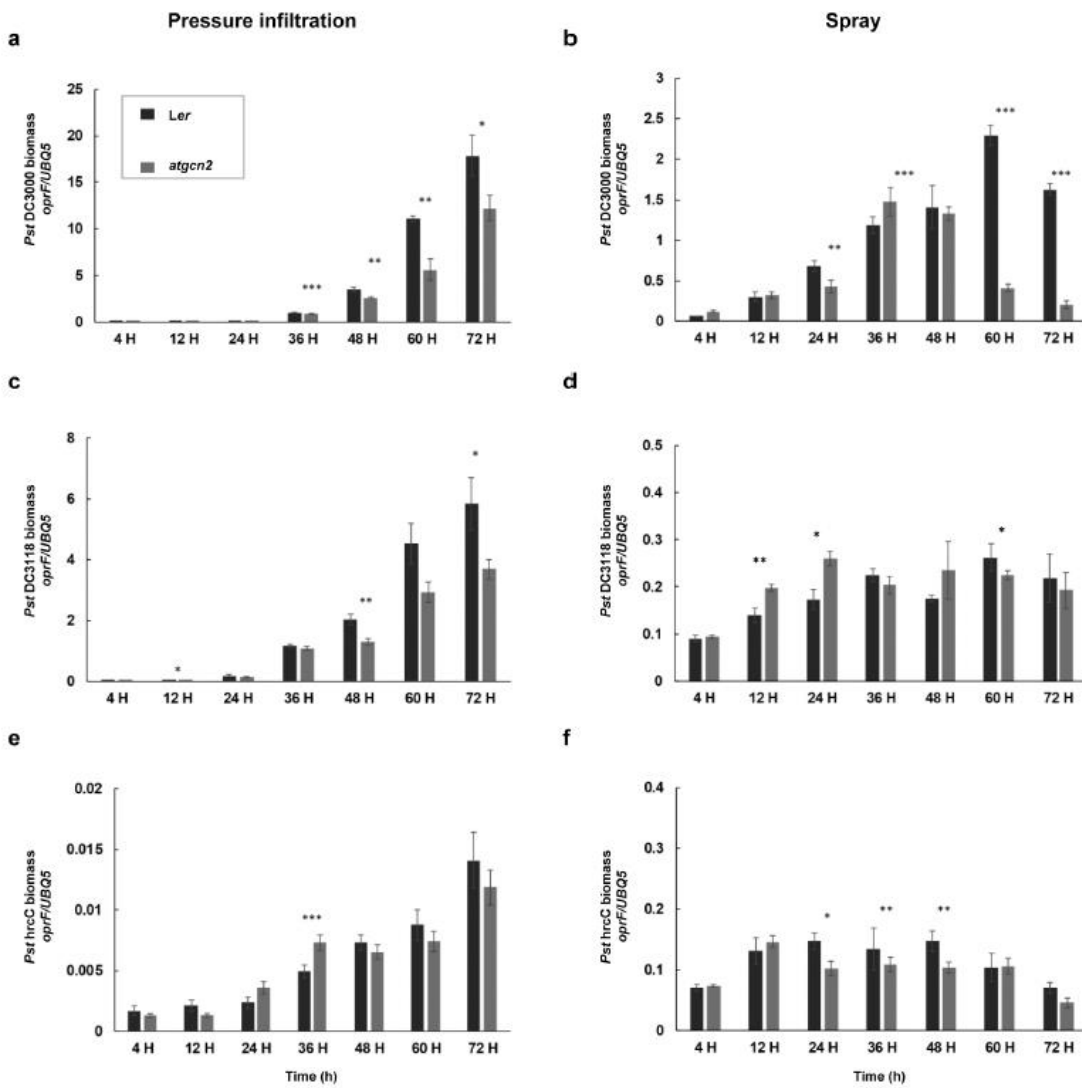




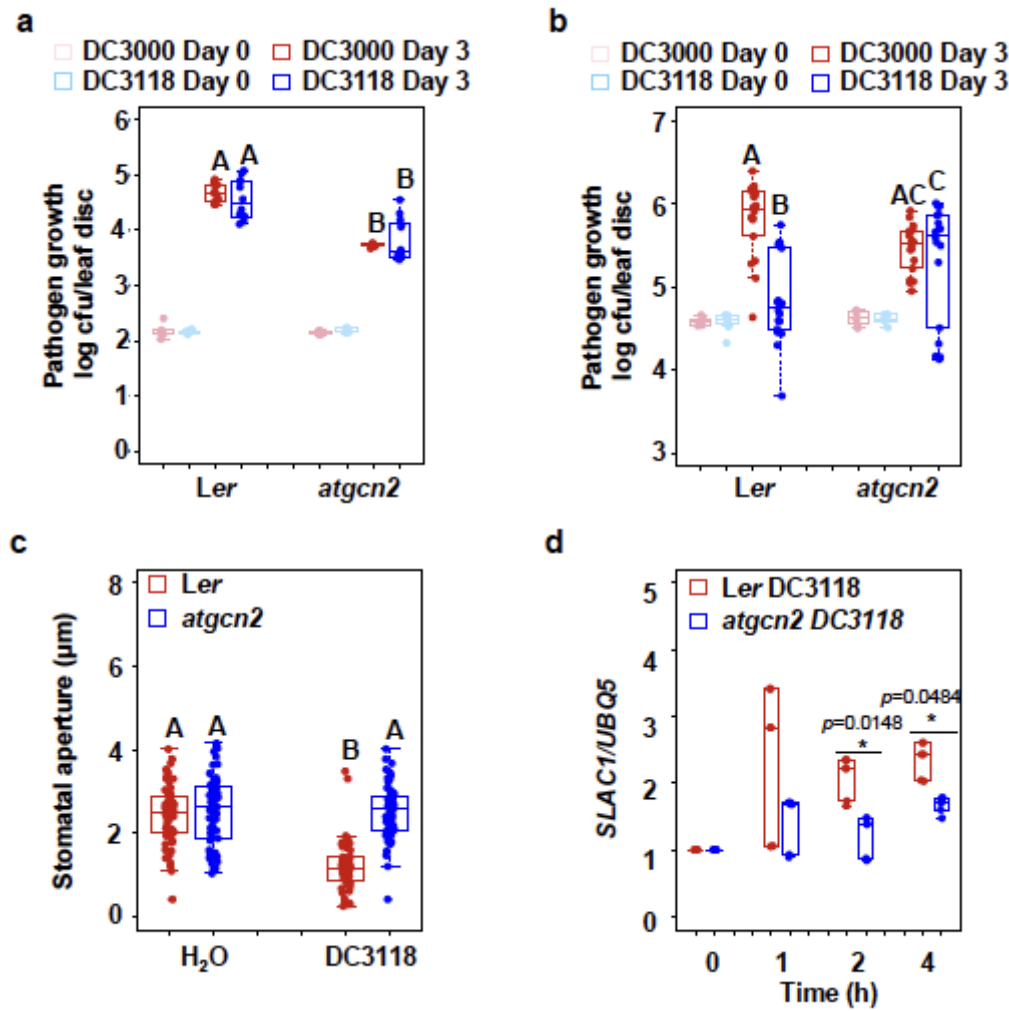
Supplementary Figure 1. AtGCN2 is essential for pathogen-triggered eIF2 $\alpha$  phosphorylation without affecting TBF1 transcript accumulation. a. Transcript accumulation of AtGCN2 was measured in four-week-old plants by real-time RT-PCR. The box plots extend from the 25th to 75th percentiles and the whiskers extend from the minimum to the maximum level. Median values are plotted in the box with data generated from three independent biological replicates, each of them representing means of two technical replicates. Statistical analysis was performed with Student's t-test, p-value is listed. b. Detection of phosphorylated form of eIF2 $\alpha$  in the samples prepared from two-week-old plants treated with Pst DC3000 or Pst DC3118 (OD600nm = 0.02) at the indicated time points in hours (h) (full blots for Fig. 1a). Phosphorylation state specific (S51) anti-human eIF2 $\alpha$  antibody was used. Ponceau S staining shows loading

amounts. c. Detection of phosphorylated form of eIF2 $\alpha$  in the samples prepared from two-week-old plants treated with Pst DC3000 (OD600nm = 0.02) or control H<sub>2</sub>O at the indicated time points in hours (h). Phosphorylation state specific (S51) anti-human eIF2 $\alpha$  antibody was used. Ponceau S staining was used to determine loading. d. Full blots for Supplementary fig. 1c. e. Detection of phosphorylated form of eIF2 $\alpha$  in the samples prepared from two-week-old plants treated with Pst DC3000 or Pst hrcC (OD600nm = 0.02) at the indicated time points in hours (h) (full blots for Fig. 1b). Phosphorylation state-specific (S51) anti-human eIF2 $\alpha$  antibody was used. Ponceau S staining shows loading amounts. f. Detection of phosphorylated form of eIF2 $\alpha$  in the samples prepared from two- week-old plants treated with Psm ES4326/avrRpm1 (OD600nm = 0.02) at the indicated time points in hours (h). Phosphorylation state-specific (S51) anti-human eIF2 $\alpha$  antibody was used. Ponceau S staining was used to determine loading. g. Full blots for Supplementary fig. 1f. h. Time course analysis of total eIF2 $\alpha$  protein accumulation in two- week-old plants upon Psm ES4326/avrRpm1 (OD600nm = 0.02) challenge. Time points are shown in hours (h). Ponceau S staining was used to determine loading. i. Full blots for Supplementary fig. 1h. j. Transcript accumulation of eIF2 $\alpha$  was measured in four-week- old plants by real-time RT-PCR. The box plots extends from the 25th to 75th percentiles and the whiskers extend from the minimum to the maximum level. Median values are plotted in the box with data generated from three independent biological replicates, each of them represented as means of two technical replicates. Statistical analysis was performed with Student's t-test and no significant difference was detected. k. Time course total eIF2 $\alpha$  protein accumulation in two-week-old plants upon Pst DC3000 or Pst hrcC (OD600nm = 0.02) challenge. Time points are shown in hours (h)

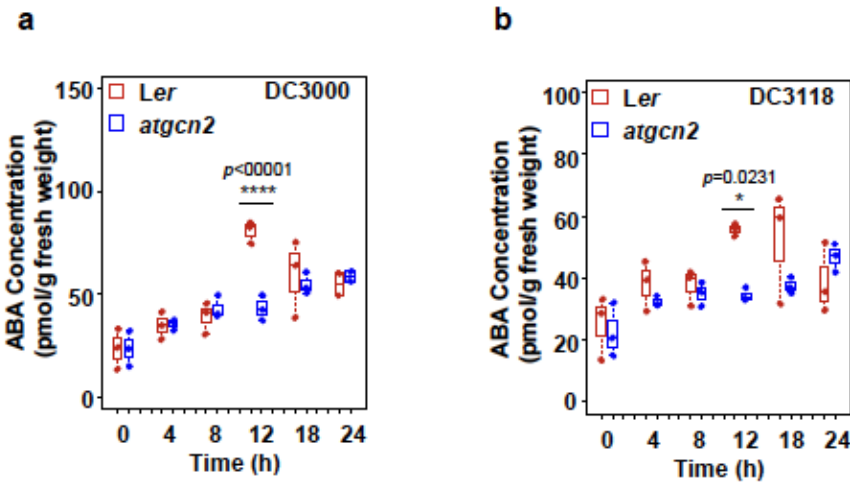
(full blots for Fig. 1c). Ponceau S staining shows loading amounts. l. Transcript accumulation of iudA (encoding the GUS reporter) was measured by real-time RT-PCR in four-week-old transgenic T3 plants uORF1-uORF2-GUS (Ler), uorf1-uorf2-GUS (Ler) and uORF1-uORF2-GUS (atgcn2) treated with Pst DC3000 (OD<sub>600nm</sub> = 0.02), sampled at indicated time points. Data represent the mean and standard error of three independent biological replicates. m. Transcript accumulation of iudA (encoding the GUS reporter) was measured by real- time RT-PCR in four-week-old transgenic T3 plants uORF1- uORF2-GUS (Ler), uorf1- uorf2-GUS (Ler) and uORF1-uORF2-GUS (atgcn2) treated with Psm ES4326/avrRpm1 (OD<sub>600nm</sub> = 0.02), sampled at indicated time points. Data represent the mean and standard error of three independent biological replicates.



Supplementary Figure 2. Time-course quantification of *P. syringae* biomass. Ler and *atgcn2* plants were infected with *Pst* DC3000 (a, b), *Pst* DC3118 (c, d), or *Pst* DC3000 *hrcC* (e, f) by pressure infiltration (OD<sub>600nm</sub>=0.0002) (a, c, e) or spray (OD<sub>600nm</sub>=0.2) (b, d, f). Pathogen growth were quantified in four weeks old infected plants at indicated time points (4, 12, 24, 36, 48, 60, and 72 hpi) by qPCR analyses. Data represent the mean and standard error of three independent biological replicates. Two sample t-test was performed for statistical analysis, asterisks indicate significant differences compared to wild-type Ler (\* p<0.05, \*\* p<0.01, \*\*\*p<0.001).

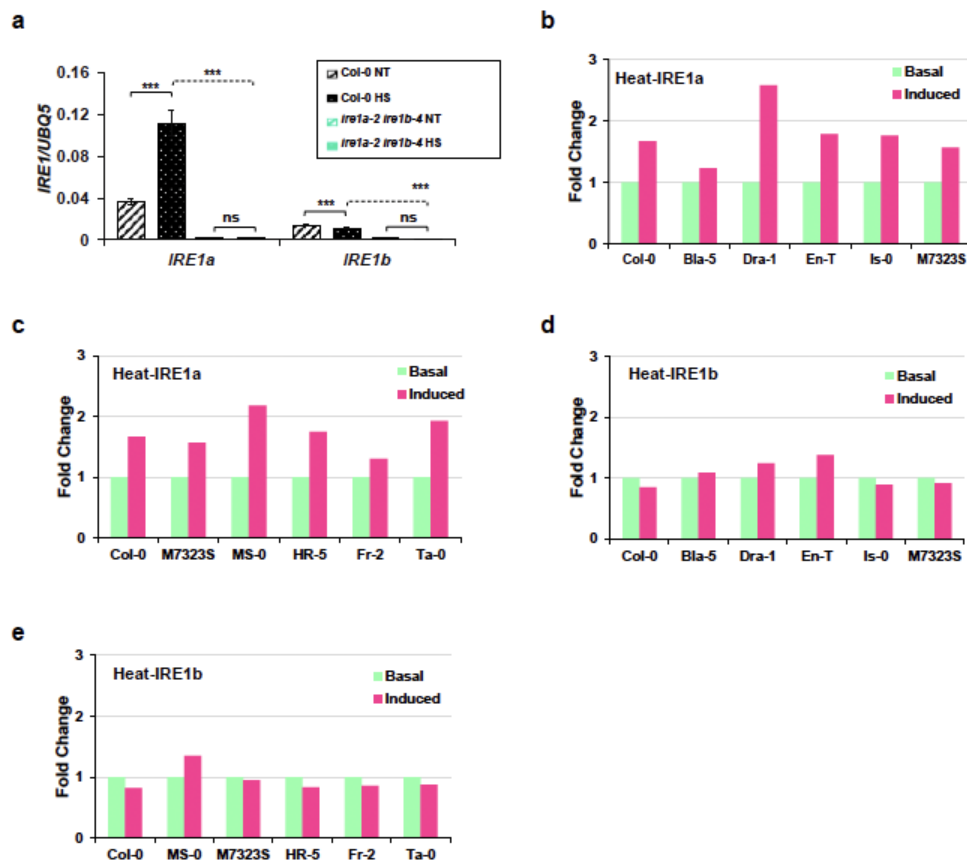


Supplementary Figure 2. Time-course quantification of *P. syringae* biomass. Ler and *atgcn2* plants were infected with Pst DC3000 (a, b), Pst DC3118 (c, d), or Pst DC3000 hrcC (e, f) by pressure infiltration (OD<sub>600nm</sub>=0.0002) (a, c, e) or spray (OD<sub>600nm</sub>=0.2) (b, d, f). Pathogen growth were quantified in four weeks old infected plants at indicated time points (4, 12, 24, 36, 48, 60, and 72hpi) by qPCR analyses. Data represent the mean and standard error of three independent biological replicates. Two sample t-test was performed for statistical analysis, asterisks indicate significant differences compared to wild-type Ler (\* p<0.05, \*\* p<0.01 ; \*\*\*p<0.001).



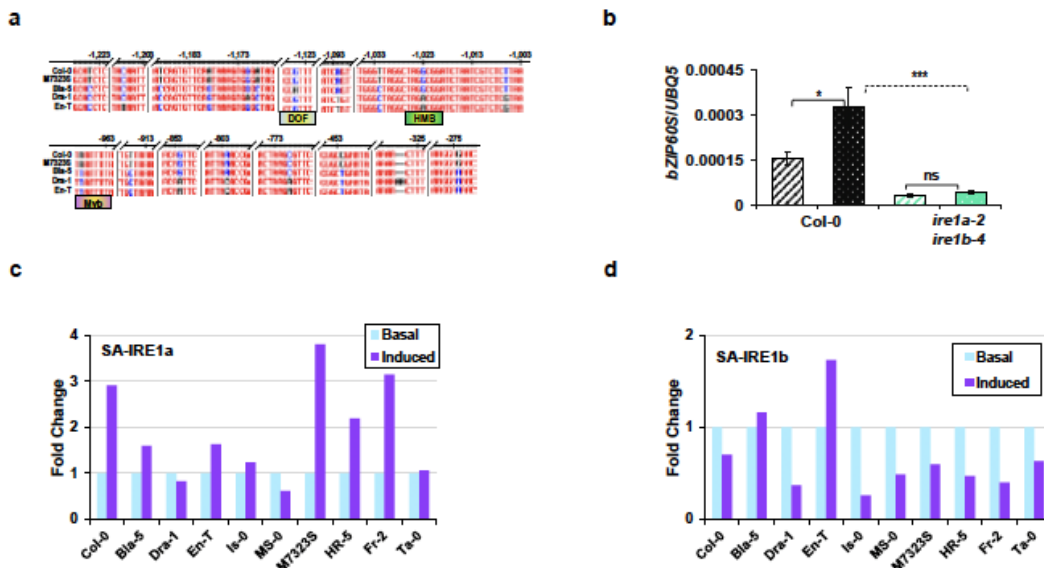
Supplementary Figure 4. AtGCN2 affects ABA accumulation upon pathogen infection. a-b. ABA concentration was determined in two-week-old Ler and atgcn2 at the indicated time points after Pst DC3000 (OD<sub>600nm</sub> = 0.2) (a) or Pst DC3118 (OD<sub>600nm</sub> = 0.2) (b) dip inoculation. The box plots extend from the 25th to 75th percentiles and the whiskers extend from the minimum to the maximum level. Median values are plotted in the box with data generated from three independent biological replicates, each of them shown as means of four technical replications. Two-way ANOVA with Tukey's test was performed, asterisks indicate significant differences compared to wild-type Ler (p-values are listed).

CHAPTER 4 PROBING NATURAL VARIATION OF IRE1 EXPRESSION AND  
ENDOPLASMIC RETICULUM STRESS RESPONSES IN ARABIDOPSIS  
ACCESSIONS



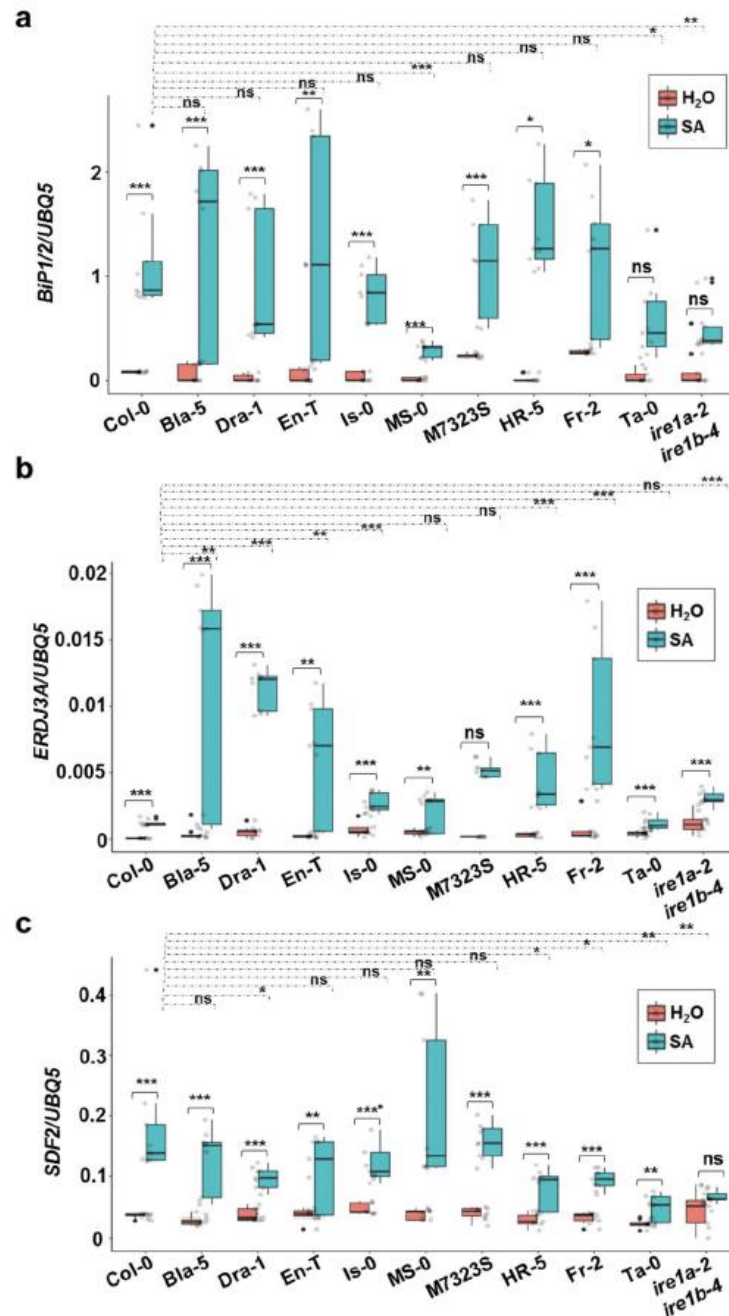
**Supplementary Figure 1: Analysis of relative *IRE1a* and *IRE1b* expression levels before and after heat stress.** (a) Basal and induced mRNA expression levels of *IRE1a* and *IRE1b* in Col-0 (black bars) and double mutant *ire1a-2 ire1b-4* (green bars) were measured in leaf tissue of 1-month-old Arabidopsis plants that were untreated or heat-stressed at 37°C for 90 minutes. Transcript accumulation was assessed via qRT-PCR and normalized to housekeeping gene UBQ5 (Ubiquitin 5). Dashed bars represent basal expression levels, and dotted bars correspond to heat-induced expression levels.

Statistical analyses were performed in Excel by One-Way ANOVA. At least three independent biological replicates, each with three technical replicates were performed. Error bars show mean  $\pm$  SD. Significant differences are indicated by asterisks (\*\* p<0.001, \*\* p<0.01, \* p<0.05). Solid lines connecting bars represent the comparison of basal to heat-induced expression levels for each individual genotype, while dashed lines represent the comparison of induced expression levels between Col-0 and ire1a-2 ire1b-4 plants. (b,c) The fold change of induced IRE1a expression compared to the respective basal expression levels in the selected members of the IRE1a-accession group (b) and IRE1b-accession group (c) upon heat stress. (d,e) The fold change of induced IRE1b expression compared to the respective basal expression levels in the selected members of the IRE1a-accession group (d) and IRE1b-accession group (e) upon heat stress. The fold change was calculated by dividing the average (from 3 biological replications) of induced expression value with average (from 3 biological replications) of basal expression value. Treatment groups are represented according to legends.

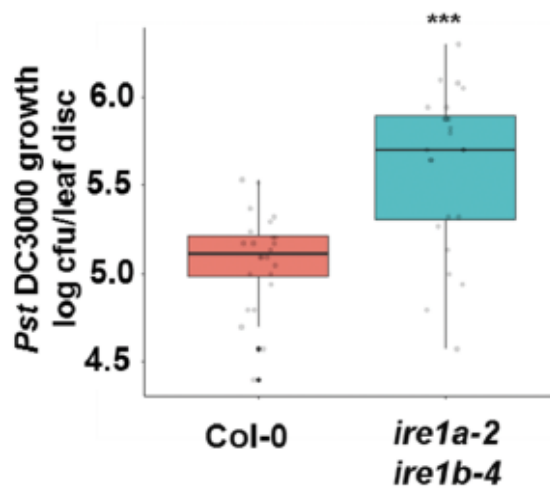


Supplementary Figure 2: (a) multiple sequence alignment of the promoter regions of the IRE1a gene among five ecotypes. Upstream regulatory sequences of IRE1a from Col-0, M7323S, Bla-5, Dra-1, and En-T were obtained and aligned to identify polymorphic regions. For clarity, only the sequence regions showing polymorphisms (17 SNPs and one InDel) among these accessions are shown. Positions are relative to the point of translation initiation coding sequence in Col-0. Predicted binding sites for transcription factors DOF (DNA binding with one finger), Myb (Myb-related DNA binding proteins), and HMB (Arabidopsis homeobox protein) are indicated with rectangular boxes. (b) Basal and induced mRNA expression levels of spliced bZIP60 (bZIP60s) in Col-0 (black bars) and double mutant ire1a-2 ire1b-4 (green bars) were measured in leaf tissue of 1-month-old Arabidopsis plants that were untreated or heat-stressed at 37°C for 90 minutes. Transcript accumulation was assessed via qRT-PCR and normalized to housekeeping gene UBQ5 (Ubiquitin 5). Dashed bars represent basal expression levels, and dotted bars correspond to heat-induced expression levels. Statistical analyses were performed in Excel by One-Way ANOVA. At least three independent biological replicates, each with three technical replicates were performed. Error bars show mean ± SD. Significant differences are indicated by asterisks (\*\*\*( $p<0.001$ ), \*\*( $p<0.01$ ), \*( $p<0.05$ )). Solid lines connecting bars represent the comparison of basal to heat-induced expression levels for each individual genotype, while dashed lines represent the comparison of induced expression levels between Col-0 and ire1a-2 ire1b-4 plants. (c) The fold change of induced IRE1a expression compared to the basal expression levels in all the selected accessions upon SA stress. (d) The fold change of induced IRE1b expression compared to the basal expression levels in all the selected accessions upon SA stress. The fold change was

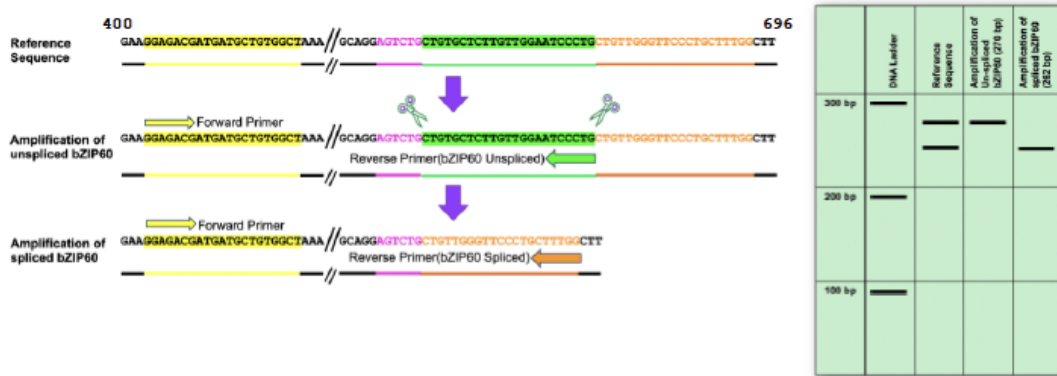
calculated by dividing the average (from 3 biological replications) of induced expression value with average (from 3 biological replications) of basal expression value. Treatment groups are represented according to legends.



Supplementary Figure 3: Quantification of relative mRNA levels of ER stress markers BiP1/2, ERDJ3A, and SDF2. Transcript levels of BiP1/2 (a), ERDJ3A (b), and SDF2 (c) were quantified using qRT-PCR in leaf tissues of 1-month-old plants that were treated with 0.5mM SA or H<sub>2</sub>O (mock) for 6 hours. Treatment groups are represented according to legends. All expression levels shown in panels a-c were measured in leaf tissues of 1-month-old *Arabidopsis* plants via qRT-PCR and were normalized to housekeeping gene UBQ5 (Ubiquitin 5). The box plots extend from the 25th to 75th percentiles and the whiskers extend from the minimum to the maximum level. Light grey dots represent individual data points. Outliers, shown as dark grey dots, were identified by the test statistics of the geom\_boxplot function in ggplot2. Median values were plotted in the boxes with the data generated from three independent biological replicates. Statistical analyses were performed in Excel by one-way ANOVA. Significant differences are indicated by asterisks (\*\*\*(p<0.001), \*\*(p<0.01), \*(p<0.05)). Solid lines connecting bars represent the comparison of basal to SA-induced expression levels for each individual accession, while dashed lines represent the comparison of SA-induced expression levels between Col-0 and an indicated accession.

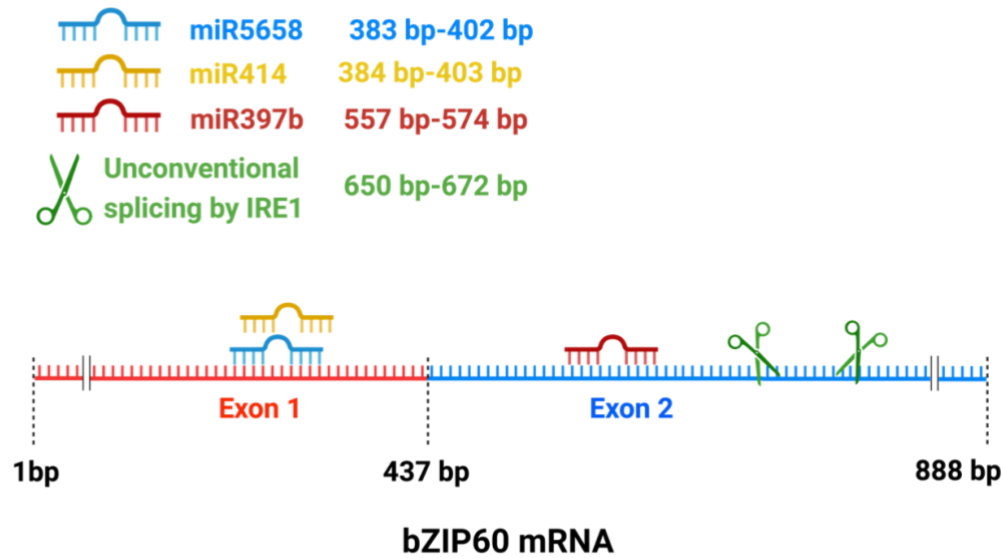


Supplementary Figure 4. Enhanced disease susceptibility to *Pseudomonas syringae* pv. tomato DC3000 in double mutant *ire1a-2 ire1b-4*. Leaves of 4 weeks old plants were syringe infiltrated with *Pseudomonas syringae* pv. tomato DC3000 (Pst DC3000). In planta bacterial growth was quantified at 3 days post-inoculation. The box plots extend from 25th to 75th percentiles and whiskers extend from minimum to maximum level. Light grey dots represent individual data points. Outliers, shown as dark grey dots, were identified by the test statistics of the geom\_boxplot function in ggplot2. Median values were plotted in the boxes with the data generated from three independent biological replicates. Statistical analyses were performed in Excel by One-Way ANOVA. Significant differences are indicated by asterisks (\*\*\*)  $p < 0.001$ .

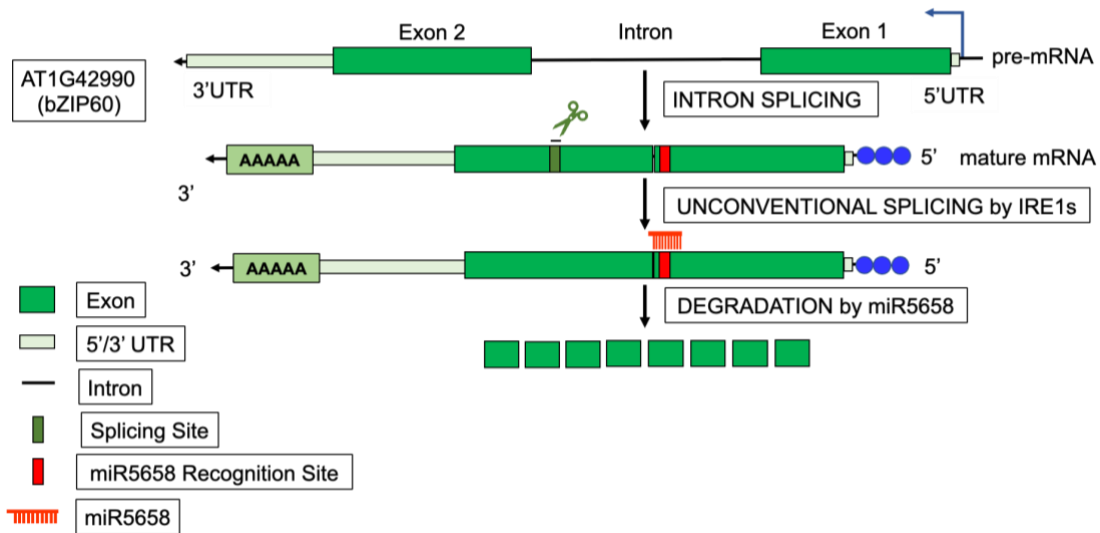


Supplementary Figure 5. Schematic representation of the q-RT-PCR assay developed to measure levels of spliced and unspliced bZIP60 variants. The binding site for the common forward primer is highlighted in yellow. The binding site for the reverse primer specific to unspliced bZIP60 is highlighted in green. Sequence marked in pink and orange constitutes the binding site for the reverse primer specific to spliced bZIP60. Sequence coordinates are indicated next to Reference Sequence (top) and are in relation to the bZIP60 CDS sequence. A schematic representation of PCR amplicon sizes is shown to the right. The unspliced bZIP60 fragment is 270bp while the spliced bZIP60 amplicon is 262bp.

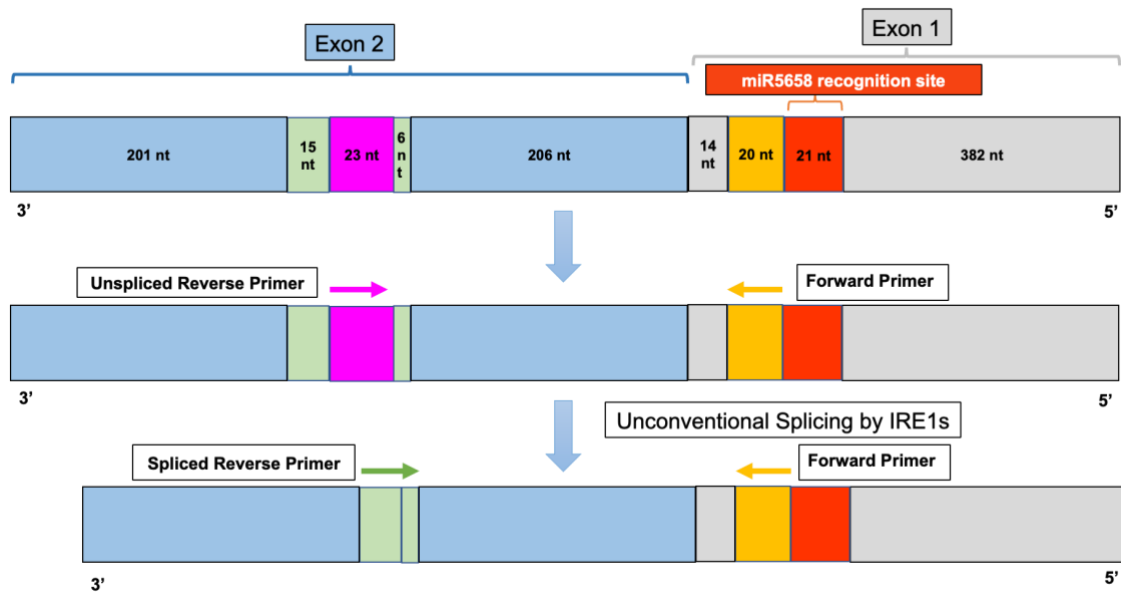
CHAPTER 5 ELUCIDATING THE ROLE OF NATURAL ANTISENSE RNA LOCI AS  
PRO-SURVIVAL TO PRO-DEATH MOLECULAR SWITCH IN THE IRE1A  
SIGNALING PATHWAY IN ARABIDOPSIS THALIANA



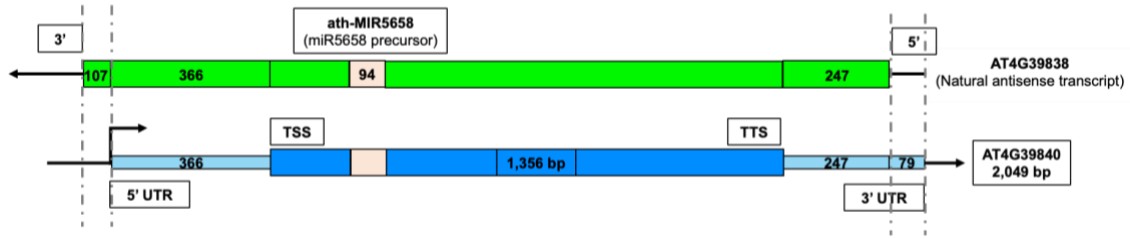
Supplemental Figure 1: The intended target locations of miRNAs (miR5658, miR414, miR397b) and the splicing site of IRE1 at bZIP60.



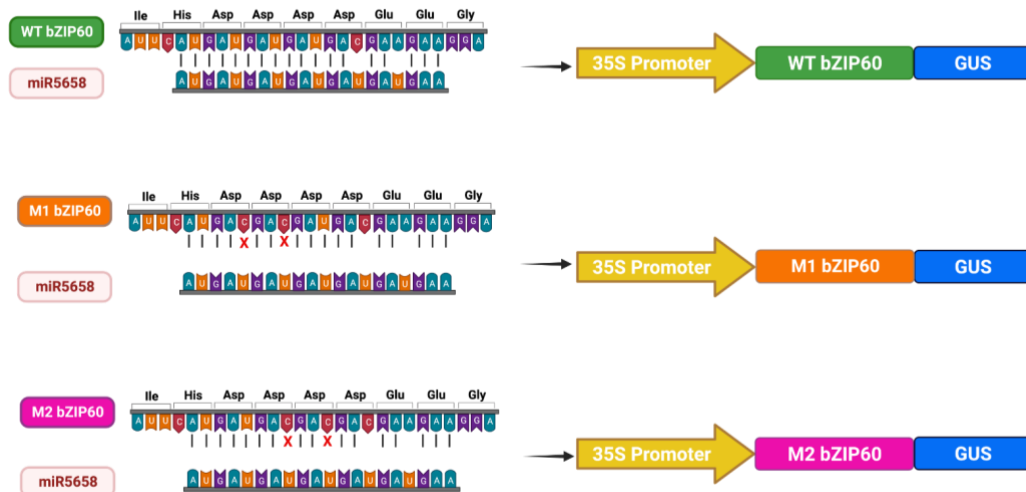
Supplemental Figure 2: The schematic representation of bZIP60, its cytoplasmic splicing site and miR5658 target site.



Supplemental Figure 3: The schematic representation of bZIP60, its cytoplasmic splicing site, the primer locations to quantify the spliced and unspliced bZIP60.



Supplemental Figure 4: The schematic of miR5658 precursor lncNAT and its sense transcript.



Supplemental Figure 5: the schematic of miR5658 target location and the synonymous point mutations to block the mir5658 binding.

	Wild Type bZIP60	M1 bZIP60
Col-0		
<i>NAT<sub>src1</sub></i>		
<i>src1</i>		
<i>npr1-1</i>		
<i>bZIP60</i>		

Supplemental Figure 6: Histochemical GUS assay in Col-0, *NAT<sub>SRCL</sub>*, *src1*, *npr1-1* and bZIP60 leaves transiently expressing transcriptional 35S::WT bZIP60-GUS and 35S::M1 bZIP60-GUS reporter

**APPENDIX B**

**SUPPLEMENTAL TABLES**

**CHAPTER 2 ARABIDOPSIS GCN2 KINASE CONTRIBUTES TO ABA  
HOMEOSTASIS AND STOMATAL IMMUNITY**

Supplemental Table 1. Summary of genes associated with ABA response whose transcription is TBF1-dependent upon *elf18* challenge.

	<b>AGI</b>	<b>Gene Model Description</b>	<b># TL1 degenerate</b>	<b># TL1 exact</b>
Induced by TBF1	AT3G20310	ERF/AP2 transcription factor family (ATERF-7), involved in ABA-mediated responses.	4	0
	AT5G46790	a member of the PYR/PYL/RCAR family proteins and mediate ABA-dependent regulation of protein phosphatase 2Cs ABI1 and ABI2.	2	2
	AT2G40330	a member of the PYR/PYL/RCAR family proteins and mediate ABA-dependent regulation of protein phosphatase 2Cs ABI1 and ABI2.	0	0
	AT5G01560	LecRKA4.3 which negative regulates ABA response in seed germination.	0	0
	AT5G05440	a member of the PYR/PYL/RCAR family proteins and mediate ABA-dependent regulation of protein phosphatase 2Cs ABI1 and ABI2.	0	0
Repressed by TBF1	AT3G57530	Calcium-dependent Protein Kinase and regulates the ABA-responsive gene expression via ABF4.	6	0
	AT5G66880	a member of SNF1-related protein kinases (SnRK2) in the ABA signaling during seed germination, dormancy and seedling growth.	4	0
	AT1G72450	jasmonate-zim-domain protein 6 (JAZ6).	2	2
	AT3G11410	Encodes protein phosphatase 2C. Negative regulator of ABA signalling.	2	2
	AT3G62030	nuclear-encoded chloroplast stromal cyclophilin CYP20-3 (also known as ROC4) which is modulated in response to ABA.	2	0
	AT5G02240	Protein is tyrosine-phosphorylated and its phosphorylation state is modulated in response to ABA in <i>Arabidopsis thaliana</i> seeds.	2	2
	AT5G24030	The SLAH3 protein has similarity to the SLAC1 protein involved in ion homeostasis in guard cells.	2	0
	AT5G63980	Encodes a bifunctional protein that is involved in the response to cold, drought (negative regulator of drought tolerance), and ABA.	2	0
	AT1G01260	basic helix-loop-helix (bHLH) DNA-binding superfamily protein shows similarity to ABA-inducible transcription factor (AT2G46510.1).	0	0
	AT1G17380	jasmonate-zim-domain protein 5 (JAZ5).	0	0
	AT1G32640	MYC2	0	0
	AT1G70700	jasmonate-zim-domain protein 9 (JAZ9).	0	0
	AT1G75380	nucleases AtBBD1 involved in ABA-mediated callose deposition.	0	0
	AT2G05710	ACO3 is tyrosine-phosphorylated and its phosphorylation state is modulated in response to ABA in <i>Arabidopsis thaliana</i> seeds.	0	0
	AT2G18960	a plasma membrane proton ATPase which affect stomatal closure towards drought and ABA.	0	0
	AT2G33380	Encodes a calcium binding protein whose mRNA is induced upon treatment with NaCl, ABA and in response to desiccation.	0	0
	AT2G34600	jasmonate-zim-domain protein 7 (JAZ7).	0	0
	AT2G46510	Encodes a nuclear localized BLH domain containing transcriptional activator involved in response to ABA.	0	0
	AT3G17860	jasmonate-zim-domain protein 3 (JAZ3).	0	0
	AT3G50500	SNRK2.2 which is involved in the ABA signaling during seed germination, dormancy and seedling growth.	0	0
	AT3G55610	encodes delta 1-pyrroline-5-carboxylate synthetase B. Gene expression is induced by dehydration, high salt and ABA.	0	0
	AT4G38970	Protein is tyrosine-phosphorylated and its phosphorylation state is modulated in response to ABA in <i>Arabidopsis thaliana</i> seeds.	0	0
	AT5G20900	jasmonate-zim-domain protein 12 (JAZ12)	0	0
	AT5G25610	responsive to dehydration 22 (RD22) mediated by ABA	0	0
	AT5G67030	ABA1 which functions in first step of the biosynthesis of the abiotic stress hormone abscisic acid (ABA).	0	0

Supplemental Table 2. List of primers used in this study.

Primer name	Sequence 5' -> 3'	Application
AtGCN2-F	CAACACTTCCCCTTCAG	qPCR
AtGCN2-R	GTTGACACTGCACCTGAGTAG	qPCR
eIF2α-F	ACTCACAACTCACACCCATTAC	qPCR
eIF2α-R	TTCCCTCATCACCCTCATTT	qPCR
TBF1-F	GTTGGTTCGCCCTCTG	qPCR
TBF1-R	CCACACCCCAAACAAT	qPCR
PP2CA-F	AAGATCGGTACGACGTCGGTTGT	qPCR
PP2CA-R	TCTGCACTCTCCGCAACATGAGA	qPCR
ABI2-F	ACACGTGGCAAGAGAACATGGAAGA	qPCR
ABI2-R	CCGCAATTGCGACAAAGATGTGA	qPCR
FRK1-F	AAGATGGCGACTTCG	qPCR
FRK1-R	GCAGGTTGGCCTGTAA	qPCR
SLAC1-F	CCGGGCTCTAGCACTCA	qPCR
SLAC1-R	TCAGTGATGCGACTCTT	qPCR
MYC2-F	CAAGGAGGAGTGTGGGATGC	qPCR
MYC2-R	GTCGAAAAATTAAAGTTCTCGGGAG	qPCR
ANAC019-F	GCATCTCGCTCGCTCAG	qPCR
ANAC019-R	CTCGACTTCCTCCCTCG	qPCR
ANAC055-F	GCGCTGCCTCATAGTC	qPCR
ANAC055-R	CGAGGAATCCCCTCAGT	qPCR
NCED5-F	CCTCGTTAGTTCACCAACACT	qPCR
NCED5-R	GGTGTGCGAGACGGAGTT	qPCR
ABA3-F	TCCTGAAGATTACAGTTGCTTATTAC	qPCR
ABA3-R	TGGGTCCACGGAAAAGTCTCT	qPCR
oprF-F	AACTGAAAACACCTGGGC	qPCR
oprF-R	CCTGGGTTGTTGAAGTGGTA	qPCR
UBQ5-F	GTAAACGTAGGTGAGTCC	qPCR
UBQ5-R	GACGCTTCATCTCGTCC	qPCR

CHAPTER 4 PROBING NATURAL VARIATION OF IRE1 EXPRESSION AND  
ENDOPLASMIC RETICULUM STRESS RESPONSES IN ARABIDOPSIS  
ACCESSIONS

**Supplementary Table S1.** Primers used in this study.

Application	Gene	Sequence	Fwd/Rev
clone (attB flanked)	IRE1a	GGGG ACA AGT TTG TAC AAA AAA GCA GGC TCC GCAAGATAATATTGCATACCTAAGA	F1
clone (attB flanked)	IRE1a	GGGG ACC ACT TTG TAC AAG AAA GCT GGG TC AATAGTAGTAAGAAGAAAAGATGGC	R1
clone (attB flanked)	IRE1a	GGGG ACA AGT TTG TAC AAA AAA GCA GGC TCC CCTAACATGCAGAGGATGGAAGAAA	F2
clone (attB flanked)	IRE1a	GGGG ACC ACT TTG TAC AAG AAA GCT GGG TC TTAACATGCAGAGGATGGAAGAAA	R2
clone (attB flanked)	IRE1b	GGGG ACA AGT TTG TAC AAA AAA GCA GGC TCC GACATCATGCATCATGTTGATACTC	F1

clone (attB flanked)	IRE1b	GGGG ACC ACT TTG TAC AAG AAA GCT GGG TC GAGATAGATTGTCATAGAACTTGG	R1
clone (attB flanked)	IRE1b	GGGG ACA AGT TTG TAC AAA AAA GCA GGC TCC CCCAACAGAGACATCATGCATCATG	F2
clone (attB flanked)	IRE1b	GGGG ACC ACT TTG TAC AAG AAA GCT GGG TC CCGATCGGATTGAGAGATTGATTG	R2
clone (attB flanked)	IRE1a	GGGGACCACTTGTACAAGAAAGCTG GGTC AGGACATCTCGCGGCATGGT	R3
clone (attB flanked)	IRE1a	GGGGACCACTTGTACAAGAAAGCTG GGTC TAGTAAGAAGAAAAGATGGCGGAG	R4
clone (attB flanked)	IRE1b	GGGGACCACTTGTACAAGAAAGCTG GGTC GATTGGAGATAGATTGTCAT	R3
clone (attB flanked)	IRE1b	GGGGACCACTTGTACAAGAAAGCTG GGTC GATCGGATTGAGAGATTGAT	R4
clone (attB flanked)	IRE1b	GGGG ACC ACT TTG TAC AAG AAA GCT GGG TC AGATAGATTGTCATAGAACTTGG	R5

clone (attB flanked)	IRE1b	GGGG ACC ACT TTG TAC AAG AAA GCT GGG TC GATCGGATTGAGAGATTGATTG	R6
Bigdye	IRE1a	ctaaccattttgcagaagata	F1
Bigdye	IRE1a	gagacg atta gatc cgcc tagc	R1
Bigdye	IRE1a	cggttctattaatcagttag	F2
Bigdye	IRE1a	catata catt agac atag tgcc	R2
Bigdye	IRE1a	gcgcttaagcggagggtcacccgc	F3
Bigdye	IRE1a	cgttc tcct ttgc aatc ttct	R3
Bigdye	IRE1a	acgcataattggctcggtcgcc	F4
Bigdye	IRE1a	tatgg agaa tccg aaca gaga	R4
Bigdye	IRE1a	ctcgccggacagagacggaga	F5
Bigdye	IRE1a	aactaa gtat tttt aaac atgc	R5
Bigdye	IRE1b	AAACGTTATATAACAAGGTCCGTT	F1
Bigdye	IRE1b	GTG TGA CAA TTT CTA ATT GAC CAC	R1
Bigdye	IRE1b	AATTAGAAATTGTCACACGTCTCTA	F2
Bigdye	IRE1b	AT TAT ATG TTG GTT TAG GCA AAC	R2
Bigdye	IRE1b	AGAATATGTTGCCTAACCAAC	F3
Bigdye	IRE1b	TT AAA GAT GTT TTT GTT TGT TTG	R3
Bigdye	IRE1b	AATCACCGATTAAACCGATAA	F4
Bigdye	IRE1b	AA TGT CAA ATG AAT CAA ACG AAA	R4
Bigdye	IRE1a	gcaagataatgcatacCTAAGA	F6a
Bigdye	IRE1a	cctttgctatcaacaatt	R6a

Bigdye	IRE1a	gccactatgtctaatttatgtg	F7a
Bigdye	IRE1a	TAGTAAGAAGAAAAGATGGCG	R7a
Bigdye	IRE1b	ATCATGCATCATgttgatact	F5b
Bigdye	IRE1b	agtttgttagattttttcc	R5b
Bigdye	IRE1b	ccaaatttggatgacacttat	F6b
Bigdye	IRE1b	ataacaaacaataaccggatc	R6b
Bigdye	IRE1b	aaccaatgatttaccaaattg	F7b
Bigdye	IRE1b	AGATAGATTGTCACTagaacctgg	R7b
Bigdye	pDNOR207	TCGCGTTAACGCTAGCATGGATCTC	F
Bigdye	pDNOR207	GTAACATCAGAGATTTGAGACAC	R
Bigdye	GUS	CGGTGAACAG GTATGGAATT TCGC	F
Bigdye	GUS	TTCCCACCAA CGCTGATCAA TTCC	R
qPCR	IRE1a F	GCTTCAGACCTCATATCCCG	F
qPCR	IRE1a R	AGCATCACGAAGGAAAGACAG	R
qPCR	IRE1b F	GGTGGGATGAGAAACTGGATAG	F
qPCR	IRE1b R	AGTTTGTTCGTATGACCCG	R
qPCR	UBQ5 F	GACGCTTCATCTCGTCC	F
qPCR	UBQ5 R	gtaaacgttaggtgagtcca	R
qPCR	ERDJ3B	CAAATACGAACGGGAGGGATAC	F
qPCR	ERDJ3B	GGTCGCCGTCTTCATAGAAA	R
qPCR	SDF2	TCAAGAGTGGAGCAACCATTAG	F
qPCR	SDF2	CCAAAGCAGCTAACCTCTAAGT	R
qPCR	ERdj3A	GGTAGCTCATCGAATGCTGAA	F

qPCR	ERdj3A	GGTCCACAACGTCCCTTATAG	R
qPCR	BIP3	CGGTCCAAGGTGGAGTATTAAG	F
qPCR	BIP3	CGCCTCCGACAGTTCAATA	R
qPCR	BIP1/2	CTGCTGTTCAGGGTGGTATT	F
qPCR	BIP1/2	TCATCACTCCTCCTACAGTCTC	R
qPCR	bZIP60us_F WD	GGAGACGATGATGCTGTGGCT	
qPCR	bZIP60u_RE V	caggattccaacaagagcacaG	
qPCR	bZIP60s_RE V	CAGGGAACCCAACAGCAGACT	

**CHAPTER 5 ELUCIDATING THE ROLE OF NATURAL ANTISENSE RNA LOCI AS  
PRO-SURVIVAL TO PRO-DEATH MOLECULAR SWITCH IN THE IRE1A  
SIGNALING PATHWAY IN ARABIDOPSIS THALIANA**

Supplemental Table 1: Primers Used in the Project.

Primer Name	Sequence (5' to 3')	Application
LP #1 / At4g39840 homo #097507	CTCTACGATTCCGTAGACCCC	Genotyping
RP #1 / At4g39840 homo #097507	CATTCTGGCTAGACGACGAAG	Genotyping
LP #6/At4g39838 homo #047112	AAAGTGTGTTTTGGTCTCC	Genotyping
RP #6/At4g39838 homo #047112	TAGGAGGAGGAGGAAGATTGG	Genotyping
#1 LP	GAAGCTCAATTCCGGAAACA	Genotyping
#1 RP	CTGACGAAGCACACCCAT	Genotyping
LP #5 / At4g39840 homo #093172	GCAGATCTGCTAAATCAAGC	Genotyping
RP #5 / At4g39840 homo #093172	AAAAGTTCCAACCATTCCACC	Genotyping
stem loop RT primer for miR5658	GTGTGATTCAGTGCAAGGTCGAGGTATTGCACTGGATAACGACTTTCA	stem loop RT Primer
forward qpcr primer	GCGGGGGATGATGATGATGATG	forward qpcr primer
Entry clone Sequencing F1	CTGATAAAGTTCTAACCGTCG	Cloning
Entry clone Sequencing F2	GCTTAATGATTCTGTAGCGG	Cloning
Entry clone Sequencing R1	GGTAGTATTATTGCCATTACCC	Cloning
Entry clone Sequencing R2	AGGGATTCCAACAAGAGC	Cloning
stem loop RT primer for miR414	GTC GTA TCC AGT GCA GGG TCC GAG GTA TTC GCA CTG GAT ACG AC TGACGA	stem loop RT Primer
forward qpcr primer miR414	GCG GCG TCA TCT TCA TC	forward qpcr primer
stem loop RT primer for miR397b	GTC GTA TCC AGT GCA GGG TCC GAG GTA TTC GCA CTG GAT ACG AC CATCAA	stem loop RT Primer
forward qpcr primer miR397b	GCC GCC TCA TTG AGT GCA T	forward qpcr primer
universal reverse primer	GTC CAG GGT CGG AGG TA	qPCR
snoR101 FP	CTTCACAGGTAAGTTCCCTG	qPCR
snoR101 RP	AGCATCAGCAGACAGTAGTT	qPCR
mir5658 (precursor) F1	GCTCTATTCCAGTCTCTCTTATT	qPCR
mir5658 (precursor) R1	AGAAGAGATGGGTTAACGGAGC	qPCR
mir5658 (precursor) F2	GAACCAATCTCTCTCTCTC	qPCR
mir5658 (precursor) R2	GGTCTGGGATTAGGGATCTTG	qPCR
mir5658 (precursor) F3	CCGAGTAGAGAAGATTGTTGGT	qPCR
mir5658 (precursor) R3	<u>GTGGTCITGGCGAGTTAGT</u>	qPCR
40 F1	<u>CTGGTGATGGTTGGAAACT</u>	qPCR
40 R1	<u>TCTCGCCGTCACATTTC</u>	qPCR
40 F2	<u>AGCTGAGAAATGCAATAGAAAGAAC</u>	qPCR
40 R2	<u>AGTTCCAACCATCACCAAG</u>	qPCR
40 F3	<u>AAGAACAAATTCTGGTGGATGG</u>	qPCR
40 R3	<u>CGGTCACATTTACAACATA</u>	qPCR
38 F1	<u>AGTTTCAATTGACGTGAGTAGTAGT</u>	qPCR
38 R1	<u>AGATCTCGCAAATGATTGCTATTG</u>	qPCR
38 F2	<u>GTGTGTAACGATAAGAGAGAAAGA</u>	qPCR
38 F3	<u>GTGATTGTTGATTTGGTAGGTGA</u>	qPCR
38 R3	CTACTCACGTACAATGAAACCTTCC	qPCR
Cloning sense FW	GGGG ACA AGT TTG TAC AAA AAA GCA GGC TCC ATGTCTCACTAAGTACTTGTG	Cloning
Cloning sense RV	GGGG ACC ACT TTG TAC AAG AAA GCT GGG TC TCAATTCTCTCTCTGTCA	Cloning
Cloning antisense FW	GGGG ACA AGT TTG TAC AAA AAA GCA GGC TCC GTCACACATTCAACATATTGTAA	Cloning
Cloning antisense RV	GGGG ACC ACT TTG TAC AAG AAA GCT GGG TC AAAATGTCTCTTATAATTATATAAG	Cloning
Cloning miR promo RV	GGGG ACC ACT TTG TAC AAG AAA GCT GGG TC GGTTACTAAGAAGAACCAAGCTCC	Cloning
Tagged s(pr)RT Primer 2	GACTGGAGCACGAGGACACT CCGAGTGAGAAGAGATGG	stem loop RT Primer
Tagged as(pr)RT Primer 2	GACTGGAGCACGAGGACACT GGTGGAAGAAGAAGAGATGG	stem loop RT Primer
F_Primer (qPCR) (Tag)	GACTGGAGCACGAGGACACT	qPCR
R_s(pr)_Primer 2 (qPCR)	GAGATGGGTTAACGGAGCTGG	qPCR
R_as(pr)_Primer 2 (qPCR)	CCGAGTAGAGAAGATTGTTGGTG	qPCR
SEQ FW	GAAGAAGGAGACGATGATGC	Sequencing
SEQ RV	TCATCTCGAGTAAATCTATGC	
Mutation at D1D2 FW	CTGGTAGCGAGATTGATGACGAGCATGACGAAGAAGGGAGC	
Mutation at D1D2 RV	CGTCTCCCTCTCGTCATCGTCATGAACTCGCTACAG	
Mutation at D2D3 FW	GGTAGCGAGATTGATGACGACGACGAGAAGGAGACGATG	
Mutation at D2D3 RV	CATCGTCCTCTCTCGTCATGATGAATCTCGCTACC	Site directed mutagenesis for miR5658 resistant bZIP60